Universidade de Aveiro Departamento de Química

2019

Luís Filipe Baptista Fontes

Synthesis and photophysical properties of triphenylpyridine derivatives

Síntese e caracterização fotofísica de derivados de trifenilpiridinas

Universidade de Aveiro Departamento de Química

2019

Luís Filipe Baptista Fontes

Synthesis and photophysical properties of triphenylpyridine derivatives

Síntese e caracterização fotofísica de derivados de trifenilpiridinas

Tese apresentada à Universidade de Aveiro para cumprimento dos requisitos necessários à obtenção do grau de Mestre em Química, realizada sob a orientação científica do Doutor Samuel Guieu, Investigador do Departamento de Química da Universidade de Aveiro (Portugal), e da Doutora Raquel Nunes da Silva, Investigadora de Pós-Doutoramento do Departamento de Química e do Departamento de Ciências Médicas da Universidade de Aveiro (Portugal).

O Júri

Presidente: Professora Helena Isabel Seguro Nogueira

Professora auxiliar do Departamento de Química da Universidade de Aveiro

Doutor Samuel Guieu

Investigador do Departamento de Química da Universidade de Aveiro

Doutora Eduarda M. P. Silva

Investigadora do Departamento de Ciências Químicas, Faculdade de Farmácia, Universidade do Porto

Dedico esta tese à minha família.

Acknowledgements

To Professor Artur Silva for his support and guidance.

To my supervisors Dr Samuel Guieu and Dr Raquel Nunes da Silva for the excellent challenge they proposed to me, for the advices, patience and for inspiring me to pursue my goals.

To my family that saw me changing my life and pursue the uncertainty of a dream. I hope that one day I will make them proud for doing something meaningful.

To my friends that received me in Aveiro, especially Ana Monteiro for being so kind and dear friend, Sofia Soares for pushing me to be better, Hélio Albuquerque for encouraging me to pursue my crazy ideas. Also, to my friends and colleagues from Chemistry and Biochemistry Vasco Baptista, João Pereira, Sara Gamelas, Carlos Silva, João Ferreira, Inês Cardoso and Sónia Pedro.

To all the Chemistry department staff, especially Mónica Valega that respected and helped me to have the same working conditions as any other researcher.

To Professor Hans Peter Wessel for believing in my potential.

To any person that in any way helped me and is part of my life.

Resumo

Neste estudo foram sintetizados e caracterizados derivados de trifenilpiridinas. Os derivados de trifenilpiridina apresentaram fluorescência, com alguns derivados a apresentarem rendimentos quânticos de fluorescência acima do composto de referência (antraceno). O composto [*4-(2-(2-metoxifenil)-6-fenilpiridin-4-il)-N,N-dimetilanilina]* apresenta ser o derivado com valores superiores de rendimento quântico de fluorescência. Os estudos realizados permitiram identificar a importância do grupo *2-(piridin-2-il)fenol* para obter fluorescência em estado sólido e não em solução. Foi tentada a complexação de boro com os derivados de *2-(piridin-2-il)fenol* com eterato de trifluoreto de boro no entanto os complexos obtidos não mostraram ser estáveis em solução. Cinco dos derivados foram analisados por cristalografia de raio-x: -os resultados permitiram avaliar as interações intramoleculares e intermoleculares em estado sólido. Todos os derivados apresentaram fluorescência em estado sólido demonstrando o potencial de fluoróforos baseados em trifenilpiridina para futuros estudos de luminescência em estado sólido.

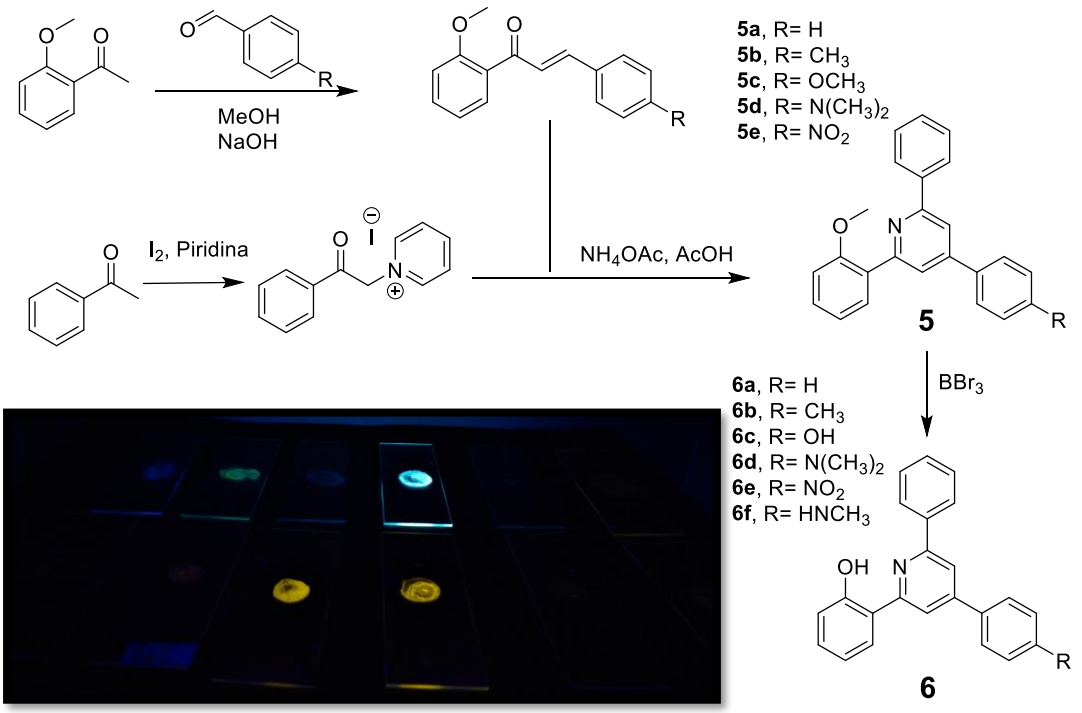

Palavras-chave: Luminescência, Fluorescência, Fluorescência promovida por agregação, Fluorescência em estado-sólido, Síntese de piridinas, Cristalografia de raio-x.

Abstract

In this study, triphenylpyridine derivatives were synthetized and fully characterized, including their photophysical properties. The triphenylpyridine core presented fluorescence in solution with quantum yields that surpass anthracene's, with compound [*4-(2-(2-methoxyphenyl)-6-phenylpyridin-4-yl)-N,N-dimethylaniline*] being the brightest. This study allowed to identify the importance of *2-(pyridin-2-yl)phenol* moiety for achieving fluorescence in solid state and not in solution. Complexation of boron was attempted for *2-(pyridin-2-yl)phenol* derivatives with boron trifluoride, however the complex was not stable in solution. Five derivatives were analysed by single crystal x-ray diffraction and their structural features were indicative of the possibility of solid-state emission with very weak intermolecular and intramolecular interactions. All derivatives presented solid-state fluorescence with three compounds showing potential for further solid-state luminescence studies.

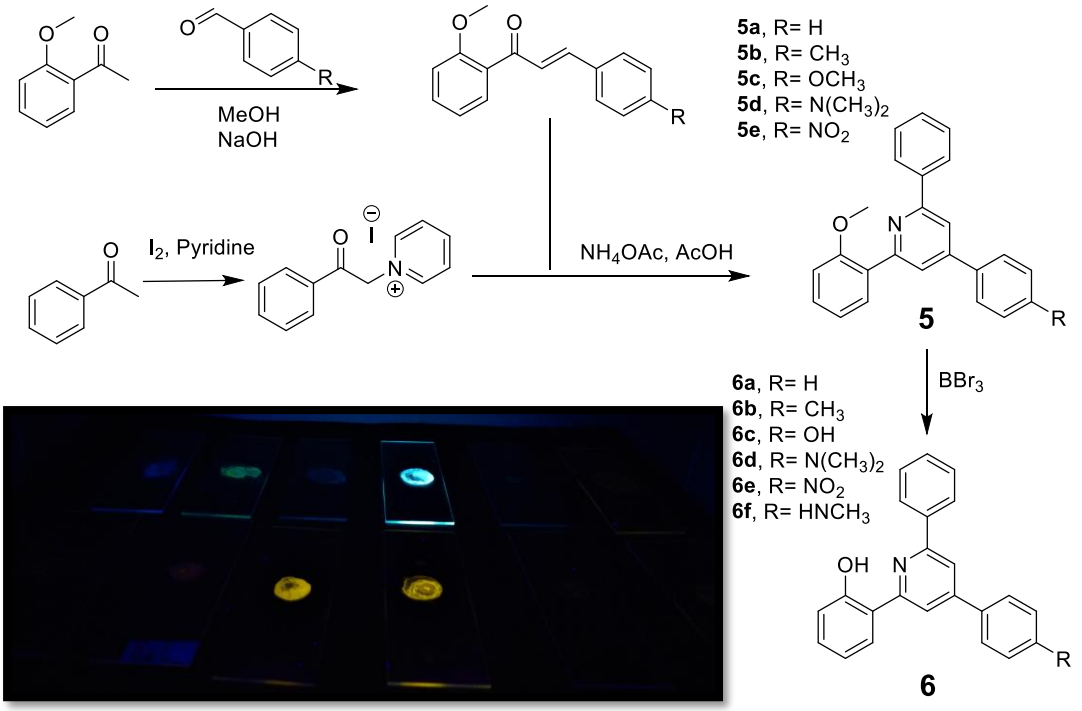

Keywords: Luminescence, Fluorescence, Aggregation-Induced Emission Enhancement, Solid state fluorescence, Pyridine synthesis, X-ray diffraction.

Index

List of figures, schemes and tables

List of symbols and abbreviations

π-pi orbitals

Φ: quantum yield

AIEE: aggregation induced emission enhancement

ACQ: aggregation caused quenching

BODIPY: boron-dipyrromethene

EML: emission layer

ETL: electron transport layer

HPS: hexaphenylsilole

HMBC-heteronuclear multiple bond connectivity

HOMO-highest occupied molecular orbital

HSQC-heteronuclear single quantum correlation

IC: internal conversion

ISC: intersystem crossing

LUMO-lowest unoccupied molecular orbital

OLED: organic light-emitting diode

OPD: organic photodiodes

PCT: photoinduced charge transfer

Py: pyridine

RIR: restrictions of intramolecular rotation

S_0: fundamental singlet state

S_1: singlet excited state

T_1: triplet state

ϵ: molar extinction coefficient

UV-vis: ultraviolet-visible

Chapter I. State of the art

In this chapter, information is provided about the photophysical phenomena related to fluorophores, especially organo-boron compounds. In the first section, fundamental concepts, such as fluorescence and the effect of different moieties, are explained using the Perrin-Jablonski's diagram and HOMO-LUMO transitions. In the second part, a overview of organo-boron complexes that are benchmarks in fluorescence is presented, focussing on BODIPY and analogues. Finally, in a third part, several *via* of synthesis of pyridine are described, introducing the *via* of synthesis chosen to achieve boranils based on a triphenyl-pyridinium backbone.

1. Photophysics

1.1. Luminescence

Luminescence is defined as the emission of light (radiation) from a substance due to electron excitation. There are several types of luminescence, like radioluminescence (excitation by ionizing radiation, e.g.: x-rays), chemiluminescence (excitation by chemical reactions, e.g.: oxidation) but in this work only photoluminescence will be discussed.[1]

In more detail, there are some parameters that affect photoluminescence. After excitation, a molecule has different ways of relaxation to the fundamental state. If the relaxation goes by radiative decay, there are two main ways of doing so, by fluorescence or by phosphorescence. Fluorescence is the phenomenon by which a molecule emits light (photons) immediately after excitation. Phosphorescence is the delayed emission of radiation after inter-system crossing.[1] To better understand these concepts, the Perrin-Jablonski's diagram interpretation is presented after a brief historical context of fluorescence.

The term fluorescence was used for the first time by George Stokes in "On the refrangibility of light" published in 1852, in order to describe a phenomenon that had already been observed by spanish physician Nicolas Monardes in 1565 of an extraction of wood from Mexico that had a peculiar blue colour.[2] The phenomenon observed in different samples – organic (e.g.: quinine) and inorganic (e.g.: fluorite crystals) (Figure 1) – was due to the emission of light.

a)  b) 

Figure 1-a) Quinine and b) Fluorite crystals under UV.

Stokes perceived that the emitted light has longer wavelength than the absorbed light and this led to what is called the Stokes shift in his honour, but the process was only better understood with the development of quantum mechanics. During the twentieth century, several physicists explored the process of fluorescence. The electronic transition principle is illustrated in the Perrin-Jablonski's diagram (Figure 2).

1.2. Mechanism of fluorescence and Perrin-Jablonski's diagram

The Perrin-Jablonski's diagram (Figure 2) is often used to illustrate the principles related with transitions of organic molecules from fundamental to excited state. These principles rely on quantum mechanics studies that suggest the possibility for a molecule to acquire an excited state of higher energy (S_1) without ionization. This state is transitory, and the molecule quickly returns to a lower energy state (S_0, or ground state) which leads to the release of energy in different forms (heat, vibration or photon emission by fluorescence or phosphorescence). Fluorescence is the emission of photons from the direct decay from S_1 to S_0, phosphorescence is the delayed emission of radiation after inter-system crossing. Phosphorescence occurs from the unfavourable transition form singlet (paired electrons with opposite spin) S_1 to triplet (paired electrons with same spin) T_1. In inter-system crossing, the triplet state-singlet state energy transfer "forbidden transition" is a slower process than singlet state decay, creating a slow and continuous release of energy that can take seconds to hours.[3]

In both fluorescence and phosphorescence, efficiency is measured by what is called the quantum yield. The quantum yield is the ratio of the total number of photons emitted over the total number of photons that were absorbed by the molecule; this process is

time-dependent and gives the effectiveness. Quantifying the conversion of energy by the molecule to radiation allows to estimate the quantity of energy loss by non-radiative phenomena.[1,2]

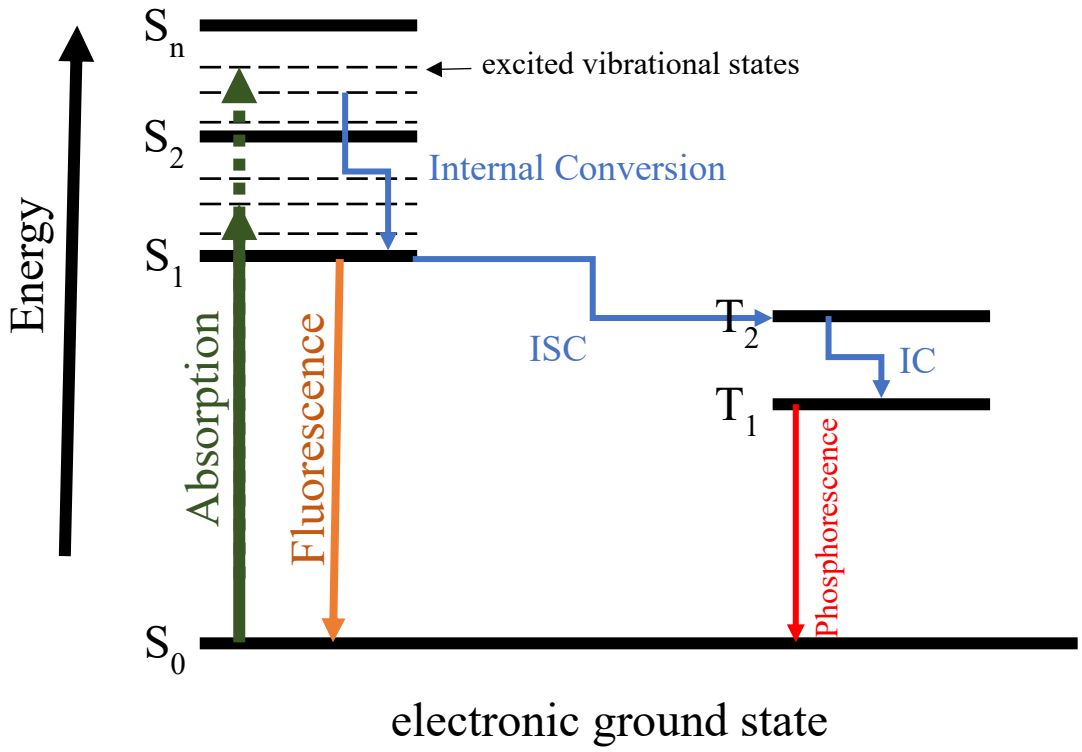

Figure 2-Perrin-Jablonski's diagram.[2]

1.3. Energy absorption and emission

There are several molecular characteristics that influence the transition of electrons from fundamental to excited state. The electronic transition of an electron is dependent of the type of bond it is involved in, σ bond's electrons require more energy to promote them to an excited state than π bond's electrons. This lower energy requirement allows the promotion of π electrons to excited states π* (π-π* transition) by photons of appropriate energy. These transitions are often called HOMO-LUMO transitions, being HOMO-highest occupied molecular orbitals and LUMO-lowest unoccupied molecular orbitals (Figure 3).

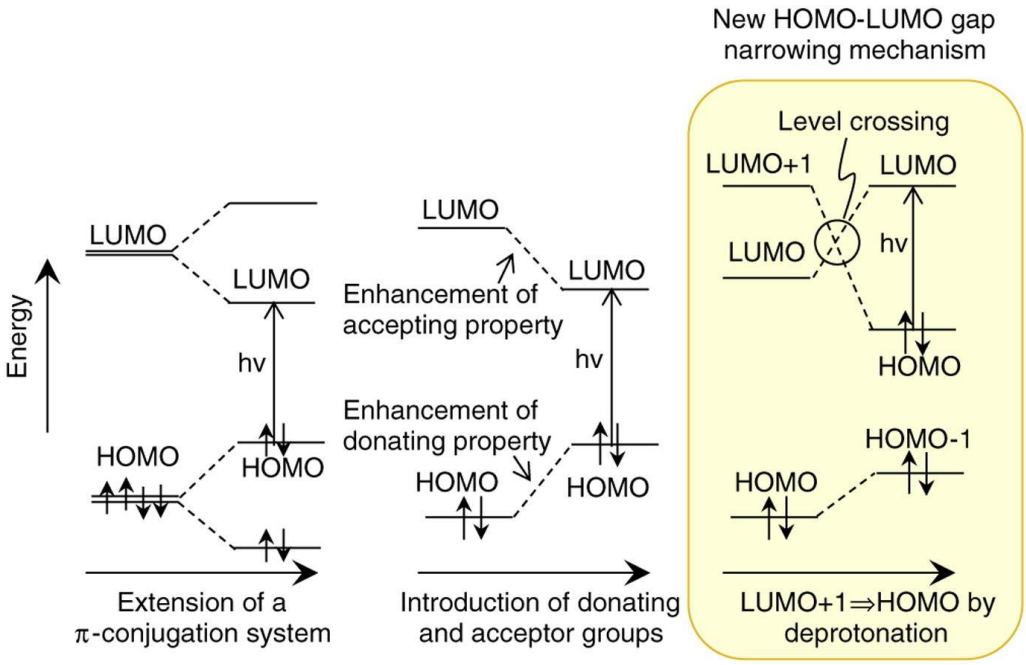

Figure 3-HOMO-LUMO transitions.[4]

The extension of the π electron system lowers the necessary energy to excite an electron in the system, this means that π-π* transitions becomes possible with excitation at longer wavelengths. It was noticed that increasing the conjugation of π electrons lowers the π-π* gap. The highly conjugated systems are one of the strategies applied to synthetize molecules that have low π-π* transitions energies, and therefore longer wavelengths of excitation and emission. To achieve fluorescence, it is better to have as much electrons as possible with low energy π-π* transitions. Several studies have indicated that achieving low HOMO-LUMO gaps could be made by high π conjugation, and it can also be obtained by using heterocyclic compounds and atoms with non-bonded electron orbitals that could interact with π orbitals, such as: O, N, for examples. Other way to achieve low HOMO-LUMO gaps is the complexation with metals creating organo-metallic complexes. Molecules that have small HOMO-LUMO gaps present further red absorption/emission spectra, and this characteristic provides an excellent starting point for tuneable scaffolds.[4]

It is important to highlight that a balance of the quantity of electrons with low π-π* transition energies must be taken in consideration because a highly conjugated molecule that absorbs greatly does not necessarily emit greatly: graphene is one of the most well-known examples.[2]

1.3.1. Structural effects on energy emission

As referred previously, conjugation is important to achieve lower energy π-π* transitions, this can be also addressed as resonance of the structure or degree of conjugation, higher conjugated structures mean lower energy for π-π* transitions, so longer wavelength. That is one of the reasons why many fluorescent compounds are aromatic (Figure 4).

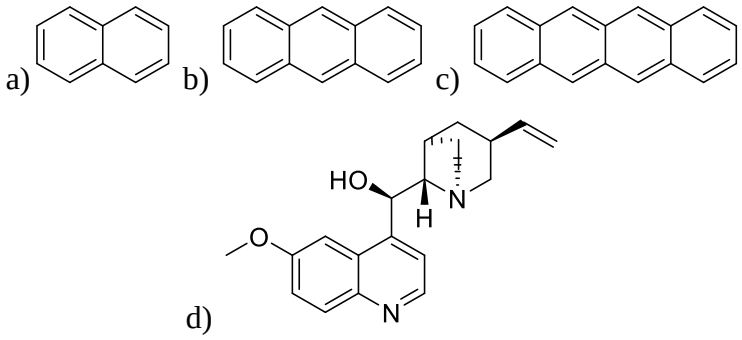

Figure 4-Aromatic compounds that are fluorescent: a) Naphthalene, b) Anthracene, c)Tetracene, d) Quinine

The substitution of aromatic compounds with chemical groups such as -OH, -NH_2, -COOH are known for their effect on the absorption and emission spectra; this modification is described as auxochromic effect.[2]

Compounds that present one or more nitrogen atoms (Figure 5) included in the ring system usually present higher quantum yields. The azarene nitrogens make S_0-S_1 transitions much more favourable than only-carbon aromatic compounds. The nitrogen that is single bonded to carbon (e.g: tryptophan) has a lone electron pair which forms a no-bonding orbital that has a conformation perpendicular to the ring making this non-bonding orbital available for the overlap of π orbitals that increases the conjugation. In general, this improves the quantum yield. This feature, along with the introduction of polarity by nitrogen, makes this nitrogen based moieties more interesting for biological applications and some examples, like tryptophan, are present in natural compounds.[5]

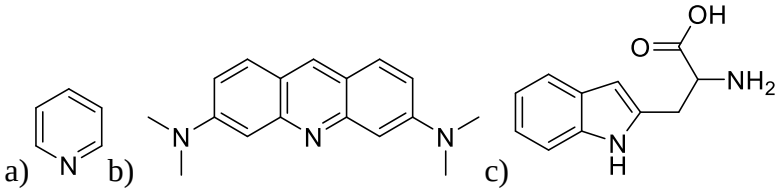

Figure 5-Azarenes: a) Pyridine, b) Acridine orange and c) Tryptophan.

Other molecules have similar proprieties due to the presence of atoms that also have lone electron pairs (Figure 6), for example xanthene that have oxygen instead of nitrogen.[2,6]

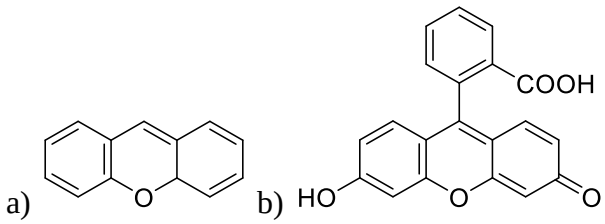

Figure 6-a) Xanthene b) Fluorescein.

Electron donating groups that have lone pairs of electrons, such as -OH, -OR, -NH_2, -NHR, -NR_2, change the molar absorption coefficients and lead to a shift in the absorption/emission spectra. The presence of lone pairs of this nature (not like carbonyl or nitro, electron withdrawing) increases the electronic density of the π conjugated systems of aromatic compounds and therefore improves the absorption by the aromatic ring.[2,7,8]

In opposition to the electron-donating groups, electron withdrawing groups such as carbonyl and nitro usually induce low quantum yields. The aromatic rings lose some of the electron density with the addition of these groups and this leads to lower absorptions by the π conjugated systems, another effect that in some cases like carbonyl or nitro groups favours intersystem crossing transitions.[2,9]

When added simultaneously to the structure of a fluorophore, electron donating and electron withdrawing groups create a dipole moment (push and pull). This effect is often denominated photoinduced charge transfer (PCT). Fluorescein is a good example that includes substitutions that create a dipolar moment. Another good example of PCT is Rhodamine B and Rhodamine 101 (Figure 7) where Rhodamine 101 presents high quantum yield. The reason comes from the cyclization of the amine groups. Besides decreasing the possibility of internal rotations, it simultaneously maximizes the conjugation between non-bonded electron pairs and the aromatic rings. In this case the presence of electron withdrawing groups promotes high photoinduced charge transfer (high dipole moment).[7,10]

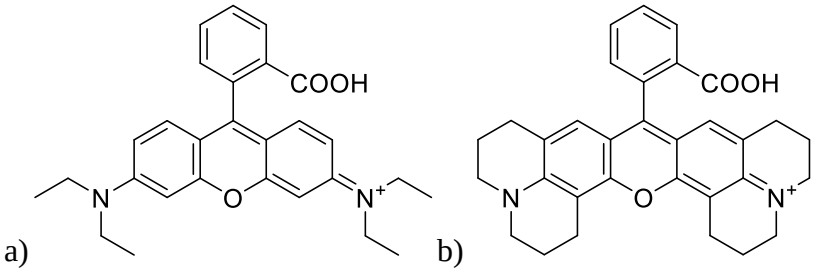

Figure 7-a) Rhodamine B and b) Rhodamine 101.

Other factors such as the pH or the polarity of the solvents can change the nature of some of the groups mentioned previously. For example, a change of pH can transform amines or carbonyl groups into charged groups, changing the electronegativity of the groups and leading to different fluorescence proprieties. Changes in conformation can also affect fluorescence.[2,5,11]

1.4. Fluorescence in solution and in aggregate state

Fluorescence is dependent of the state of matter of the compound: a compound that is fluorescent in solution is not necessarily fluorescent in solid state. This decrease of brightness in solid state comes from the promotion of non-radiative decay and is called quenching. Quenching is the loss of energy by non-radiative phenomena such as vibrations or inter-molecular interactions. This phenomenon depends on the structure of the molecule, but also depends on the environment.[12,13] The process where high concentration of the compound induces quenching is referred as Aggregation Caused Quenching (ACQ).

For this study a focus will be put into the structural effects on fluorescence emission. To minimize non-radiative phenomena one strategy is to rigidify the structure avoiding the release of energy by vibration.[12,14,15] This phenomenon in called Aggregation Induced Emission Enhancement (AIEE).

AIEE, in opposition to ACQ, is the enhancement of fluorescence by the minimization of vibrational non-radiative decay associated with rotatory substituents.[16] This process was described by Ben Zhong Tang[16] who presented an example of a molecule that is fluorescent in solution (perylene) but at high concentrations or in solid-state is non-emissive. In opposition to perylene, a molecule of hexaphenylsilole (HPS), which is not luminescent in solution, becomes emissive in the solid state due to the restrictions of intramolecular rotation (RIR) (Figure 8).

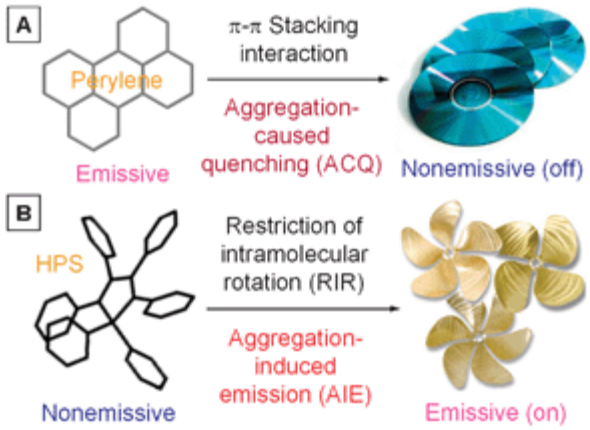

Figure 8-Aggregation Caused Quenching *vs* Aggregation Induced Emission Enhancement.[16]

Several structures have been designed to achieve AIEE, mostly designed with rotational groups that are blocked in the solid state (Figure 9).[17] AIEE is important in several technological applications where quenching due to concentration is a problem, or when the compound must be used in the solid state.[18] Two examples where AIEE is important are biological imaging[19] and Organic Light-Emitting Diodes (OLED).[20] Some applications are presented below (Figure 9).

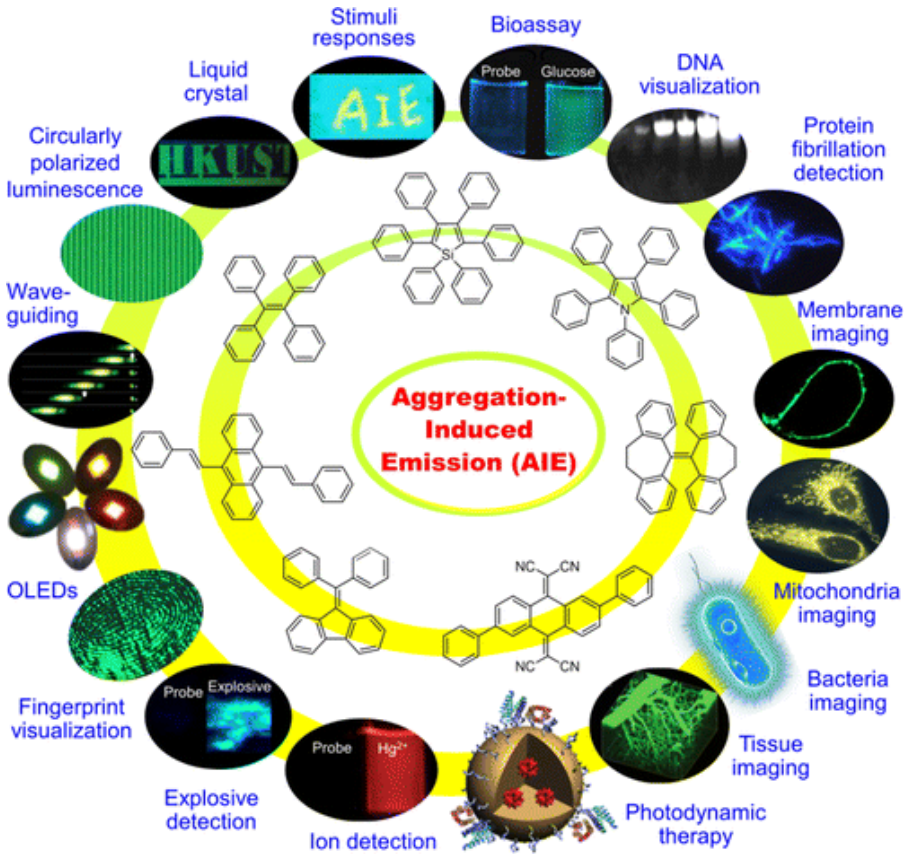

Figure 9-Examples of fluorophores with AIEE and technologic applications.[17]

1.5. Applications

1.5.1. OLED systems

Organic light-emitting devices or diodes can convert electric energy into light. OLED systems (Figure 10) have some drawbacks, one of them is that very compact multilayers of chromophores sometimes lead to quenching events that lower considerably the quantum yield.[21,22] One reason relies on one characteristic very common to fluorophores, the presence of planar π conjugated systems make them susceptible of π-π stacking interactions leading to quenching when in the solid state.

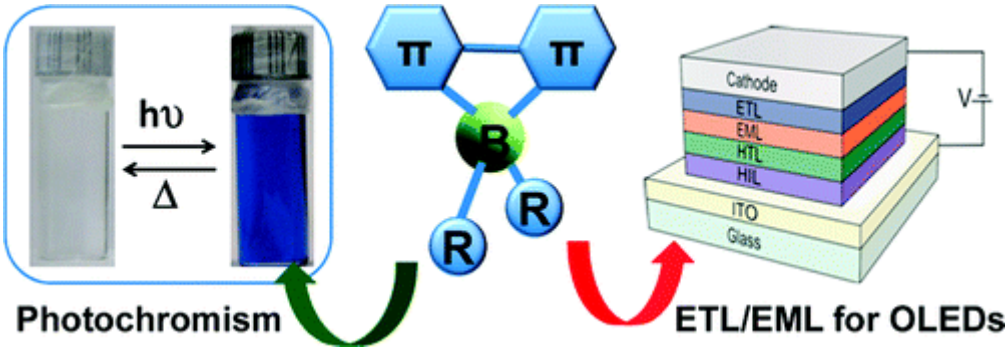

Figure 10-Organo-boron complexes for optoelectronic applications.[22]

1.5.2. Fluorescent Light-up Probe for the Detection of Protein Aggregates

Protein aggregates are related with several pathological conditions, for example neurodegenerative disorders often have protein aggregates present. One well-known example is β-amyloid aggregates,[23] a hallmark of Alzheimer's disease. One strategy to analyse/detect these aggregates is to use fluorophores that can interact with these aggregates[24] and change or enhance their fluorescence in the presence of these aggregates[25,26] (Figure 11). One example is the interaction between thioflavin and β-amyloid aggregates, where a change in the absorption/emission spectra of thioflavin is observed due to structural rigidification.

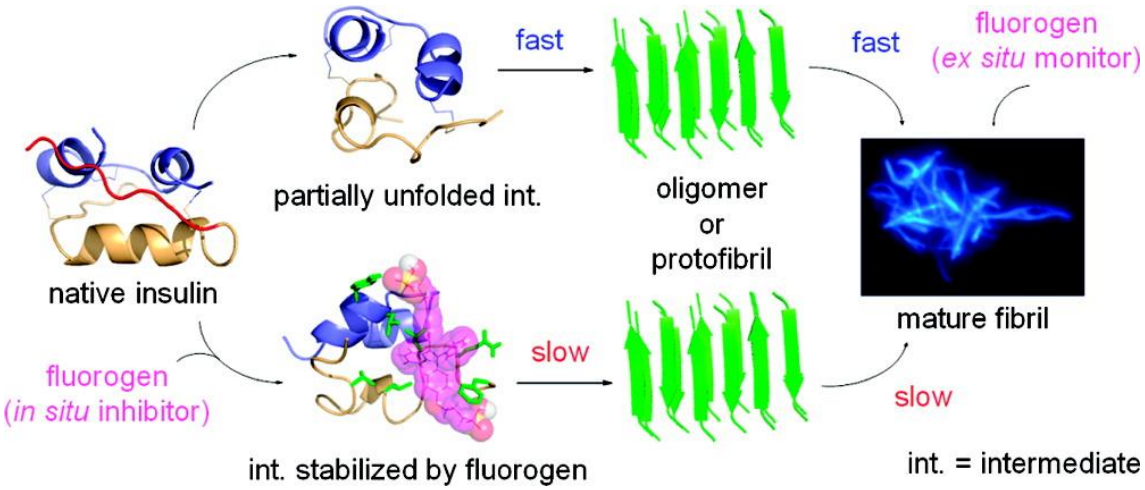

Figure 11-AIEgen example for monitoring misfolding kinetics with protein model insulin aggregates.[25]

2. Boron complexes

2.1. Boron complexes-main scaffolds and synthesis

Boron complexes based on N and O ligands (Figure 12) have been studied for several luminescence applications. Metal complexes offer the possibility to have conjugations between π-conjugated systems and π orbitals of the metals that have positive charges, creating a dipole moment that provides an essential condition for large Stoke shifts while having low HOMO-LUMO gaps.[20]

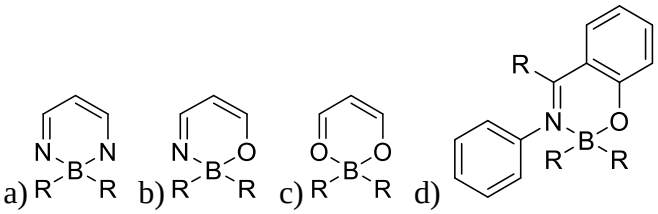

Figure 12-Generic classes of boron chelates. a) N-B-N, b) N-B-O, c) O-B-O d) Boranils.

The complexation of boron can be achieved by reacting the ligand (such as diketones) with a tetrahedral boron coordinated like boron trifluoride–diethyl etherate in the presence of a base like triethylamine (Scheme 1), leading to the formation of a new complex.[27,28] One exception noticed is that sometimes the base is absent.[27]

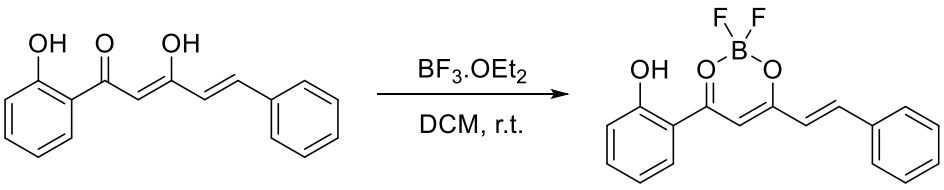

Scheme 1-Complexation of boron with diketonates.[27]

2.2. BODIPY fluorophores

BODIPY compounds have an indacene like structure (Figure 13) where two nitrogen atoms bond to a boron atom creating a rigid dipyrromethene boron difluoride with high fluorescence quantum yields. This series presents high versatility due to the possibility of the substitution of the pyrrole moieties that allow the extension of the conjugation, the variation of electron density or photoinduced charge transfer allowing the adjustment of the desired properties from tuning (changes in emission wavelength) to larger molar absorption coefficients and higher quantum yields. BODIPY compounds are relatively stable compared to other fluorophores and their insensibility to solvent or pH changes make them a good lead scaffold for biologic applications.[29–35]

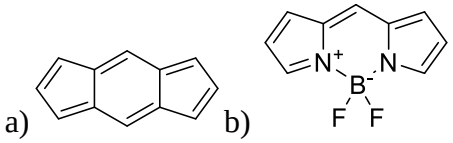

Figure 13-a) Indacene and b) BODIPY.

BODIPY are among the most interesting fluorophores due to the high brightness that they present in comparison to other well-known structures (Figure 14). This is important to achieve high sensitivity. They are also very stable and can emit in the red part of the visible spectrum. This class of fluorophores will be further discussed into more details with some examples from the literature that are relevant to this study, among other fluorophores that are known as benchmarks.[36]

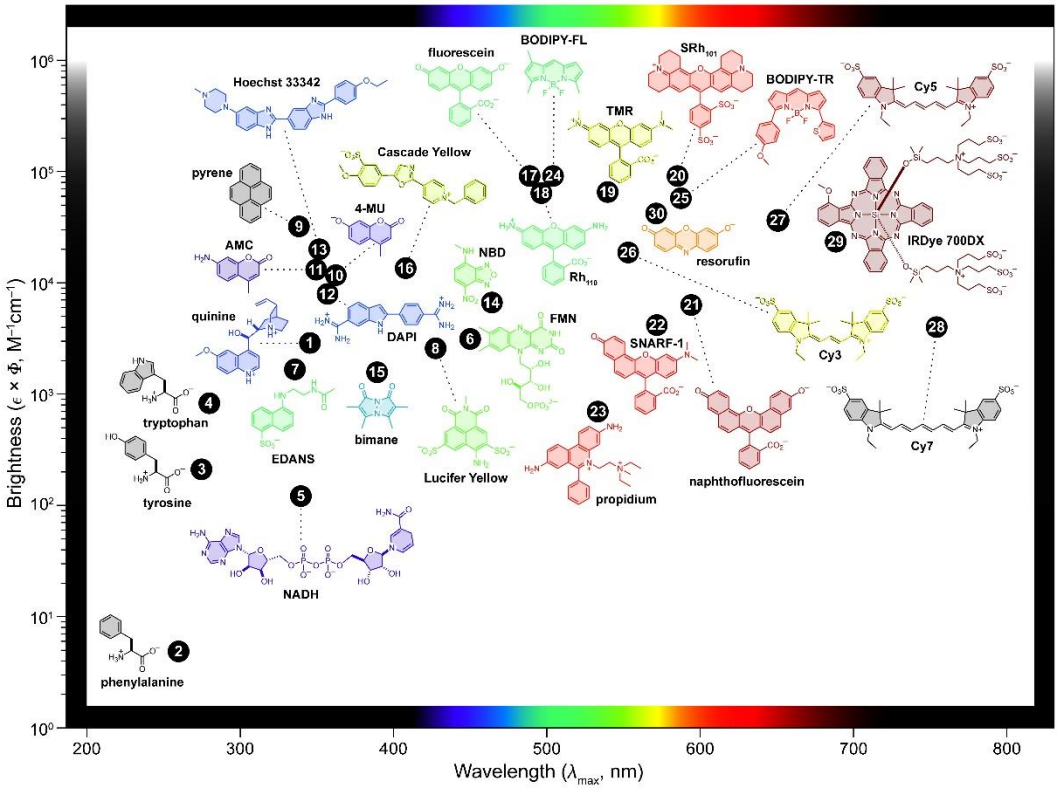

Figure 14-Examples of fluorophore brightness ($\epsilon \times \Phi$) vs the wavelength of maximum absorption (λ_{max}) for the major classes of fluorophores.[36]

One of the first BODIPYs used as probe for biological applications was studied by Richard P. Haugland's group,[30] who presented one, at the time new, scaffold that had higher brightness than the fluorescence benchmarks for studying membrane traffic in cells (Figure 15).

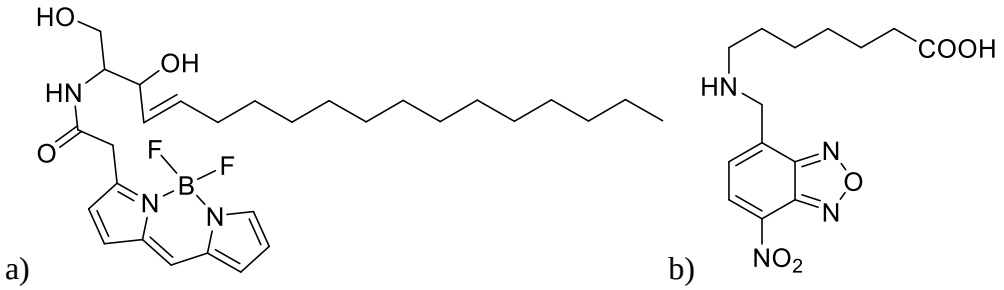

Figure 15-a) Fluorescent fatty acid containing the fluorophore boron dipyrromethene, b) NBD-X (6-(N-(7-Nitrobenz-2-oxa-1,3-diazol-4-yl) amino)hexanoic acid).[30]

This example shows that higher efficiency can be obtained with an enhancement of the fluorescence emission. This study among other pioneer studies led to a higher interest in

BODIPY scaffolds for applications such as OLED or organic photovoltaic devices (OPD).

One interesting work was published in 2014, in which André Bessette and Garry S. Hanan[37] examined the advantages of BODIPY such as their high molar extinction coefficients, their absorption/emission near to infrared (lower energy of excitation) and the tuning of their emission wavelength by simple derivatization. This work highlights the potential that BODIPY derivatives still offer today for several applications.

2.3. Other boron complexes

2.3.1 Boranils

Boranils is the domination for a broader class that besides diaza-s–indacene cores typic of BODIPY includes other coordination possibilities. Boranils include aromatic-nitrogen-boron-oxygen-aromatic complexes. An aniline where the nitrogen is linked to a phenyl or a substituted phenyl can be called an anil. These structures after complexation with boron form a boron-anils (boranils for short). This class increases the possibilities for achieving boron complexes with a large amount of derivative possibilities, starting with the moieties that provide nitrogen and oxygen that coordinate with boron.[11–14,29,38–40]

One group that also studies boranils is Raymond Ziessel's.[11,12,29,33,40] They have been studying the optical and photoelectric charge transfer properties of these compounds and they achieved high quantum yields (up to 90%) with these systems, pointing them as potential antennae for photoactive modules (Scheme 2).

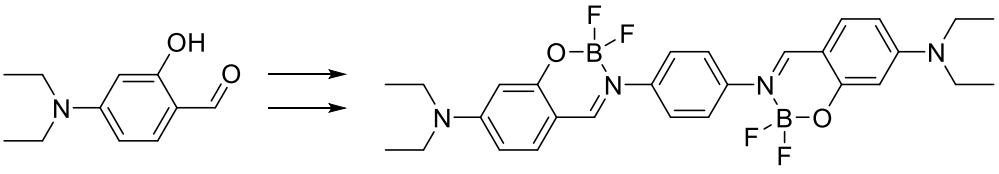

Scheme 2-Synthesis of bis-boranils.[29]

Very recent studies have shown that not only these compounds present fluorescence in solution, but also in the solid state, and AIEE can be observed.[12,15] This characteristic can be relatively important in biological probes where aggregates of the compounds can lead to quenching phenomenon that decreases the quantum yield and therefore the brightness.[11]

New boranils based on chiral benzylamines and their photophysical properties were studied by Samuel Guieu's group.[41] These complexes exhibit fluorescence in solution and in the solid state, and exhibit AIEE.[41]

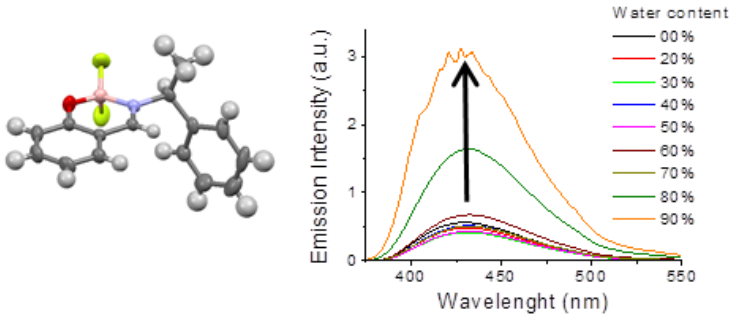

Figure 16-New fluorescent boranils based on chiral benzylamines.[41]

Until now the most common scaffolds for boranils design were based on aniline-boron-phenol cores. The replacement of aniline by pyridine represents a strategy that has been done before[42], but the synthesis is complex and was not explored further.

2.3.2 Boranils based on pyridine ligands

Pyridine-based systems are analogous to BODIPY classic structures whereas instead of complexing the boron with a nitrogen from a pyrrole group, they belong to pyridine moieties (Figure 17). One example is a study where pyridine based BODIPY were used as chemosensors of hydrazine.[43] The results also show that these compounds present fluorescence even in the solid state.

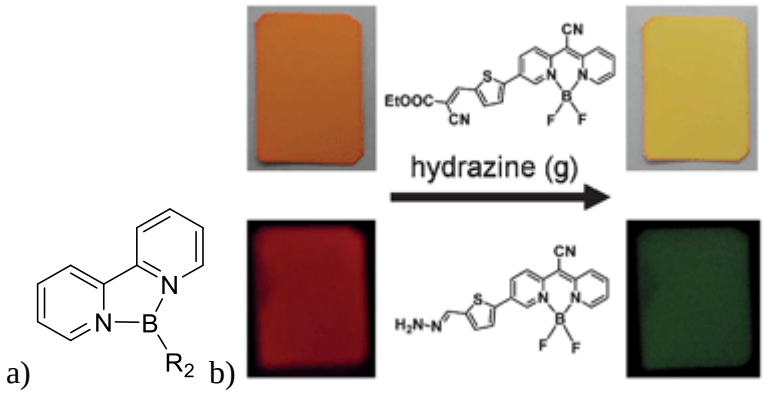

Figure 17-a) Pyridine-boron core, b) Pyridine based BODIPY as chemosensors.[43]

2.4. Pyridine synthesis

For the synthesis of multi-substituted pyridines, several *via* of synthesis were studied, and some are presented here, with some emphasis on Kröhnke's *via*. These strategies

always rely on the reaction between one aldehyde, two ketones, and ammonia, with some adaptations (Scheme 3).

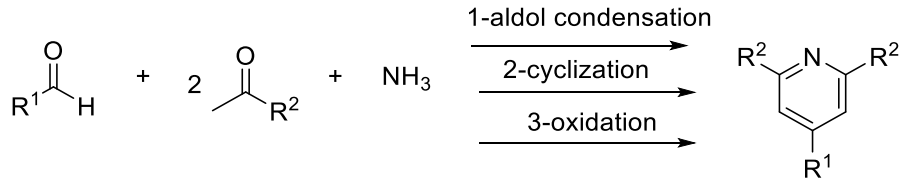

Scheme 3-Synthesis of pyridine.

The classic *via* for the synthesis of pyridine, until mid-twentieth century, was Hantzsch's pyridine synthesis[44] that consisted in a multi-component one-pot synthesis with one first step where an aldehyde, two equivalents of β-keto-ester and a nitrogen donor like ammonium acetate are reacted (Scheme 4).

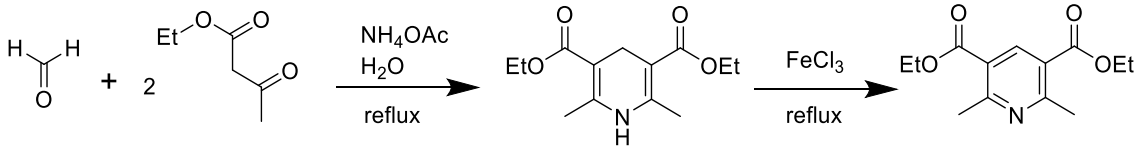

Scheme 4-Hantzsch pyridine synthesis.

Chichibabin method was reported in 1924, and consists in a condensation reaction of aldehydes, ketones and α, β-unsaturated carbonyl compounds with compounds containing ammonia.[45] To exemplify with simple molecules, the method involved a first step, the formation of acrolein from acetaldehyde and formaldehyde. In a second step, acetaldehyde and acrolein are reacted with ammonia to form the pyridine (Scheme 5).

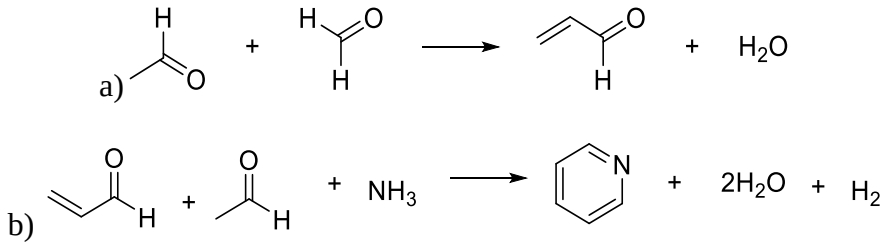

Scheme 5-a) Formation of acrolein and b) formation of pyridine.

Fritz Kröhnke later described a new strategy to achieve di, tri and tetra substituted pyridines, being a more versatile *via* of synthesis than the previously proposed methods (Scheme 6). Contrary to Hantzsch's *via*, the final oxidation step was not necessary and made one-pot-synthesis possible. This allowed the synthesis of a library of compounds

in a simpler manner. The mechanism involves the α-pyridinium methyl ketone salts and α, β-unsaturated carbonyl compounds with ammonium acetate under acidic conditions.[46,47]

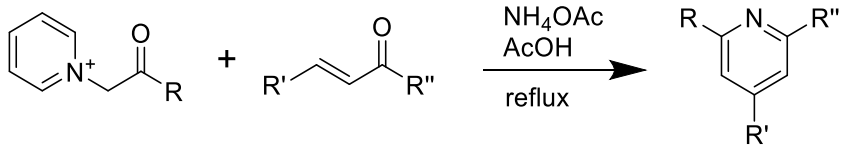

Scheme 6-Kröhnke's pyridine synthesis.

Kim D. Janda's group has been recently applying this method to synthetize large libraries with more than 200 compounds that were tested on antiviral assays.[47,48] The mechanism involves the Michael addition of the pyridinium on an α, β-unsaturated ketone, after some intermediates (Scheme 7) the pyridinium cation is eliminated and with a subsequent dehydration a final tri-substituted pyridine is obtained.

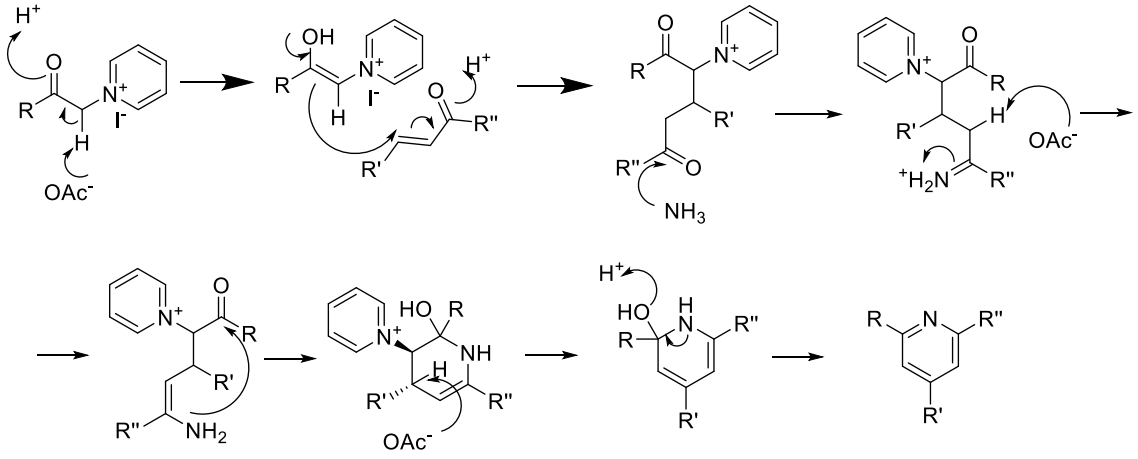

Scheme 7-Mechanism for the synthesis of pyridine *via* Kröhnke.

For the Kröhnke's synthesis a α-pyridinium methyl ketone salt must be prepared previously, the classical approach is to follow L. Carrol King's *via* where one equivalent of acetophenone reacts with one equivalent of iodine and two equivalents (excess) of pyridine to give 1-(2-oxo-2-phenylethyl)pyridin-1-ium iodide (Scheme 8).[49,50]

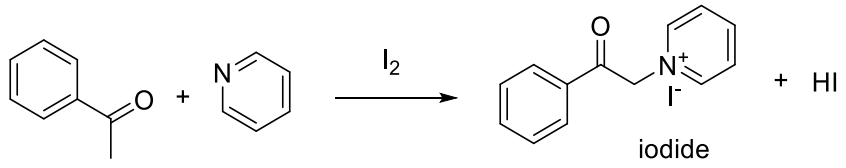

Scheme 8-Synthesis of pyridinium salts *via* Kröhnke.

Modifications of the Kröhnke's pyridine synthesis have been proposed, one approach involves a one-pot synthesis with a chalcone, ammonium acetate and acetic acid (Scheme 9). This approach seems to be viable, simple and quick but has the limitation of having the same substitution pattern on the two aromatic groups at the *ortho* position.[51]

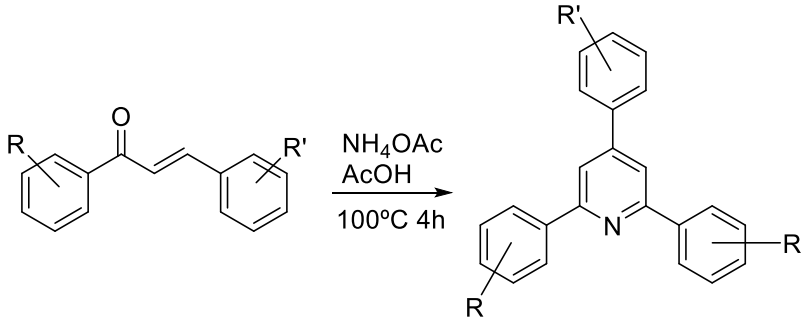

Scheme 9-Alternative via for the synthesis of pyridinium salts.[51]

Other similar studies to find simple ways of synthesis of multi-substituted pyridines have been done, mostly because there has been a crescendo interest in these structures for several applications from biologic probes[52] to OLED systems.[20] There are still possibilities not yet explored and this makes multi-substituted pyridine scaffolds appealing for further studies, and the same can be said for boron-complexes.

Aims

From the available information, a triphenylpyridine with the particularity of having a phenol in *ortho* position to allow the complexation with boron was chosen as the main scaffold (Scheme 10). The Kröhnke's pyridine synthesis *via* was considered the most relevant for this study due to its versatility. Full characterization of the compounds, including crystallographic studies, were intended to be conducted during this study. The fluorescence properties of the compounds would also be addressed, and according to the results, other studies regarding applications can and will be considered.

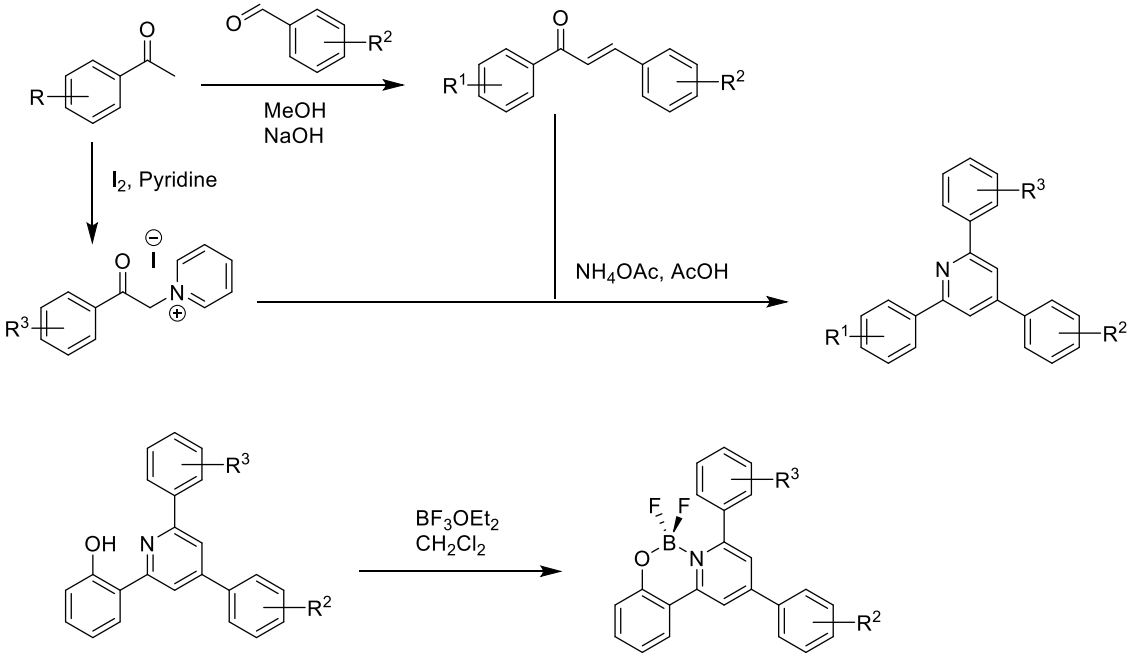

Scheme 10-Synthesis of new boranils with a pyridine scaffold.

Chapter II. Results and discussion

In this section, the synthesis of the fluorophores will first be presented. A first synthetic route was assessed[47,53], but has to be altered after the first attempts proved to be unsuccessful. The synthesis of the fluorophores, following the strategy depicted in Scheme 11, is then presented, together with the characterization of all new compounds. The study of the photophysical properties of two sets of fluorophores, bearing a methoxy or a hydroxyl group, was carried out in solution and upon aggregation. Comparing the properties of both series, some conclusions could be drawn relatively to the influence of the intramolecular hydrogen bond on the optoelectronic properties of the dyes.

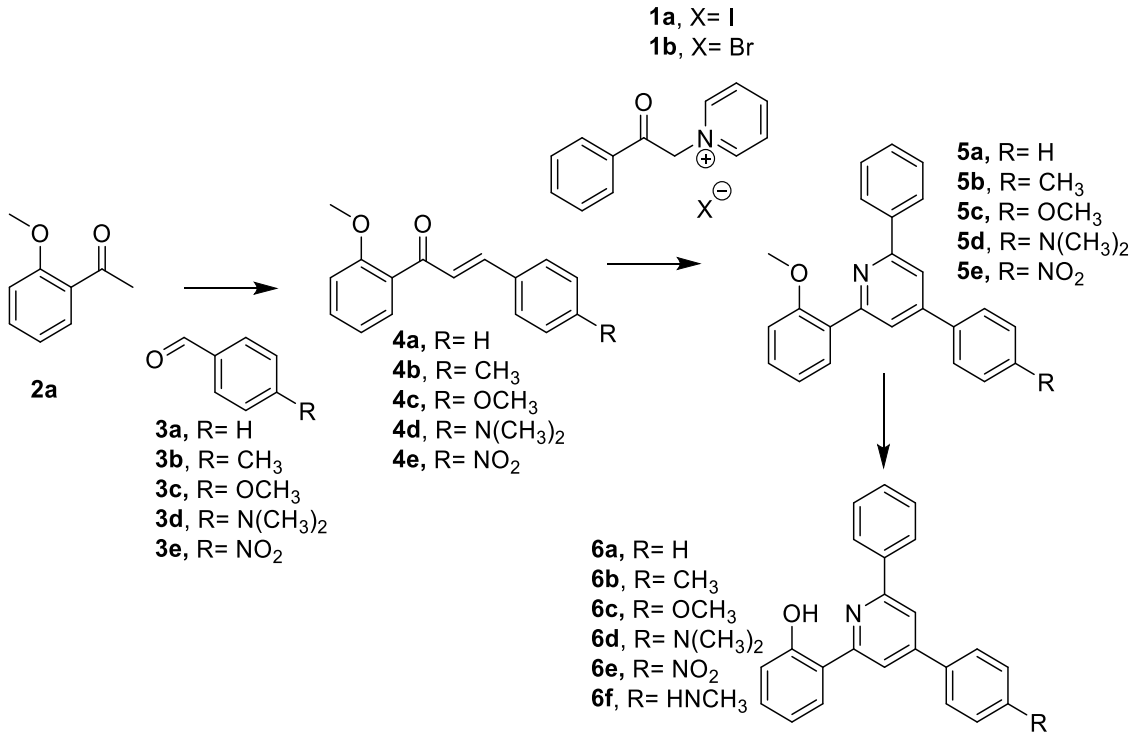

Scheme 11-Synthesis of 2-(2-methoxyphenyl) pyridine and 2-(pyridin-2-yl)phenol derivatives.

1. Synthesis

1.1. First attempt

1.1.1. Synthesis of 2-(*p*-tolyl)-4*H*-chromen-4-one

A straightforward synthesis was first attempted, trying to condense the unprotected chalcone [1-(2-hydroxyphenyl)-3-(*p*-tolyl)prop-2-en-1-one] with the pyridinium salt **1a**, under the conditions of the Kröhnke synthesis (Scheme 12).

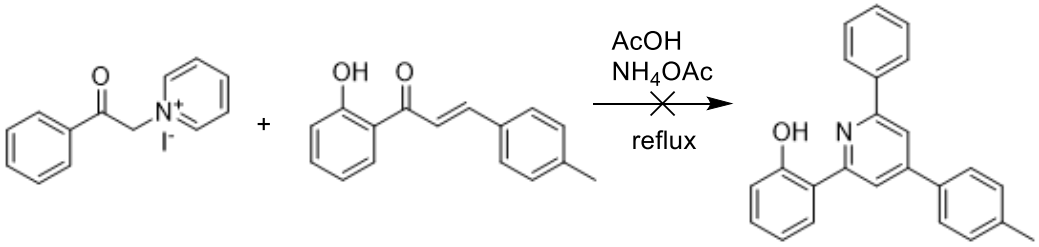

Scheme 12-Attempted synthesis of [2-(6-phenyl-4-(*p*-tolyl)pyridin-2-yl)phenol].

Instead of the intended triphenylpyridine, a cyclization of the chalcone into a chromone was obtained (Figure 18). The structure of the obtained chromone was confirmed by ^{1}H-NMR. The ^{1}H-NMR spectrum showed that the expected product was not obtained, being the most important peaks a singlet at δ = 6.81 ppm corresponding to the only single proton of chromone core. The absence of peaks corresponding to the 5 protons of the aryl group in position 6 of the expected pyridine, and of the characteristic peaks of position 3 and 5 of the pyridine core also confirmed that the product was not obtained.

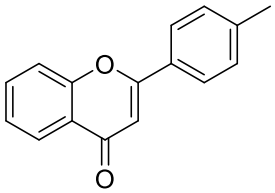

Figure 18-2-(*p*-tolyl)-4*H*-chromen-4-one.

This result meant that a protection of the hydroxyl group was needed in order to obtain the desired product under acidic conditions. For that, two additional steps were necessary: protection of the hydroxyl group of 2-hydroxy-acetophenone prior to aldol condensation or protection of the hydroxyl group of the resulting chalcone followed by a deprotection of the same group after the pyridine was obtained. The decision was in a

first approach to protect 2-hydroxy-acetophenone to allow its use in all the aldol condensations.

1.2. Synthesis of the pyridines using protected chalcones

1.2.1. Synthesis of chalcones 4a-4e

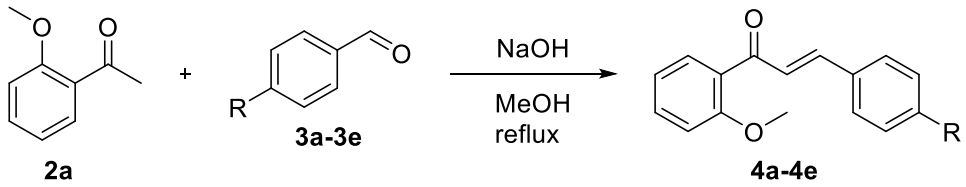

Scheme 13-Synthesis of the protected chalcones.

The chalcones **4a** to **4e** were obtained following a Claisen–Schmidt condensation[54] of 1-(2-methoxyphenyl)ethan-1-one **2a** with the corresponding benzaldehyde **3a-3e**. The products could be isolated in moderate to good yields (Yields: 45-80%) after simple purification by column chromatography.

The structure and purity of the products were confirmed by ^{1}H-NMR, with the most relevant peaks being:

- the two doublets corresponding to the protons of the double bond at δ = 7-7,9 ppm, with coupling constants about $J_{\alpha-\beta}$ 15-16 Hz that confirmed the *E* configuration.
- a singlet corresponding to the methoxy group at δ = 3,90 ppm.
- peaks of substitution groups such as the methyl group at δ = 2,40 ppm (chalcone **4b**), the singlet of the methoxy group at δ = 3,85 ppm (chalcone **4c**), the singlet of dimethylamine protons at δ = 3,00 ppm (chalcone **4d**).

1.3 Synthesis of triphenylpyridine derivatives 5a-5e

The triphenyl pyridines **5a-5e** were obtained by a modified Kröhnke *via* (Scheme 14), and could be isolated in low to moderate yields (20-50%).

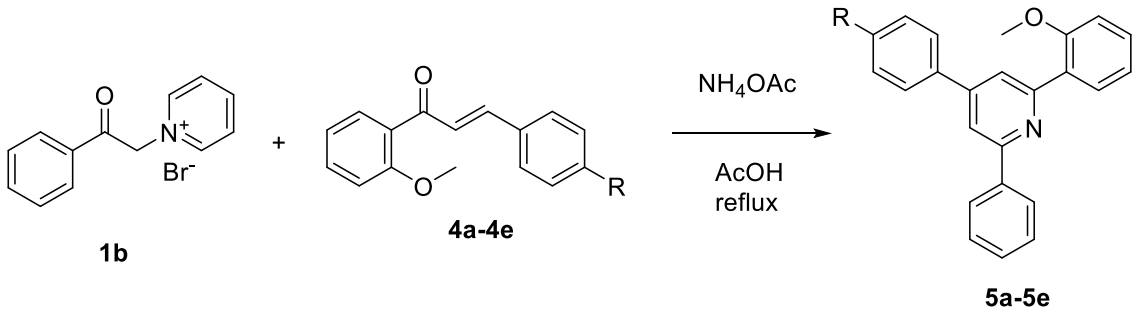

Scheme 14-Synthesis of triphenyl pyridines **5a-5e.**

The conditions were optimized in order to assure the best yields for the obtained products, the variations include:

- Variation of the pyridine salt (**1a** or **1b**) without significant difference between yields.
- Quantity of ammonium acetate from 10 equivalents up to 30 equivalents in one addition and 30 equivalents in multiple additions of 5 equivalents, being multiple additions of 5 equivalents up to 30 equivalents the conditions that presented the best results.
- The temperature of the reaction was lowered from reflux to inferior to 100ºC, but the yields decreased and, in some cases, there was no reaction at all.

All compounds were fully characterized using ^{1}H-NMR, ^{13}C-NMR, HSQC and HMBC, COSY, NOESY spectra, as well as ESI-MS. An analysis of compound **5c** is presented as an example.

Considering the ^{1}H-NMR spectrum of **5c** (Figure 19), the most important information is the presence of the corresponding peaks for all the protons with the multiplicity, coupling constants and chemical shift according to what is expected.

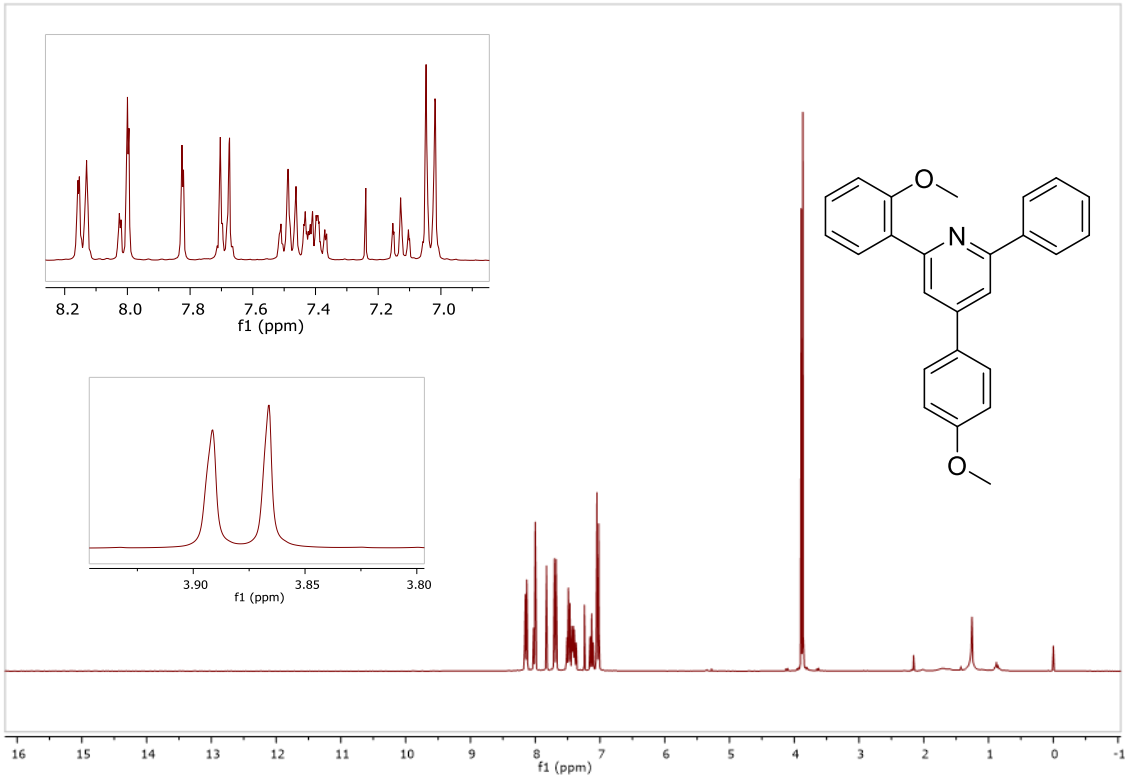

Figure 19-^{1}H-NMR spectrum of compound **5c**.

The most important peaks:

- Two singlets each with integration of 3 at 3.87 and 3.91 ppm corresponding to the methoxy groups. NOESY spectra allowed to establish a correlation between the singlet at δ = 3.91 ppm and the doublet at δ = 7.05 ppm, which correspond to the proton at position 11. This NOESY correlation happens for H28 with H16 + H18, but due to the overlap of the peaks of H16 + H18 and H11, it is not possible to distinguish, however NOESY from **5d** does not have an overlap of these peaks and it is possible to assign a correlation of protons from dimethylamine with H16 + H18 and H11 with H26 (Figure 20).

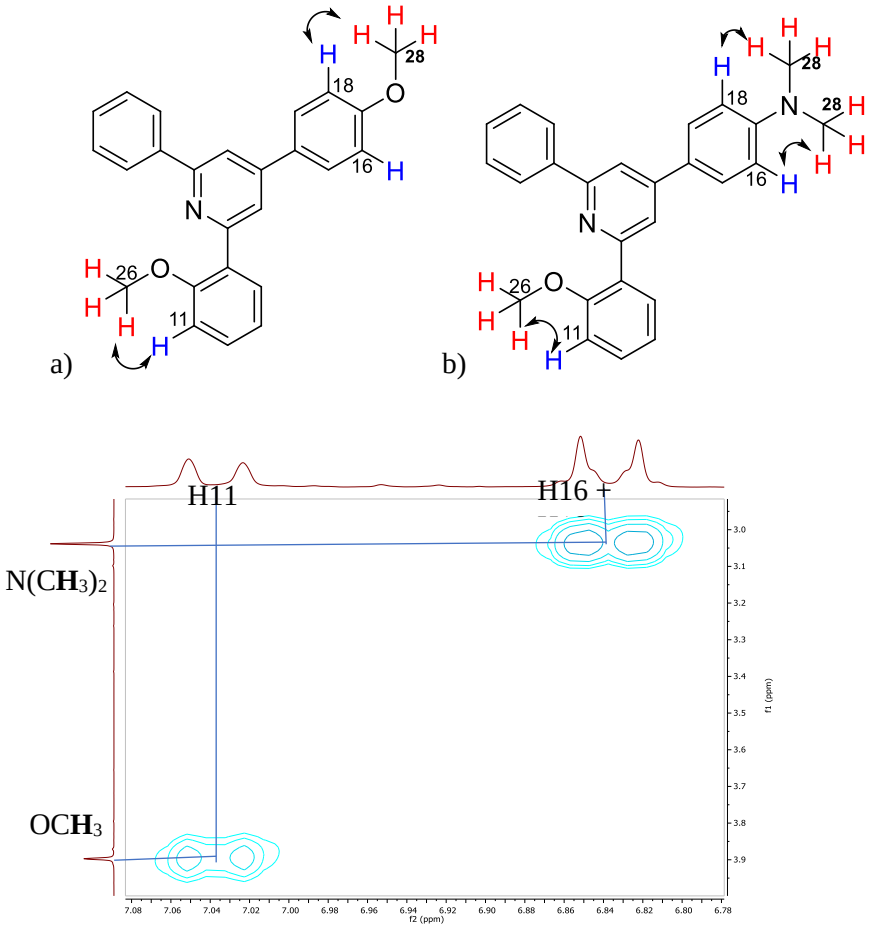

Figure 20-NOESY correlations of H26, H28 (R group) a) compound **5c**; b) compound **5d** and its NOESY spectrum.

- Two doublets, each integrating for two protons, corresponding to the aryl group in para-position to pyridine, one from H16 and H18 at δ = 7.05 ppm (overlapping with H11) being shielded by the methoxy group at *ortho*-position, and the doublet of H15 and H19 at δ = 7.71 ppm less shielded by the methoxy group. Both doublets have a coupling constant of J = 8.8 Hz which supports the assignment made using the COSY correlation (Figure 21).

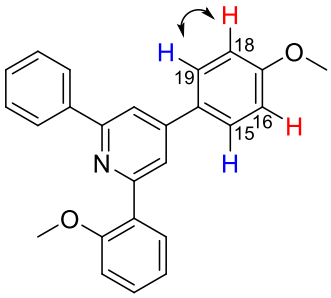

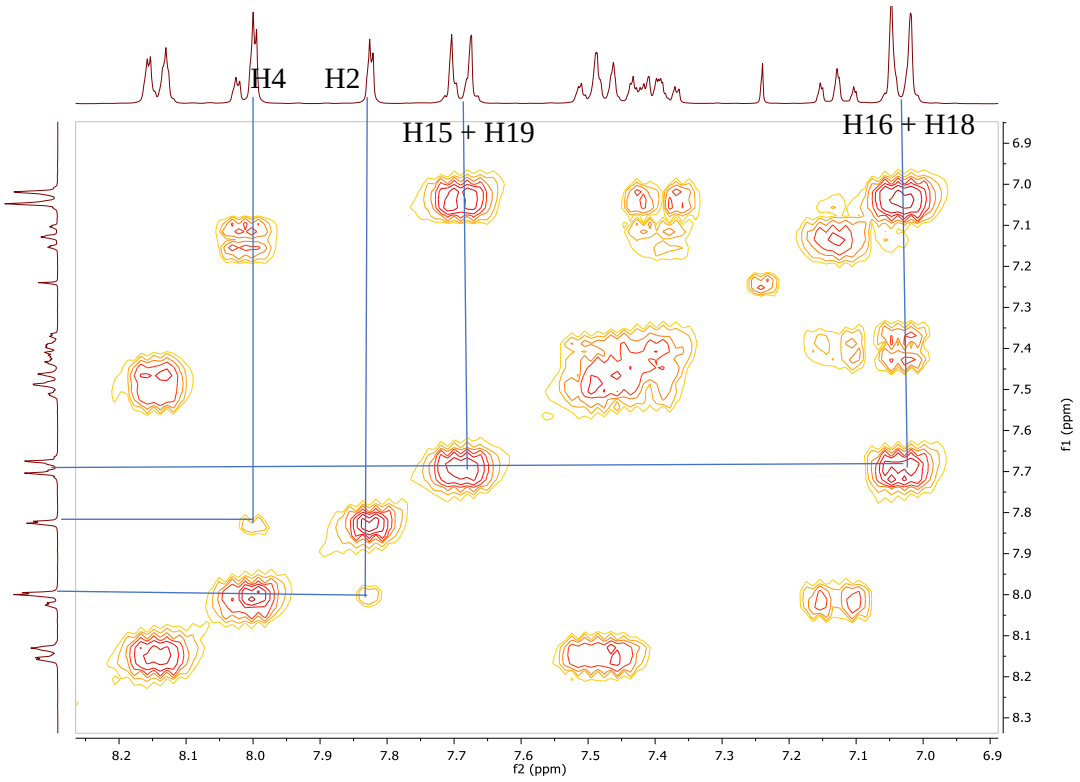

Figure 21-COSY correlations of H15 + H19 with H16 + H18 and H2 with H4 for compound **5c.**

- Two doublets, each integrating for one proton, at δ = 7.80 ppm and δ = 8.00 ppm with coupling of *J* = 1.5 Hz, corresponding to the protons in positions 2 and 4, characteristic of protons at *meta*-positions in substituted pyridines.
- The NOESY correlation between the doublet at δ = 8.14 ppm, attributed to H20 + H24, and the doublet at δ = 7.80 ppm, allowed its attribution to H4 (Figure 22).

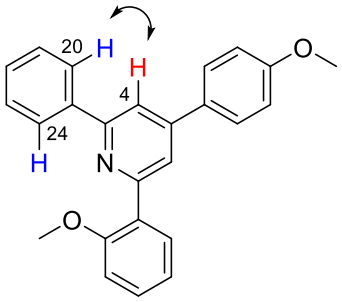

Figure 22-NOESY relation of H20 + H24 to H4 for compound **5c.**

- The doublet of doublets (ddd) from H12 at δ = 7.37-7.56 ppm could be assigned by COSY. There is a correlation with H11 at δ = 7.05 ppm and the doublet of

doublets (ddd) H13 at δ = 7.15 ppm. The proton H14 can be assigned to a doublet at δ = 8.03 ppm (Figure 23).

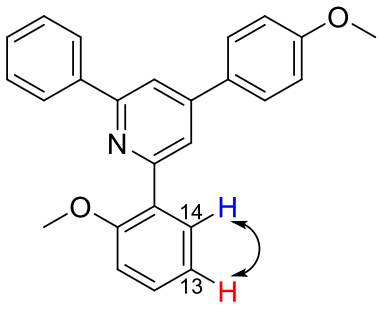

Figure 23-COSY relation of H14 to H13 for compound **5c.**

- The triplet of doublets from H21+H23 and triplet triplet from H22 can be found at δ = 7.35-7.52 ppm. COSY relations between them could be observed. The peak from H21+H23 also has correlation with doublet of H20 + H24 (Figure 24).

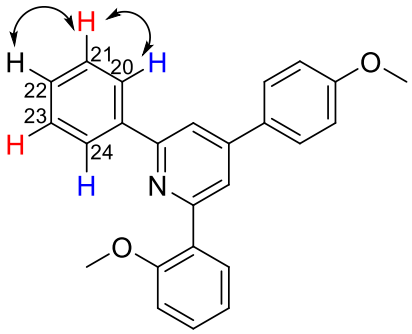

Figure 24-COSY relations of H21+H23 for compound **5c.**

All the protons were assigned to each peak presented in the ^{1}H-NMR spectrum, using COSY and NOESY spectra to eliminate doubts (Figure 25).

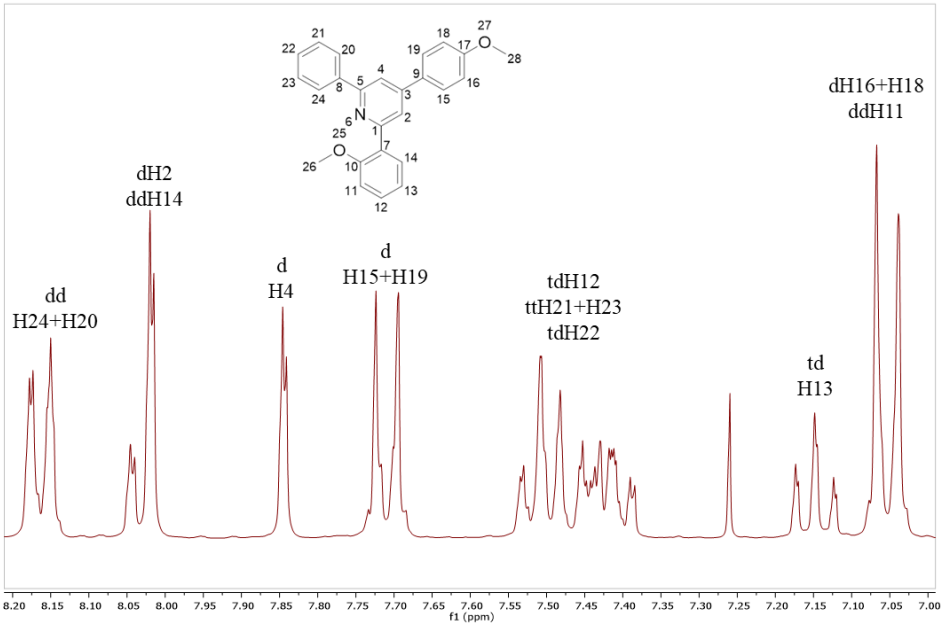

Figure 25-^{1}H-NMR assignments for compound **5c**.

Following the same strategies, it was possible to assign all the protons of each compound **5a**-**5e**. The most important variations were noticed in the aryl group in the *para*-position to the pyridine where the substitution group led to the major differences as can be seen in the following

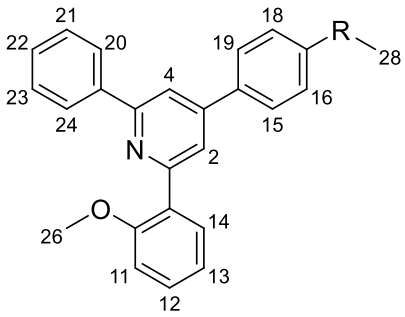

Table 1.

The signals of protons H15 + H19 and H16 + H18 were the most affected by the substitution. With the introduction of electron donor groups [CH_3, OCH_3, $N(CH_3)_2$] there was a deviation upfield of the doublet in *ortho* position H16 + H18 due to shielding. In compound **5e** the opposite effect was observed, a downfield deviation due to the presence of electron withdrawing group (NO_2).

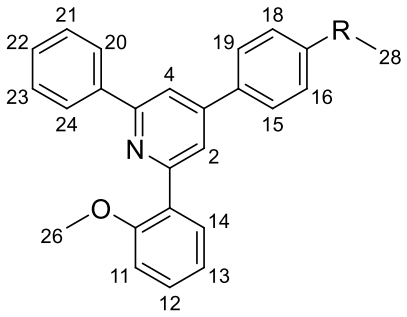

Table 1-^{1}H-NMR assignment for compounds **5a-5e.**

^{1}H-NMR Signal	**5a** R = H	**5b** R = CH_3	**5c** R = OCH_3	**5d** R = $N(CH_3)_2$	**5e** R = NO_2
2	δ 8.05; J = 1.5	δ 8.02; J = 1.5	δ 8.02; J = 1.5	δ 8.00; J = 1.6	δ 8.07; J = 1.5
4	δ 7.87; J = 1.5	δ 7.86; J = 1.5	δ 7.84; J = 1.5	δ 7.84; J = 1.6	δ 7.85; J = 1.5
11	δ 7.05	δ 7.05	δ 7.05	δ 7.04	δ 7.06
12	δ [7.37-7.56]	δ [7.37-7.54]	δ [7.38-7.54]	δ [7.34-7.52]	δ [7.39-7.55]
13	δ 7.14	δ 7.14	δ 7.15	δ 7.13	δ 7.15
14	δ 8.02	δ 8.01	δ 8.03	δ 8.00	δ 8.04
15+19	δ 7.74	δ 7.65; J = 8	δ 7.70; J = 8.9	δ 7.68; J = 8.9	δ 7.88; J = 8.8
16+18	δ [7.37-7.56]	δ 7.33; J = 8	δ 7.05; J = 8.9	δ = 6.84; J = 8.9	δ 8.38; J = 8.8
20+24	δ 8.16	δ 8.15	δ 8.16	δ 8.14	δ 8.16
21+23	δ [7.37-7.56]	δ [7.37-7.54]	δ [7.38-7.54]	δ [7.34-7.52]	δ [7.39-7.55]
22	δ [7.37-7.56]	δ [7.37-7.54]	δ [7.38-7.54]	δ [7.34-7.52]	δ [7.39-7.55]
26	δ 3.91	δ 3.91	δ 3.91	δ 3.90	δ 3.92
R	δ [7.37-7.56]	δ 2.44	δ 3.89	δ 3.04	----------

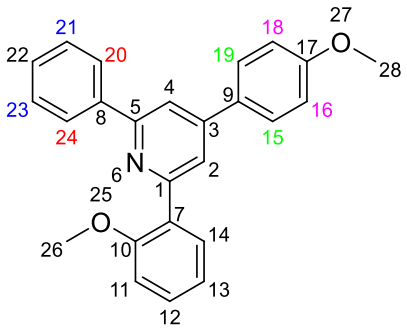

Figure 26-Compound **5c** carbon numeration with colours representing carbons with similar chemical environments.

Considering the compound **5c** again as an example, ^{13}C-NMR, HSQC and HMBC allow to increase the certainty of the characterization. The first important analysis is:

- For compound **5c** in a total of 25 atoms of carbon there are 21 peaks that appear in the ^{13}C-NMR spectrum due to the equivalence of some carbons that have the same chemical environment: C16 + C18, C15 + C19, C20 + C24 and C21 + C23 (Figure 26).
- The methyl groups, and the aromatic carbons bearing a proton can be identified using the proton-carbon correlation HSQC (Figure 27): C28 δ = 55.43; C26 δ = 55.79; C16 + C18 δ = 114.32; C15 + C19 δ = 128.40; C4 δ = 116.35; C2 δ = 121.36; C14 δ = 131.58; C13 δ = 121.12; C12 δ = 128.69; C11 δ = 129.50; C20 + C24 δ = 127.12; C21 + C23 δ = 128.60; C22 δ = 128.96.

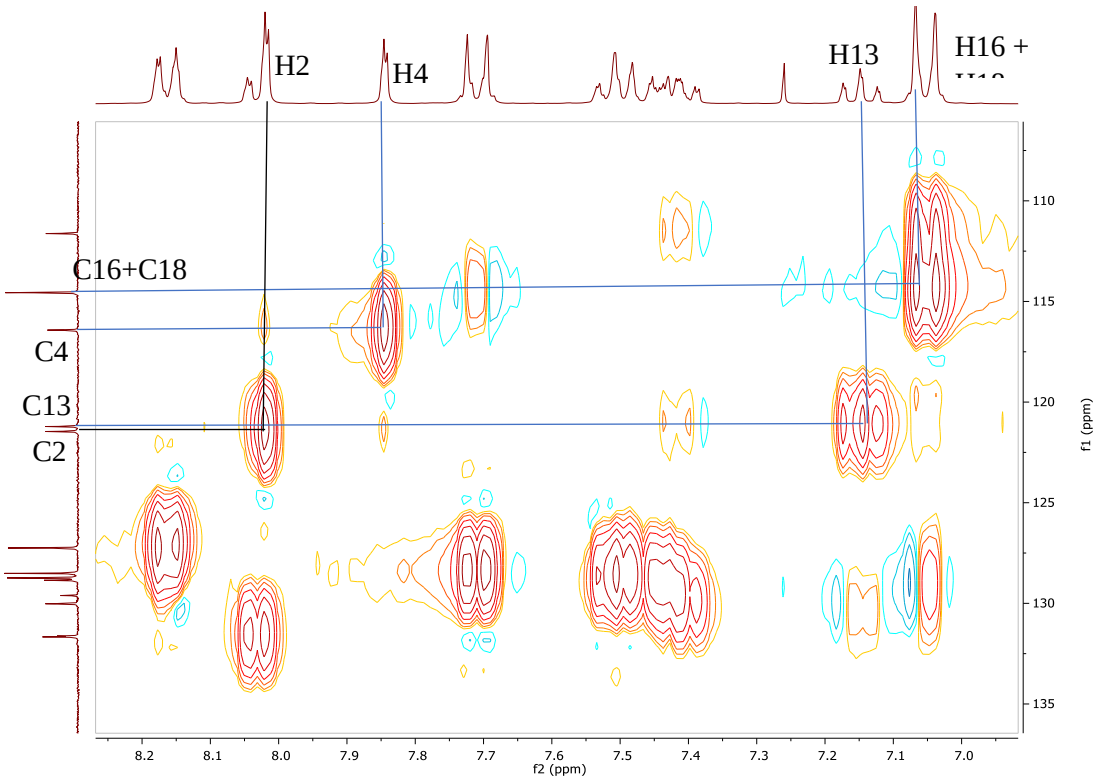

Figure 27-Example of some of the carbon assignments by HSQC in compound **5c**.

- For the carbons that do not have protons (C1, C3, C5, C7, C8, C9, C10 and C17) some carbons could be assigned using HMBC correlations:
  - C17 has a J_3 correlation with H28 and H15 + H19 and J_2 with H16 + H18, therefore C17 δ = 160.29 and C10 δ = 157.26 correlates at J_3 with H26, H12 and H14 and J_2 with H11 (Figure 28).

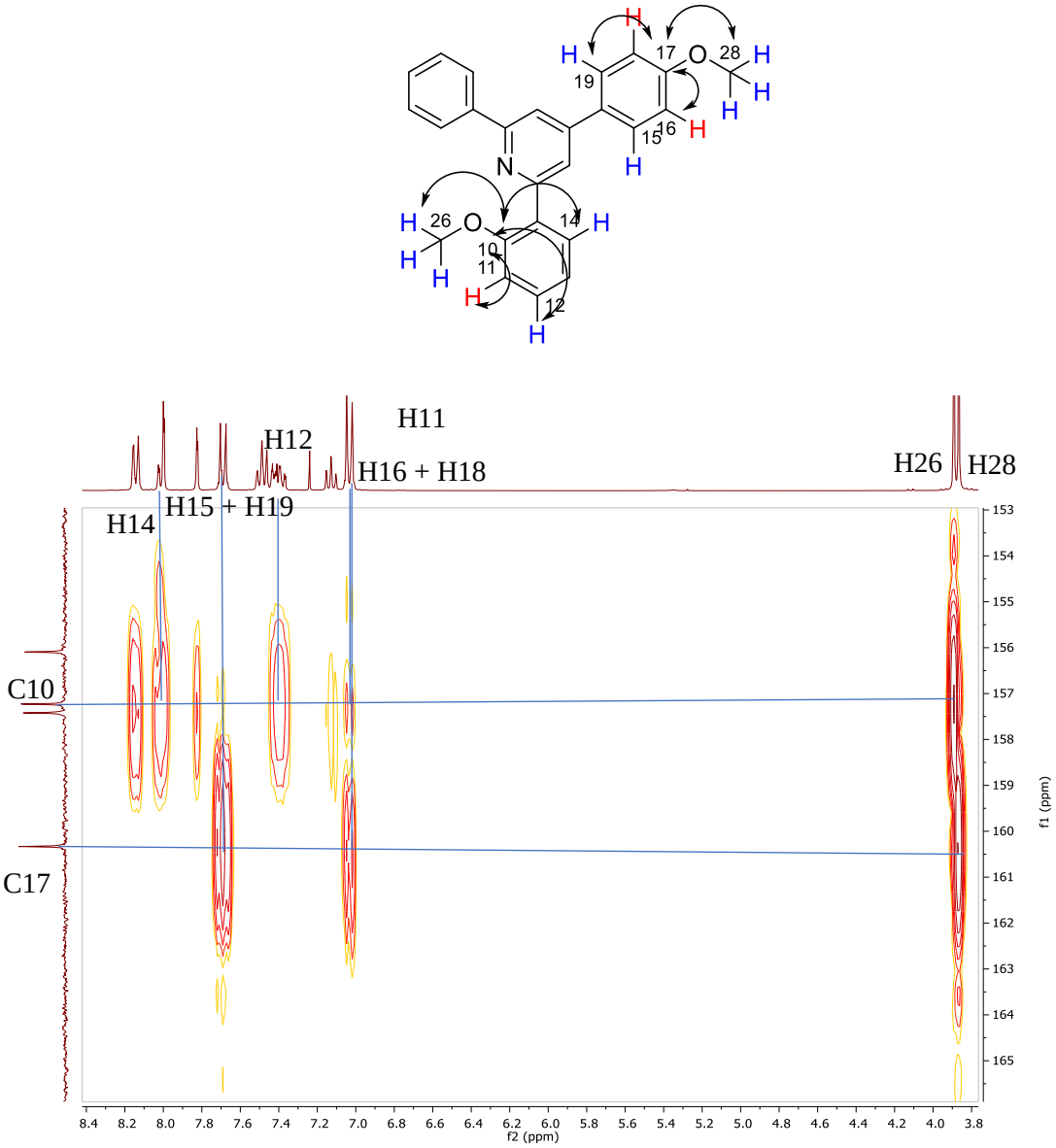

Figure 28-HMBC correlation of carbon C10 and C17 for compound **5c**.

- C7 is assigned to δ = 156.13 by the J_2 correlations with proton H14 and J_3 with H13, H11 and H2 (pyridine) (Figure 29).

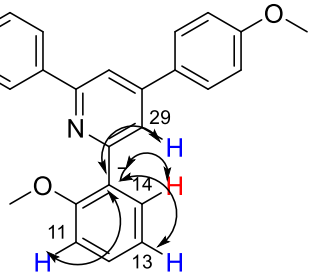

Figure 29-HMBC correlations of C7 for compound **5c**.

- C3 peak is at δ = 148.5 and only has a J_3 correlation with H15 + H19 ; with that the last non-protonated carbon that relates with H15 + H19 and H2 and H4 is at δ = 131.5 and there is only one possibility left that is C9 (Figure 30).

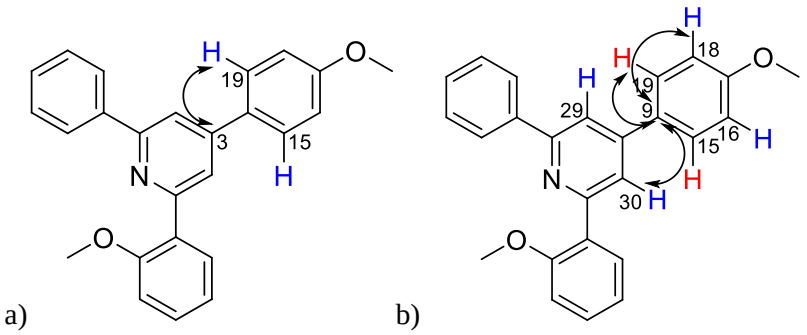

Figure 30-HMBC correlations of C9 and C3 for compound **5c**.

- For peaks of carbons at position C1 δ = 157.4 and C5 δ = 157.20 two assessments can be made, first there is a J_2 correlation of C1 to H2 and a J_3 with H14 while for C5 there is a J_2 correlation with H4 and J_3 with H20 + H24 (Figure 31).

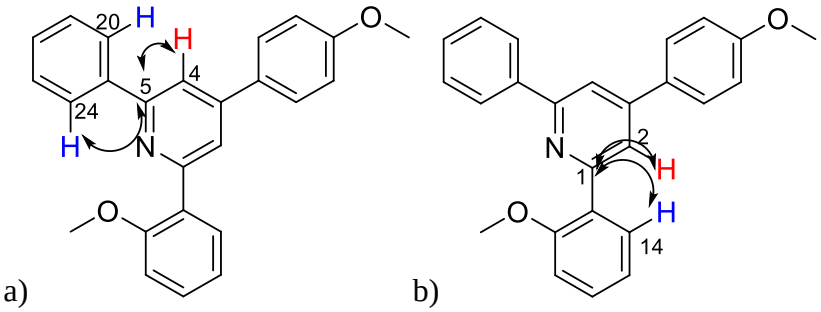

Figure 31-HMBC correlations of C1 and C5 for compound **5c**

- For C8 there is a peak at δ = 128.70 that has a J_2 correlation with H20 + H24 and J_3 with H4 and H21+H23 (Figure 32).

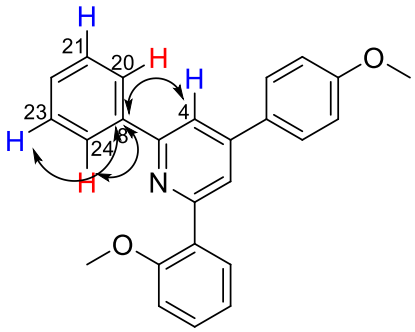

Figure 32-HMBC correlations of C8 for compound **5c**.

The results indicate that all the proton and carbons appear to have the expected correlations and therefore all the peaks were assigned. For compounds **5a**, **5b**, **5d** and **5e** the same approach can be made having similar interactions except for **5a** that has no substitution in the aryl group in *para*-position.

The results obtained by Electrospray Ionisation Mass Spectrometry (ESI-MS) were consistent with the theoretical expected masses. The lack of fragmentation as well as the presence of a dominant peak corresponding to the mass of the molecule plus one proton (M+H) demonstrated the relative stability of the chromophores upon positive charge ionization (cationization). The stability upon cationization might be due to the pyridine group that can be easily protonated without significant loss of structural integrity (Scheme 15). For each compound **5a-5e** ESI-MS results were consistent with the theoretical exact mass (Table 2).

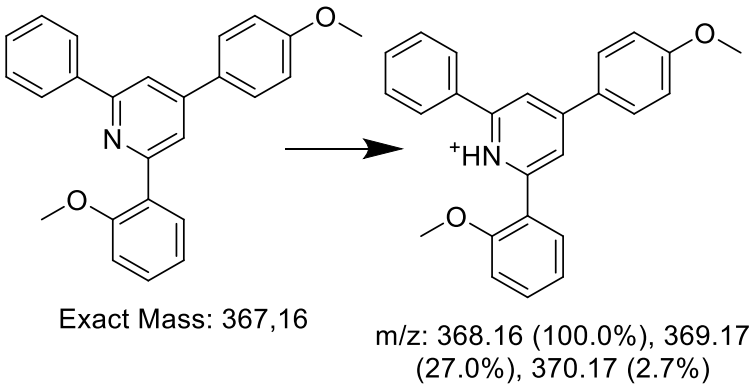

Scheme 15-Representation of cationic form of compound **5c**.

Table 2-Electrospray Ionisation Mass Spectrometry results of compounds **5a**-**5e**

Compound	Exact mass	m/z
5a	337.15	338.2
5b	351.16	352.2
5c	367.16	368.2
5d	380.19	381.2
5e	382.13	383.2

1.2.4. Synthesis of phenol-pyridine derivatives 6a-6e

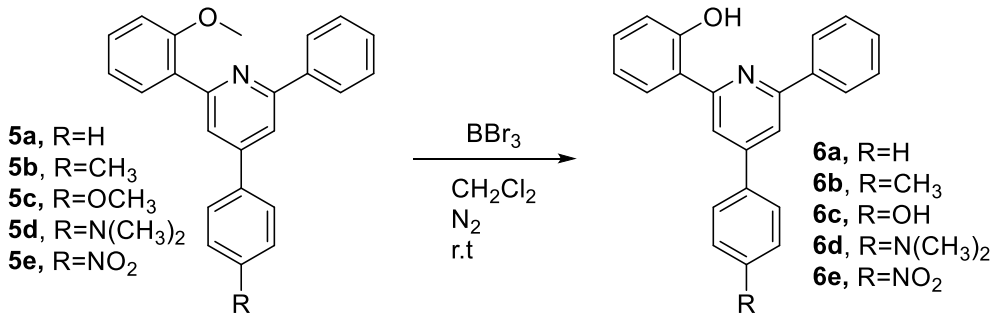

Scheme 16-Deprotection of the anisole groups of pyridines **5a**-**5e**.

The pyridines **6a-e** were obtained by O-demethylation of the anisole groups with BBr_3, in reasonable to excellent yields (37-95%).

Some problems had to be overcome in the O-demethylation step:

-First the solvent (CH_2Cl_2) had to be distilled and dried over molecular sieves (sodium aluminium silicates) in order to remove all traces of water in the solvent. This step was necessary to guaranty that none of the BBr_3 would be hydrolysed by water that could be present. For additional dry conditions the reaction was carried out under pressure of N_2.

-The compound **5c** had two methoxy groups and it would be necessary to purify the products from the deprotection using 1 equivalent, instead it was decided that the two methoxy groups would be deprotected, using 2 equivalents of BBr_3. With two hydroxyl groups it would be possible to functionalize both phenolic groups, opening a lot of possibilities.

-The compound **5d** has a dimethylamine group that with excess of BBr_3 also reacted leading to a secondary amine that corresponds to compound **6f**. The compound **5d** also had another problem related with its low solubility in CH_2Cl_2 under the acidic conditions obtained after the addition of BBr_3. (Scheme 17).

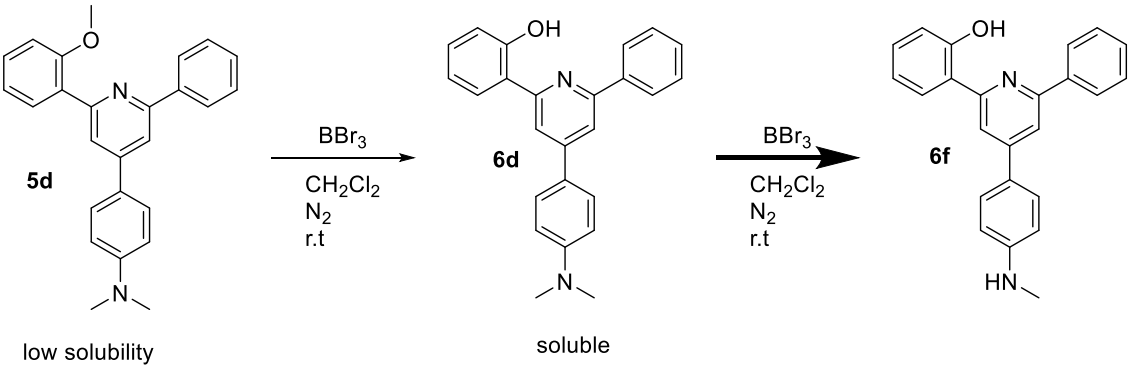

Scheme 17-Synthesis of compound **6f.**

For the structural characterization discussion, ^{1}H-NMR, ^{13}C-NMR, HSQC and HMBC, COSY, NOESY spectra will be considered, as well as ESI-MS and X-ray diffraction. For compound **6f** only ^{1}H-NMR was considered.

An analysis of compound **6e** will be presented as an example of a complete assignment of proton and carbon.

Considering the ^{1}H-NMR spectrum the most important information is the presence of the corresponding peaks for all the protons expected with the multiplicity, coupling constants and chemical shift according to what was expected. The results were also analysed taking into consideration ^{1}H-NMR from compounds **5a**-**5e** that apart from the peaks of the methoxy groups all the other protons should appear and with similar multiplicity. In this analysis the compound **6e** will be used as example. The compound **6f** was not intended to be obtained but because it was the compound tested in alternative to compound **6d**, it was important to include it in this discussion.

- The most evident difference of spectrum from compound **6e** to **5e** is the lack of peak at δ = 3.92 ppm that corresponds to the singlet of three protons from the methoxy group. Instead there is the appearance of a peak at δ = 14.63 ppm corresponding to the characteristic chemical shift of a phenol with a strong intramolecular hydrogen bond (Figure 33).

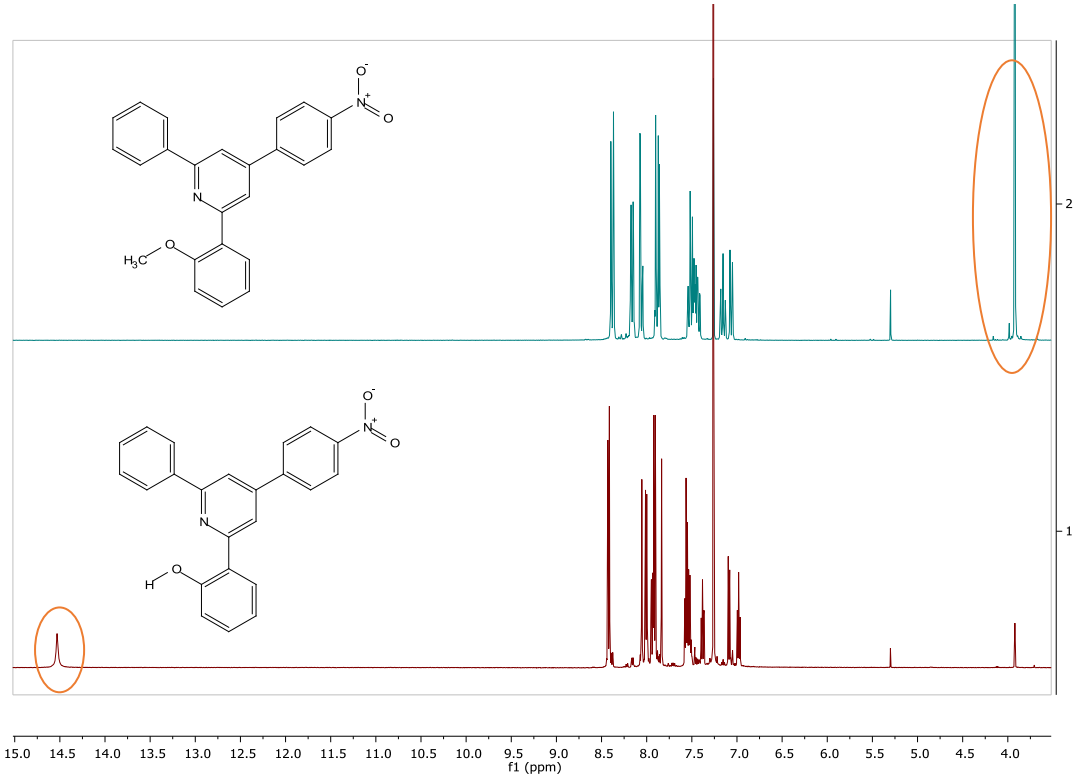

Figure 33-^{1}H-NMR spectra of compound **5e** and **6e**.

- In the aromatic region some changes of deviation can be noticed, one is the downfield deviation of proton H11 from δ = 7.06 to δ = 7.09 due to the less shielding effect of hydroxyl group compared to methoxy.
- Proton H14 being in *meta*-position in relation to the phenol has an upfield deviation from δ = 8.06 to δ = 7.94. The doublet of doublets (ddd) from H12 suffers similar upfield deviation from δ = 7.44 to δ = 7.38.
- Proton H13 has an upfield deviation from δ = 7.16 to δ = 6.98, so that all peaks corresponding to the protons of the phenol ring suffer a shift deviation.

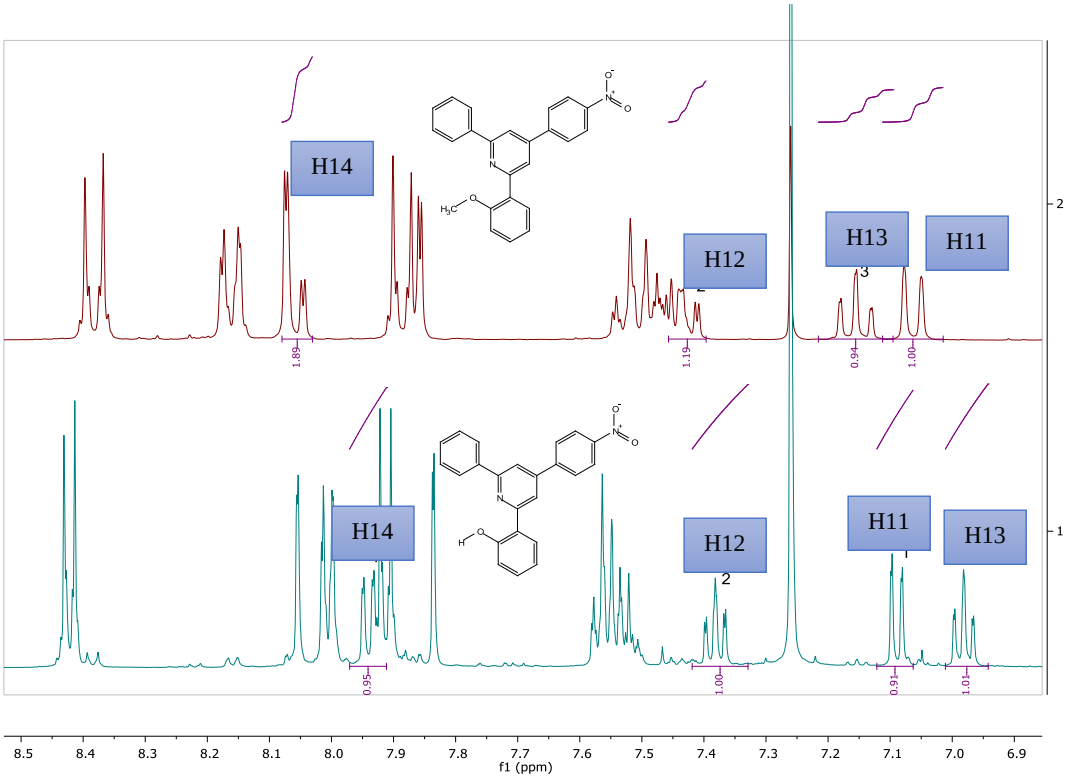

Figure 34-^{1}H-NMR spectra of aromatic protons of compounds **5e** and **6e**.

Other peaks belonging to aromatic protons of the other aryl groups, including pyridine, are not significantly affected by O-demethylation.

Compound **6c** has two O-demethylations what leads to a shift deviation of proton pairs H16 + H18 (*orto*-position to phenol) with downfield deviation and H15 + H19 (*meta*-position) with upfield deviation.

Table 3-^{1}H-NMR peak assignment of phenol group of compounds **6a-6f**.

^{1}H-NMR Signal	**6a** R = H	**6b** R = CH_3	**6c*** R = OH	**6d** R = $N(CH_3)_2$	**6e** R = NO_2	**6f** R = $NHCH_3$
11	δ = 7.08	δ = 7.14	δ = 6.99	δ = 7.06	δ = 7.09	δ = 7.06
12	δ = 7.36	δ = 7.36	δ = 7.34	δ = 7.33	δ = 7.38	δ = 7.34
13	δ = 6.97	δ = 6.97	δ = 6.99	δ = 6.95	δ = 6.98	δ = 6.95
14	δ = 7.96	δ = 7.95	δ = 8.13	δ = 7.95	δ = 7.94	δ = 7.95
26	δ = 14.85	δ = 14.93	----	δ = 15.07	δ = 14.53	δ = 15.08

*-For ^{1}H-NMR of compound **6c** the solvent used was CD_3OD, all the others were dissolved in $CDCl_3$; Highlights in orange represent upfield shift variations and in blue are represented the downfield shift variations.

Also, with the COSY spectrum of compound **6d**, it is possible to establish a correlation between H11, H12, H13 and H14, increasing the certainty of having the right assignments made (Figure 35).

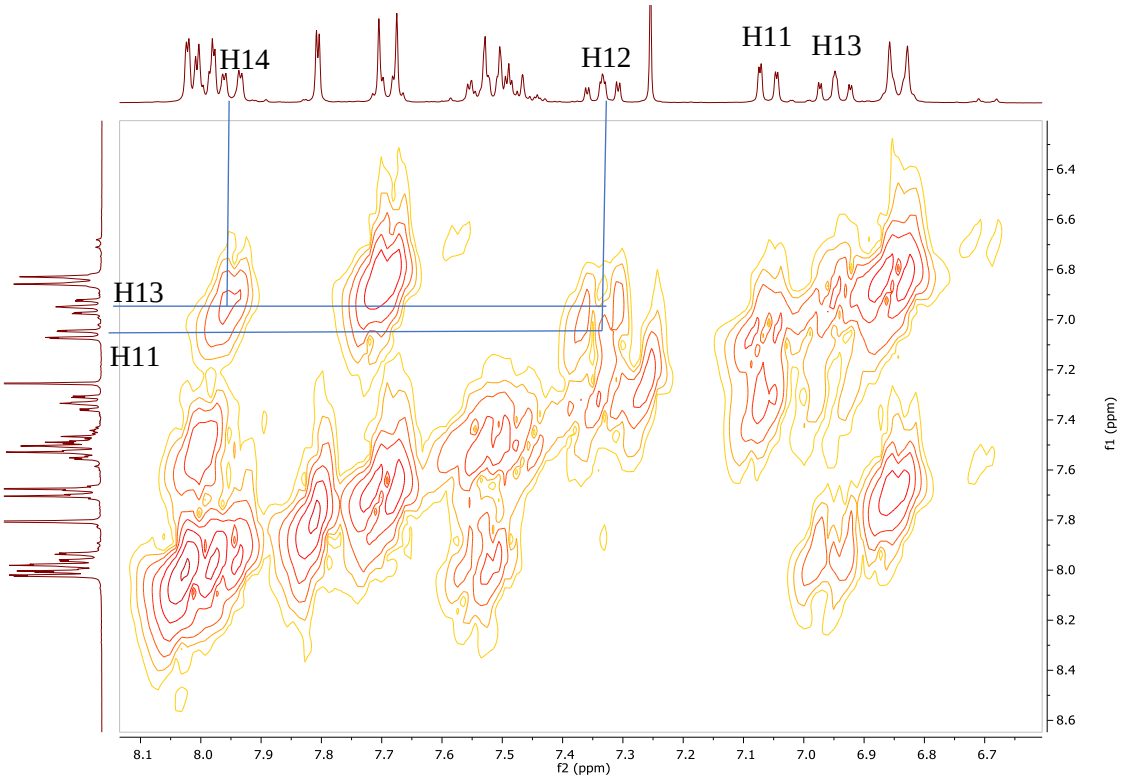

Figure 35-COSY spectrum of compound **6d** with highlight of H12 correlations.

In relation to ^{13}C-NMR, HSQC and HMBC, spectra the same approach can be made in relation to the ^{1}H-NMR comparison made previously between compounds **5a-5e** and **6a-6e**. The most significant changes are like in ^{1}H-NMR the absence of methoxy group at position C10, and because of it, the most affected carbon peaks are the ones that belong to the phenol group.

Other feature that is important to highlight is that HSQC and HMBC are quite consistent with the previous assignments, for compounds **6a-6e** it is possible to identify easily some of the quaternary carbons that had correlations overlapped in compounds **5a-5e**.

For the compound **6d** there are twenty non-equivalent carbons with pairs presenting the same chemical environment being 2C28, C18+C16, C15+C19, C20+C24 and C21+C23, in comparison to compound **5d** there is only one carbon less in this case from methoxy group (C26) (Figure 36).

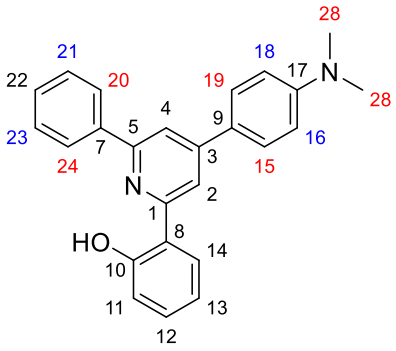

Figure 36-Compound **6d** carbon numeration with colours to highlight carbon pairs with the same chemical environments.

Using HSQC, it is possible to directly identify: C2 δ = 114.33; C4 δ = 116.6; C11 δ = 118.46; C13 δ = 118.73; C14 δ = 126.36; C12 δ = 131.35; C16+C18 δ = 112.5; C15+C19 δ = 127.98; C20+C24 δ = 127.06; C21+C23 δ = 129.06; C22 δ = 129.23.

To identify the remaining carbons, HMBC spectrum can be used, for carbon C10 correlations with protons H12 and H14 in J_3 and J_2 with H11 can be detected. Using HMBC spectrum of compound **6d** as an example it can be seen a correlation between C10 δ = 160.25 and H12 (Figure 37) that previously in compound **5d** was difficult to assign due to an overlap of proton peaks H12, H21+H23 and H22 in the region δ [7.34-7.52].

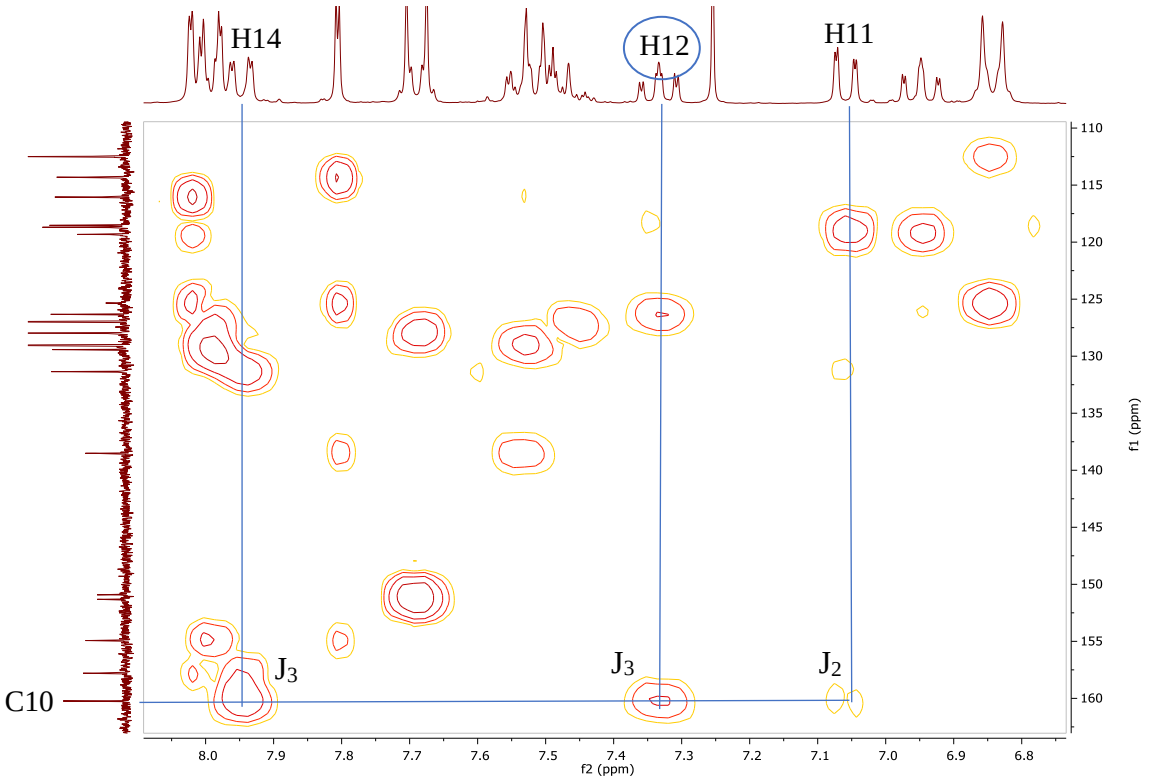

Figure 37-HMBC correlations of carbon C10 in compound **6d**.

For the assignment of the correspondent peak of carbon C8 δ = 119.36 there are J_3 correlations with H2, H11 and H13. Carbon C7 δ = 138.44 can be assigned with a strategy similar to C8, in this case C7 has a J_3 correlations with H4 and the pair H21+H23 and J_2 with H20 + H24 (Figure 38).

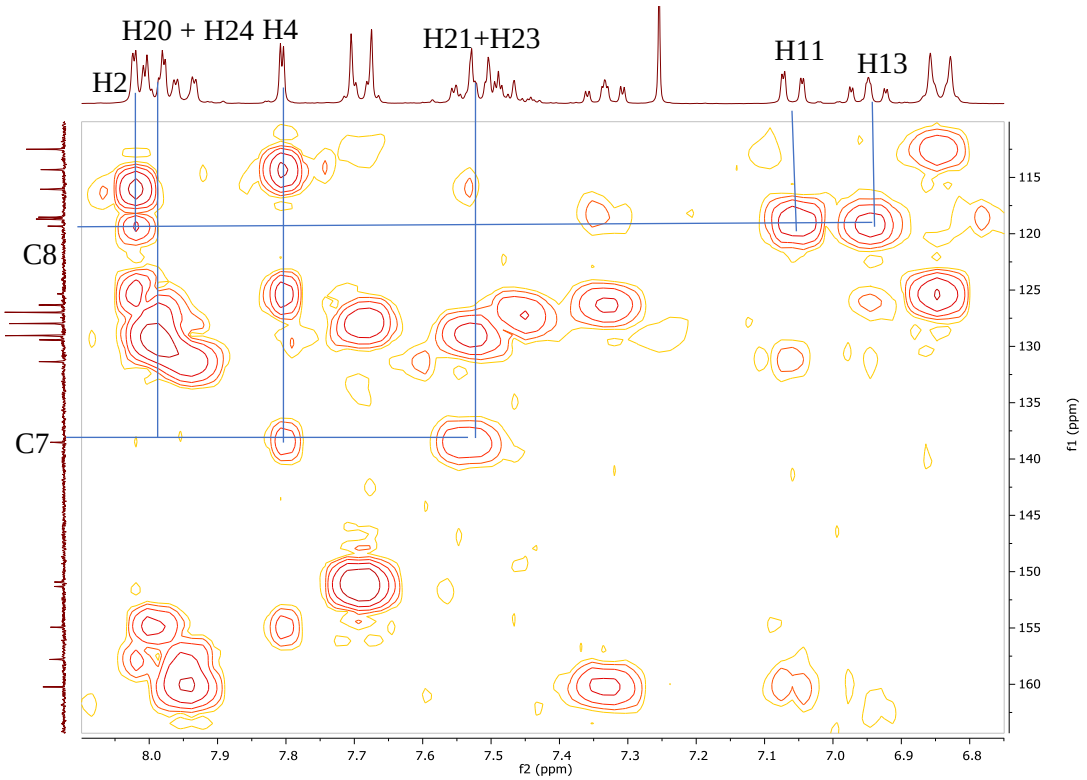

Figure 38-HMBC correlations of carbon C7 and C8 for compound **6d**.

C1 has a J_2 correlation with H2 and J_3 with H14 therefore it has a shift of δ = 157.85, in parallel C5 δ = 154.84 can also be identified by correlations J_2 with H4 and J_3 with pair H20 + H24 (Figure 39).

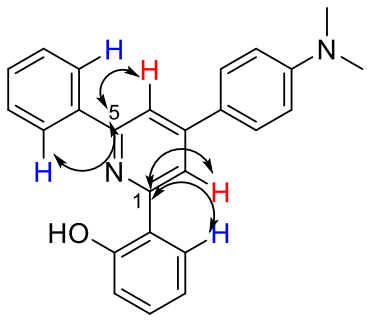

Figure 39-HMBC correlations of C1 and C5 for compound **6d**.

C17 is the only carbon with correlation with the protons of the dimethylamine group and the pair H15 + H19 , so it can be assigned to peak C17 δ = 151.31 (Figure 40).

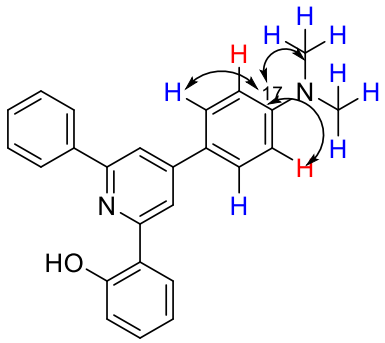

Figure 40-HMBC correlations of C17 for compound **6d.**

The carbon at position C9 δ = 125.40 is assigned by the J_3 correlation with both pyridine protons H2 and H4 and H16 + H18. For last carbon C3 can be assigned by J_2 correlation with H2 and H4 and J_3 with pair H15 + H19 so C3 δ = 150.92 (Figure 41).

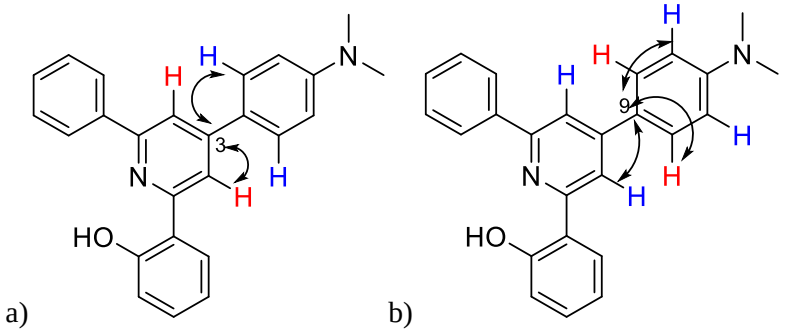

Figure 41-HMBC correlations of C3 and C9 for compound **6d.**

The results obtained by Electrospray Ionisation Mass Spectrometry (ESI-MS) were consistent with the theoretical expected mass (Scheme 18). For each compound **6a-6e** ESI-MS results were consistent with the theoretical exact mass (Table 4).

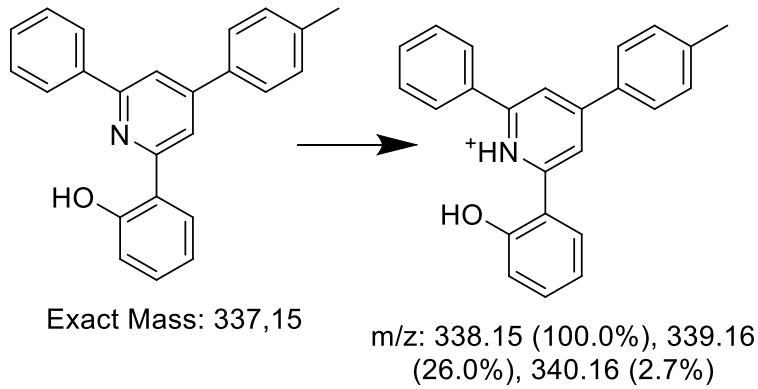

Scheme 18-Representation of cationic form of compound **6b.**

Table 4-Electrospray Ionisation Mass Spectrometry results of compounds **6a**-**6c** and **6e.**

Compound*	Exact mass	m/z
6a	323.13	324.2
6b	337.15	338.2
6c	339.13	340.2
6e	368.12	369.2

*compound **6d** and **6f** were not analysed on time to be included in this discussion.

1.3. Attempted Synthesis of boranils

For the complexation of compounds **6a**-**6e,** the strategy descripted below (Scheme 19) was used in order to obtain the intended boranils, however several attempts were unsuccessful. First a complexation using compound **6b** and $BF_3 \cdot OEt_2$ dissolved in CH_2Cl_2 at room temperature was tried. The ^{19}F-NMR spectrum showed peaks corresponding to ^{19}F but there was not any ^{1}H-NMR shift of any peak and therefore a stable complex was not achieved.

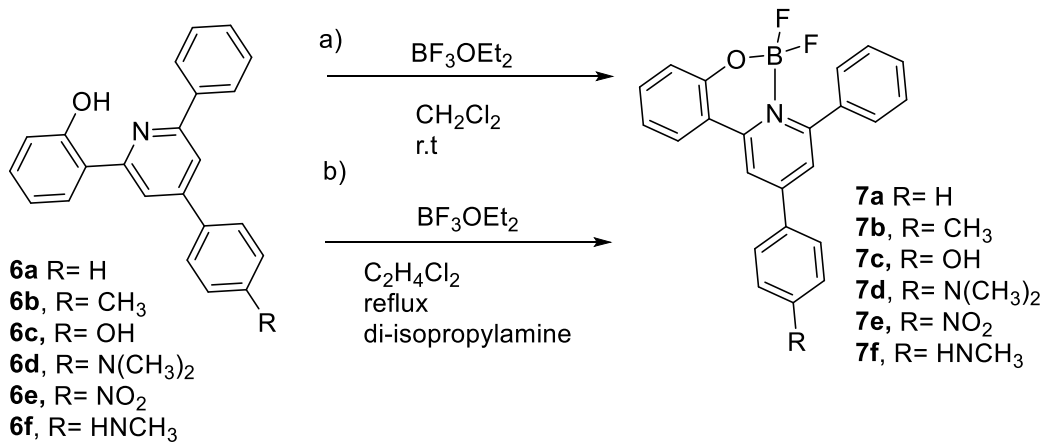

Scheme 19-Synthesis of the boranils.

In a second attempt another solvent was used ($C_2H_4Cl_2$), that allows to increase the temperature of the reaction. In parallel, a base (diisopropylamine) was used to facilitate the reaction by neutralizing the HF formed during the reaction that can lead to

protonation of the pyridine and not allowing the complexation to happen. In this second attempt, the results had a slight but relevant variation: first a cleaner ^{19}F-NMR spectrum with a cleaner peak at -143.37 ppm was obtained, and there was a slight variation in the ^{1}H-NMR spectrum that is relevant, a slight shift of the peak corresponding to proton H11 (the proton in *ortho*-position to phenol). Other explanation for the unsuccessful result is the quick hydrolysis of the complex when dissolved in the solvents used for NMR studies.

A stable complex of compound **6b** and boron was not obtained, and other attempts were done using the same conditions for compounds **6d** and **6e**, but the results were similar. It was intended to try a complexation using alternatives for $BF_3 \cdot OEt_2$ like triphenylborane however it could not be done in time for this study.

2. Photophysical characterization

2.1. In dilute solution

For the photophysical characterization of the series of compounds **5** and **6**, fluorescein was used as reference, but the quantum yields were aberrant (over 100%). Anthracene was better used as reference for its similar absorption-emission spectra, more specifically its absorption wavelength (340 nm) and emission (350-470 nm), more adequate than fluorescein (Figure 42). The chosen reference is important to get a more accurate value of the quantum yield, however there is an error associated with comparative methods that is often not taken into consideration. This study acknowledges Demas and Crosby equation[55] for determination of a corrected quantum yield, but it was decided that comparative method could be applied in this study using anthracene as reference without correction.

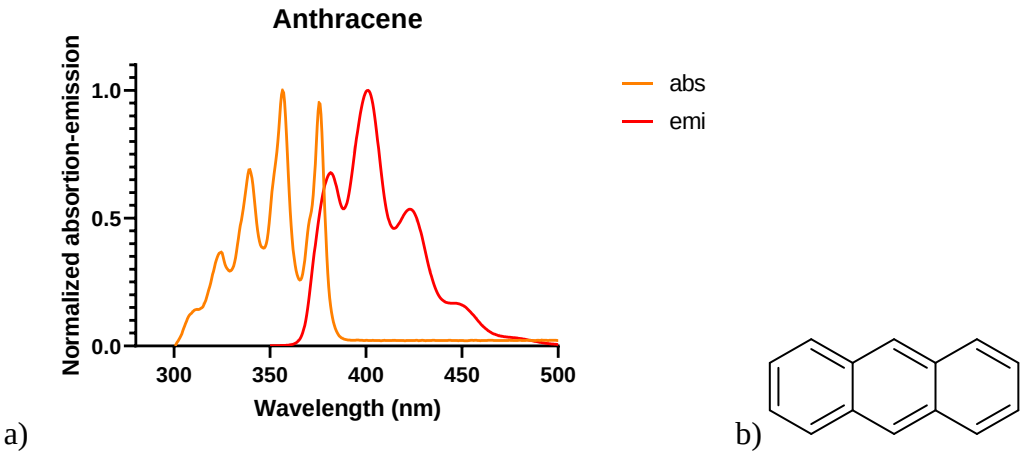

Figure 42-Anthracene a) Normalized absorption-emission spectra b) Structure

The absorption profile of compounds **5a** and **5b** has an almost profile overlap, as the only structural difference is a methyl in 4-aryl group that has weak electron donating character. Both compounds **5a** and **5b** profiles have a double band profile with a higher absorption at 260-280 nm and a second band with absorption at around 310 nm. Compound **5c** has a second band at 290-300 nm and its intensity is close to the

absorption of the band at 260-280 nm which might indicate similar electron π-π* transitions of both moieties that contribute to the absorption profile (Figure 43).

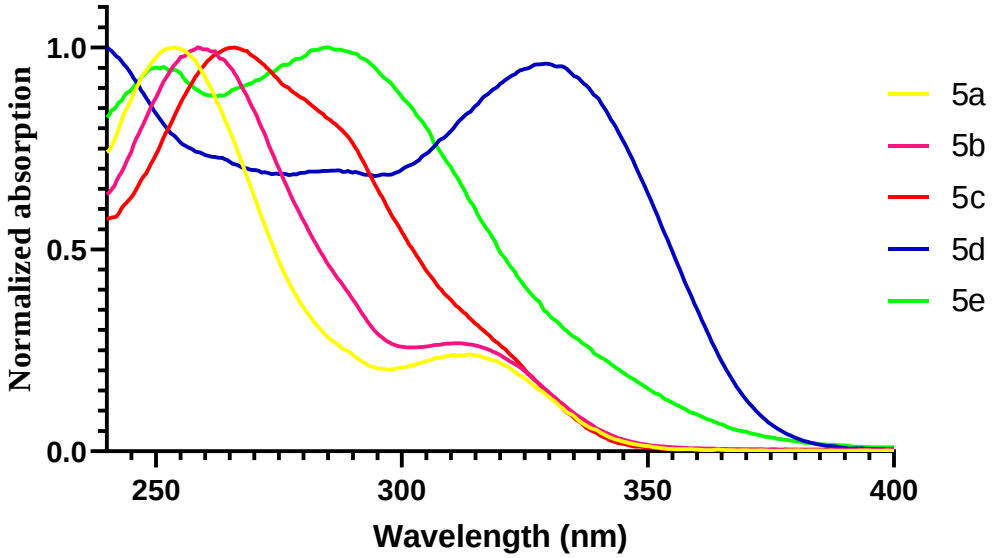

Figure 43-Absorption spectra of compound **5a**-**5e**.

The distinct profile of the several derivatives is related to the different substitutions that change the electronic distribution leading to different HOMO-LUMO transitions.[8,10] This relation between structure and absorption profile is supported by the profiles of compound **5d** and **5e** which are clearly different from compounds **5a**-**5c**. Compound **5d** has a stronger donating group at 4-aryl position than other derivatives, which significantly changes the electronic distribution, while for compound **5e** there is an electron withdrawing group, corresponding to nitro in *para*-position of the 4-aryl group (Figure 44).

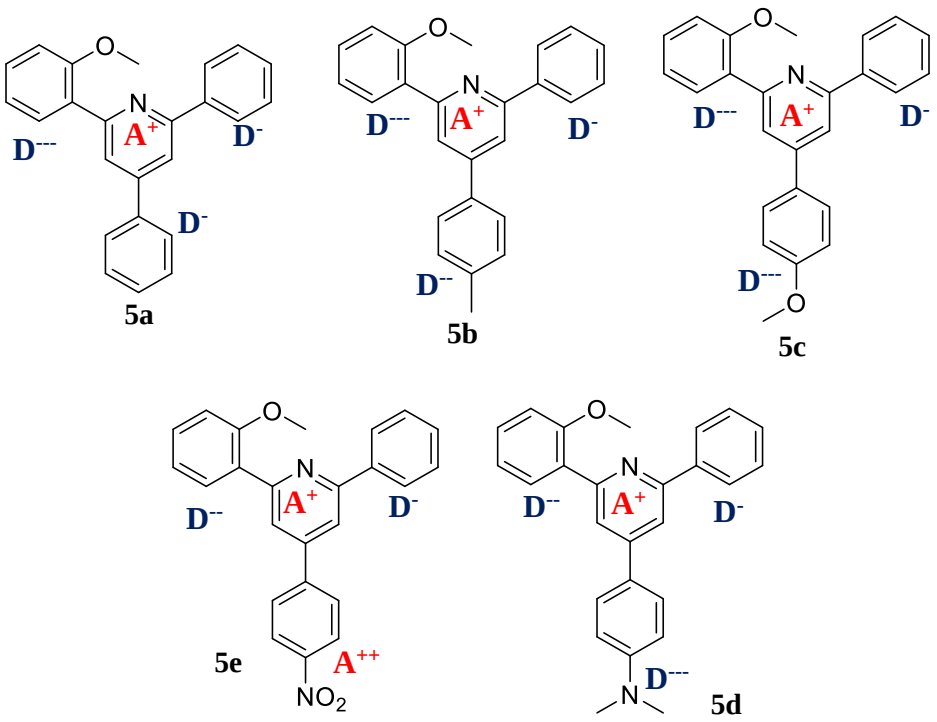

Figure 44-Donator-Acceptor character of aromatic rings in compounds **5a-5e**.

The number of donating groups and the relation donating (D^-) to accepting (A^+) groups is 3D-1A in compounds **5a-5d** while for **5e** there is 2D-2A. Compounds **5a-5d** have a similar fluorescence emission profile, compound **5e** has a double band emission however it should be mentioned that this compound has 1000 times less brightness than other compounds (Figure 45).

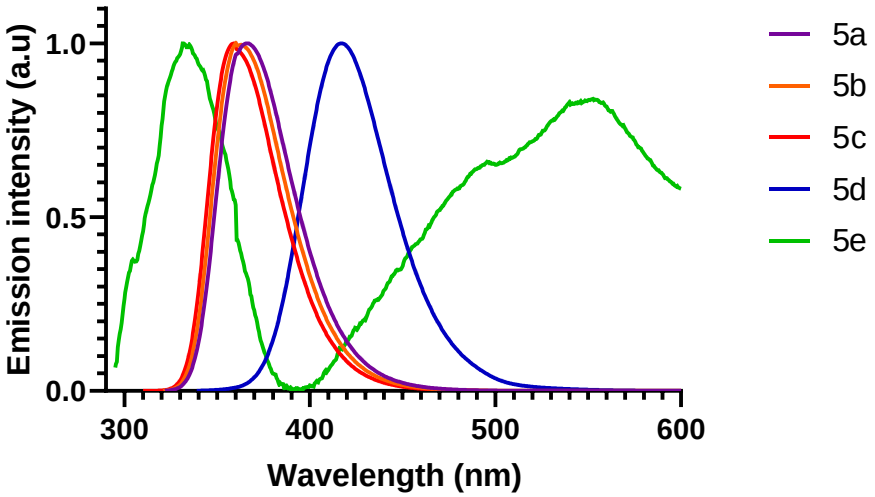

Figure 45-Emission spectra of compounds **5a-5e**.

As it was discussed previously, compounds **5a** and **5b** have a similar profile for both absorption and emission, having a maximum of absorption and emission quite close as it can be seen in Table 5. The molar absorption coefficient, quantum yield and therefore brightness are also similar. The compound that has the highest quantum yield is compound **5d** and there is an apparent relation of donor strength of 4-aryl group to quantum yield (**5a**/**5b**<**5c**<**5d**). The compound that has the highest brightness is compound **5d** which has, as expected, highest molar absorption coefficient and quantum yield combination. Compound **5e** has a high molar absorption coefficient but due to having a low quantum yield it does not have significant emission.

The results are coherent with other works that studied the importance of donor-acceptor moieties,[8] as well as the charge transfer phenomena involved in such systems,[7,10] to lead to red-shift absorption-emission as well as larger Stoke shifts.[8,10] The triphenylpyridines **5a**-**5e** in this study exhibit the properties associated with donor-π-acceptor systems and they offer the possibility to easily introduce π-extensions for tuning of the photophysical properties with the possibility of introducing different substituents independently in each aryl group creating different donor-acceptor variations.

Table 5-Photophysical characterizations of compounds **5a**-**5e**.

Compound	λ ex nm	λ f nm	Δ nm cm^{-1}	ε $M^{-1}.cm^{-1}$	Φ %	Brightness ε.Φ
5a	312	366	54 4729	8 500	29	2500
5b	311	360	49 4377	10 000	28	2800
5c	300	359.5	59.5 5517	18 200	32	5900
5d	329	417	88 6414	30 600	74	22600
5e	285	332/549	47/264 4967/ 16873	27 500	<0.1	6
Anthracene	340	401	61 4474	9 700	28	2700

Compounds **6a**-**6c**, **6e**, **6f** do not present significant fluorescence in solution, in the same conditions that compounds **5a**-**5e** were tested. First the absorption spectra of each compound seem to have a profile similar to compounds **5a**-**5e**, with **6a** and **6b** having similar profile, **6c** has a slight overlap of bands at 260-280 nm and at 300 nm like in **5c**, which also happens for compound **6e** (Figure 46).

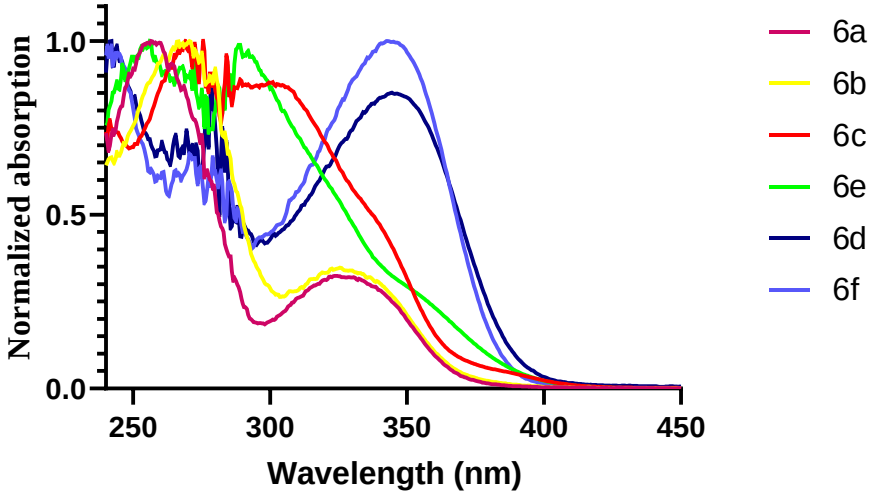

Figure 46-Absorption spectra of compounds **6a**-**6f**.

The family of compounds **6a**-**6f** does not have an intense emission compared to compounds **5a**-**5e**. Compounds **6a**-**6c** present a double emission (Figure 47).

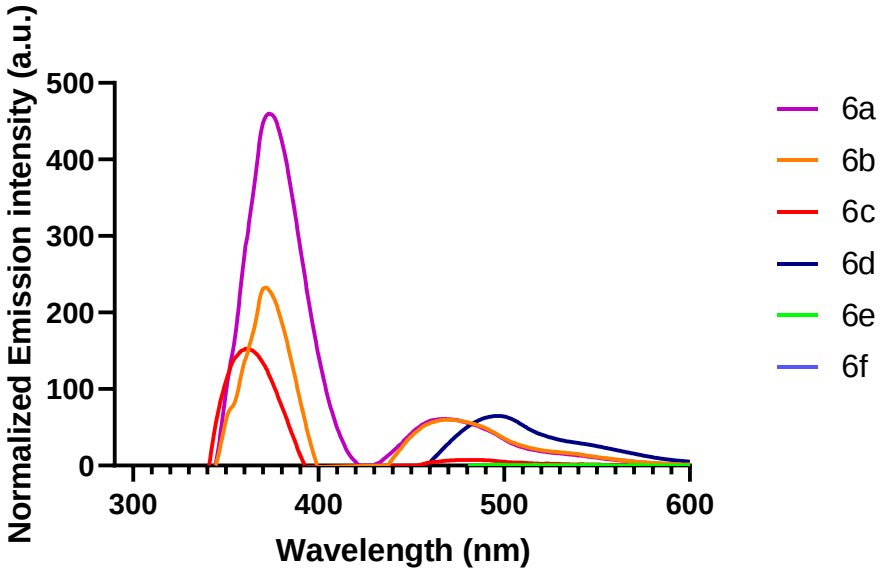

Figure 47-Emission spectra of compounds **6a**-**6f.**

The calculated molar absorption coefficients show an increase of value from compound **6a** to **6f** (Table 6). The emission of phenol-pyridine derivatives **6a**-**6c** is significantly lower than anisole-pyridine derivatives **5a**-**5d**.

The phenol-pyridine core is possibly leading to a red shift of 10-20 nm in both absorption and emission spectra. There is also a dual emission profile that should be studied in order to understand the reason for such profile.

Table 6-Photophysical characterizations of compounds **6a**-**6f**.

Compound	λ ex nm	λ f nm	Δ nm cm^{-1}	ε $M^{-1}.cm^{-1}$	Φ %	Brightness ε.Φ
6a	325	370	45 3742	16100	1.6	300
6b	325	370	45 3742	16300	1.2	200
6c	305	355	50 4617	29100	0.5	100
6f	345	-	-	44700	<0.1	-
6e	284	-	-	40700	<0.1	-
Anthracene	340	401	61 4474	9700	28	2700

The results from the photophysical characterizations in solution of triphenylpyridine derivatives, compared with some major classes of fluorophores, show that triphenylpyridine derivatives can be an alternative for some of the benchmark fluorophores (Figure 48). If we consider compound **5d** (λ_{max} 329 nm) and classes of fluorophores with similar absorption wavelengths such as pyrene (340 nm), quinine(347 nm), DAPI(358), AMC (351 nm), 4-MU (360 nm), HOECHST 33342 (350 nm), compound **5d** brightness (22 600 $M^{-1}cm^{-1}$) surpasses all of them with exception for pyrene that has a brightness of 32 000 $M^{-1}cm^{-1}$ [56]. Compound **4d** has an advantage over pyrene that is related with its non-planarity and larger Stoke-shift.

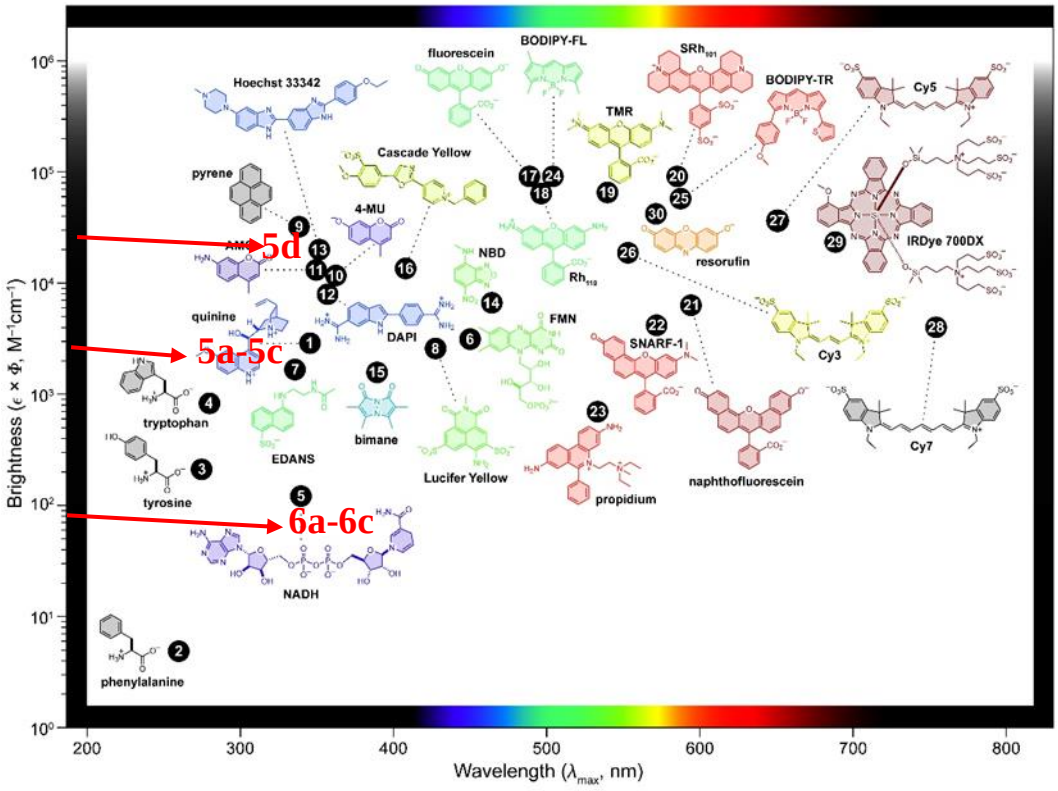

Figure 48-Examples of fluorophore brightness ($\epsilon \times \Phi$) vs the wavelength of maximum absorption (λ_{max}) for the major classes of fluorophores and triphenylpyridine derivatives of this study.[56]

2.2. Aggregation-Induced Emission Enhancement

The aggregation test was performed in order to observe an enhancement of the emission intensity that would be related to the restriction of non-radiative decay due to the rotation of aryl groups. The test was accomplished by decreasing the solvent relation THF/H_2O from 100% THF to 10% THF for compounds **5b** and **6b**. The absorption spectra of solutions 100% to 30% had a similar profile with an accentuate decrease of the band intensity at 250 nm while the band intensity at 311 nm did not have any significant decrease. For solutions at 20% and 10% there was an increase of the band intensity at 311 nm to absorption 10 times higher which indicates the formation of aggregates, having this way a colloidal solution (Figure 49).

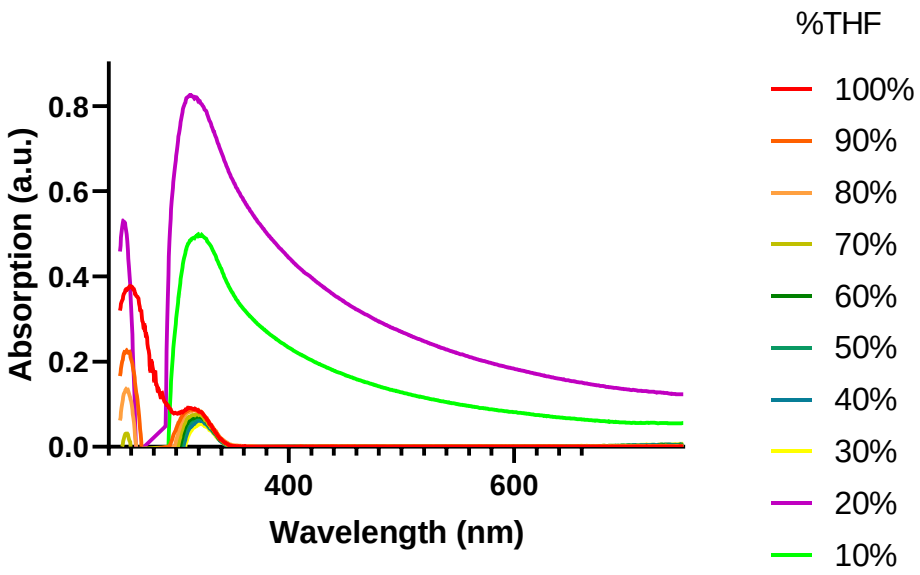

Figure 49-Absorption spectra from aggregation test of compound **5b** (100% THF to 10% THF and 90% H_2O).

For the emission, an enhancement of fluorescence would mean an increase of emission intensity with aggregation, which for compound **5b** did not occur.

The emission intensity remained unchanged for water content varying from 0% to 70% and decreased dramatically with the formation of colloidal solutions when the water content gets higher. A red shift of the emission band from 360 nm to 440 nm was also observed for these colloidal solutions. As the crystals seem highly emissive to the naked eye, it can be postulated that the water present in the colloidal solution impede the crystallization, and an amorphous solid containing water is obtained in the colloidal solution. This unorganized solid may promote the formation of extensive Pi-Pi interaction, leading to the observed quenching of the emission (Figure 50).

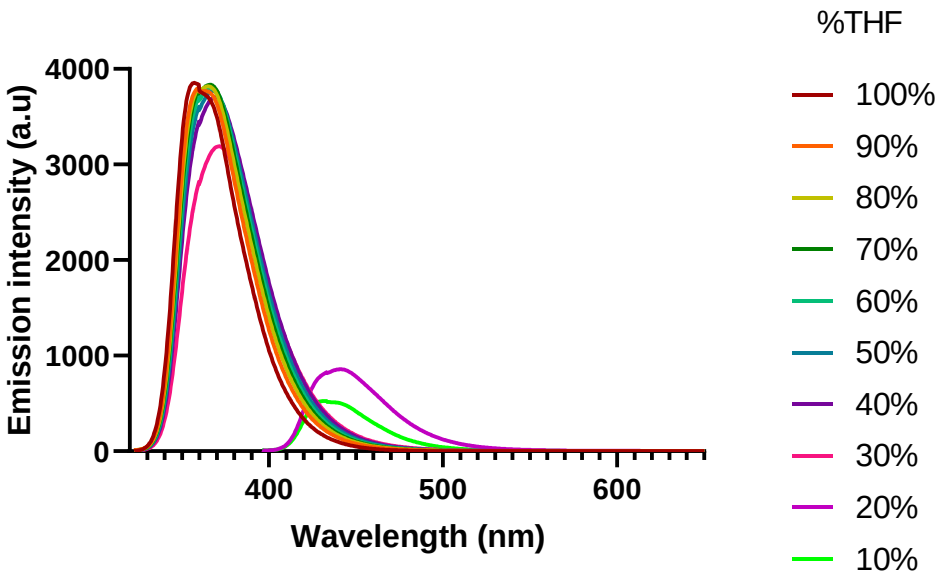

Figure 50-Emission spectra from aggregation test of compound **5b**. (100% THF to 10% THF and 90% H_2O).

The aggregation test of compound **6b** showed a similar tendency in absorption spectra. The absorption spectra of solutions 100% to 30% had a similar profile with an accentuate decrease of the band intensity at 250 nm while the band intensity at 325 nm did not have a significant decrease. For solutions at 20% and 10% there was an increase of the band intensity at 325 nm to absorption 10 times higher which indicates the formation of aggregates, having this way a colloidal solution (Figure 51).

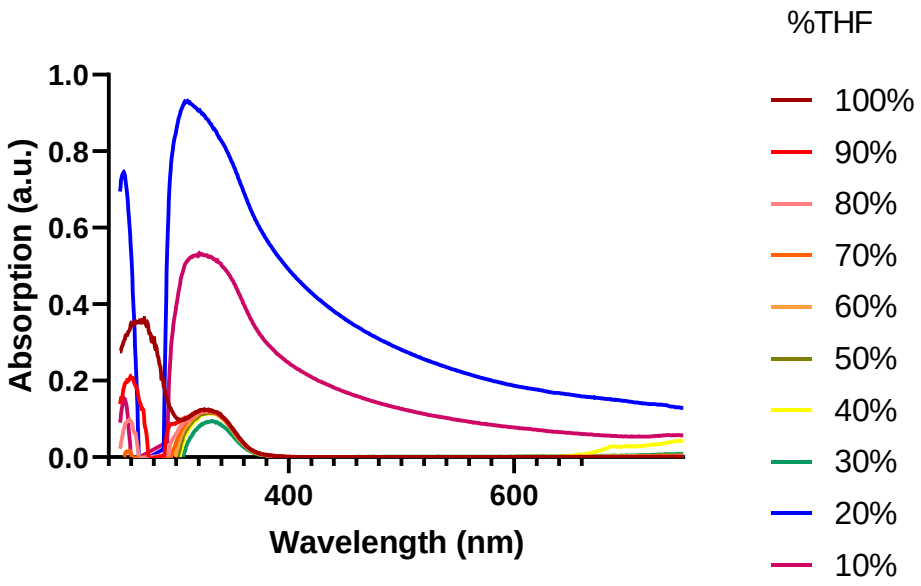

Figure 51-UV-vis spectra from aggregation test of compound **6b**. (100% THF to 10% THF and 90% H_2O).

For the emission spectra, the changes in the profile did not follow the same tendency as it was observed for compound **5b**. The addition of water led to a sudden decrease of the emission at 90% solution in opposition to compound **5b** where there was a decrease of emission intensity only at 20%. The profile of the emission of compound **6b** does not change after addition of water but at 20% and 10% solutions the emission is close to zero. The possible phenomenon that is leading to such low emission intensities might be related with the strong polar interactions that compound **6b** can have with H_2O, in opposition to compound **5b**. Other very important phenomenon responsible for the decrease of emission intensities is related to the emission bands having an overlap with the absorption band (Figure 52). There is also the possibility of having a self-quenching by intermolecular interactions due to the compound **6b**, similarly to compound **5b,** do not have such a polar character like compound **5d**, **6c**, **6d** or **6f**. For compounds with polar character, polar interactions are preponderant in opposition to Van der Walls interactions in **5b** or **6b,** leading to π-stacking.

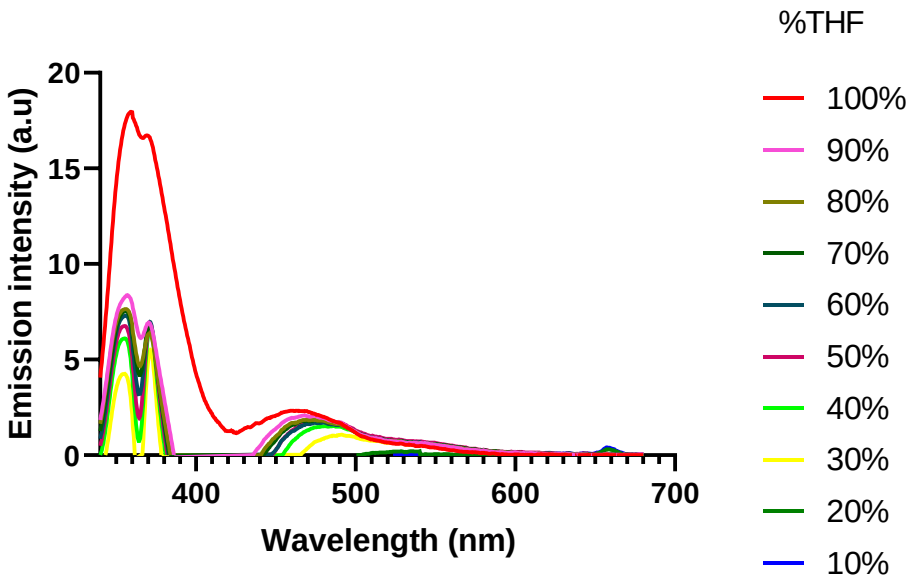

Figure 52-Emission spectra from aggregation test of compound **6b**. (100% THF to 10% THF and 90% H_2O).

2.3. Solid-state fluorescence and luminescence

The solid-state fluorescence of triphenylpyridine derivatives was not recorded in time to be included in this study, however some qualitative analysis could be done. The first observation is that some of the derivatives are fluorescence in the solid state, more significantly compounds **5d**, **6c** and **6f**, under UV light (366 nm) (Figure 53).

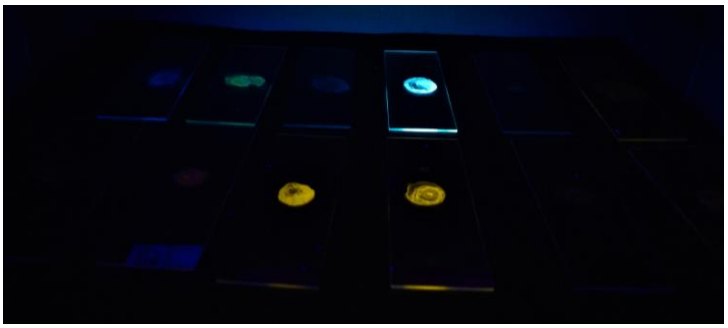

Figure 53-Photograph of dropcasted films of compounds **5a**-**5e** and **6d** (on top) and compounds **6a**-**6c**, **6f**, **6e** (bottom) under UV light (366 nm).

3. Crystal structures

Single crystals suitable for X-ray diffraction were obtained for compounds **5b-5e**, by slow evaporation of saturated solutions in CH_2Cl_2.

All the crystal structures were consistent with ^{1}H-NMR, ^{13}C-NMR and 2D spectra. With the crystallographic results (example Figure 54), it was possible to discuss some structural features that are important for the luminescence in solid state.

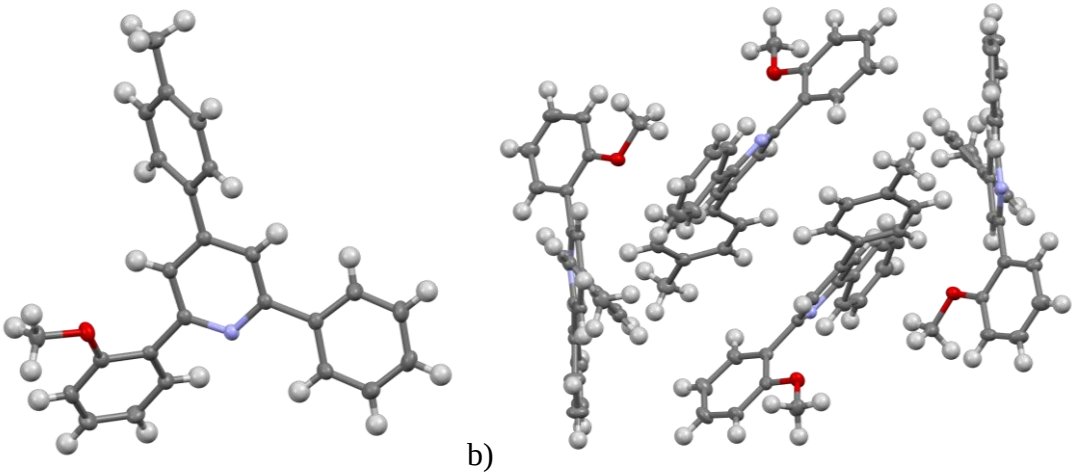

a) b)

Figure 54-Assymetric unit of compound **5b** (a) and unit cell content (b). Thermal ellipsoids are shown at the 50% probability level, hydrogen atoms are shown with an arbitrary radius (0.30Å). C, grey; O, red; N, blue; H, white.

An analysis of the crystal structures shows that there are some differences between the compounds **5b**-**5e**. One important feature is the angles between the pyridine core and the aryl groups. The importance of these angles between the pyridine core and the aryl groups is the adoption of conformations that promote larger inter-molecular distances in solid state, preventing some of the quenching phenomena discussed previously in chapter I.

Using compound **5b** as an example, the anisole ring in *ortho*-position adopts an angle of approximately 40º in relation to the pyridine ring. The aryl group in *para*-position adopts a slightly wider angle of 42º, and the aryl group in *ortho*-position has a smaller angle of 10.5º. These angles do not allow strong Van der Waals interactions

considering a cut-off of 3Å, neither intermolecular hydrogen bonds for compounds **5b-5e** (Figure 55).

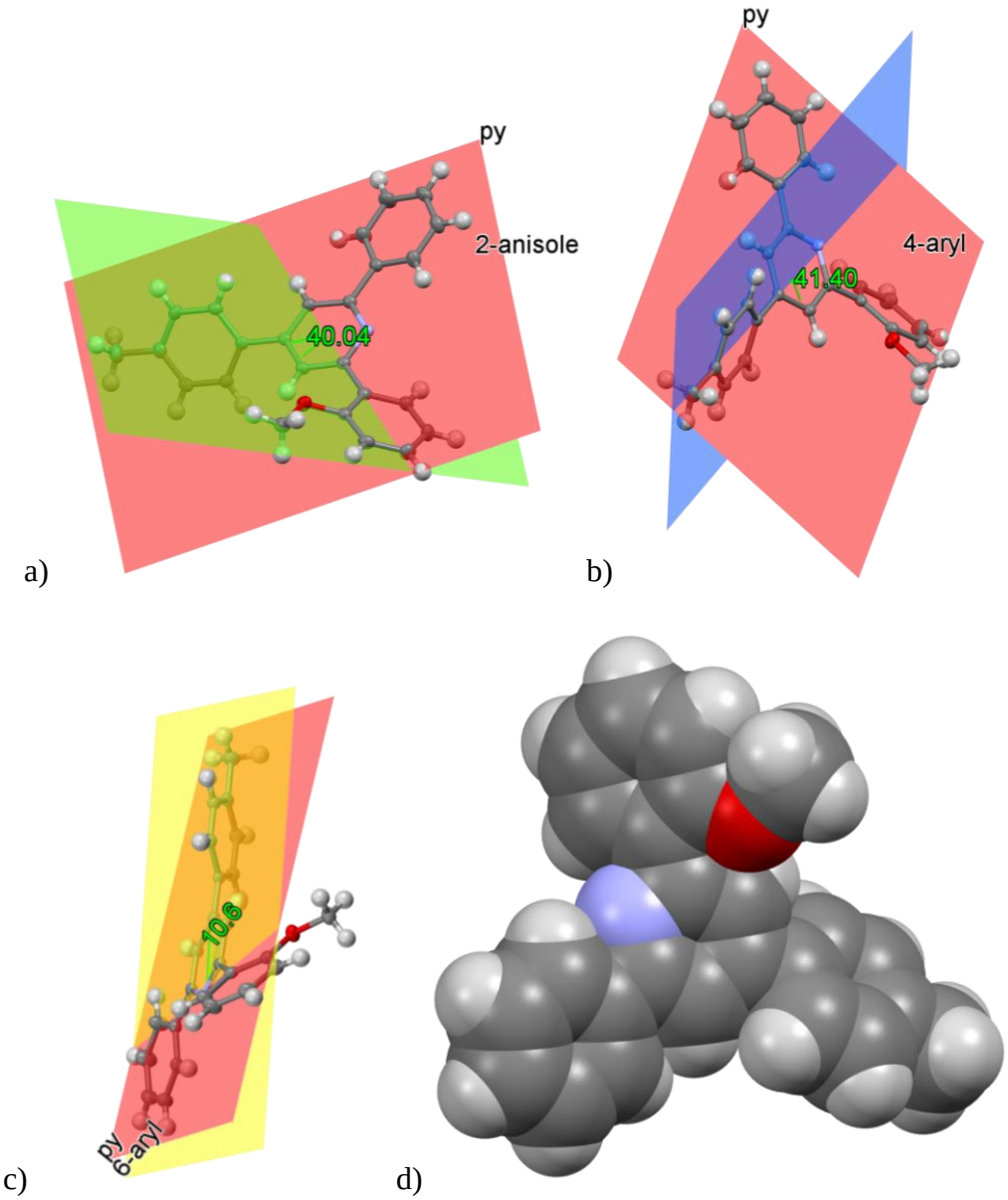

Figure 55-Representation of the angles between the planes of the pyridine core and the aryl groups in compound **5b**.

The angles that anisole, *ortho*-aryl and *para*-aryl form with the central pyridine ring promote a lack of planarity that is important to prevent a π-π stacking that is often responsible for quenching in solid state, as it was referred in chapter I.

In the following table some features mentioned above are resumed, such as the torsion angles and intermolecular distances given by the distance between two pyridine cores (py-py) for compounds **5b**-**5e.**

Table 7-Angles between the planes of the pyridine core and the aryl groups and intermolecular distances between two pyridine cores (py-py) for **5b**-**5e**.

Compound	2-anisole θ	4-aryl θ	6-aryl θ	py-py Å
5b	40.4	41.4	10.6	7.61/7.72
5c	37.9	38.5	14.5	7.52/7.69
5d	16.1	7.9	20.2	10.49/9.74/9.49
5e	7.7	30.7	20.0	4.83/12.37/15.23
6b	9.4	9.5	19.1	13.70/11.07/7.99

The influence of the 4-aryl substituents in terms of electron-donating/electron-withdrawing properties cannot be taken into consideration without an analysis of the planarity between withdrawing-donating groups in order to obtain π-π conjugation. It can be noticed that compound **5d**, bearing a dimethylamino substituent, has a noticeably smaller angle between py-(4-aryl) which can be due to strong conjugation between those groups that makes a planar core formed by these two aromatic groups. It must be considered that carbon-carbon distances of 1.54 Å are single bonds, 1.33 Å double bonds and that benzene carbon-carbon bonds have a distance 1.39 Å which is considered an intermediary (resonance) character. For derivatives **5b**-**5e** and **6b** there are three sigma bonds (σ) between the pyridine core and the aromatic substituents, one for each aryl group, and one sigma bond for R group. Each benzene ring has six pi bonds (π) which average is represented in Table 8.

Table 8-Bond length of sigma bonds (σ) and pi bond average (π) of aryl groups at crystallographic structures of **5a**-**5e** and **6b**.

	2-anisole		**6-aryl**		**4-aryl**		
Compound	σ	π	σ	π	σ	π	**R**
5b	1.491	1.392	1.490	1.383	1.482	1.389	1.507
5c	1.486	1.393	1.490	1.389	1.481	1.393	1.365*
5d	1.497	1.396	1.490	1.393	1.476	1.398	1.371*
5e	1.496	1.390	1.485	1.389	1.495	1.390	1.474*
6b	1.484	1.392	1.495	1.383	1.487	1.388	1.508

*Not carbon-carbon bonds: **5c** (C-O); **5d** (C-N); **5e** (C-N)

It can be noticed that none of the bonds have a characteristic length of single bonds, this is caused by having conjugation of pyridine core with aryl groups. Usually in conjugated systems there is a slight increase in double bonds' length of about 0.007 Å and a decrease in single bonds' length[57] of about 0.016 Å and these effect can be observed in compounds **5b**-**5e** with even higher decreases when the single bond is with electron donating group (compound **5c** and **5d**). Other indication that supports the conjugated character of sigma bond with dimethylamine in compound **5d** is the planar conformation of dimethylamine in opposition to umbrella conformation.

It must be noticed that sigma bonds corresponding to (4-aryl)-R are shorter in compounds **5d** than compounds **5a**-**5c** due to having a C-N bond involved and due to its electron donating character we must expect a strong conjugation of dimethylamine with the aryl group at *para*-position to pyridine.

Having in consideration the bond lengths and angles between the pyridine core and the aryl groups, the results indicate that the donating character of the aryl groups to pyridine is compromised mostly by the angle formed by the anisole and the 4-aryl which can led to lower π-π orbitals overlap, however this twist is slightly smaller in compound **5d** which might indicate more 4-aryl-pyridine conjugation than in compounds **5c** and **5b**.

In some cases, the conjugation might not be as favourable in solid-state as in solution because in the solid state, restricted conformations might lower the conjugation of donating groups.

Single crystals suitable for X-ray diffraction were also obtained for compound **6b**, by slow evaporation of a saturated solution in CH_2Cl_2.

The crystal structure was consistent with ^{1}H-NMR, ^{13}C-NMR and 2D spectra results. With the crystallographic results it was possible to identify some structural features that are important for the luminescence in the solid state.

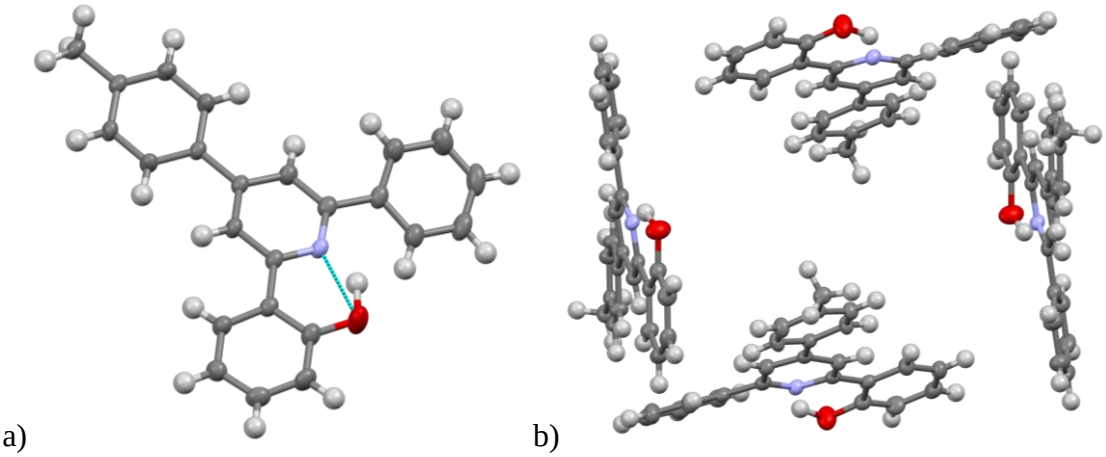

a) b)

Figure 56-Crystal structure of compound **6b**. a) Assymetric unit b) Crystal packing.

For compounds **6a**, **6c**, **6d** and **6e,** we could not obtain crystals with the dimensions necessary for X-ray diffraction. The obtained crystals had a needle shape and were too small for the apparatus we have access to.

Compound **6b** presents a distinct crystal geometry in comparison to compounds **5b**-**5e**. It has a box shaped arrangement where pyridine-pyridine intermolecular distances increase besides the structure having a flatter shape with smaller torsion angles between the aryl groups and the pyridine ring. The results suggest that non protected compound **6b** might have a stronger conjugation in the solid state when compared to protected compound **5b**. The sigma bond between the pyridine and the anisole group of compound **5b** is significantly longer than the sigma bond between the phenol and the pyridine of compound **6b,** which is related to the stronger conjugation that phenol and pyridine have.

Observing the crystal packing, there is the formation of head-to-head dimers connected by hydrogen bonds formed by two C-H-O interactions for compound **6b**, while for

compounds **5b**-**5e** there are only polymeric/chain interactions held together through one C-H-N(pyridine) hydrogen bond (Figure 57).

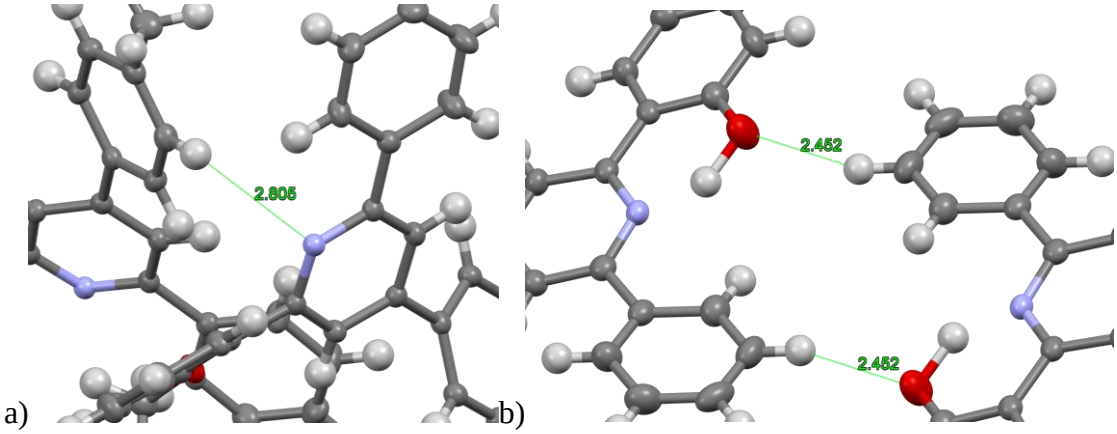

a) b)

Figure 57-Representation of weak polar interactions of a) compound **5b** and b) compound **6b**.

The formation of dimers might also be present when aggregation was studied using compound **6b,** where there was a slight red shift characteristic of aggregates. Taking in consideration the solvatochromic behavior of Reichardt's dye that has structure similarities with the compounds in this study, solvatochromic effects should be expected.[58] One indication that maybe there are no solvatochromic effects is that there is no red shift until the relation water/THF reaches 4/1. One possible explanation for the difference between emission in solid-state vs aggregation test results is that aggregates have a different intermolecular rearrangement than in the crystal form, which might promote quenching phenomena that do not occur in the crystal form.

Conclusions and perspectives

In this study, a family of fluorophores with a triphenylpyridine core were synthetized. The synthetic strategy opens the possibility of independent aryl modifications in *ortho* and *para* positions of the pyridine, which in turn allowed the introduction of different donor-acceptor substituents for the enhancement of the luminescence properties. The contribution of the donor group in 4-aryl position of pyridine was only significant for compound **5d** with a dimethylamine as electron donor, the compound has a molar absorption coefficient of 30 600 $M^{-1}.cm^{-1}$, a quantum yield of 74%, and surpasses the brightness of some of the benchmark fluorophores for the same spectral region. The next step should be the modification of the aryl groups, specifically through a pi-extension, to obtain a red shift in the absorption and emission wavelengths.

Comparing the results from the fluorescence studies of the two families of compounds **5** and **6,** it was noticed that the derivatives **6a-f,** containing a phenol-pyridine core, were less emissive than the derivatives **5a-e** that have an anisole-pyridine core. Phenol-pyridine proton bridge induced a dramatic decrease of emission in solution. Molecular orbital calculations would be important to compare the two derivatives **5** and **6** and their HOMO-LUMO gap energies.

The complexation of boron using boron trifluoride diethyl etherate did not produce stable complexes. For more stable complexes, it would be important to try other reagent. Complexation of boron using triphenylborane as alternative might lead to a more stable complex.

Some compounds are also fluorescent in the solid state, which was one of the objectives of this work. The crystal structures showed that compounds **5** and **6** have characteristics, such as torsion angles of the aryl groups, that prevent quenching by π-π stacking, which can explain the solid-state fluorescence. Further studies should include luminescence in crystal form *versus* powder which might reveal the importance of organized molecular structures for the enhancement of luminescence and reveal some quenching effects that possibly happen in non-organized structures. Other interesting analysis is the study of electroluminescence without any complex or after complexation with metals like copper, zinc, or aluminium. The synthesis of a family of

triphenylpyridines with cationization of the pyridine is also to be considered for enhancement of electroluminescence properties.

The aggregation tests did reveal a red shift on emission of compound **6b** when in aggregate form but there was no enhancement of emission, which should be related to quenching phenomena due to the lack of organization like in crystals, or due to the presence of water. It would be important to do an aggregation test with different conditions to reveal the importance of water in the lack of AIEE.

Experimental part

General.

Melting points were measured in a Reichert Thermovar apparatus fitted with a microscope and are uncorrected. NMR spectra were recorded with Bruker DRX 300 spectrometers (300 for ^{1}H and 75 MHz for ^{13}C), in $CDCl_3$ as solvent, if not stated otherwise. Chemical shifts (δ) are reported in ppm and coupling constants (J) in Hz; internal standard was residual peak of the solvent. Unequivocal ^{13}C assignments were made with the aid of 2D gHSQC and gHMBC (delays for one-bond and long-range J C/H couplings were optimised for 145 and 7 Hz, respectively) experiments. High resolution mass spectra analysis (HRMS-ESI) were performed on a microTOF (focus) mass spectrometer. Ions were generated using an ApolloII (ESI) source. Ionization was achieved by electrospray, using a voltage of 4500 V applied to the needle, and a counter voltage between 100 and 150 V applied to the capillary. Absorption spectra were collected with UV-2501PC, emission and excitation spectra were collected with *Jasco* FP-8300 Spectrofluorometer.

Column chromatography was performed with Merck silica gel 60 (70–230 mesh). All other chemicals and solvents used were obtained from commercial sources and were either used as received or dried by standard procedures.

Synthesis of Kröhnke salts

Synthesis of [1-(2-oxo-2-phenylethyl)pyridin-1-ium iodide] (**1a**)[59]

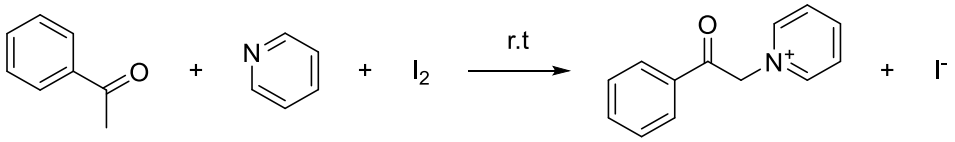

Acetophenone (1 equivalent, 4 mmol, 481 mg) was dissolved in pyridine (3 mL), iodine (1.2 equivalent, 4.8 mmol, 1.22g) was added and the resulting solution was stirred at room temperature for 7 hours. A light-yellow precipitate had formed. It was collected

by filtration, washed with water/MeOH (4/1, 10 mL) and air dried at 55ºC. Compound **1a** was obtained as a light-yellow solid (1.26g, 96% yield).

^{1}H NMR (300 MHz, DMSO-d6) δ 9.04 – 8.94 (m, 2H), 8.75 (ddd, J = 7.8, 6.5, 1.4 Hz, 1H), 8.28 (dd, J = 7.9, 6.5 Hz, 2H), 8.14 – 7.99 (m, 2H), 7.87 – 7.76 (m, 1H), 7.63 – 7.73 (m, 2H), 6.48 (s, 2H).

Synthesis of [1-(2-oxo-2-phenylethyl)pyridin-1-ium bromide] (**1b**)[60]

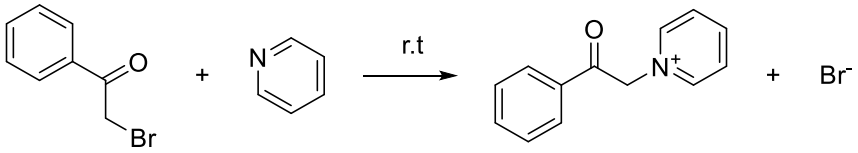

The 2-bromoacetophenone (1 equivalent, 4 mmol, 796 mg) was dissolved in pyridine (3 mL), the resulting solution was stirred at room temperature for 4 hours. A light-yellow precipitate had formed, and it was collected by filtration, washed with water/MeOH (4/1, 10 mL) and air dried at 55ºC. Compound **1b** was obtained as a light-yellow solid (1.0g, 90% yield).

^{1}H NMR (300 MHz, Acetone-d6) δ 9.49 – 9.35 (m, 2H), 8.95 – 8.81 (m, 1H), 8.48 – 8.29 (m, 2H), 8.26 – 8.13 (m, 2H), 7.81 – 7.73 (m, 1H), 7.59 – 7.69 (m, 2H), 7.06 (s, 2H).

Synthesis of the chalcone [(*E*)-1-(2-hydroxyphenyl)-3-(*p*-tolyl)prop-2-en-1-one][61]

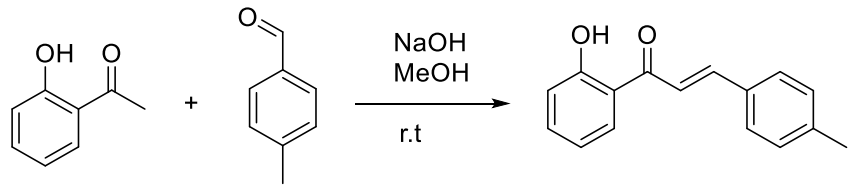

The 2′-hydroxyacetophenone (1 equivalent, 4 mmol, 550 mg) and NaOH (2 equivalent, 8 mmol, 320mg) were dissolved in MeOH (30 mL). 4-methylbenzaldehyde (1 equivalent, 4 mmol, 480mg) was added. After stirring at room temperature for 12 hours a yellow paste had formed. After evaporating the solvent under vacuum, water was added, and the product was extracted with DCM. The organic extract was dried over anhydrous sodium sulphate and then concentrated in vacuum, and a column

chromatography (CH_2Cl_2) of the organic extract was used to purify the product. [(*E*)-1-(2-hydroxyphenyl)-3-(*p*-tolyl)prop-2-en-1-one] was obtained as a yellow solid (578 mg, 61% yield).

^{1}H NMR (300 MHz, Chloroform-d) δ 16.3 (s,1H), 7.59 (d, J = 15.5 Hz, 1H), 7.59 (d, J = 1.8 Hz, 1H), 7.42 – 7.52 (m, 2H), 7.31 (d, J = 15.9 Hz, 1H), 7.20 (d, J = 7.7 Hz, 1H), 7.10 – 6.96 (m, 2H), 2.38 (s, 3H).

Synthesis of [1-(2-methoxyphenyl)ethan-1-one] (**2a**)[62]

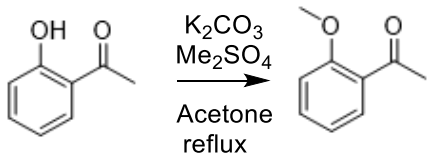

The 2′-hydroxyacetophenone (1 equivalent, 7 mmol, 1.05g) was dissolved in acetone (20mL), dimethyl sulphate (1 equivalent, 7 mmol, 0.88g) and potassium carbonate (1 equivalent, 7mmol, 0.97g) were added, and the resulting solution was refluxed for 6h, then stirred at RT for 12h. Water was added, and the product was extracted with DCM. The organic extract was dried with anhydrous sodium sulphate and then concentrated in vacuum, and a column chromatography (CH_2Cl_2/Hex 4:1) of the organic extract was used to purify the product. The compound **2a** was obtained as a colourless oil (1.25g. 92% yield).

^{1}H NMR (300 MHz, Chloroform-d) δ 7.73 (dd, J = 7.7, 1.8 Hz, 1H), 7.46 (ddd, J = 8.3, 7.3, 1.9 Hz, 1H), 7.02 – 6.94 (m, 2H), 3.91 (s, 3H), 2.61 (s, 3H).

Synthesis of chalcones 4a-4e

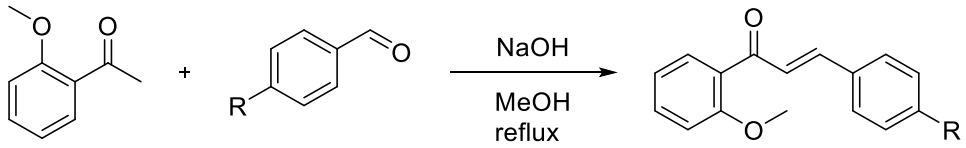

General Procedure

The chalcones **4a** to **4e** were obtained following a Claisen–Schmidt condensation with acetophenone **2a** (1 equivalent), benzaldehyde **3a**-**3e** (1 equivalent) and NaOH (2

equivalent) dissolved in MeOH. The resulting solution was stirred under reflux for 4 h and then left at room temperature for 12h. Purification: An extraction with H_2O/CH_2Cl_2 was performed, the organic extract was dried with anhydrous sodium sulphate and then concentrated in vacuum, and a column chromatography (CH_2Cl_2/Hex 4:1) of the organic extract was used to purify the product. Yield: 60-80%.

Synthesis of [(*E*)-1-(2-methoxyphenyl)-3-phenylprop-2-en-1-one] (**4a**)[63]

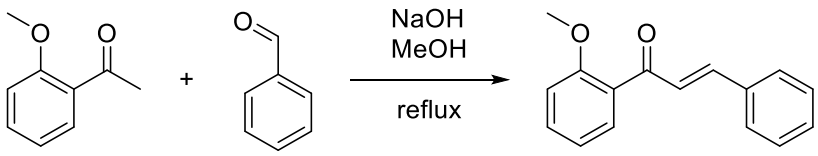

The acetophenone **2a** (1 equivalent, 3 mmol, 450 mg) and NaOH (2 equivalent, 6 mmol, 240mg) were dissolved in MeOH (15 mL). Benzaldehyde **3a** (1 equivalent, 3 mmol, 318mg) was added to the solution. After stirring at room temperature for 12h a light-yellow paste had formed. After evaporating the solvent under vacuum, water was added, and the product was extracted with DCM. The organic extract was dried with anhydrous sodium sulphate and then concentrated in vacuum, and a column chromatography (CH_2Cl_2) of the organic extract was used to purify the product. The compound **4a** was obtained as a light-yellow solid (508 mg, 71% yield).

^{1}H NMR (300 MHz, Chloroform-d) δ 7.66 – 7.57 (m, 4H), 7.48 (ddd, J = 8.4, 7.4, 1.8 Hz, 1H), 7.42 – 7.34 (m, 4H), 3.91 (s, 3H).

Synthesis of [(*E*)-1-(2-methoxyphenyl)-3-(*p*-tolyl)prop-2-en-1-one] (**4b**)[64]

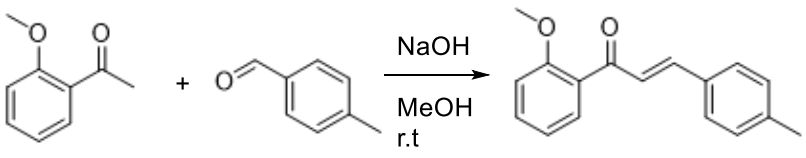

The acetophenone **2a** (1 equivalent, 2 mmol, 300 mg) and NaOH (2 equivalent, 4 mmol, 160mg) were dissolved in MeOH (15 mL). 4-methylbenzaldehyde **3b** (1 equivalent, 2 mmol, 240mg) was added to the solution. After stirring at room temperature for 12h a light-yellow paste had formed. After evaporating the solvent in vacuum, water was

added, and the product was extracted with CH_2Cl_2. The organic extract was dried with anhydrous sodium sulphate and then concentrated in vacuum, and a column chromatography (CH_2Cl_2) of the organic extract was used to purify the product. The compound **4b** was obtained as a light-yellow solid (322 mg, 77% yield).

^{1}H NMR (300 MHz, Chloroform-d) δ 7.59 (d, J = 15.5 Hz, 1H), 7.59 (d, J = 1.8 Hz, 1H), 7.42 – 7.52 (m, 2H), 7.31 (dd, J = 15.9 Hz, 1H), 7.20 (d, J = 7.7 Hz, 1H), 7.10 – 6.96 (m, 2H), 3.89 (s, 3H), 2.38 (s, 3H).

Synthesis of [(*E*)-1-(2-methoxyphenyl)-3-(4-methoxyphenyl)pro*p*-2-en-1-one] (**4c**)

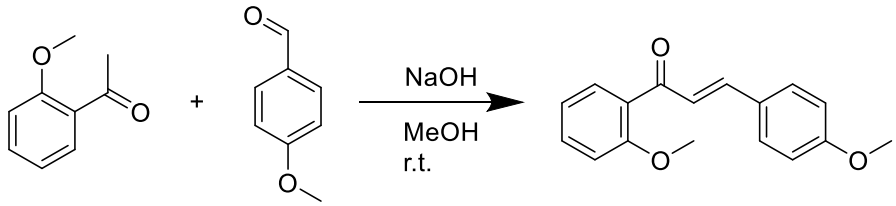

The acetophenone **2a** (1 equivalent, 2 mmol, 300 mg) and NaOH (2 equivalent, 4 mmol, 160mg) were dissolved in MeOH (15 mL). 4-methoxybenzaldehyde **3c** (1 equivalent, 2 mmol, 272mg) was added to solution. After stirring at room temperature for 12h a light-yellow paste was formed. After evaporating the solvent in vacuum, water was added, and the product was extracted with CH_2Cl_2. The organic extract was dried with anhydrous sodium sulphate and then concentrated in vacuum, and a column chromatography (CH_2Cl_2) of the organic extract was used to purify the product. The compound **4c** was obtained as a light-yellow solid (242 mg, 45% yield).

^{1}H NMR (300 MHz, Chloroform-d) δ 7.62 – 7.51 (m, 4H), 7.46 (ddd, J = 8.3, 7.4, 1.8 Hz, 1H), 7.23 (d, J = 16.1 Hz, 2H), 7.07 – 6.97 (m, 2H), 6.91 (d, J = 8.8 Hz, 2H), 3.90 (s, 3H), 3.85 (s, 3H).

Synthesis of [(E)-3-(4-(dimethylamino)phenyl)-1-(2-methoxyphenyl)prop-2-en-1-one] (**4d**)[65]

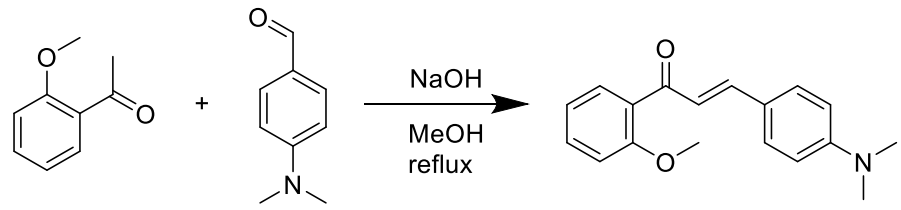

The acetophenone **2a** (1 equivalent, 2 mmol, 300 mg) and NaOH (2 equivalent, 4 mmol, 160mg) were dissolved in MeOH (15 mL). 4-(dimethylamino)benzaldehyde **3d** (1 equivalent, 2 mmol, 298mg) was added to solution. After stirring at reflux for 6h and left at room temperature for 16h a yellow paste was formed. After evaporating the solvent in vacuum, water was added, and the product was extracted with CH_2Cl_2. The organic extract was dried with anhydrous sodium sulphate and then concentrated in vacuum, and a column chromatography (CH_2Cl_2) of the organic extract was used to purify the product. The compound **4d** was obtained as a bright-yellow solid (433 mg, 70% yield).

^{1}H NMR (300 MHz, Chloroform-d) δ 7.63 – 7.37 (m, 5H), 7.12 (d, J = 15.8 Hz, 1H), 7.07 – 6.89 (m, 2H), 6.67 (d, J = 8.9 Hz, 2H), 3.88 (s, 3H), 3.03 (s, 6H).

Synthesis of [(*E*)-1-(2-methoxyphenyl)-3-(4-nitrophenyl)prop-2-en-1-one] (**4e**)

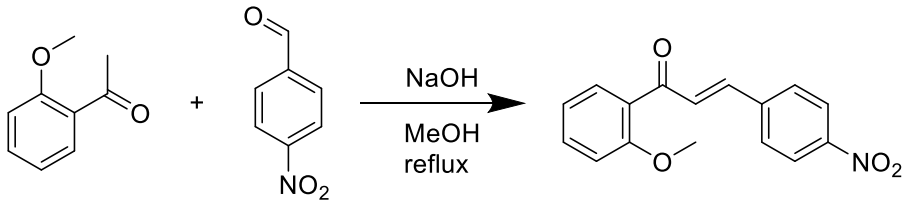

The acetophenone **2a** (1 equivalent, 2 mmol, 300 mg) and NaOH (2 equivalent, 4 mmol, 160mg) were dissolved in MeOH (15 mL). 4-nitrobenzaldehyde **3e** (1 equivalent, 2 mmol, 302mg) was added to solution. After stirring at room temperature for 16h a yellow paste was formed. After evaporating the solvent in vacuum, water was added, and the product was extracted with CH_2Cl_2. The organic extract was dried with

anhydrous sodium sulphate and then concentrated in vacuum, and a column chromatography (CH_2Cl_2) of the organic extract was used to purify the product. The compound **4e** was obtained as a orange-yellow solid (450 mg, 79% yield)

^{1}H NMR (300 MHz, Chloroform-d) δ 8.26 (d, J = 8.8 Hz, 2H), 7.78 – 7.62 (m, 4H), 7.58 – 7.48 (m, 2H), 7.13 – 6.98 (m, 2H), 3.94 (s, 3H).

Synthesis of the pyridines 5a-5e

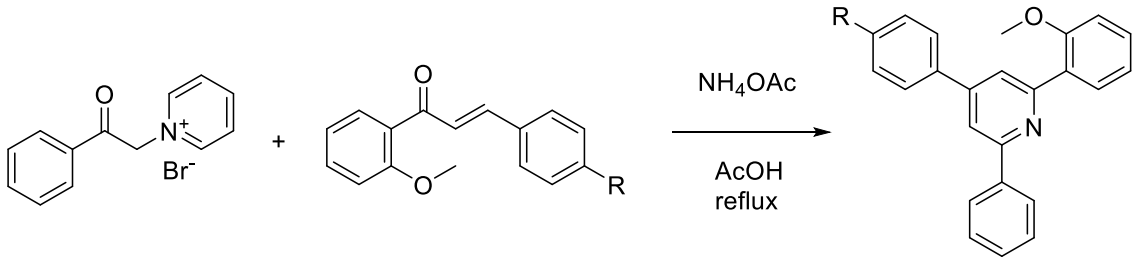

General Procedure:

The triphenyl pyridines **5a**-**5e** were obtained by a modified Kröhnke *via*. First a pyridinium salt derivative (1 equivalent) was dissolved in AcOH (4 mL), a chalcone derivative (1 equivalent) was added and after a clear solution was observed, ammonium acetate (30 equivalents) was poured. The resulting solution was stirred at reflux for 7 hours and left stirring 12 hours at room temperature. Purification: Filtration if there was a precipitate formed and washed with water/MeOH (4/1, 10 mL) or water was added and the product was extracted with DCM, the organic extract was dried with anhydrous sodium sulphate and then concentrated in vacuum, and a column chromatography (CH_2Cl_2/Hex 4:1) of the organic extract was used to purify the product. Yield: 20-50%.

Synthesis of [2-(2-methoxyphenyl)-4,6-diphenylpyridine] (**5a**)

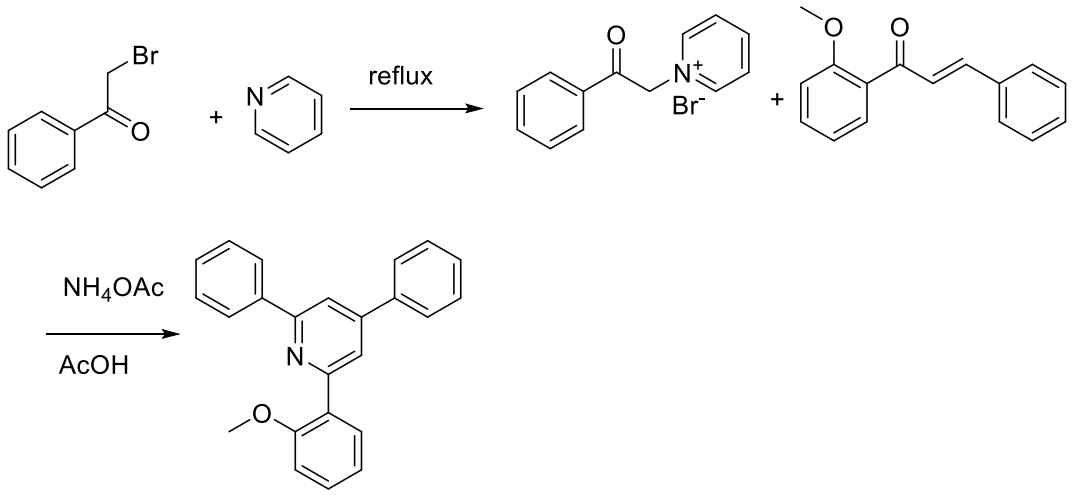

The 2-bromoacetophenone (1 equivalent, 2 mmol, 398 mg) was dissolved in an excess of pyridine (1 mL) and the resulting solution was stirred at room temperature for 4 hours. A light-yellow precipitate had formed. The excess pyridine was removed by evaporation, and the resulting solid was dissolved in AcOH (4 mL). The chalcone **4a** (1 equivalent, 2 mmol, 488 mg) was added, followed by ammonium acetate (15 equivalent, 30 mmol, 2.31 g), and the resulting solution was stirred at reflux temperature for 7 hours and for 12 hours at room temperature. The solution was neutralized to pH≈7 with water and NaOH. An extraction with CH_2Cl_2 was performed, the organic extract was dried with anhydrous sodium sulphate and then concentrated in vacuum, and a column chromatography (CH_2Cl_2/Hex 4:1) of the organic extract was used to purify the product. The compound **5a** was obtained as a light greenish oil (324 mg, 48% yield).

^{1}H NMR (300 MHz, Chloroform-d) δ 8.19 – 8.13 (m, 2H), 8.09 – 8.00 (m, 2H), 7.87 (d, J = 1.5 Hz, 1H), 7.79 – 7.71 (m, 2H), 7.57 – 7.35 (m, 7H), 7.14 (td, J = 7.5, 1.1 Hz, 1H), 7.05 (dd, J = 8.3, 1.0 Hz, 1H), 3.91 (s, 3H). ^{13}C NMR (75 MHz, Chloroform-d) δ 157.53, 157.36, 156.22, 139.38, 131.71, 130.17, 129.19, 128.99, 128.94, 128.79, 127.43, 127.31, 122.03, 121.25, 117.03, 111.64, 55.91 (O-CH_3). ESI$^+$-MS: 338.2 $[M+H]^+$

Synthesis of [2-(2-methoxyphenyl)-6-phenyl-4-(*p*-tolyl)pyridine] (**5b**)

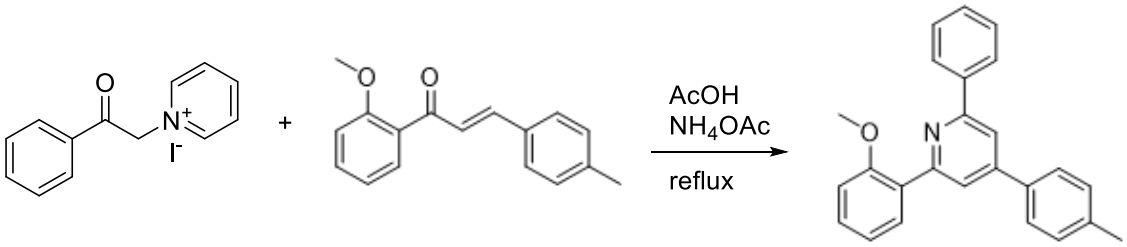

The Kröhnke salt **1a** (1 equivalent, 0,5 mmol, 550 mg) was dissolved in AcOH (4 mL). The chalcone **4b** (1 equivalent, 0.5 mmol, 162 mg) was added, followed by ammonium acetate (15 equivalents, 7.5 mmol, 578 mg), and the resulting solution was stirred at reflux temperature for 7 hours. After stirring 12 hours at room temperature, a yellow precipitate had formed. It was collected by filtration, washed with water/MeOH (4/1, 10 mL) and air dried at 55ºC. The compound **5b** was obtained as a light yellow solid (83 mg, 47% yield).

Mp 159ºC-160ºC. ^{1}H NMR (300 MHz, Chloroform-d) δ 8.17 – 8.10 (m, 2H), 8.01 (d, J =1.5 Hz, 1H), 8.01 (d, J = 8.2, 1H), 7.86 (d, J = 1.5 Hz, 1H), 7.65 (d, J = 8.2 Hz, 2H), 7.54 – 7.37 (m, 4H), 7.36 – 7.31 (m, 2H), 7.14 (td, J = 7.5, 1.0 Hz, 1H), 7.05 (dd, J = 8.3, 1.0 Hz, 1H), 3.91 (s, 3H), 2.44 (s, 3H). ^{13}C NMR (75 MHz, Chloroform-d) δ 157.36 (C=N), 157.22(C=N), 156.03(C-O), 148.96, 139.79, 138.90, 136.27, 131.57, 130.00, 129.78, 128.82, 128.65, 127.20, 127.13, 121.69, 121.11, 116.72, 111.52, 55.78(O-CH_3), 21.28(Ph-CH_3). ESI$^+$-MS: 352.2 $[M+H]^+$

Synthesis of [2-(2-methoxyphenyl)-4-(4-methoxyphenyl)-6-phenylpyridine] (**5c**)

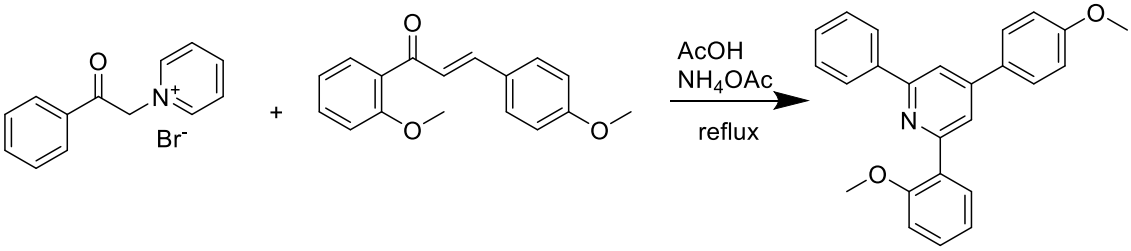

The Kröhnke salt **1b** (1 equivalent, 1.3 mmol, 362 mg) was dissolved in AcOH (4 mL). The chalcone **4c** (1 equivalent, 1.3 mmol, 349 mg) was added, followed by ammonium acetate (15 equivalents, 19.5 mmol, 1.5 g), and the resulting solution was stirred at reflux temperature for 7 hours and 12 hours at room temperature The solution was

neutralized to pH≈7 with water and NaOH. An extraction with CH_2Cl_2 was performed, the organic extract was dried with anhydrous sodium sulphate and then concentrated in vacuum, and a column chromatography (CH_2Cl_2/Hex 4:1) of the organic extract was used to purify the product. The compound **5c** was obtained as a light green solid (176 mg, 37% yield).

Mp 139ºC-141ºC. ^1H NMR (300 MHz, Chloroform-d) δ 8.16 (ddd, J = 8.2, 1.8, 1.0 Hz, 2H), 8.08 – 7.95 (m, 2H), 7.84 (d, J = 1.5 Hz, 1H), 7.71 (dd, J = 8.9, 0.9 Hz, 2H), 7.55 – 7.47 (m, 2H), 7.47 – 7.38 (m, 2H), 7.15 (td, J = 7.5, 1.1 Hz, 1H), 7.08 – 7.02 (m, 3H), 3.91 (s, 3H), 3.89 (s, 3H). ^{13}C NMR (75 MHz, Chloroform-d) δ 160.41, 157.50, 157.31, 156.18, 148.51, 140.09, 131.67, 131.63, 130.02, 129.61, 128.85, 128.74, 128.51, 127.25, 121.46, 121.22, 116.42, 114.56, 111.63, 55.88(O-CH_3), 55.51(O-CH_3). ESI^+-MS: 368.2 $[M+H]^+$

Synthesis of [4-(2-(2-methoxyphenyl)-6-phenylpyridin-4-yl)-N,N-dimethylaniline] (**5d**)

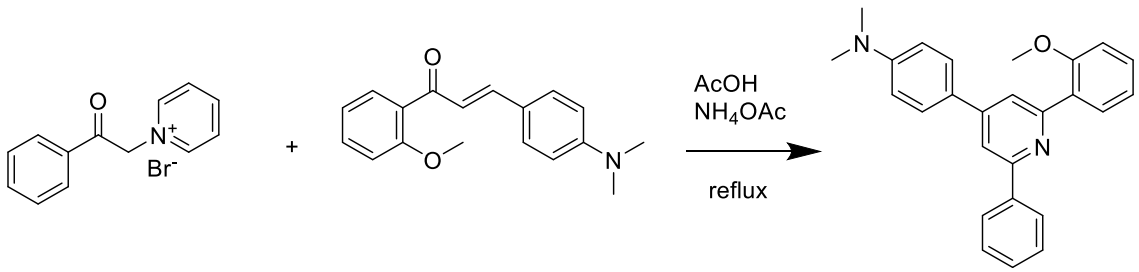

The Kröhnke salt **1b** (1 equivalent, 1.6 mmol, 445 mg) was dissolved in AcOH (4 mL). The chalcone **4d** (1 equivalent, 1.6 mmol, 457 mg) was added, followed by ammonium acetate (15 equivalents, 24 mmol, 1.85 g), and the resulting solution was stirred at reflux temperature for 7 hours and 12 hours at room temperature The solution was neutralized to pH≈7 with water and NaOH. An extraction with CH_2Cl_2 was performed, the organic extract was dried with anhydrous sodium sulphate and then concentrated in vacuum, and a column chromatography (CH_2Cl_2/Hex 4:1) of the organic extract was used to purify the product. The compound **5d** was obtained as an orange solid (147 mg, 24% yield).

Mp 146ºC-149ºC. ^{1}H NMR (300 MHz, Chloroform-d) δ 8.18 – 8.10 (m, 2H), 7.97 – 8.02 (m, 2H), 7.84 (d, J = 1.6 Hz, 1H), 7.72 – 7.64 (m, 2H), 7.55 – 7.45 (m, 2H), 7.45 – 7.35 (m, 2H), 7.13 (td, J = 7.5, 1.1 Hz, 1H), 7.04 (dd, J = 8.3, 1.0 Hz, 1H), 6.84 (d, J = 8.9 Hz, 2H), 3.90 (s, 3H), 3.04 (s, 6H). ^{13}C NMR (75 MHz, Chloroform-d) δ 157.41, 157.33, 156.04, 151.06, 148.83, 140.36, 131.68, 129.88, 128.70, 128.06, 127.29, 126.52, 121.20, 120.89, 115.94, 112.62, 111.65, 55.92(O-CH_3), 40.54(N-CH_3). ESI$^+$-MS: 381.2 $[M+H]^+$

Synthesis of [2-(2-methoxyphenyl)-4-(4-nitrophenyl)-6-phenylpyridine] (**5e**)

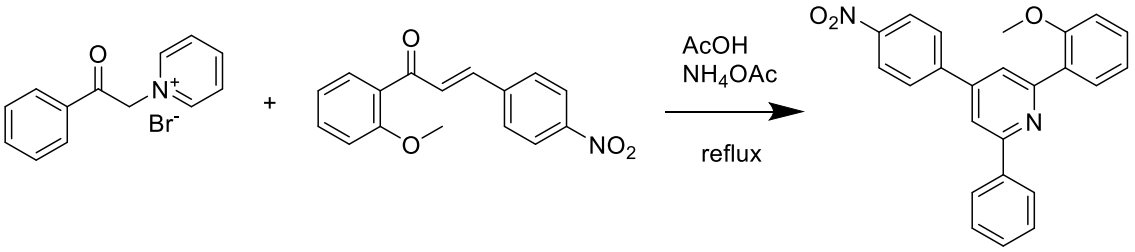

The Kröhnke salt **1b** (1 equivalent, 1.6 mmol, 445 mg) was dissolved in AcOH (4 mL). The chalcone **4e** (1 equivalent, 1.6 mmol, 450 mg) was added, followed by ammonium acetate (15 equivalents, 24 mmol, 1.85 g), and the resulting solution was stirred at reflux temperature for 7 hours and 12 hours at room temperature The solution was neutralized to pH≈7 with water and NaOH. An extraction with CH_2Cl_2 was performed, the organic extract was dried with anhydrous sodium sulphate and then concentrated in vacuum, and a column chromatography (CH_2Cl_2/Hex 4:1) of the organic extract was used to purify the product. The compound **5e** was obtained as a light yellow solid (295 mg, 48% yield).

Mp 162ºC-163ºC. ^{1}H NMR (300 MHz, Chloroform-d) δ 8.38 (d, J = 8.8 Hz, 2H), 8.22 – 8.12 (m, 2H), 8.06 (dd, J = 8.2, 1.6 Hz, 2H), 7.94 – 7.82 (m, 3H), 7.61 – 7.37 (m, 4H), 7.16 (td, J = 7.5, 1.0 Hz, 1H), 7.06 (dd, J = 8.3, 1.0 Hz, 1H), 3.92 (s, 3H). ^{13}C NMR (75 MHz, Chloroform-d) δ 157.96, 157.33, 156.65, 148.17, 146.75, 145.86, 139.36, 131.69,

130.54, 129.36, 128.91, 128.77, 128.35, 127.26, 124.46, 121.95, 121.35, 116.74, 111.64, 55.90(O-CH_3). ESI^+-MS: 383.2 $[M+H]^+$

Synthesis of compounds 6a-6f

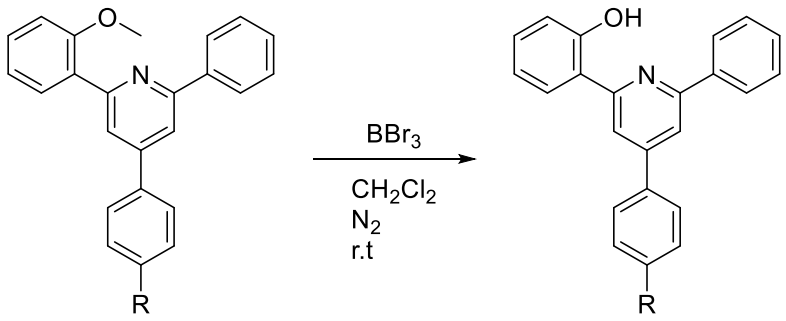

General Procedure

The pyridines **6a** to **6e** were obtained by O-demethylation of anisole groups with BBr_3. To each pyridine derivative **5a**-**5e** (1 equivalent) was added BBr_3 (1 equivalent) in dry CH_2Cl_2 as solvent under N_2 atmosphere. The resulting solution was left at room temperature for 12h. Purification: water was added, an extraction with CH_2Cl_2 was performed, the organic extract was dried with anhydrous sodium sulphate and then concentrated in vacuum, and a column chromatography (CH_2Cl_2/Hex 4:1) of the organic extract was used to purify the product. Yield: 37-95%.

Synthesis of [2-(4,6-diphenylpyridin-2-yl)phenol] (**6a**)

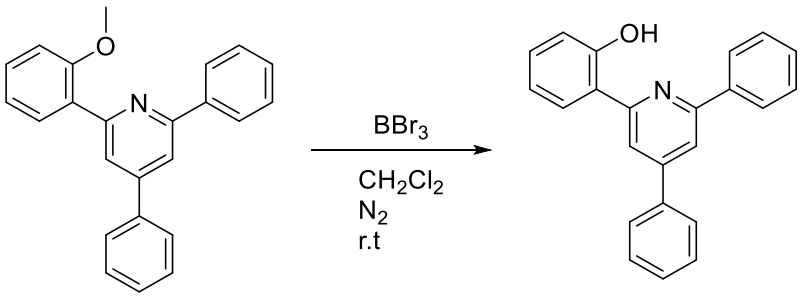

Pyridine **5a** (1 equivalent, 0.35 mmol, 118 mg) was dissolved in CH_2Cl_2 (5 mL) under N_2 atmosphere. BBr_3 (1.1 equivalent, 0.39 mmol, 0.39 mL, 1M in methylene chloride solution) was slowly added, the resulting solution was stirred for 16 hours at room temperature. Water was added, an extraction with CH_2Cl_2 was performed, the organic extract was dried with anhydrous sodium sulphate and then concentrated in vacuum,

and a column chromatography (CH_2Cl_2) of the organic extract was used to purify the product. The compound **6a** was obtained as a light yellow-green solid (108 mg, 95% yield).

Mp 165-168ºC. ^{1}H NMR (500 MHz, Chloroform-d) δ 14.85 (s, 1H), 8.07 (d, J = 1.4 Hz, 1H), 8.03 – 7.98 (m, 2H), 7.96 (dd, J = 8.0, 1.6 Hz, 2H), 7.85 (d, J = 1.4 Hz, 1H), 7.79 – 7.73 (m, 2H), 7.59 – 7.48 (m, 6H), 7.36 (ddd, J = 8.5, 7.2, 1.6 Hz, 1H), 7.08 (dd, J = 8.2, 1.3 Hz, 1H), 6.96 (ddd, J = 8.2, 7.1, 1.3 Hz, 1H). ^{13}C NMR (126 MHz, Chloroform-d) δ 160.26, 158.21, 155.43, 151.50, 138.70, 138.22, 131.82, 129.85, 129.61, 129.41, 129.30, 127.42, 127.15, 126.55, 119.14, 119.02, 118.75, 117.46, 115.97. ESI$^+$-MS: 324.2 $[M+H]^+$

Synthesis of [2-(6-phenyl-4-(*p*-tolyl)pyridin-2-yl)phenol] **(6b)**

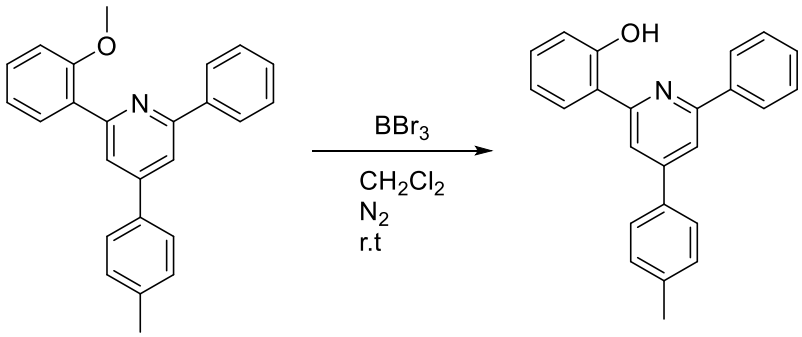

Pyridine **5b** (1 equivalent, 0.7 mmol, 240 mg) was dissolved in CH_2Cl_2 (5 mL) under N_2 atmosphere. BBr_3 (1.1 equivalent, 0.8 mmol, 0.8 mL, 1M in methylene chloride solution) was slowly added, the resulting solution was stirred for 16 hours at room temperature. Water was added, an extraction with $CH_2Cl_2$was performed, the organic extract was dried with anhydrous sodium sulphate and then concentrated in vacuum, and a column chromatography (CH_2Cl_2) of the organic extract was used to purify the product. The compound **6b** was obtained as a pale yellow solid (213 mg, 90% yield).

Mp 192-193ºC. ^{1}H NMR (300 MHz, Chloroform-d) δ 8.07 (d, J = 1.4 Hz, 1H), 8.02 – 7.97 (m, 2H), 7.95 (dd, J = 8.1, 1.6 Hz, 1H), 7.85 (dd, J = 1.5, 0.5 Hz, 1H), 7.67 (d, J = 8.2 Hz, 2H), 7.59 – 7.48 (m, 3H), 7.41 – 7.32 (m, 3H), 7.14 (dd, J = 8.2, 1.2 Hz, 1H), 7.01 – 6.92 (m, 1H), 2.46 (s, 3H). ^{13}C NMR (126 MHz, Chloroform-d) δ 160.19,

157.87, 155.11, 151.67, 140.01, 137.92, 135.55, 131.96, 130.17, 129.96, 129.35, 127.26, 127.14, 126.58, 119.10, 118.91, 118.83, 117.29, 115.77, 21.47. ESI$^+$-MS: 338.2 $[M+H]^+$

Synthesis of [2-(4-(4-hydroxyphenyl)-6-phenylpyridin-2-yl)phenol] **6c**[53]

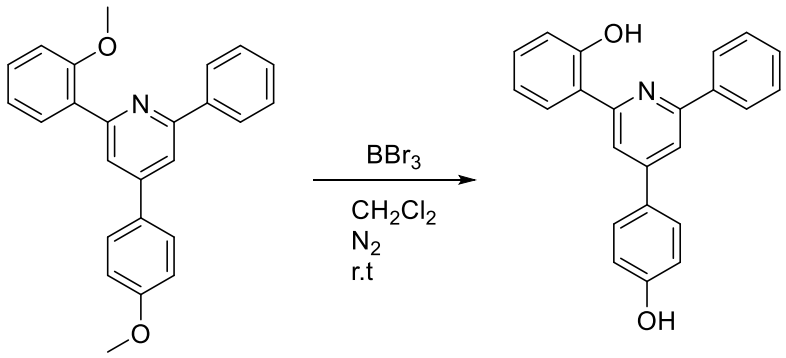

Pyridine **5c** (1 equivalent, 0.3 mmol, 127 mg) was dissolved in CH_2Cl_2 (5 mL) under N_2 atmosphere. BBr_3 (2 equivalent, 0.6 mmol, 0.6 mL, 1M in methylene chloride solution) was slowly added, the resulting solution was stirred for 16 hours at room temperature. The precipitate that had formed was collected by filtration and washed with diethyl ether. The compound **6c** was obtained as an orange solid (80 mg, 79% yield).

Mp 236-237ºC. ^{1}H NMR (500 MHz, Methanol-d4) δ 8.23 (d, J = 1.4 Hz, 1H), 8.13 (dd, J = 7.9, 1.6 Hz, 1H), 8.07 – 8.02 (m, 2H), 8.00 (d, J = 1.4 Hz, 1H), 7.81 (d, J = 8.6 Hz, 2H), 7.59 (t, J = 7.4 Hz, 2H), 7.55 – 7.50 (m, 1H), 7.34 (ddd, J = 8.6, 7.3, 1.6 Hz, 1H), 7.04 – 6.95 (m, 4H). ^{13}C NMR (126 MHz, Methanol-d4) δ 160.88, 160.50, 159.29, 156.53, 152.75, 139.76, 132.47, 130.69, 130.27, 130.21, 129.78, 127.95, 120.50, 120.27, 119.07, 117.52, 117.12, 115.97, 30.68. ESI$^+$-MS: 340.2 $[M+H]^+$

Synthesis of [2-(4-(4-(dimethylamino)phenyl)-6-phenylpyridin-2-yl)phenol] **(6d)**[60]

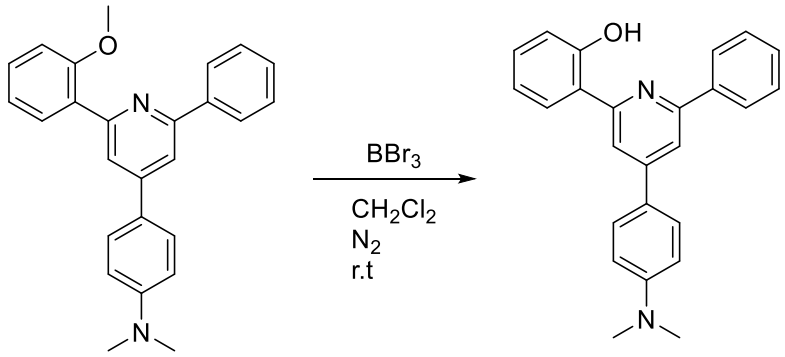

Pyridine **5d** (1 equivalent, 0.3 mmol, 112 mg) was dissolved in CH_2Cl_2 (5 mL) under N_2 atmosphere. BBr_3 1M in methylene chloride solution (1.1 equivalent, 0.33 mmol, 0.33 mL) was slowly added, the resulting solution was stirred for 16 hours at room temperature. Water was added, an extraction with CH_2Cl_2 was performed, the organic extract was dried with anhydrous sodium sulphate and then concentrated in vacuum, and a column chromatography (CH_2Cl_2) of the organic extract was used to purify the product. The compound **6d** was obtained as an orange solid (40 mg, 36% yield).

Mp 247-250ºC ^{1}H NMR (300 MHz, Chloroform-d) δ 15.08 (s, 1H), 8.06 – 7.92 (m, 4H), 7.81 (d, J = 1.5 Hz, 1H), 7.70 (d, J = 8.9 Hz, 2H), 7.58 – 7.46 (m, 3H), 7.34 (ddd, J = 8.6, 7.2, 1.6 Hz, 1H), 7.06 (dd, J = 8.2, 1.3 Hz, 1H), 6.95 (ddd, J = 8.3, 7.2, 1.3 Hz, 1H), 6.85 (d, J = 9.0 Hz, 2H), 3.06 (s, 6H). ^{13}C NMR (75 MHz, Chloroform-d) δ 160.36, 157.93, 155.06, 151.45, 151.05, 138.64, 131.49, 129.56, 129.18, 128.11, 127.10, 126.46, 125.48, 119.45, 118.83, 118.66, 116.18, 114.44, 112.63, 40.46.

Synthesis of [2-(4-(4-nitrophenyl)-6-phenylpyridin-2-yl)phenol] **(6e)**

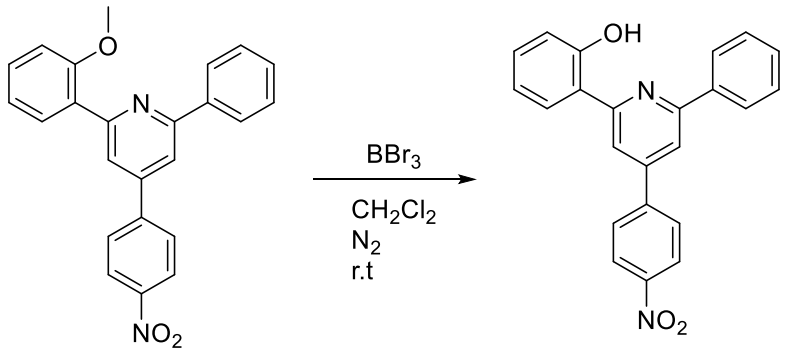

Pyridine **5e** (1 equivalent, 0.8 mmol, 292 mg) was dissolved in CH_2Cl_2 (5 mL) under N_2 atmosphere. BBr_3 (1.1 equivalent, 0.9 mmol, 0.9 mL, 1M in methylene chloride solution) was slowly added, the resulting solution was stirred for 16 hours at room temperature. Water was added, an extraction with CH_2Cl_2 was performed, the organic extract was dried with anhydrous sodium sulphate and then concentrated in vacuum, and a column chromatography (CH_2Cl_2) of the organic extract was used to purify the product. The compound **6e** was obtained as a yellow solid (266 mg, 90% yield).

Mp 233-234ºC. ^{1}H NMR (500 MHz, Chloroform-d) δ 14.53 (s, 1H), 8.42 (d, J = 8.7 Hz, 2H), 8.05 (d, J = 1.4 Hz, 1H), 8.01 (dd, J = 8.2, 1.4 Hz, 2H), 7.96 – 7.89 (m, 3H), 7.84 (d, J = 1.4 Hz, 1H), 7.61 – 7.47 (m, 3H), 7.38 (ddd, J = 8.4, 7.1, 1.6 Hz, 1H), 7.09 (dd, J = 8.2, 1.2 Hz, 1H), 6.98 (ddd, J = 8.3, 7.1, 1.3 Hz, 1H). ^{13}C NMR (126 MHz, Chloroform-d) δ 160.25, 158.77, 156.12, 149.09, 148.56, 145.05, 137.80, 132.25, 130.21, 129.42, 128.49, 127.18, 126.58, 124.64, 119.22, 118.90, 118.80, 117.28, 116.01. ESI$^+$-MS: 369.2 $[M+H]^+$

References

1. Lakowicz, J. R. Chapter 1 Principles of Fluorescence. *Princ. Fluoresc. Spectrosc.* 1–26 (2006).

2. Valeur, B. & Berberan-Santos, M. N. *Handbook of Fluorescence Spectroscopy and Imaging Fluorescence Applications in Biotechnology and Life Sciences Surface Enhanced Raman Spectroscopy Applied and Industrial Photochemistry*. (2012).

3. Yan, Z., Wang, Y., Ding, J., Wang, Y. & Wang, L. Highly Efficient Phosphorescent Furo[3,2-c]pyridine Based Iridium Complexes with Tunable Emission Colors over the Whole Visible Range. *ACS Appl. Mater. Interfaces* **10**, 1888–1896 (2018).

4. Fujisawa, J. An unusual mechanism for HOMO–LUMO gap narrowing in a minimal near-IR dye generated by the deprotonation of bis(dicyanomethylene)indan. *Chem. Phys. Lett.* **608**, 355–359 (2014).

5. Marcu, L., French, P. M. W. & Elson, D. S. *Fluorescence Lifetime Spectroscopy and Imaging*. (CRC Press, 2014). doi:10.1201/b17018

6. Whitaker, J. E., Haugland, R. P. & Prendergast, F. G. Spectral and photophysical studies of benzo[c]xanthene dyes: Dual emission pH sensors. *Anal. Biochem.* **194**, 330–344 (1991).

7. Liu, Z. *et al.* Trivalent Boron as an Acceptor in Donor–π–Acceptor-Type Compounds for Single-and Two-Photon Excited Fluorescence. *Chem. -A Eur. J.* **9**, 5074–5084 (2003).

8. Tarkuç, S., Eelkema, R. & Grozema, F. C. The relationship between molecular structure and electronic properties in dicyanovinyl substituted acceptor-donor-acceptor chromophores. *Tetrahedron* **73**, 4994–5004 (2017).

9. Kim, J. H., Lee, D. R., Han, S. H. & Lee, J. Y. Over 20% external quantum efficiency in red thermally activated delayed fluorescence organic light-emitting diodes using a reverse intersystem crossing activating host. *J. Mater. Chem. C* **6**,

5363–5368 (2018).

10. Sasaki, S., Drummen, G. P. C. & Konishi, G. Recent advances in twisted intramolecular charge transfer (TICT) fluorescence and related phenomena in materials chemistry. *J. Mater. Chem. C* **4**, 2731–2743 (2016).

11. Dobkowski, J. *et al.* Substituent and Solvent Effects on the Excited State Deactivation Channels in Anils and Boranils. *Chem. -A Eur. J.* **21**, 1312–1327 (2015).

12. Benelhadj, K. *et al.* Solution-and Solid-State Luminescent Borate Complexes Based on a Substituted π-Conjugated 2-(6′-Hydroxy-5′-benzofuryl) Scaffold. *European J. Org. Chem.* **2014**, 7156–7164 (2014).

13. Chen, S. *et al.* Boranil dyes bearing tetraphenylethene: Synthesis, AIE/AIEE effect properties, pH sensitive properties and application in live cell imaging. *Tetrahedron Lett.* **59**, 2671–2678 (2018).

14. Frath, D., Benelhadj, K., Munch, M., Massue, J. & Ulrich, G. Polyanils and Polyboranils: Synthesis, Optical Properties, and Aggregation-Induced Emission. *J. Org. Chem.* **81**, 9658–9668 (2016).

15. Vaz, P. A. A. M., Rocha, J., Silva, A. M. S. & Guieu, S. Aggregation-induced emission enhancement in halochalcones. *New J. Chem.* **40**, 8198–8201 (2016).

16. Hong, Y., Lam, J. W. Y. & Tang, B. Z. Aggregation-induced emission. *Chem. Soc. Rev.* **40**, 5361 (2011).

17. Mei, J., Leung, N. L. C., Kwok, R. T. K., Lam, J. W. Y. & Tang, B. Z. Aggregation-Induced Emission: Together We Shine, United We Soar! *Chem. Rev.* **115**, 11718–11940 (2015).

18. Guieu, S., Cardona, F., Rocha, J. & Silva, A. M. S. Tunable Color of Aggregation-Induced Emission Enhancement in a Family of Hydrogen-Bonded Azines and Schiff Bases. *Chem. -A Eur. J.* **24**, 17262–17267 (2018).

19. Qin, W. *et al.* Biocompatible Nanoparticles with Aggregation-Induced Emission

Characteristics as Far-Red/Near-Infrared Fluorescent Bioprobes for In Vitro and In Vivo Imaging Applications. *Adv. Funct. Mater.* **22**, 771–779 (2012).

20. Li, D., Zhang, H. & Wang, Y. Four-coordinate organoboron compounds for organic light-emitting diodes (OLEDs). *Chem. Soc. Rev.* **42**, 8416 (2013).

21. Rao, Y.-L. & Wang, S. Four-Coordinate Organoboron Compounds with a π-Conjugated Chelate Ligand for Optoelectronic Applications. *Inorg. Chem.* **50**, 12263–12274 (2011).

22. Wang, S. Luminescence and electroluminescence of Al(III), B(III), Be(II) and Zn(II) complexes with nitrogen donors. *Coord. Chem. Rev.* **215**, 79–98 (2001).

23. Chiti, F. & Dobson, C. M. Protein Misfolding, Functional Amyloid, and Human Disease. *Annu. Rev. Biochem.* **75**, 333–366 (2006).

24. Nunes da Silva, R. *et al.* Fluorescent Light-up Probe for the Detection of Protein Aggregates. *Chem. – An Asian J.* **14**, 859–863 (2019).

25. Hong, Y. *et al.* Monitoring and Inhibition of Insulin Fibrillation by a Small Organic Fluorogen with Aggregation-Induced Emission Characteristics. *J. Am. Chem. Soc.* **134**, 1680–1689 (2012).

26. Levine, H. Thioflavine T interaction with synthetic Alzheimer's disease β-amyloid peptides: Detection of amyloid aggregation in solution. *Protein Sci.* **2**, 404–410 (2008).

27. Guieu, S., Pinto, J., Silva, V. L. M., Rocha, J. & Silva, A. M. S. Synthesis, Post-Modification and Fluorescence Properties of Boron Diketonate Complexes. *European J. Org. Chem.* **2015**, 3423–3426 (2015).

28. Liu, Y., Guo, J., Zhang, H. & Wang, Y. Highly Efficient White Organic Electroluminescence from a Double-Layer Device Based on a Boron Hydroxyphenylpyridine Complex. *Angew. Chemie Int. Ed.* **41**, 182–184 (2002).

29. Frath, D., Azizi, S., Ulrich, G., Retailleau, P. & Ziessel, R. Facile Synthesis of Highly Fluorescent Boranil Complexes. *Org. Lett.* **13**, 3414–3417 (2011).

30. Pagano, R. E. A novel fluorescent ceramide analogue for studying membrane traffic in animal cells: accumulation at the Golgi apparatus results in altered spectral properties of the sphingolipid precursor. *J. Cell Biol.* **113**, 1267–1279 (1991).

31. Boens, N., Leen, V. & Dehaen, W. Fluorescent indicators based on BODIPY. *Chem. Soc. Rev.* **41**, 1130–1172 (2012).

32. Chen, Y. *et al.* Insights into the binding mechanism of BODIPY-based photosensitizers to human serum albumin: A combined experimental and computational study. *Spectrochim. Acta Part A Mol. Biomol. Spectrosc.* **203**, 158–165 (2018).

33. Ulrich, G., Ziessel, R. & Harriman, A. The Chemistry of Fluorescent Bodipy Dyes: Versatility Unsurpassed. *Angew. Chemie Int. Ed.* **47**, 1184–1201 (2008).

34. Rohand, T., Qin, W., Boens, N. & Dehaen, W. Palladium-Catalyzed Coupling Reactions for the Functionalization of BODIPY Dyes with Fluorescence Spanning the Visible Spectrum. *European J. Org. Chem.* **2006**, 4658–4663 (2006).

35. Rohand, T., Baruah, M., Qin, W., Boens, N. & Dehaen, W. Functionalisation of fluorescent BODIPY dyes by nucleophilic substitution. *Chem. Commun.* 266–268 (2006). doi:10.1039/B512756D

36. Lavis, L. D. & Raines, R. T. Bright Building Blocks for Chemical Biology. *ACS Chem. Biol.* **9**, 855–866 (2014).

37. Bessette, A. & Hanan, G. S. Design, synthesis and photophysical studies of dipyrromethene-based materials: insights into their applications in organic photovoltaic devices. *Chem. Soc. Rev.* **43**, 3342–3405 (2014).

38. Guieu, S., Cardona, F., Rocha, J. & Silva, A. M. S. Luminescent bi-metallic fluoroborate derivatives of bulky salen ligands. *New J. Chem.* **38**, 5411–5414 (2014).

39. Manav, N., Tyagi, A., Pandey, V. & Gupta, I. Ferrocene and triphenylamine

appended boranils. *J. Chem. Sci.* **130**, 79 (2018).

40. Frath, D., Azizi, S., Ulrich, G. & Ziessel, R. Chemistry on Boranils: An Entry to Functionalized Fluorescent Dyes. *Org. Lett.* **14**, 4774–4777 (2012).

41. Vaz, P. A. A. M., Rocha, J., Silva, A. M. S. & Guieu, S. Aggregation-induced emission enhancement of chiral boranils. *New J. Chem.* **42**, 18166–18171 (2018).

42. Frath, D., Massue, J., Ulrich, G. & Ziessel, R. Luminescent Materials: Locking π-Conjugated and Heterocyclic Ligands with Boron(III). *Angew. Chemie Int. Ed.* **53**, 2290–2310 (2014).

43. Lin, Y. & Chow, T. J. A pyridomethene–BF2 complex-based chemosensor for detection of hydrazine. *RSC Adv.* **3**, 17924 (2013).

44. Hantzsch, A. Condensationsprodukte aus Aldehydammoniak und ketonartigen Verbindungen. *Berichte der Dtsch. Chem. Gesellschaft* **14**, 1637–1638 (1881).

45. Sagitullin, R. S., Shkil', G. P., NosonovA, I. I. & Ferber, A. A. Synthesis of pyridine bases by the chichibabin method (review). *Chem. Heterocycl. Compd.* **32**, 127–140 (1996).

46. Kröhnke, F. *et al.* Syntheses Using the Michael Adddition of Phridinium Salts. *Angew. Chemie Int. Ed. English* **1**, 626–632 (1962).

47. Fujimori, T., Wirsching, P. & Janda, K. D. Preparation of a Kröhnke Pyridine Combinatorial Library Suitable for Solution-Phase Biological Screening. *J. Comb. Chem.* **5**, 625–631 (2003).

48. Miranda, P. O., Cubitt, B., Jacob, N. T., Janda, K. D. & de la Torre, J. C. Mining a Kröhnke Pyridine Library for Anti-Arenavirus Activity. *ACS Infect. Dis.* **4**, 815–824 (2018).

49. King, L. C. The Reaction of Iodine with Some Ketones in the Presence of Pyridine. *J. Am. Chem. Soc.* **66**, 894–895 (1944).

50. Sowmiah, S., Esperança, J. M. S. S., Rebelo, L. P. N. & Afonso, C. A. M.

Pyridinium salts: from synthesis to reactivity and applications. *Org. Chem. Front.* **5**, 453–493 (2018).

51. Adib, M., Tahermansouri, H., Koloogani, S. A., Mohammadi, B. & Bijanzadeh, H. R. Kröhnke pyridines: an efficient solvent-free synthesis of 2,4,6-triarylpyridines. *Tetrahedron Lett.* **47**, 5957–5960 (2006).

52. Qing, X., Wang, T., Zhang, F. & Wang, C. One-pot synthesis of 2,4,6-triarylpyridines from β-nitrostyrenes, substituted salicylic aldehydes and ammonium acetate. *RSC Adv.* **6**, 95957–95964 (2016).

53. Karki, R. *et al.* Dihydroxylated 2,4,6-triphenyl pyridines: Synthesis, topoisomerase I and II inhibitory activity, cytotoxicity, and structure–activity relationship study. *Eur. J. Med. Chem.* **49**, 219–228 (2012).

54. Powers, D. G. *et al.* Automated parallel synthesis of chalcone-based screening libraries. *Tetrahedron* **54**, 4085–4096 (1998).

55. Crosby, G. A. & Demas, J. N. Measurement of photoluminescence quantum yields. Review. *J. Phys. Chem.* **75**, 991–1024 (1971).

56. Lavis, L. D. & Raines, R. T. Bright Ideas for Chemical Biology. *ACS Chem. Biol.* **3**, 142–155 (2008).

57. Craig, N. C., Groner, P. & McKean, D. C. Equilibrium Structures for Butadiene and Ethylene: Compelling Evidence for Π-Electron Delocalization in Butadiene. *J. Phys. Chem. A* **110**, 7461–7469 (2006).

58. Fletcher, K. A., Storey, I. A., Hendricks, A. E., Pandey, S. & Pandey, S. Behavior of the solvatochromic probes Reichardt's dye, pyrene, dansylamide, Nile Red and 1-pyrenecarbaldehyde within the room-temperature ionic liquid bmimPF6. *Green Chem.* **3**, 210–215

59. Conlon, I. L. *et al.* Kröhnke pyridines: Rapid and facile access to Mcl-1 inhibitors. *Bioorg. Med. Chem. Lett.* **28**, 1949–1953 (2018).

60. Chapman, G., Solomon, I., Patonay, G. & Henary, M. Synthesis and pH-

Dependent Spectroscopic Behavior of 2,4,6-Trisubstituted Pyridine Derivatives. *J. Heterocycl. Chem.* **52**, 861–872 (2015).

61. Stompor, M., Kałużny, M. & Żarowska, B. Biotechnological methods for chalcone reduction using whole cells of Lactobacillus, Rhodococcus and Rhodotorula strains as a way to produce new derivatives. *Appl. Microbiol. Biotechnol.* **100**, 8371–8384 (2016).

62. Zhu, D., Yang, Y., Buynak, J. D. & Hua, L. Stereoselective ketone reduction by a carbonyl reductase from Sporobolomyces salmonicolor. Substrate specificity, enantioselectivity and enzyme-substrate docking studies. *Org. Biomol. Chem.* **4**, 2690 (2006).

63. Martelli, L. S. R. *et al.* Organocatalytic asymmetric vinylogous 1,4-addition of α,α-Dicyanoolefins to chalcones under a bio-based reaction media: Discovery of new Michael adducts with antiplasmodial activity. *Tetrahedron* **75**, 3530–3542 (2019).

64. Jiang, Q., Jia, J., Xu, B., Zhao, A. & Guo, C.-C. Iron-Facilitated Oxidative Radical Decarboxylative Cross-Coupling between α-Oxocarboxylic Acids and Acrylic Acids: An Approach to α,β-Unsaturated Carbonyls. *J. Org. Chem.* **80**, 3586–3596 (2015).

65. Cheng, X. *et al.* Organic Crystals with Near-Infrared Amplified Spontaneous Emissions Based on 2′-Hydroxychalcone Derivatives: Subtle Structure Modification but Great Property Change. *Angew. Chemie Int. Ed.* **54**, 8369–8373 (2015).

Copyrights

Figure 1. a) Quinine and b) Fluorite crystals under UV. Copyright free from a) (https://en.wikipedia.org/wiki/File:Tonic_water_uv.jpg) originally from C.Löser 2019 b) (https://commons.wikimedia.org/wiki/File:Fluorite-Quartz-120451.jpg) originally from Robert M. Lavinsky at http://www.mindat.org/photo-120451.html 2019.

Figure 3. HOMO-LUMO transitions. Reprinted from Fujisawa, J. An unusual mechanism for HOMO–LUMO gap narrowing in a minimal near-IR dye generated by the deprotonation of bis(dicyanomethylene)indan. *Chem. Phys. Lett.* **608**, 355–359 (2014) with permition from Elsevier 2019.

Figure 8. Aggregation Caused Quenching vs Aggregation induced emission. Reproduced with permission of Royal Society of Chemistry, from Hong, Y., Lam, J. W. Y. & Tang, B. Z. Aggregation-induced emission. Chem. Soc. Rev. 40, 5361 (2011); permission conveyed through Copyright Clearence Center, Inc 2019.

Figure 9. Examples of fluorophores with AIE and technologic applications. Reprinted with permission from Mei, J., Leung, N. L. C., Kwok, R. T. K., Lam, J. W. Y. & Tang, B. Z. Aggregation-Induced Emission: Together We Shine, United We Soar! Chem. Rev. 115, 11718–11940 (2015). Copyright 2019 American Chemical Society.

Figure 10. Organo-boron complexes for optoelectronic applications. Reprinted with permission from Rao, Y.-L. & Wang, S. Four-Coordinate Organoboron Compounds with a π-Conjugated Chelate Ligand for Optoelectronic Applications. Inorg. Chem. 50, 12263–12274 (2011). Copyright 2019 American Chemical Society.

Figure 11. AIEgen example for monitoring misfolding kinetics with protein model insulin aggregates. Reprinted with permission from Hong, Y. et al. Monitoring and Inhibition of Insulin Fibrillation by a Small Organic Fluorogen with Aggregation-Induced Emission Characteristics. J. Am. Chem. Soc. 134, 1680–1689 (2012). Copyright 2019 American Chemical Society.

Figure 14. Examples of fluorophore brightness (ϵ × Φ) vs the wavelength of maximum absorption (λmax) for the major classes of fluorophores. Reprinted with

permission from Lavis, L. D. & Raines, R. T. Bright Building Blocks for Chemical Biology. ACS Chem. Biol. 9, 855–866 (2014). Copyright 2019 American Chemical Society.

Figure 16-New fluorescent boranils based on chiral benzylamines. Reproduced with permission of Royal Society of Chemistry, from Vaz, P. A. A. M., Rocha, J., Silva, A. M. S. & Guieu, S. Aggregation-induced emission enhancement of chiral boranils. New J. Chem. 42, 18166–18171 (2018). Permission conveyed through Copyright Clearence Center, Inc 2019.

Figure 17-a) Pyridine-boron core, b) Pyridine based BODIPY as chemosensors. Reproduced with permission of Royal Society of Chemistry, from Lin, Y. & Chow, T. J. A pyridomethene–BF2 complex-based chemosensor for detection of hydrazine. RSC Adv. 3, 17924 (2013). Permission conveyed through Copyright Clearence Center, Inc 2019.

Attachments

Attachments

Illustrations

^{1}H-NMR peaks of the solvents used

Solvent		$CDCl_3$	$(CD_3)_2CO$
H_2O	-OH	1.56	2.84
acetic acid	$-CH_3$	2.10	1.96
acetone	$-CH_3$	2.17	2.09
Chloroform	-CH	7.26	8.02
CH_2Cl_2	$-CH_2$	5.30	5.63
EtOH	$-CH_3$ $-CH_2$ -OH	1.25 3.72 1.32	1.12 3.57 3.39
Ethyl acetate	$-CH_3CO$ $-C\mathbf{H}_2CH_3$ $-CH_2C\mathbf{H}_3$	2.05 2.46 1.26	1.97 4.05 1.20
H grease	$-CH_3$ $-CH_2$	0.84-0.87 1.25	0.90 1.29
n-Hexane	$-CH_3$ $-CH_2$	0.88 1.26	0.88 1.28
MeOH	$-CH_3$ -OH	3.49 1.09	3.31 3.12

Photophysical characterization

Molar absorption coefficient (ε) $M^{-1}.cm^{-1}$:

$$\varepsilon = \frac{A}{cL}$$

A is the amount of light absorbed by the sample for a wavelength.

L is the distance that the light travels through the solution (cm).

c is the concentration of the compound (moles/L) or M.

$\varepsilon_{anthracene}$= 9700 $M^{-1}.cm^{-1}$

Quantum yield (Φ):

$$\Phi = \frac{\#\ photons\ emitted}{\#\ photons\ absobed}$$

$$\Phi = \Phi_{ref} \times \frac{\eta^2}{\eta_{ref}^2} \times \frac{I}{A} \times \frac{A_{ref}}{I_{ref}}$$

$$\Phi = \Phi_{ref} \times \frac{Grad_x}{Grad_{ref}} \times \frac{\eta^2}{\eta_{ref}^2}$$

I is the integrated fluorescence intensity.

η is the refractive index of the solvent.

$\Phi_{anthracene}$ = 0.27

η_{EtOH}= 1.36; η_{CH2Cl2}= 1.424; η_{THF}= 1.407

Brightness (B) $M^{-1}.cm^{-1}$:

$$B = \varepsilon \times \Phi$$

Note: The absorbances were kept in between A = <0.1 in order to avoid inner filter effects and ensure linear response on the intensity. The compounds and reference were prepared in solutions between 10^{-4} M and 10^{-7} M until Beer-Lambert Law (linearity) was achieved.

Anthracene (reference)

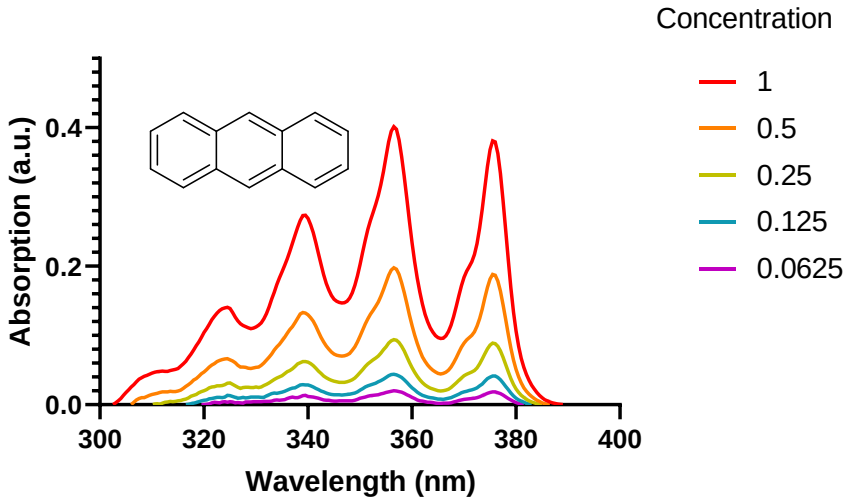

Figure 1-Absorption spectra of anthracene

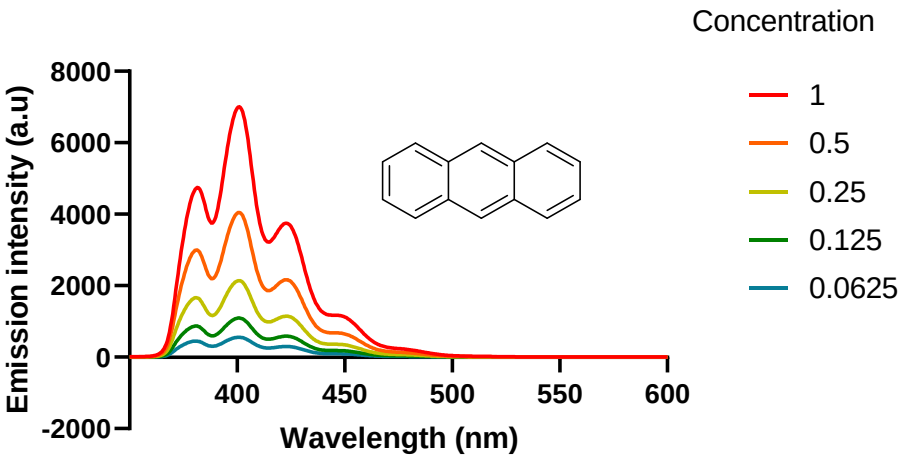

Figure 2-Emission spectra of anthracene

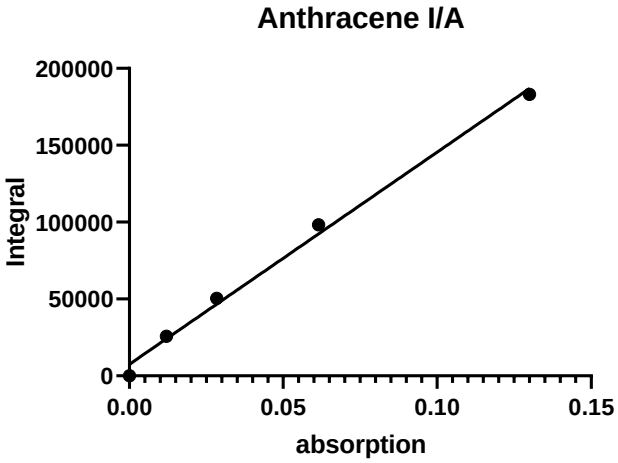

Figure 3-Ratio of Integrated fluorescence intensity over absorption of anthracene

Kroenke salt 1a

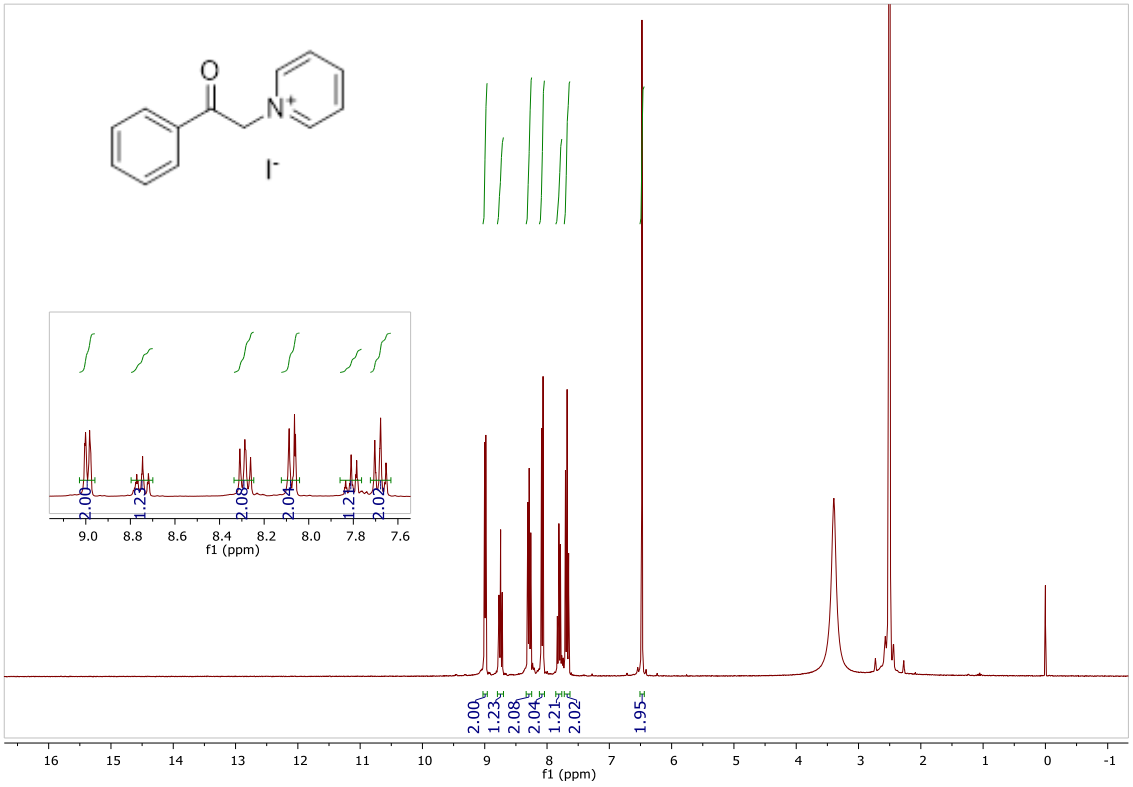

*Figure 4-^{1}H-NMR spectrum of compound **1a***

Kroenke salt 1b

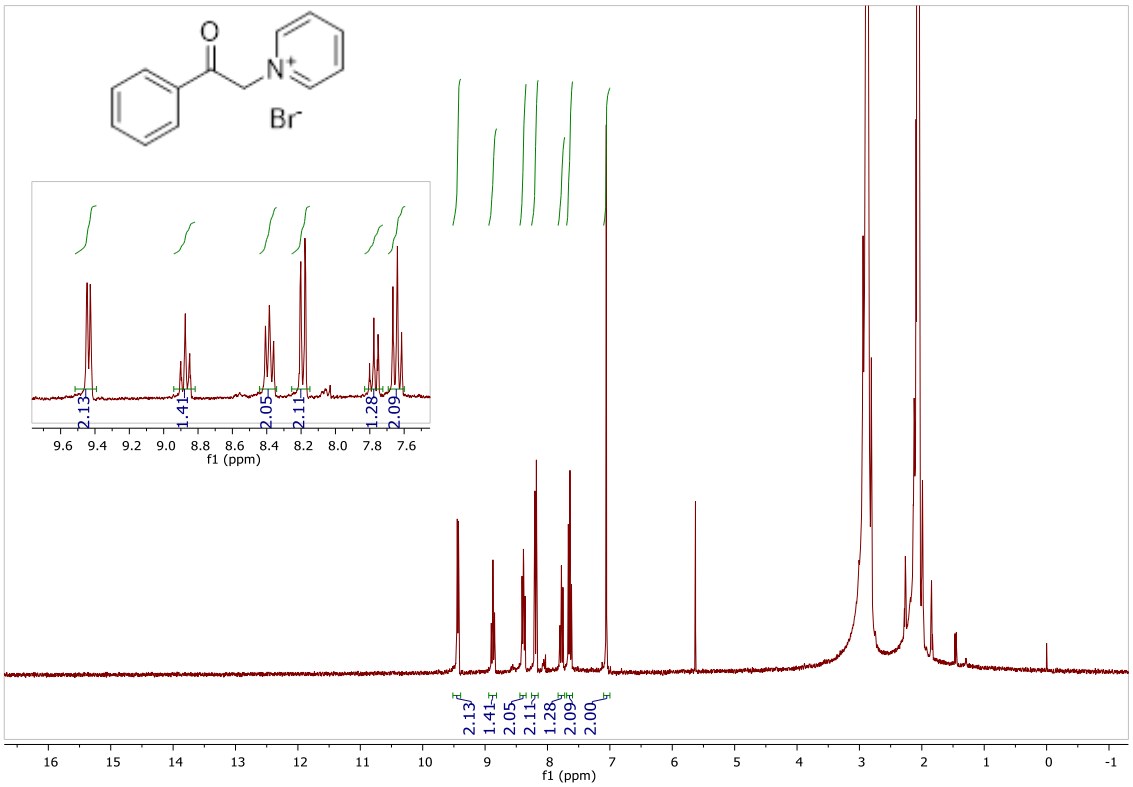

*Figure 5-^{1}H-NMR spectrum of compound **1b***

Acetophenone 2a

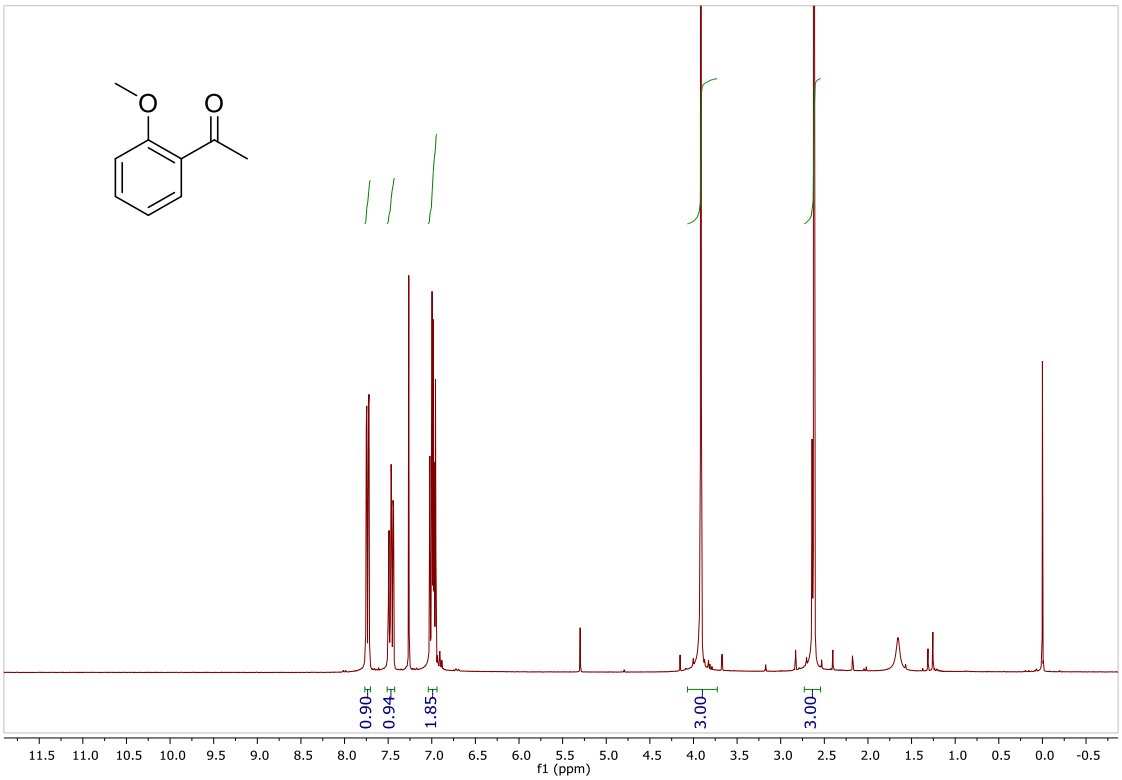

*Figure 6-^{1}H-NMR spectrum of compound **2a***

Chalcone [(E)-1-(2-methoxyphenyl)-3-(4-nitrophenyl)prop-2-en-1-one]

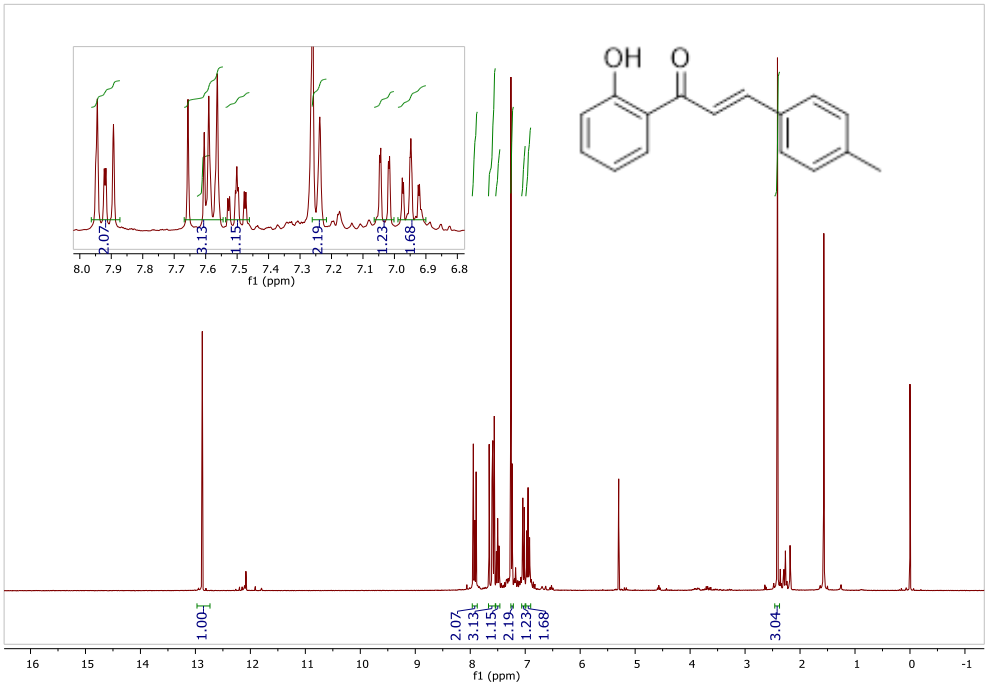

*Figure 7-^{1}H-NMR spectrum of **[(E)-1-(2-methoxyphenyl)-3-(4-nitrophenyl)prop-2-en-1-one]***

Chalcone 4a

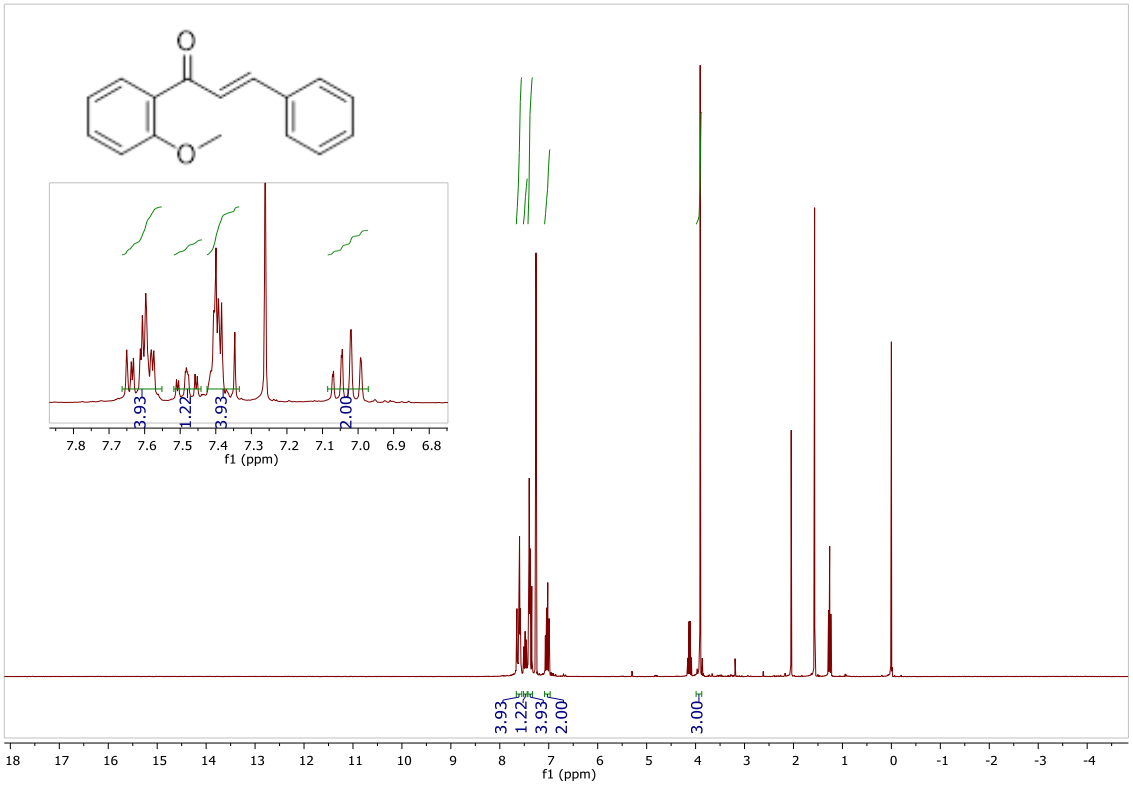

*Figure 8-^{1}H-NMR spectrum of compound **4a***

Chalcone 4b

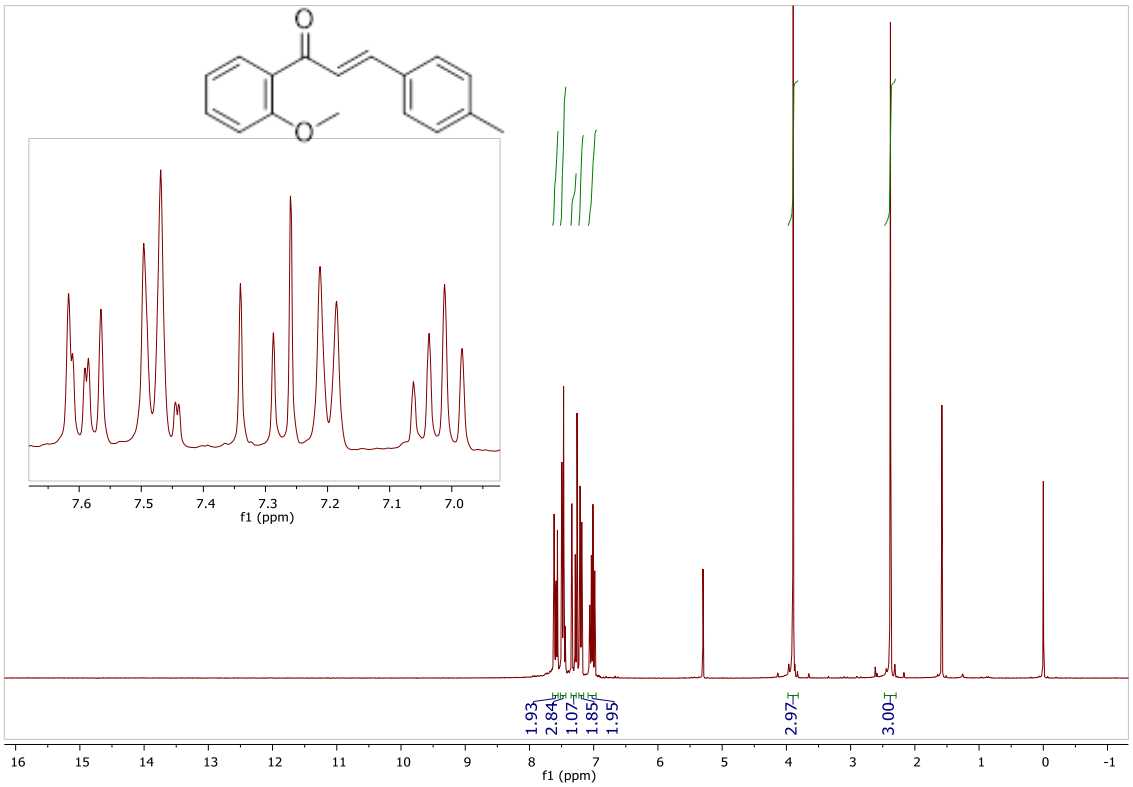

*Figure 9-^{1}H-NMR spectrum of compound **4b***

Chalcone 4c

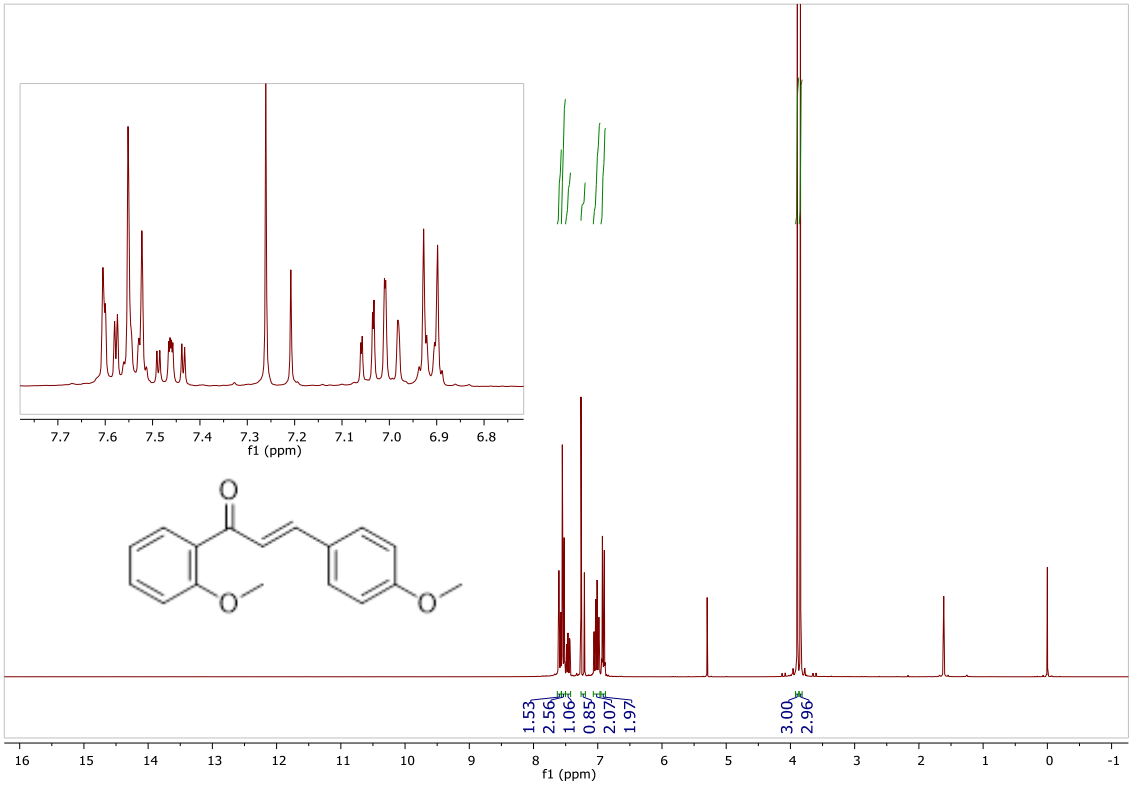

*Figure 10-^{1}H-NMR spectrum of compound **4c***

Chalcone 4d

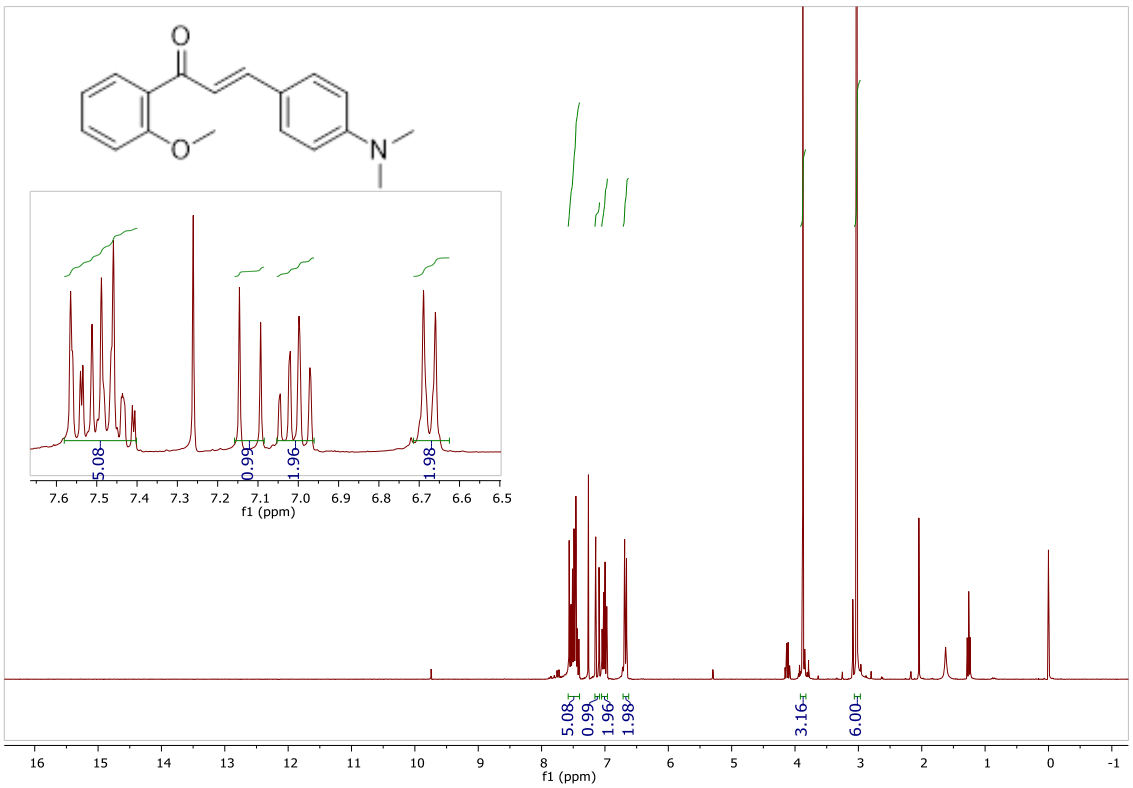

*Figure 11-^{1}H-NMR spectrum of compound **4d***

Chalcone 4e

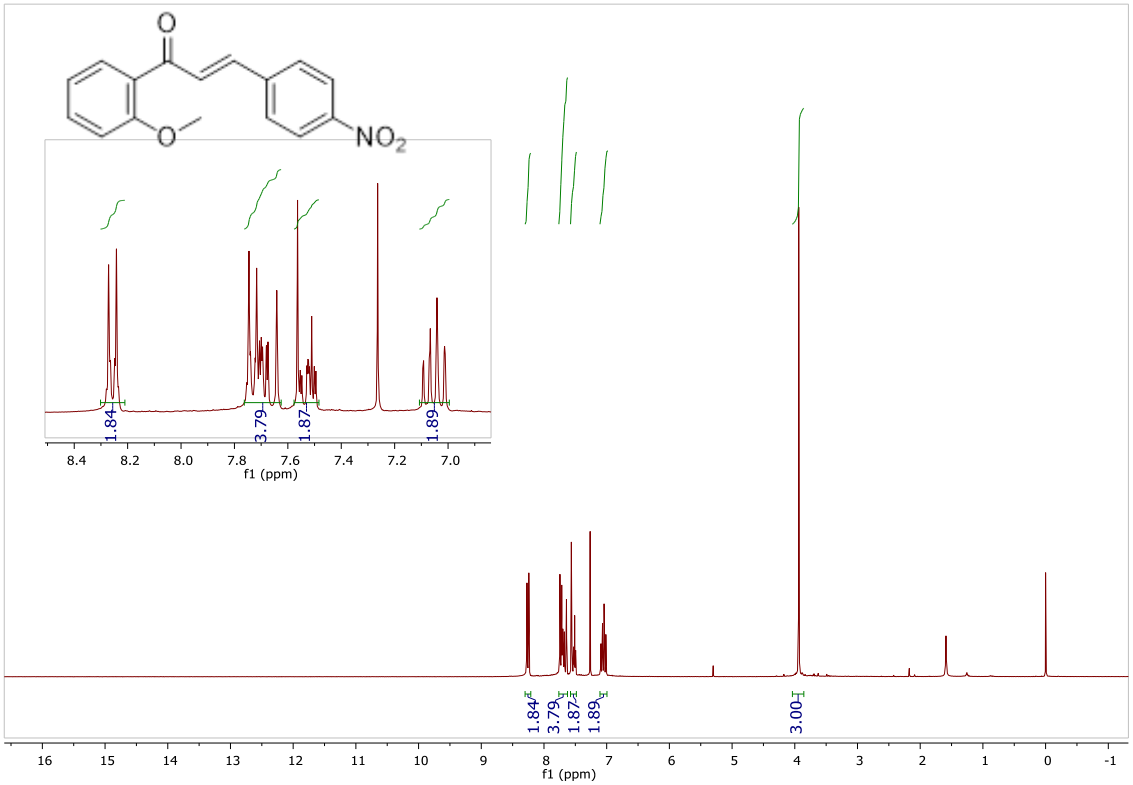

*Figure 12-^{1}H-NMR spectrum of compound **4e***

Pyridine 5a

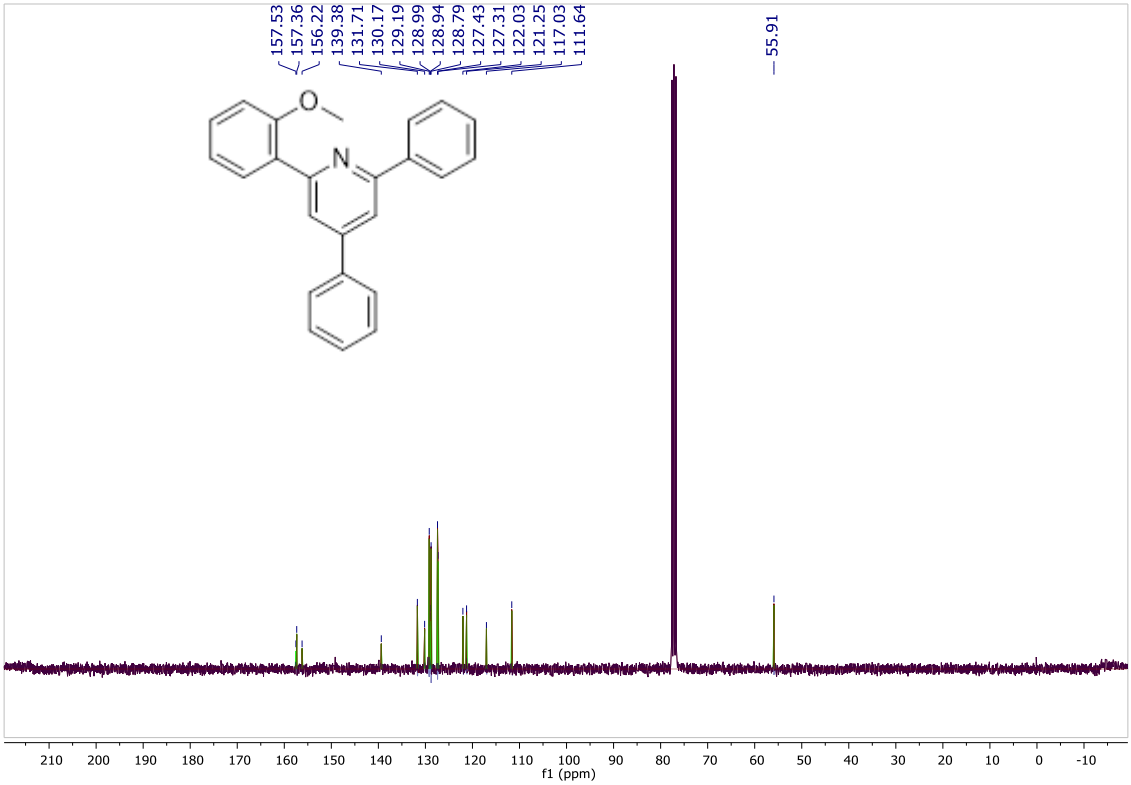

*Figure 13-^{13}C-NMR spectrum of compound **5a***

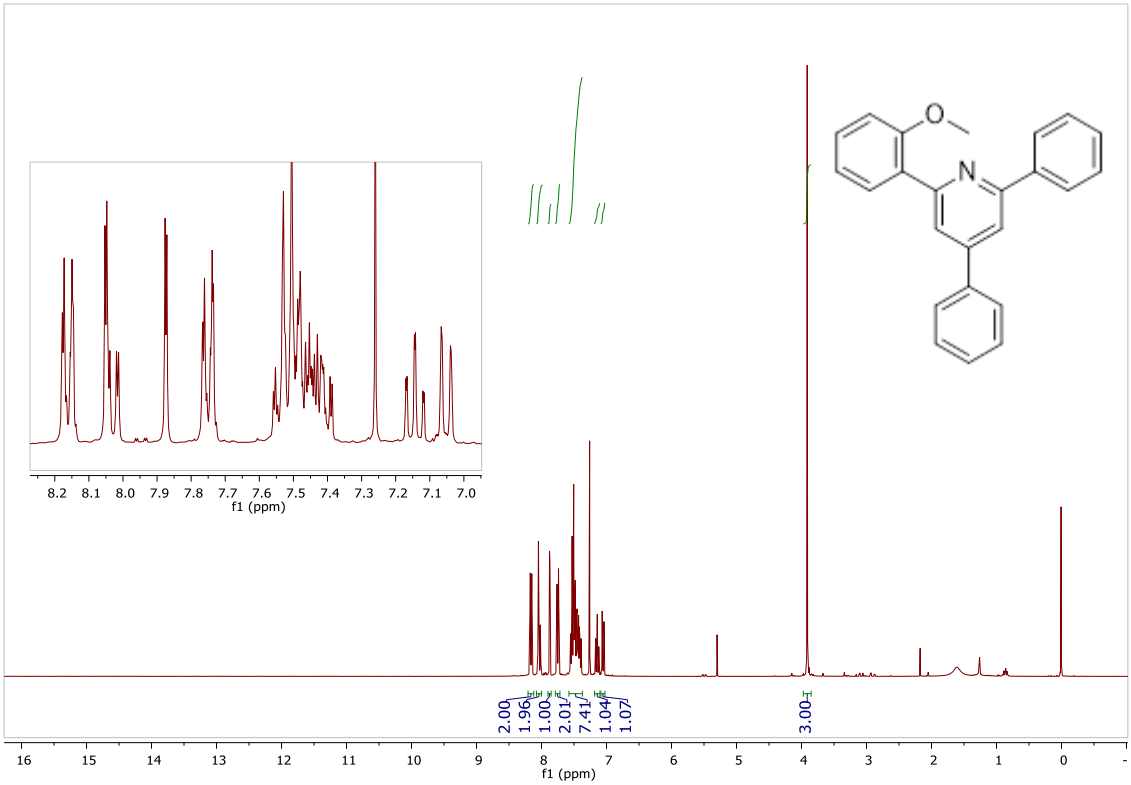

*Figure 14-^{1}H-NMR spectrum of compound **5a***

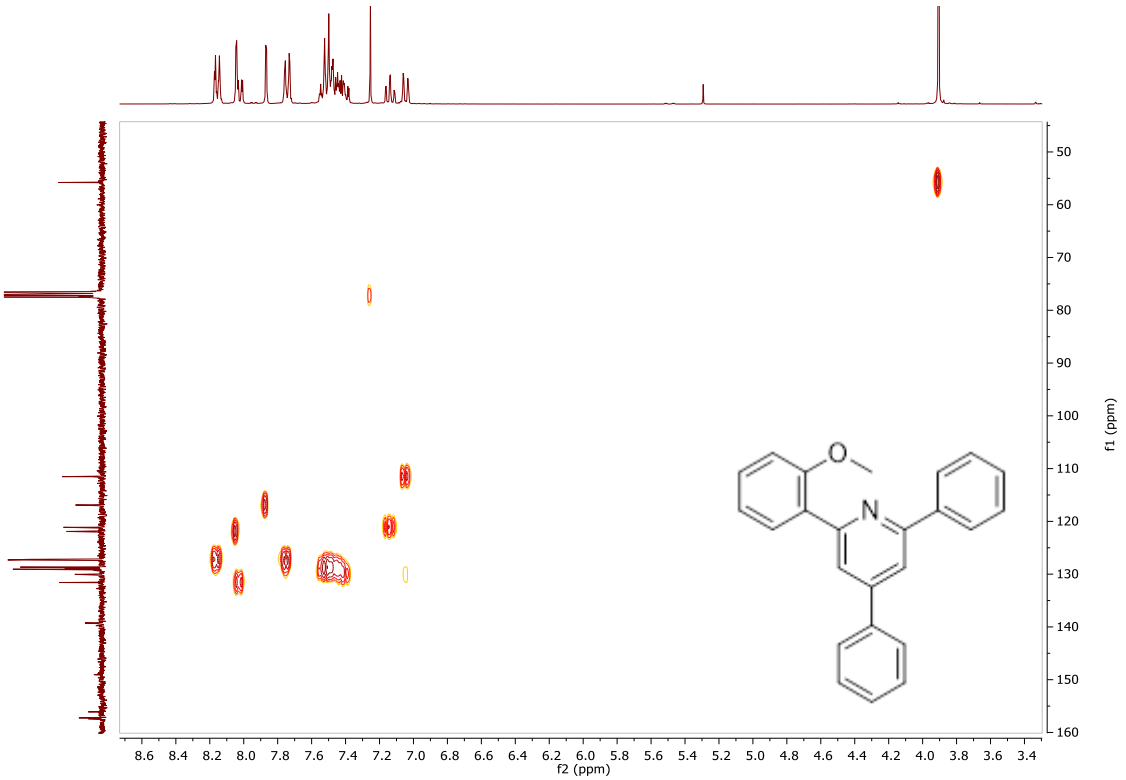

*Figure 15- HSQC spectrum of compound **5a***

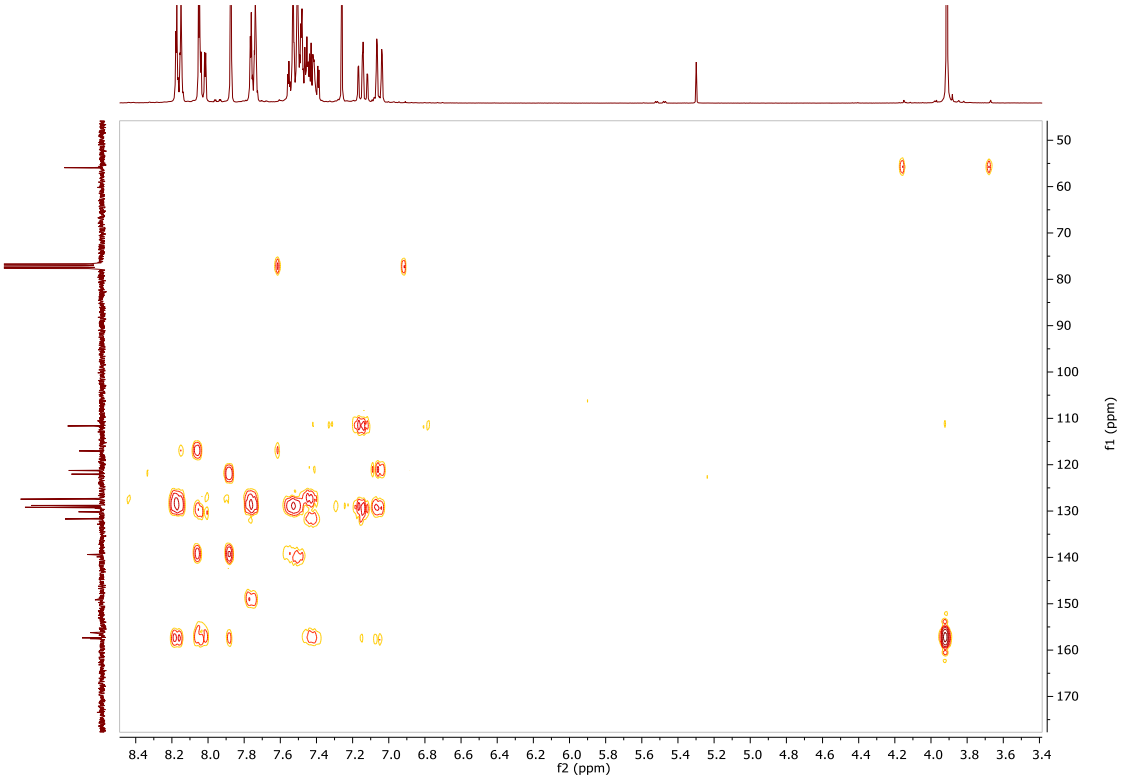

*Figure 16-HMBC spectrum of compound **5a***

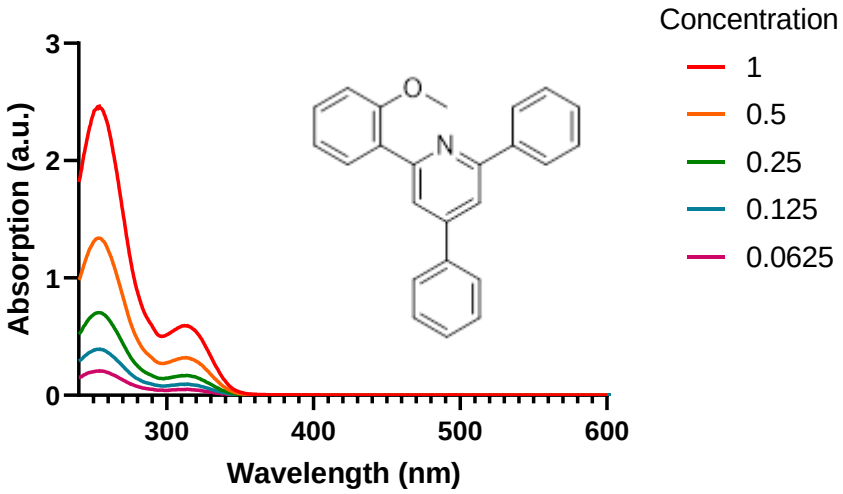

*Figure 17- Absorption spectra of compound **5a***

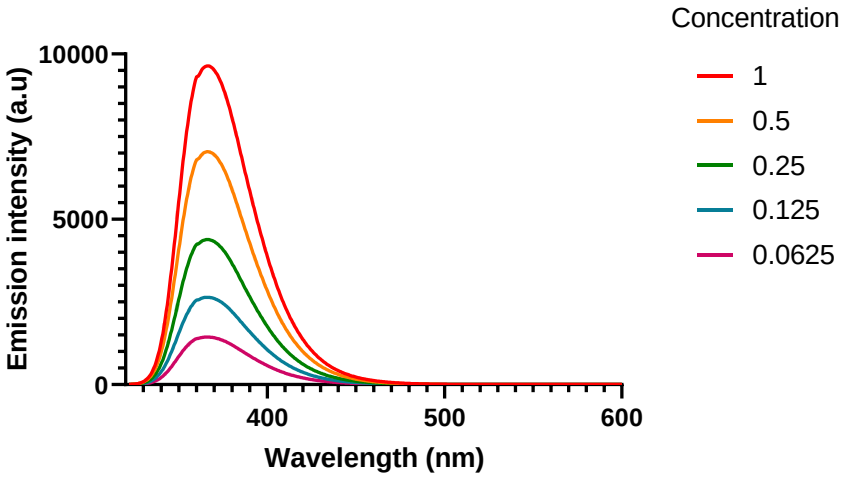

*Figure 18- Emission spectra of compound **5a***

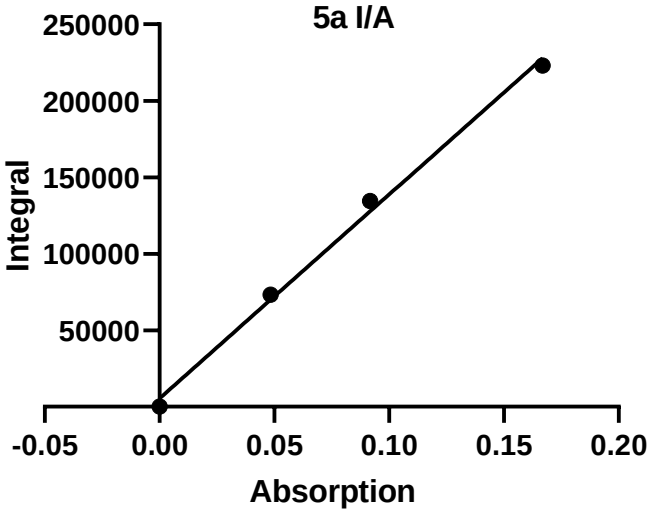

*Figure 19- Ratio of Integrated fluorescence intensity over absorption of compound **5a***

Pyridine 5b

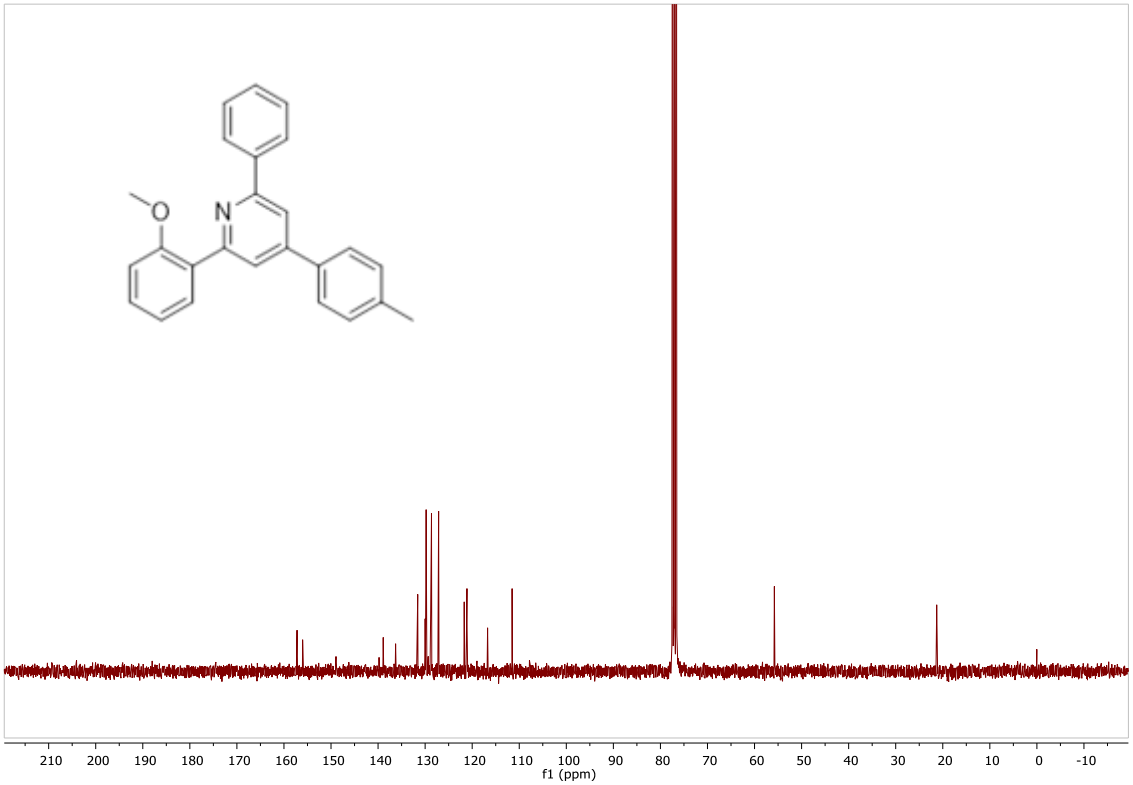

*Figure 20-^{13}C-NMR spectrum of compound **5b***

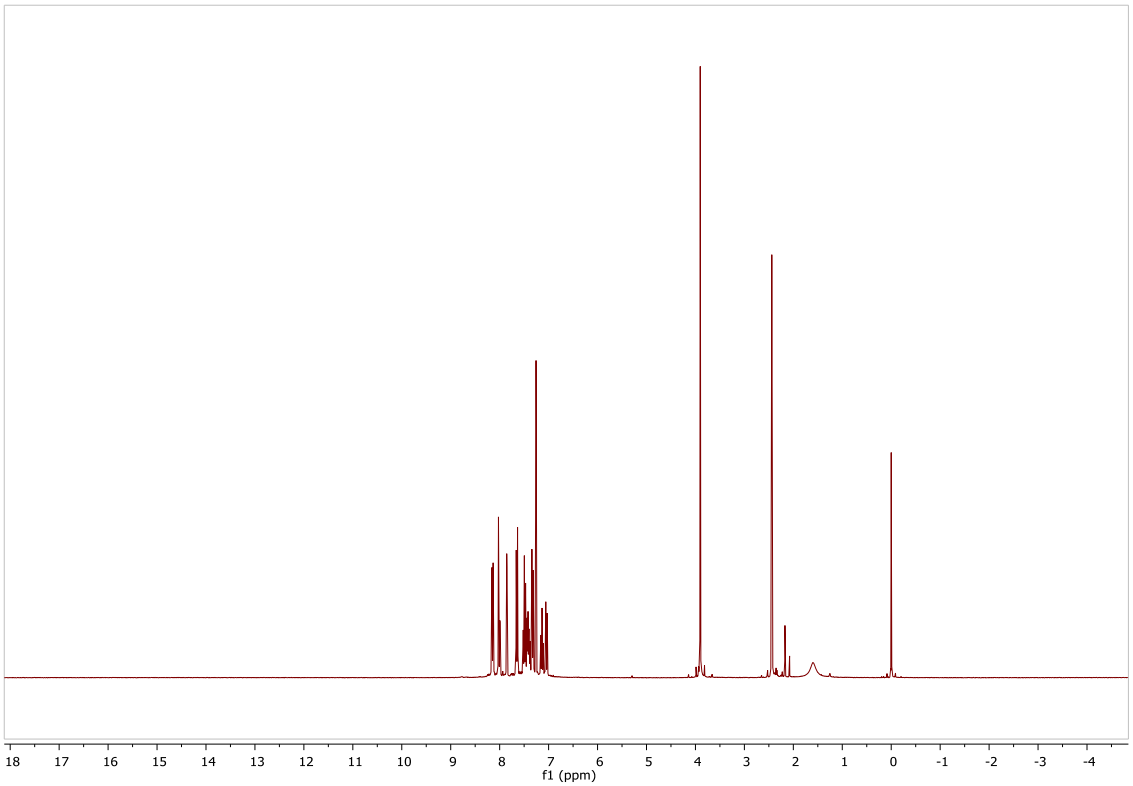

*Figure 21-^{1}H-NMR spectrum of compound **5b***

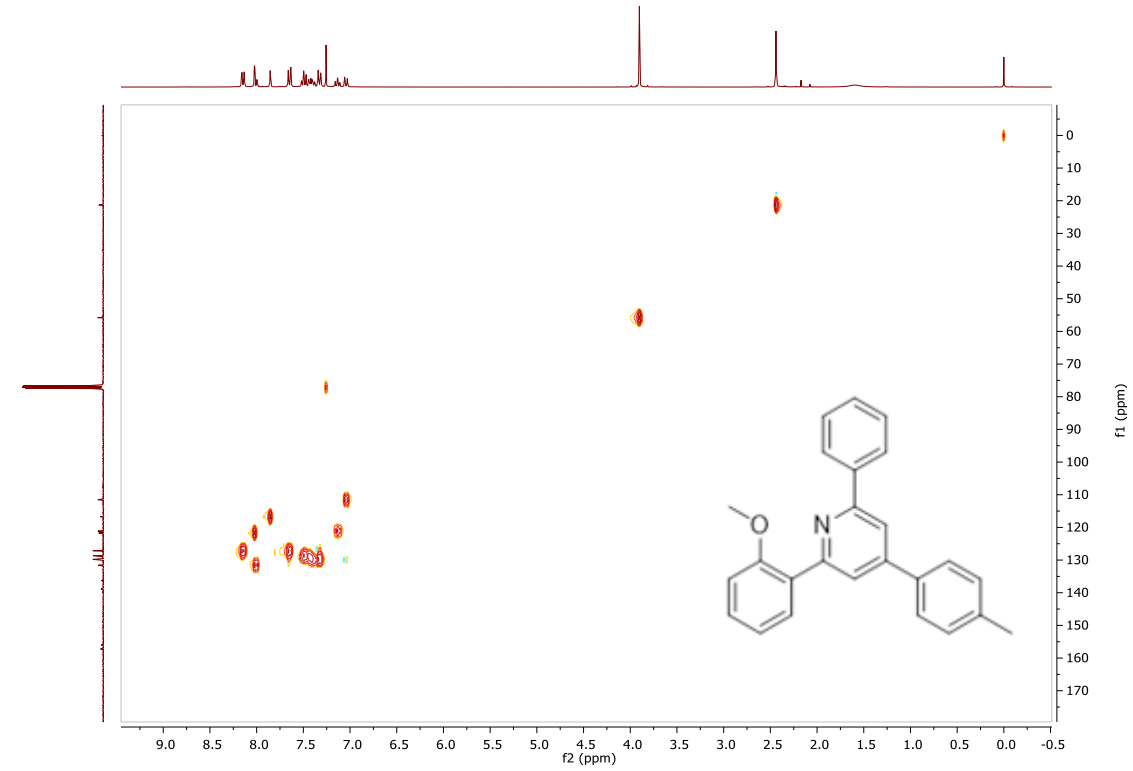

*Figure 22-HSQC spectrum of compound **5b***

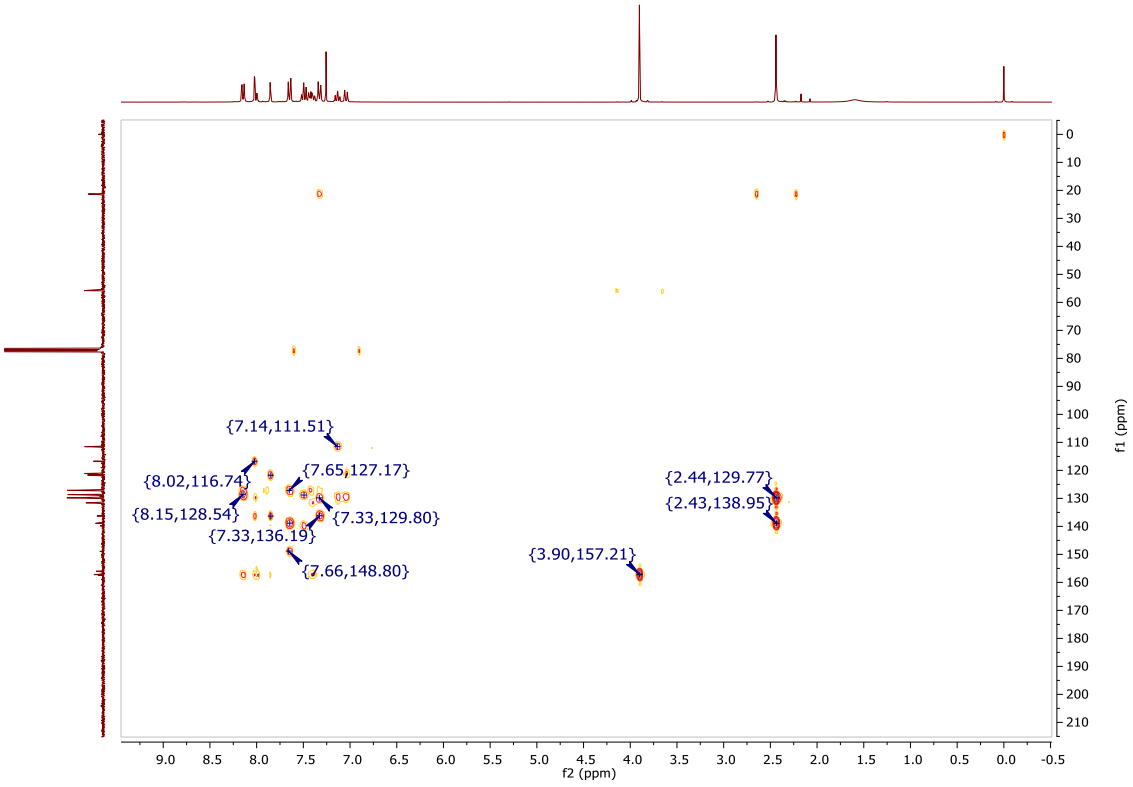

*Figure 23-HMBC spectrum of compound **5b***

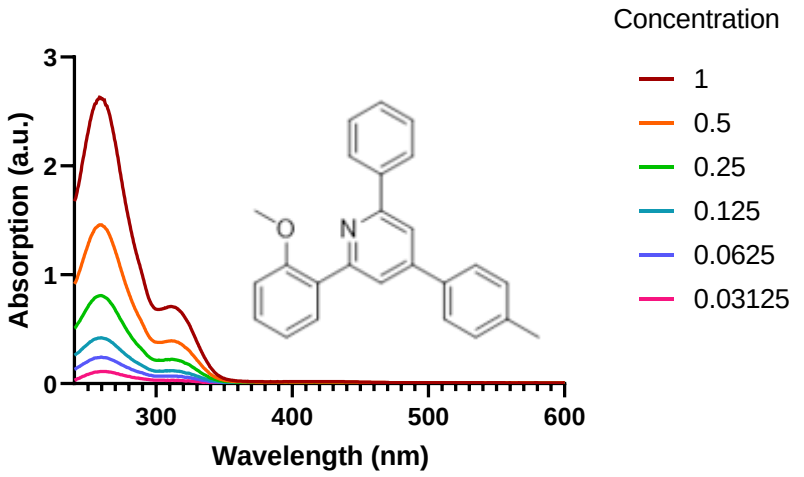

*Figure 24- Absorption spectra of compound **5b***

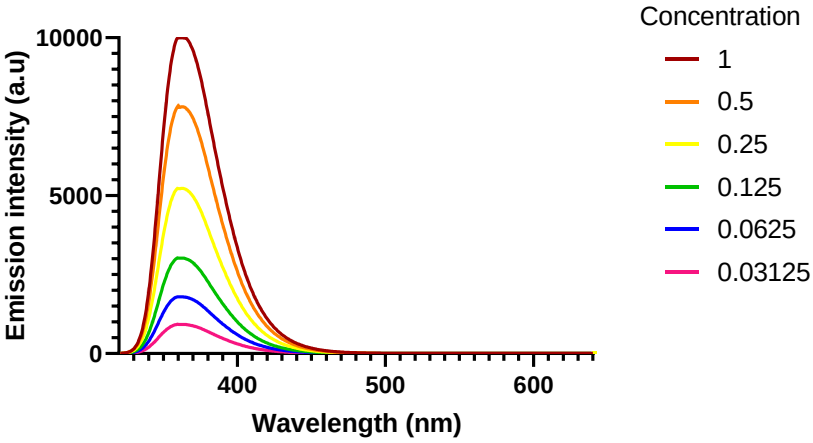

*Figure 25- Emission spectra of compound **5b***

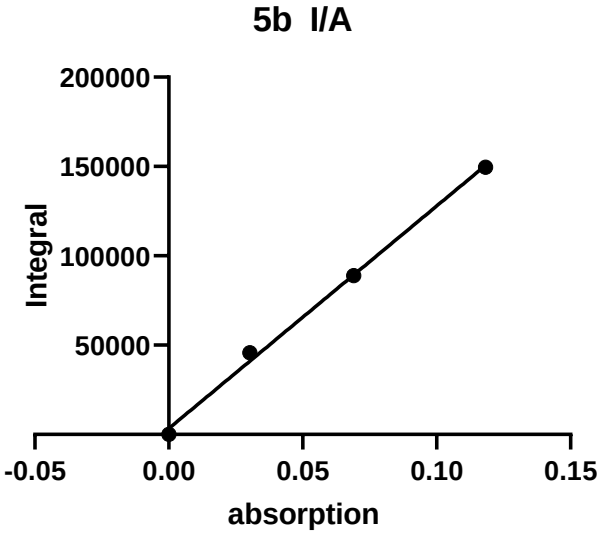

*Figure 26- Ratio of Integrated fluorescence intensity over absorption of compound **5b***

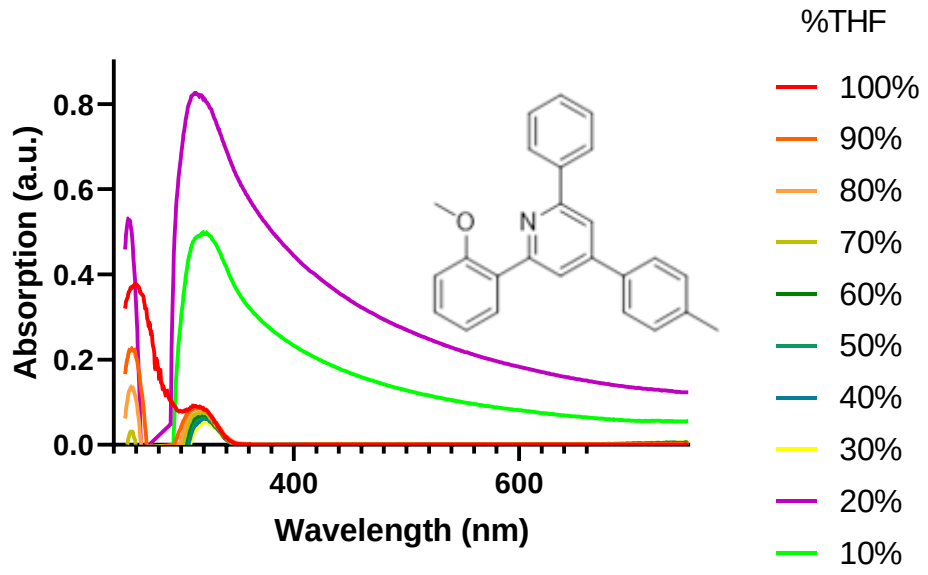

*Figure 27-Absorption spectra of compound **5b** (aggregation test)*

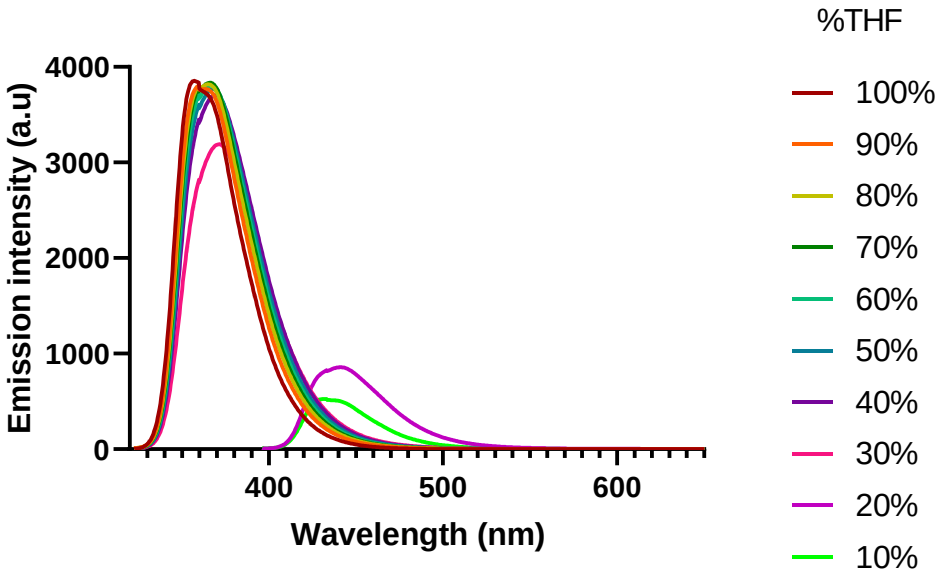

*Figure 28-Emission spectra of compound **5b** (aggregation test)*

Pyridine 5c

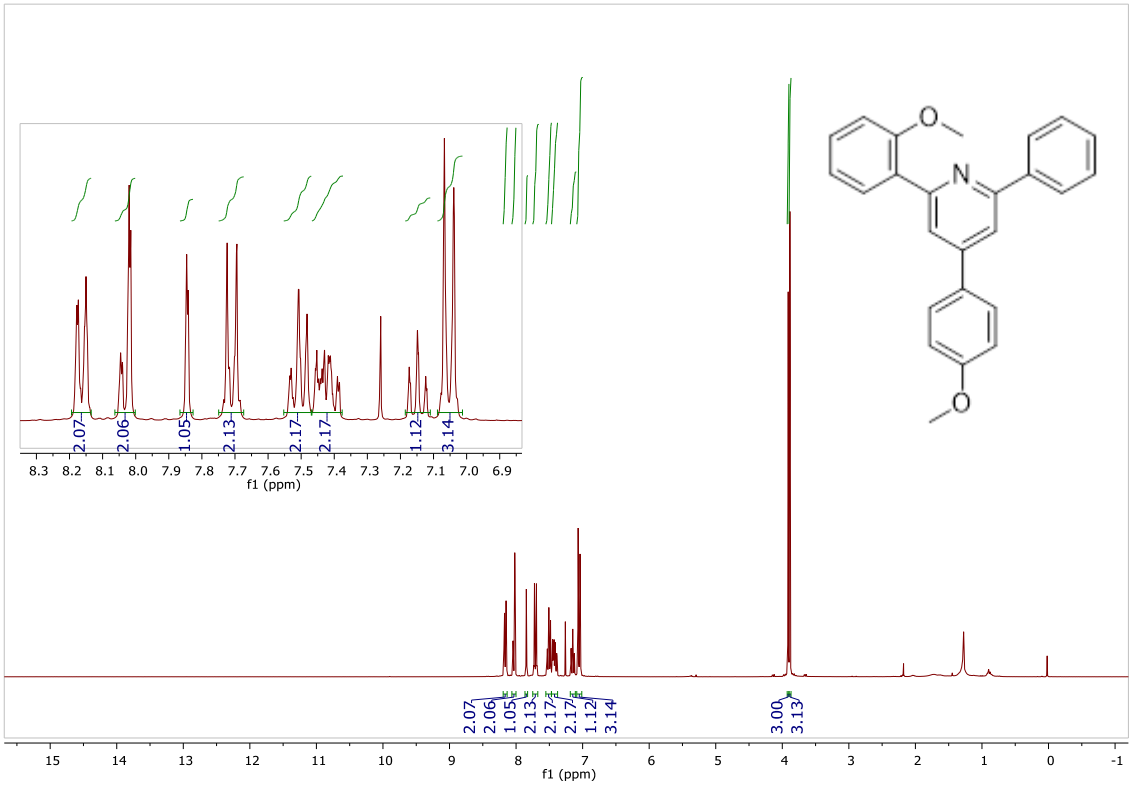

*Figure 29-^{1}H-NMR spectrum of compound **5c***

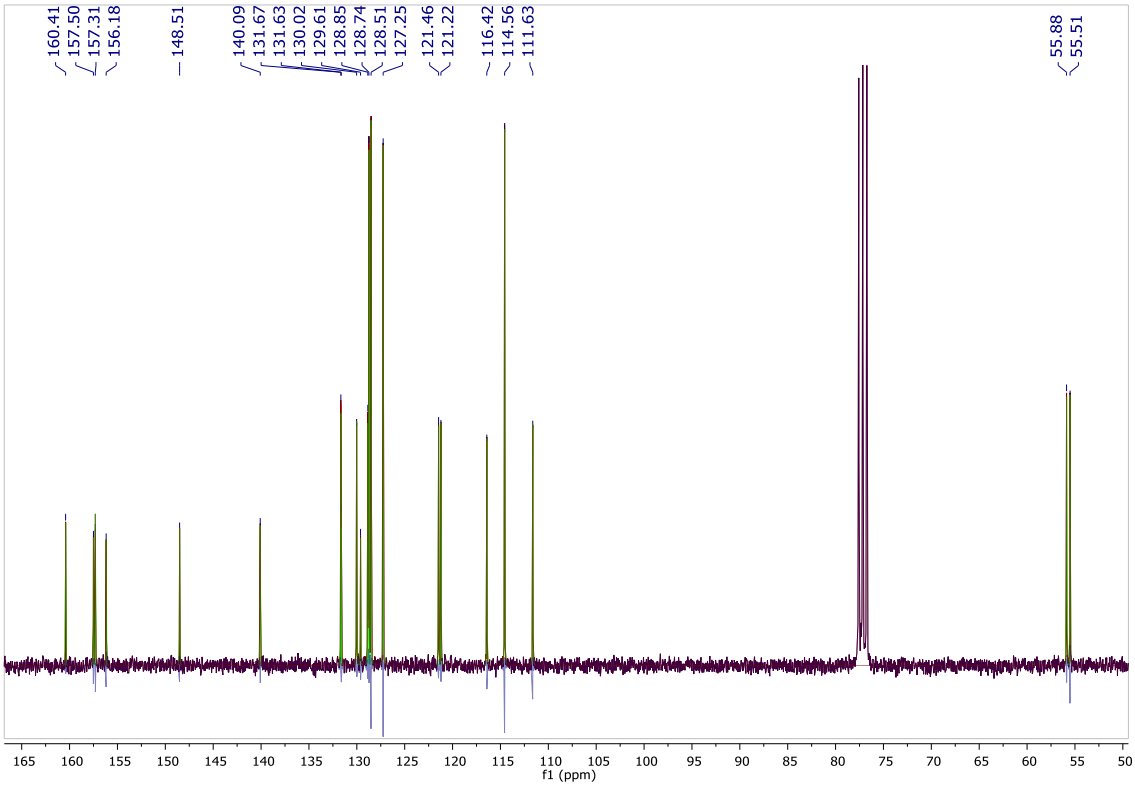

*Figure 30-^{13}C-NMR spectrum of compound **5c***

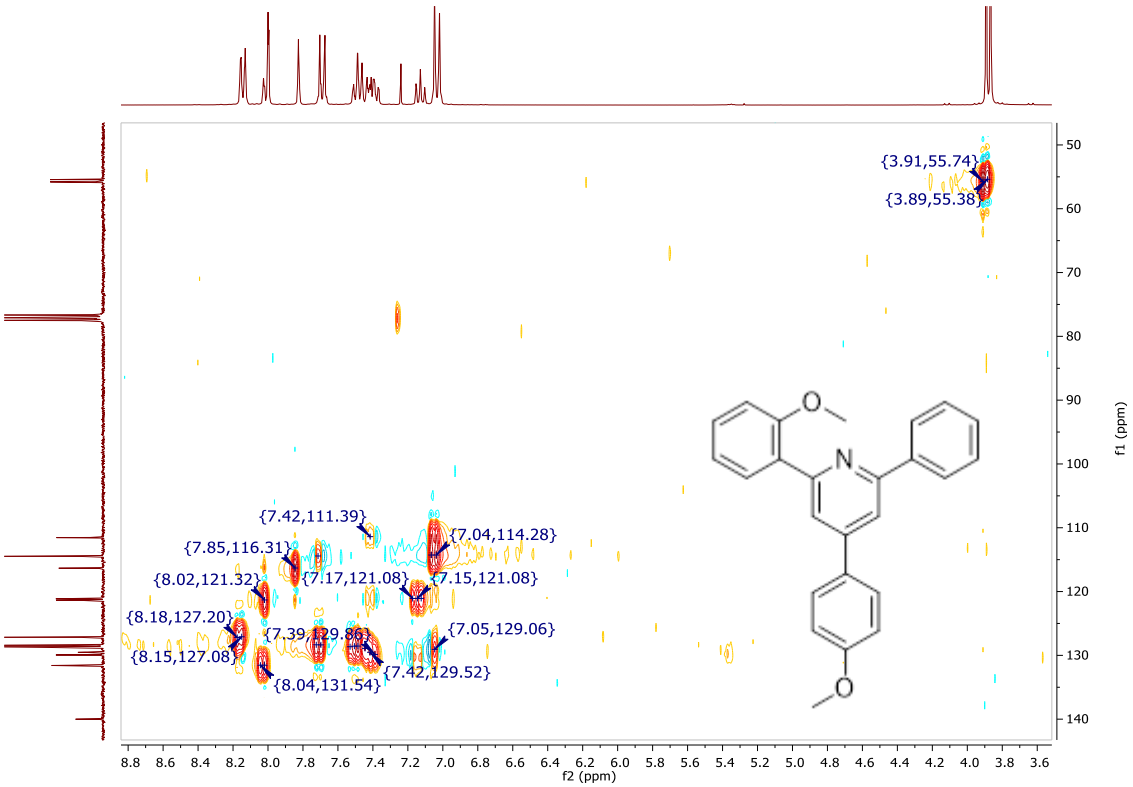

*Figure 31-HSQC spectrum of compound **5c***

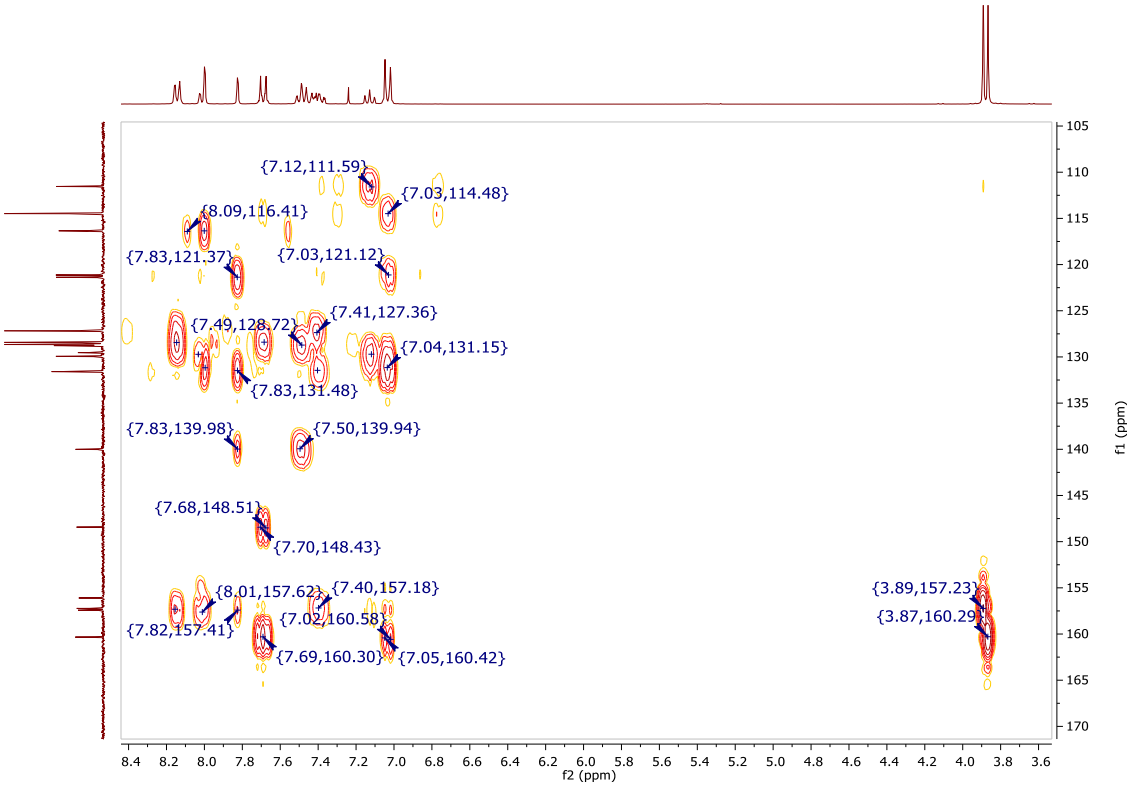

*Figure 32-HMBC spectrum of compound **5c***

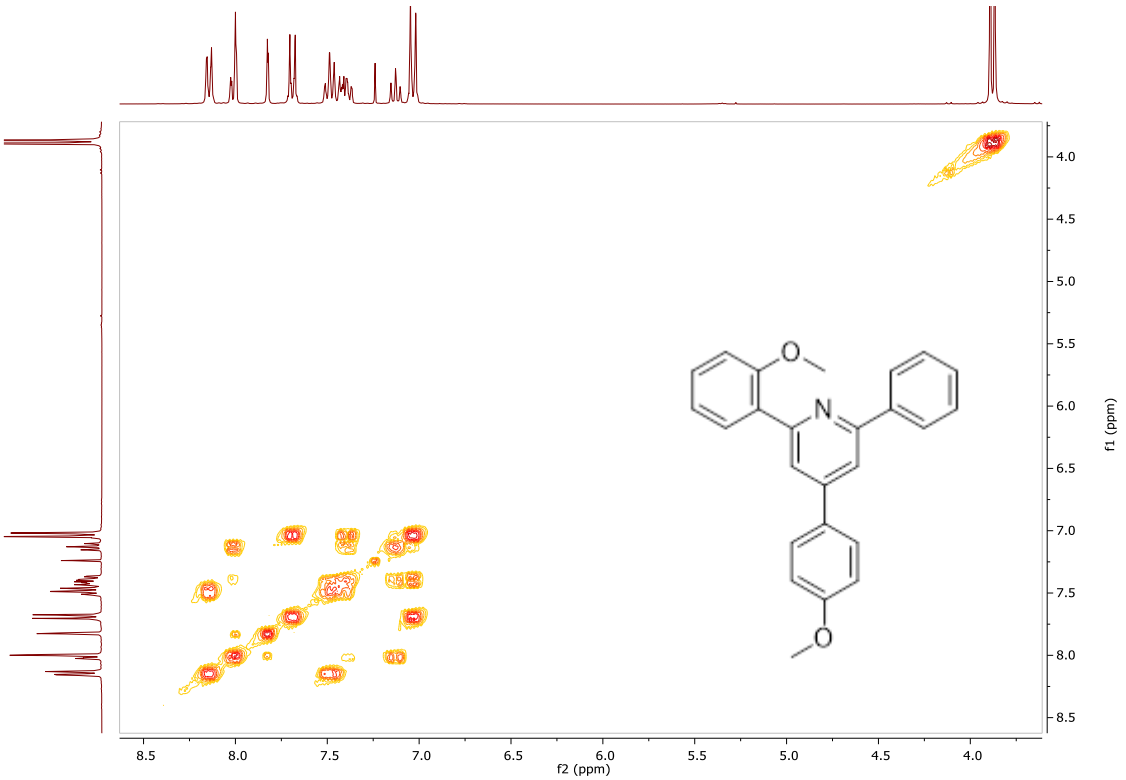

Figure 33-COSY spectrum of compound ***5c***

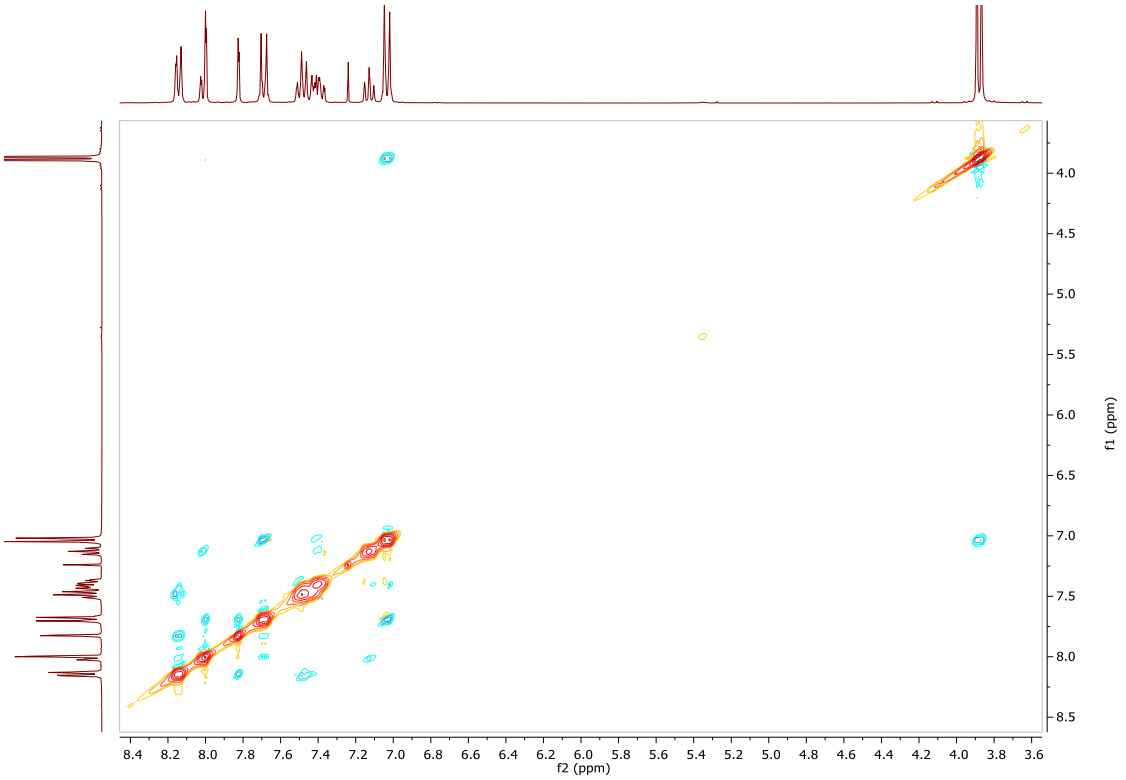

Figure 34-NOESY spectrum of compound ***5c***

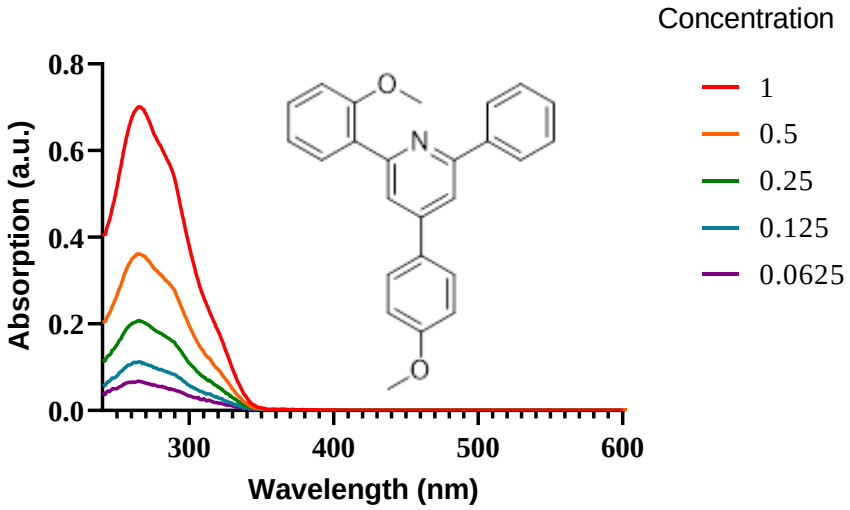

*Figure 35- Absorption spectra of compound **5c***

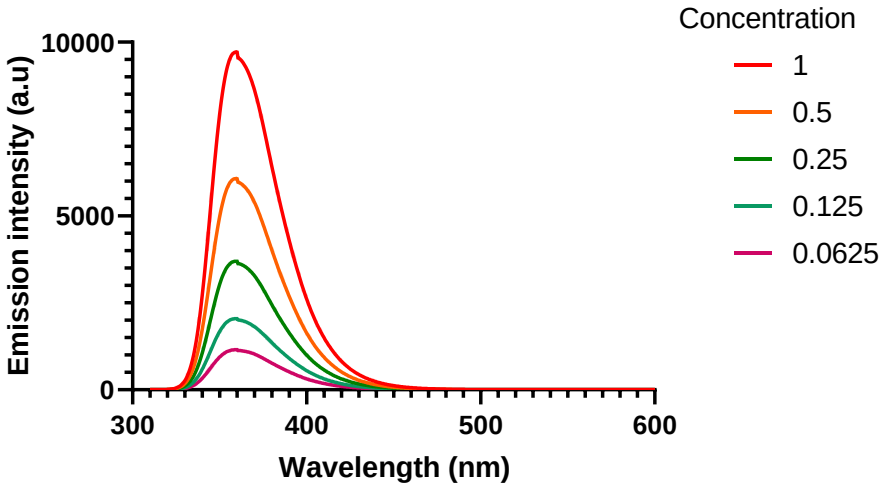

*Figure 36- Emission spectra of compound **5c***

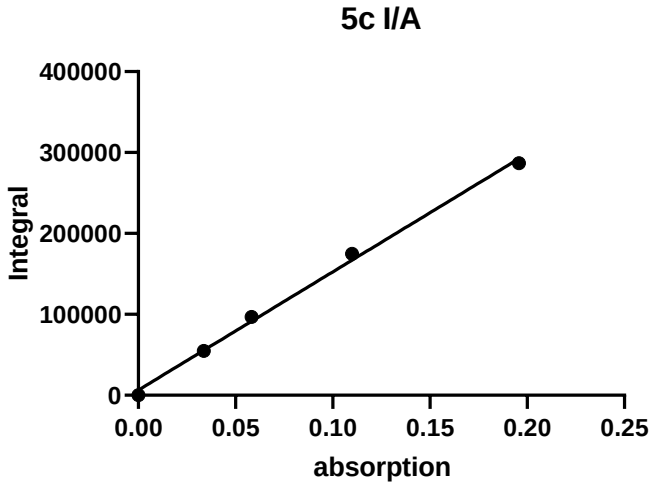

*Figure 37- Ratio of Integrated fluorescence intensity over absorption of compound **5c***

Pyridine 5d

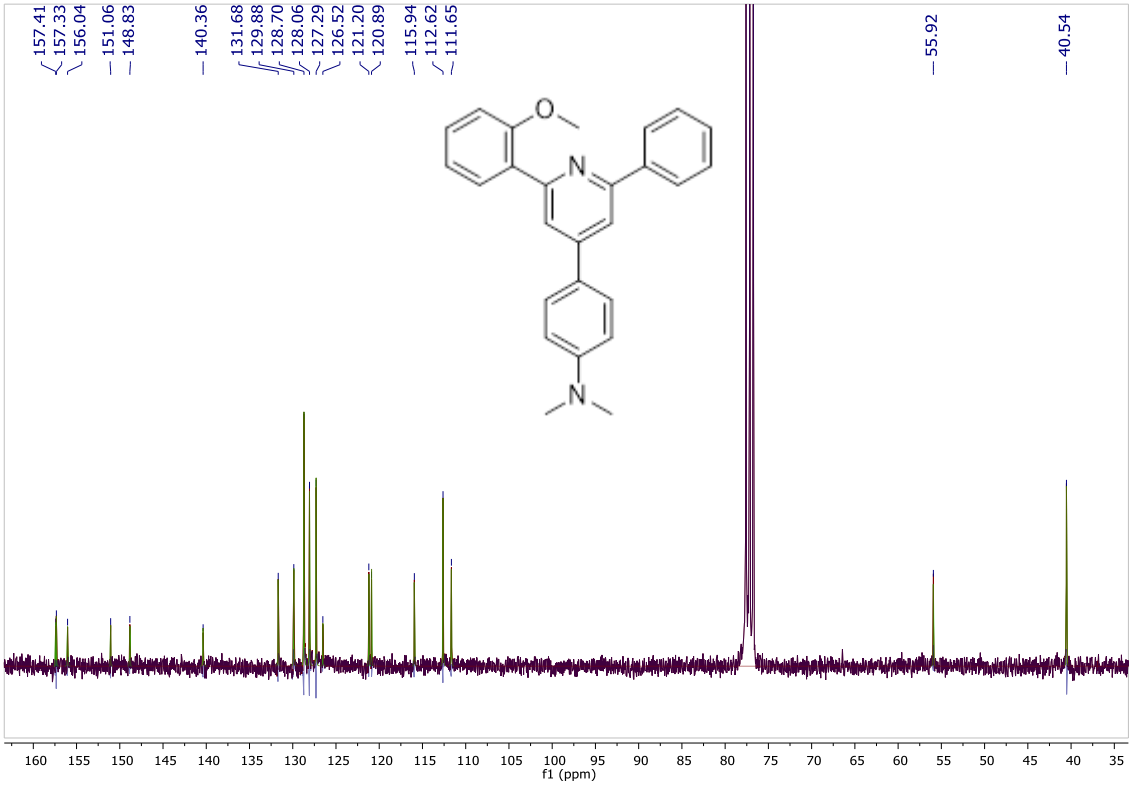

*Figure 38-^{13}C-NMR spectrum of compound **5d***

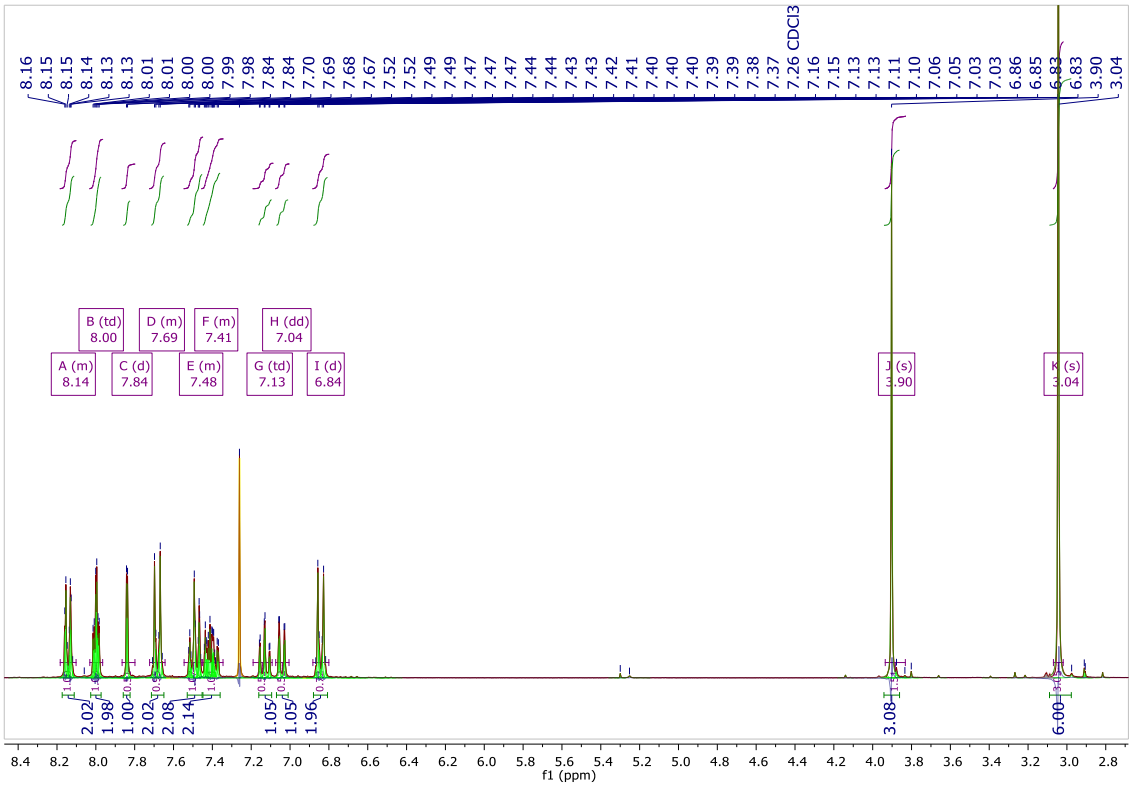

*Figure 39-^{1}H-NMR spectrum of compound **5d***

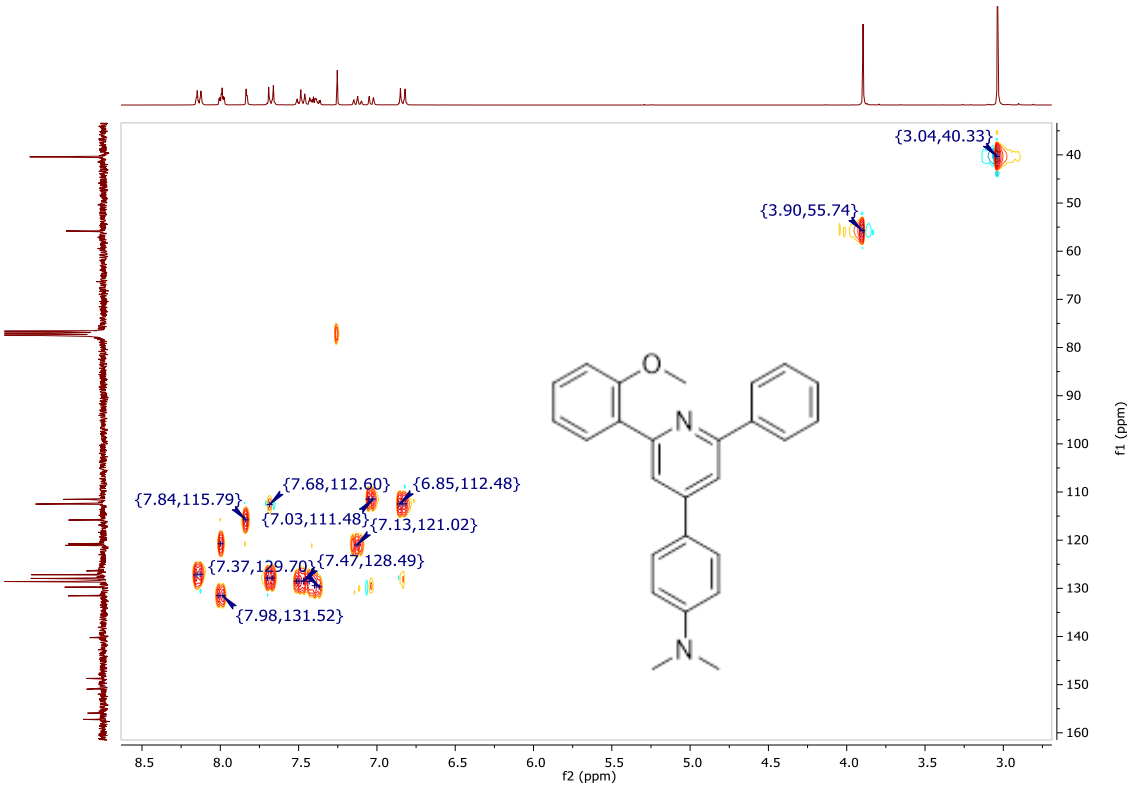

*Figure 40-HSQC spectrum of compound **5d***

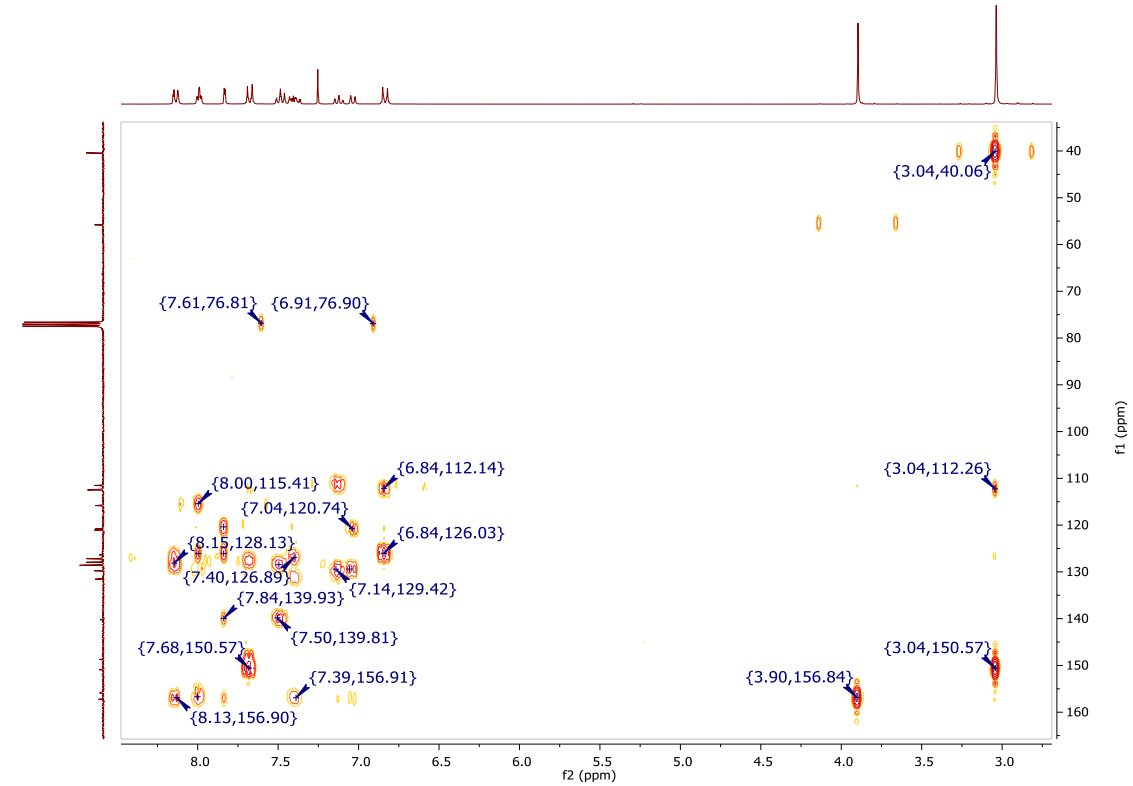

*Figure 41-HMBC spectrum of compound **5d***

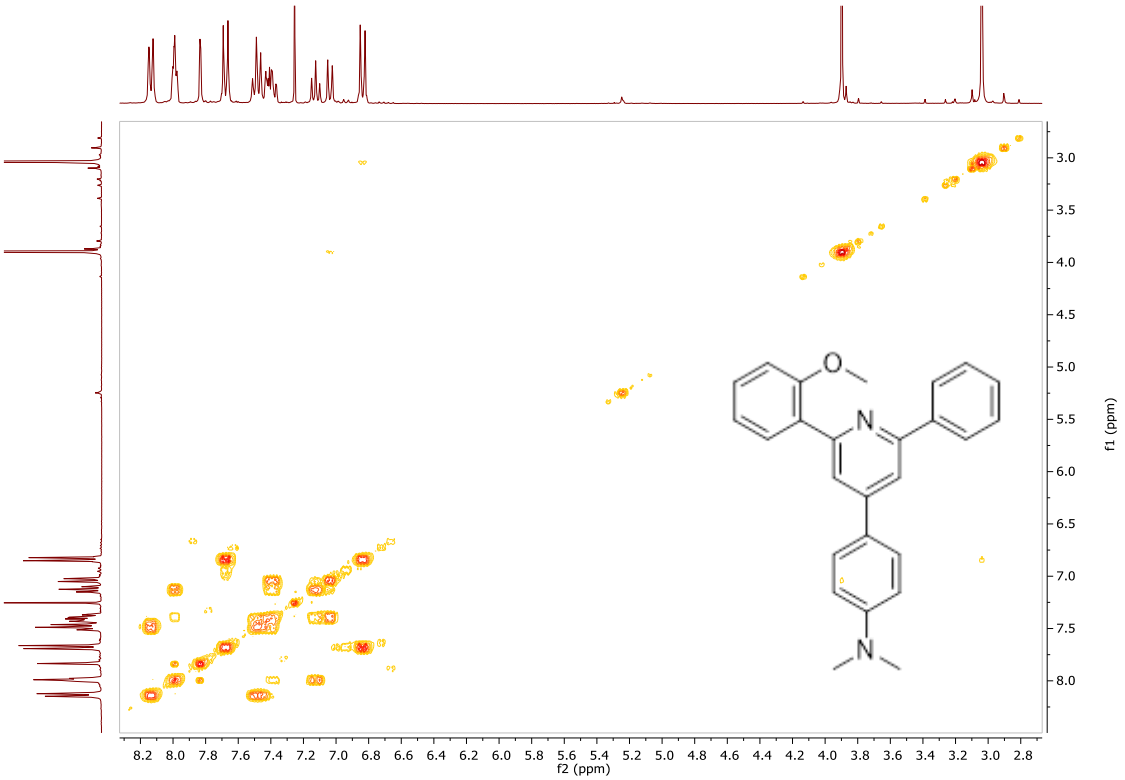

*Figure 42-COSY spectrum of compound **5d***

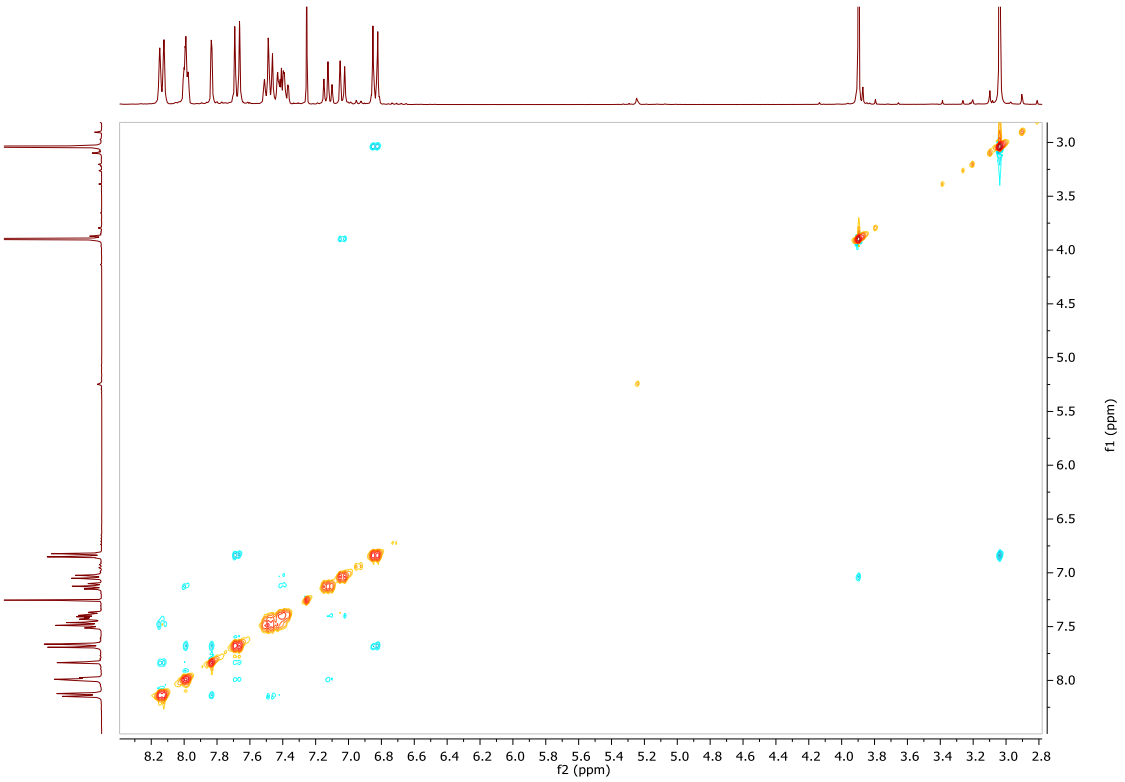

*Figure 43-NOESY spectrum of compound **5d***

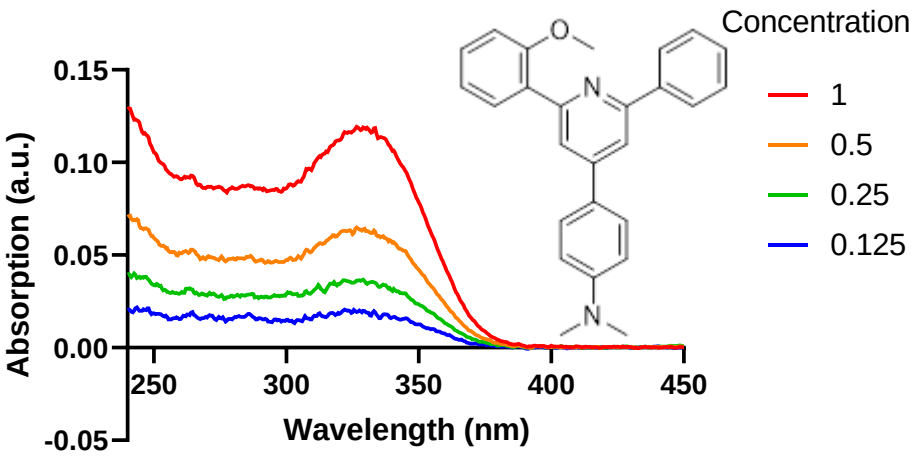

*Figure 44- Absorption spectra of compound **5d***

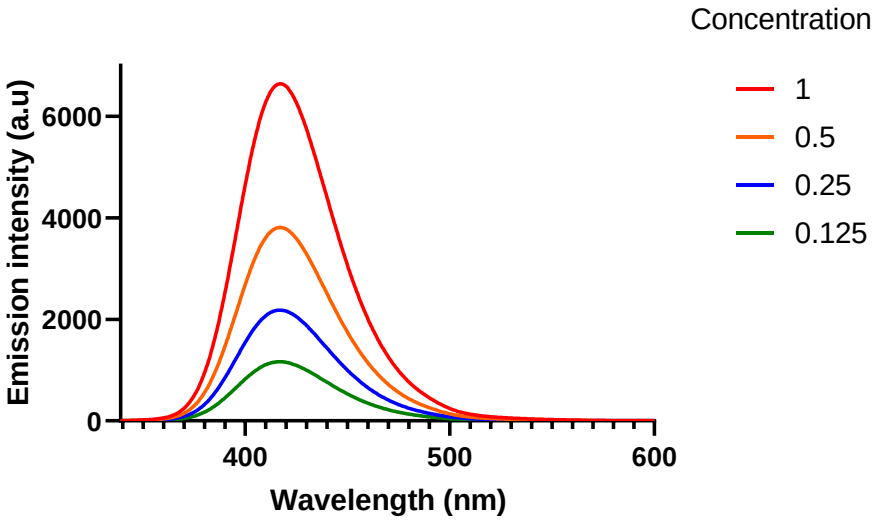

*Figure 45- Emission spectra of compound **5d***

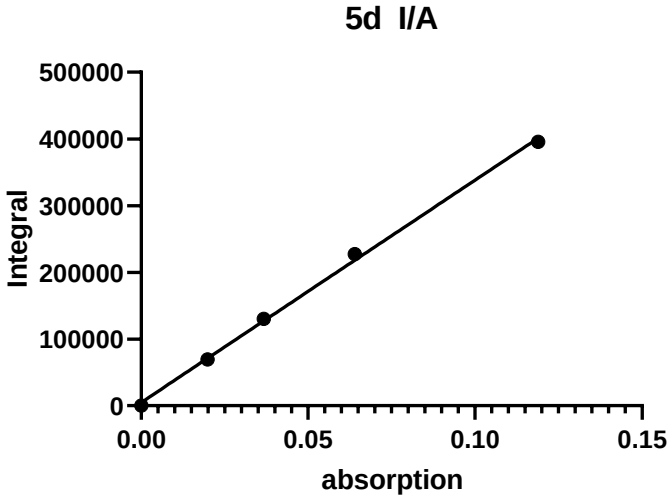

*Figure 46- Ratio of Integrated fluorescence intensity over absorption of compound **5d***

Pyridine 5e

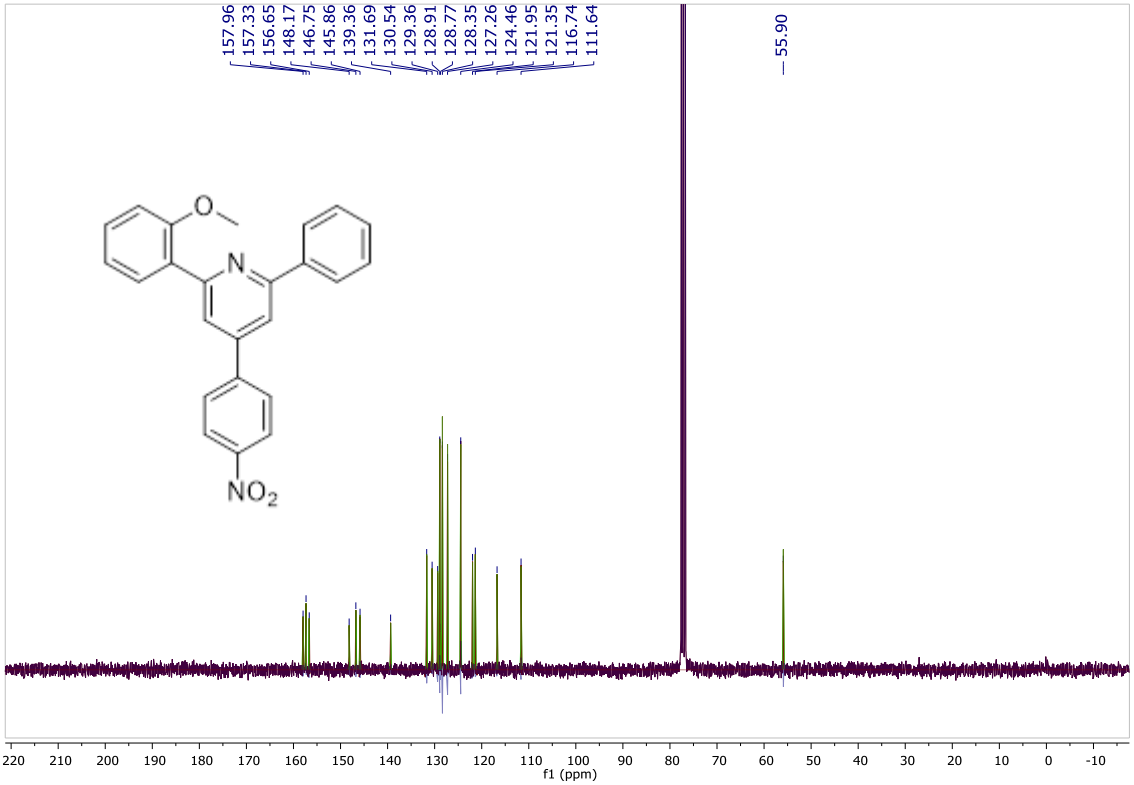

*Figure 47-^{13}C-NMR spectrum of compound **5e***

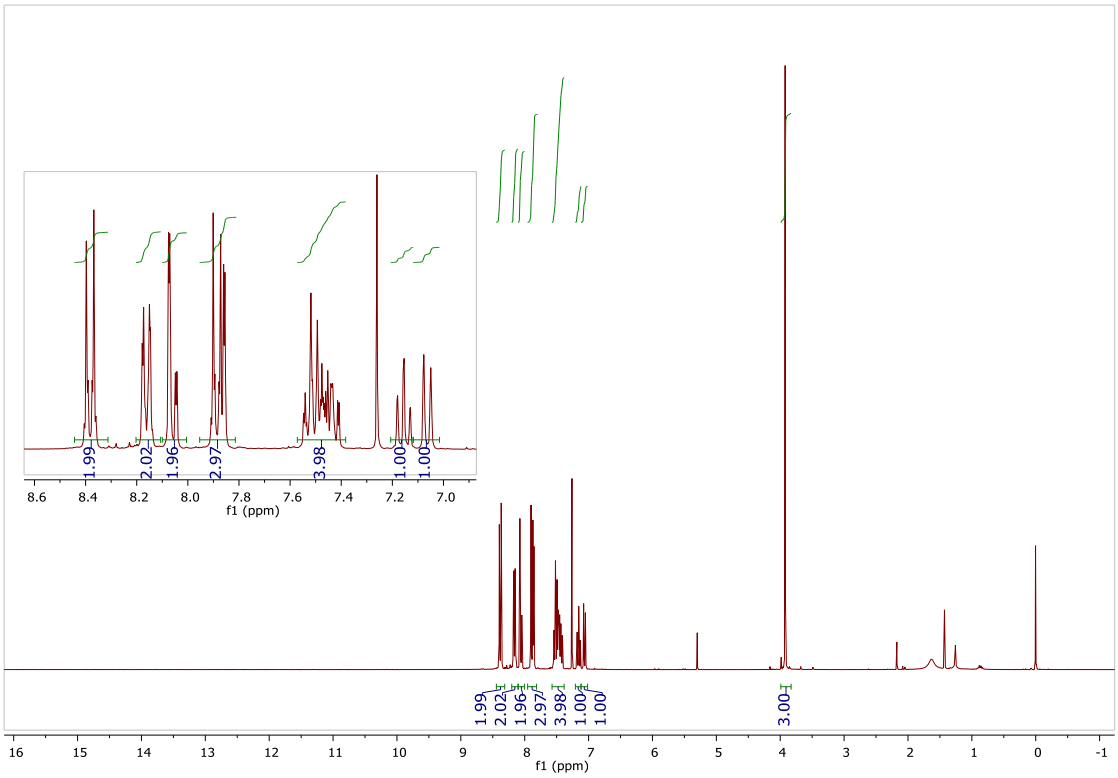

*Figure 48-^{1}H-NMR spectrum of compound **5e***

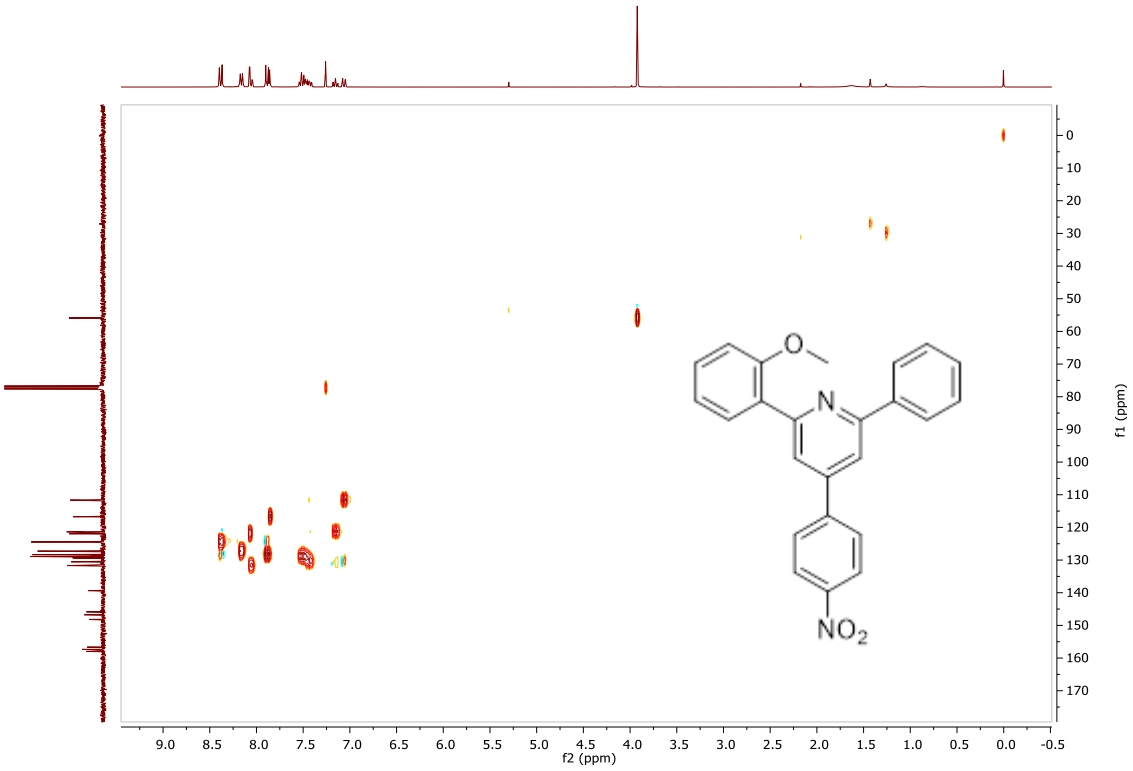

*Figure 49-HSQC spectrum of compound **5e***

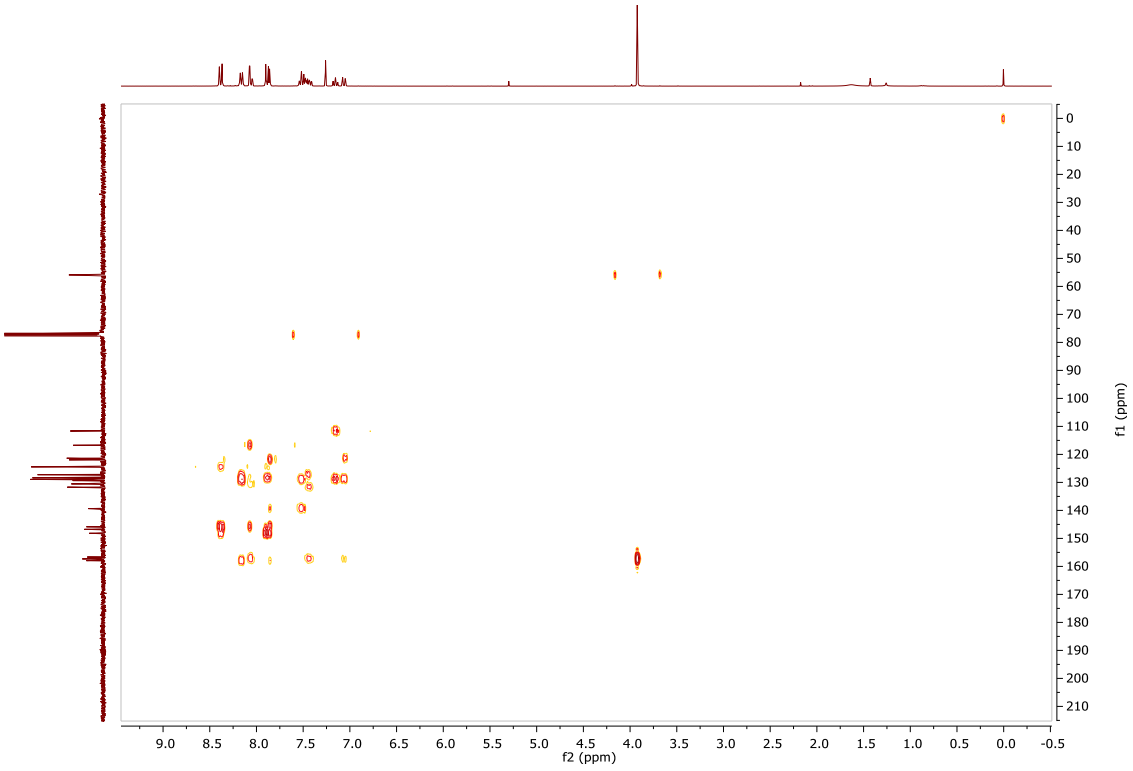

*Figure 50-HMBC spectrum of compound **5e***

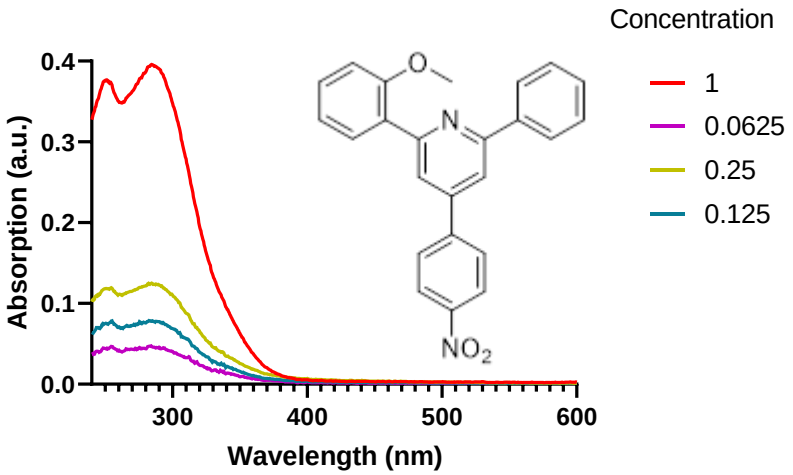

*Figure 51- Absorption spectra of compound **5e***

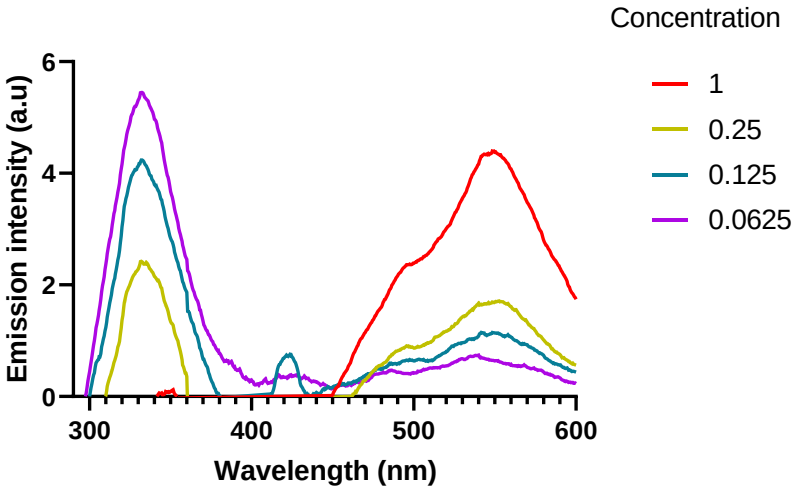

*Figure 52- Emission spectra of compound **5e***

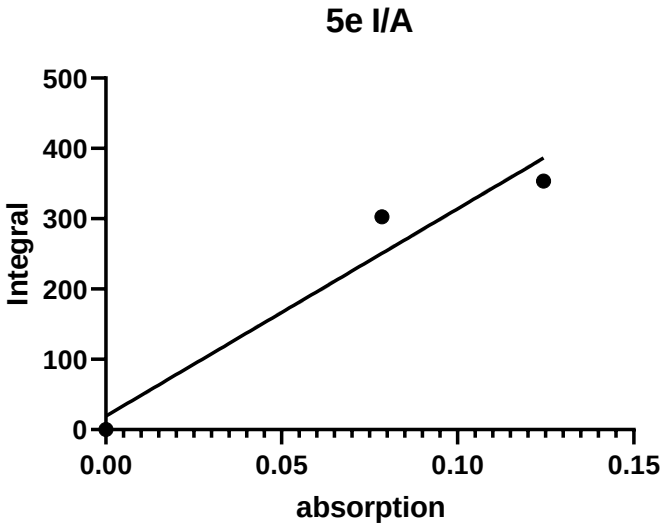

*Figure 53- Ratio of Integrated fluorescence intensity over absorption of compound **5e***

Pyridine 6a

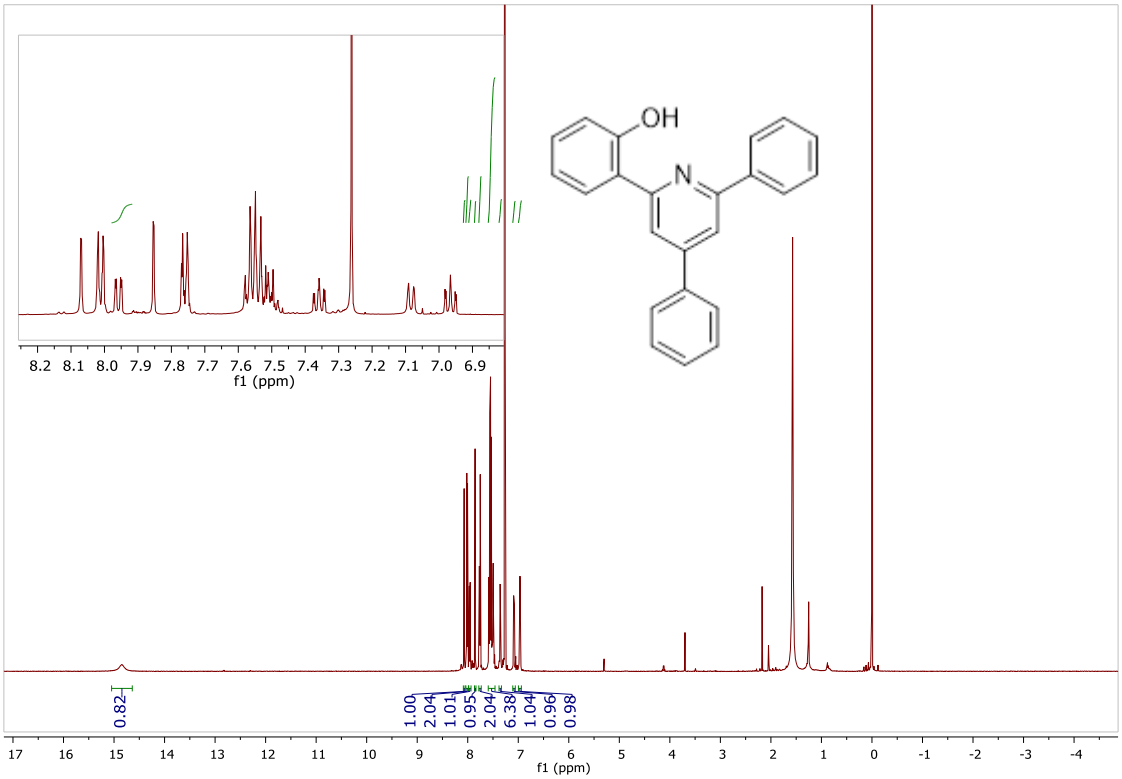

*Figure 54-^{1}H-NMR spectrum of compound **6a***

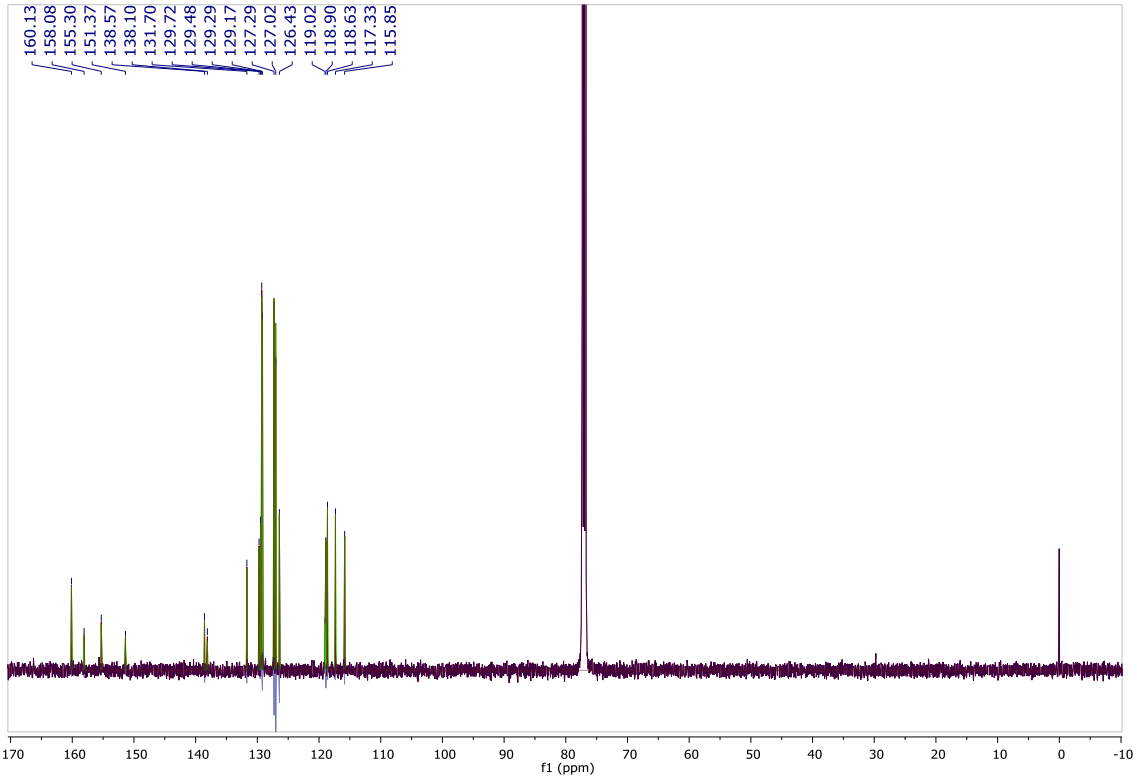

*Figure 55-^{13}C-NMR spectrum of compound **6a***

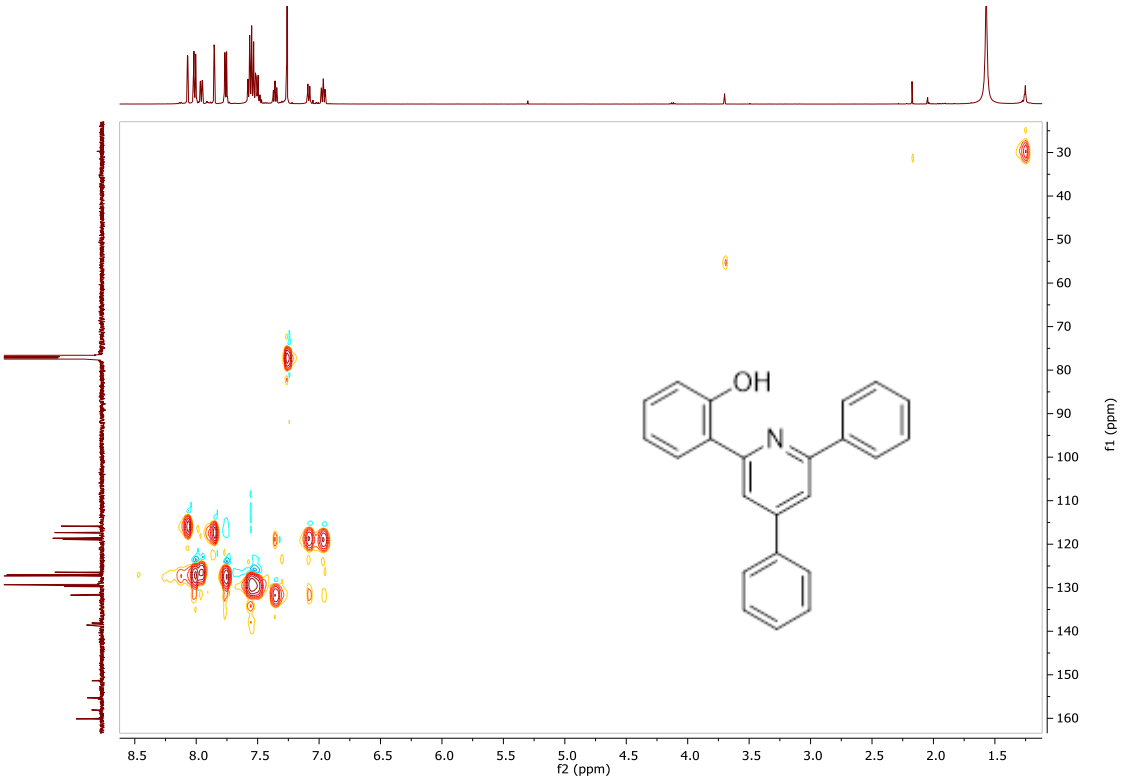

*Figure 56-HSQC spectrum of compound **6a***

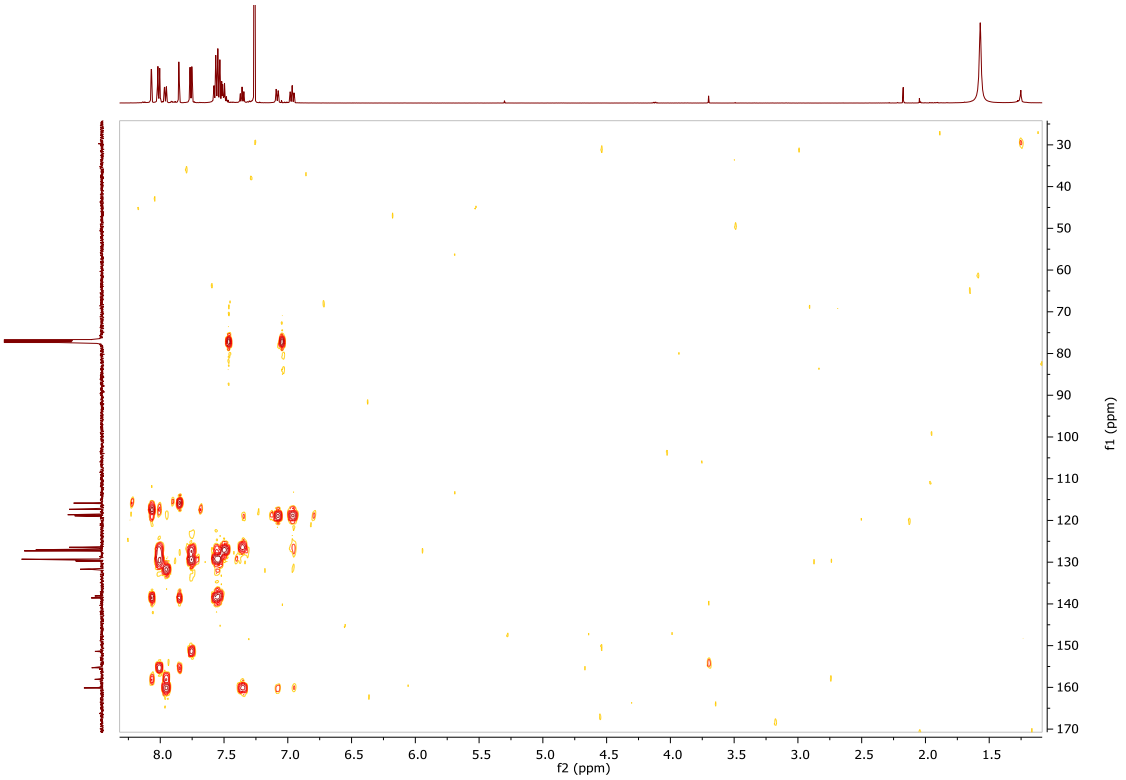

*Figure 57-HMBC spectrum of compound **6a***

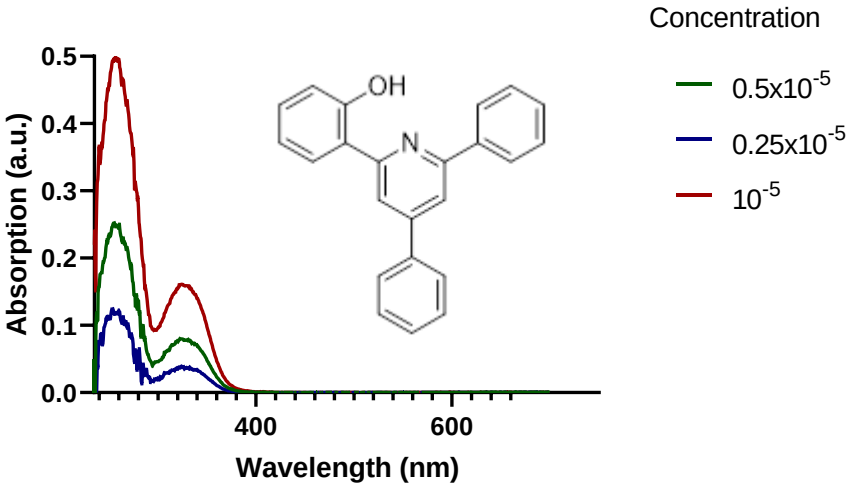

*Figure 58- Absorption spectra of compound **6a***

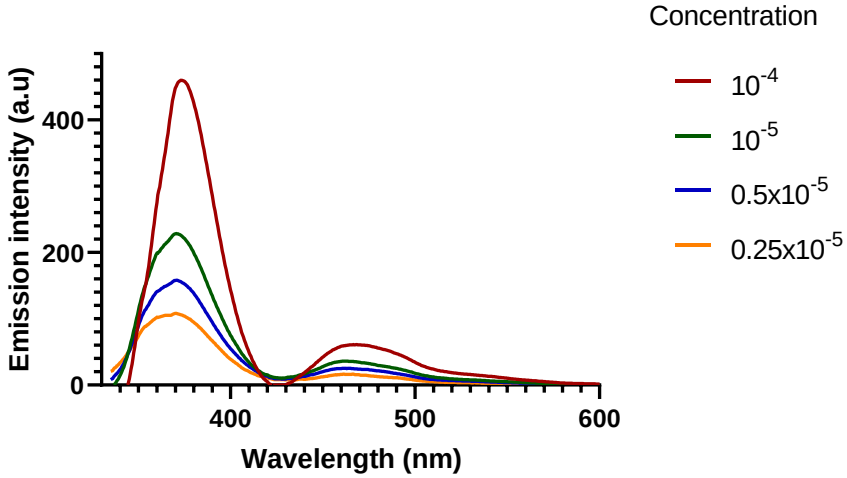

*Figure 59- Emission spectra of compound **6a***

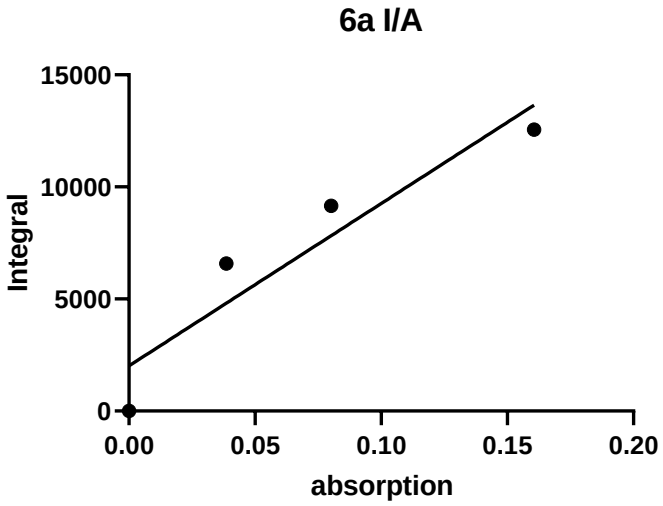

*Figure 60- Ratio of Integrated fluorescence intensity over absorption of compound **6a***

Pyridine 6b

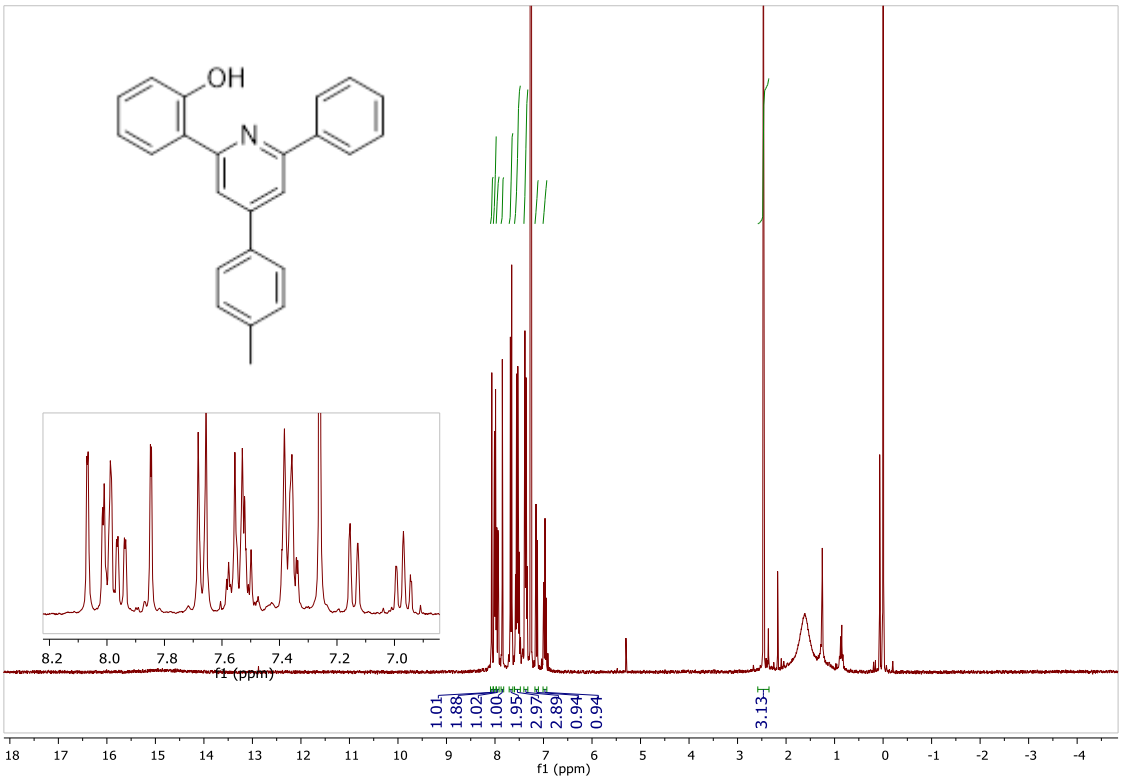

*Figure 61-^{1}H-NMR spectrum of compound **6b***

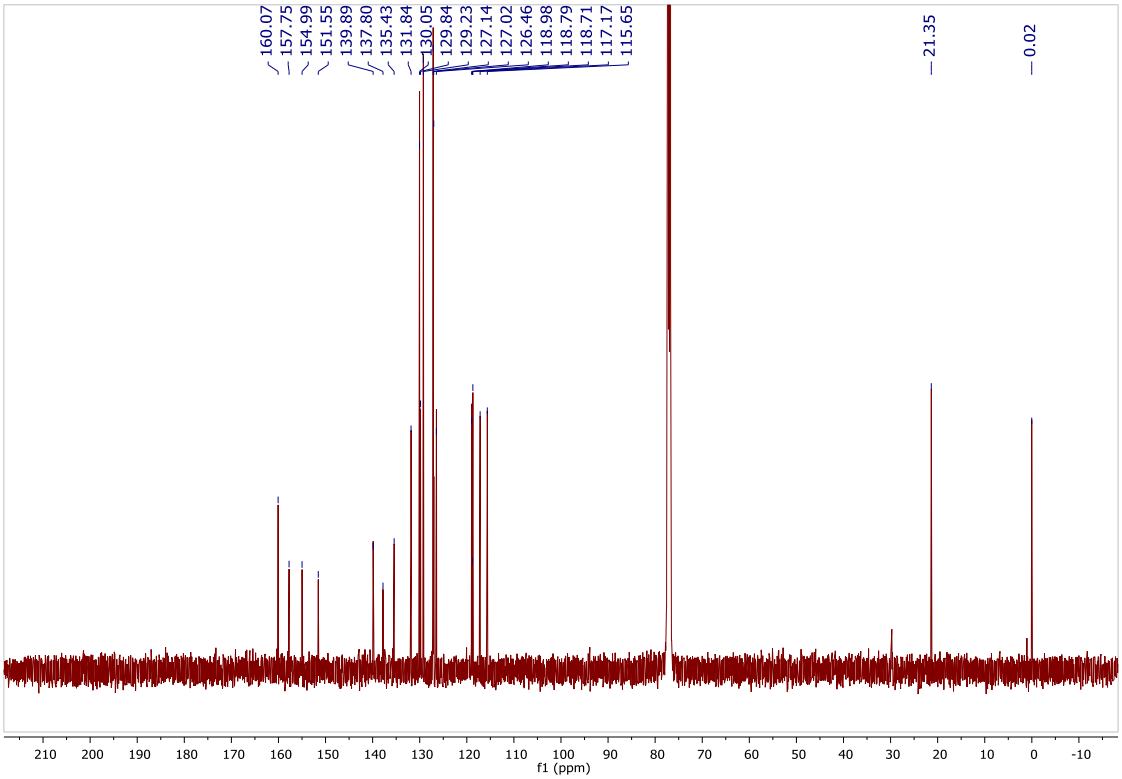

*Figure 62-^{13}C-NMR spectrum of compound **6b***

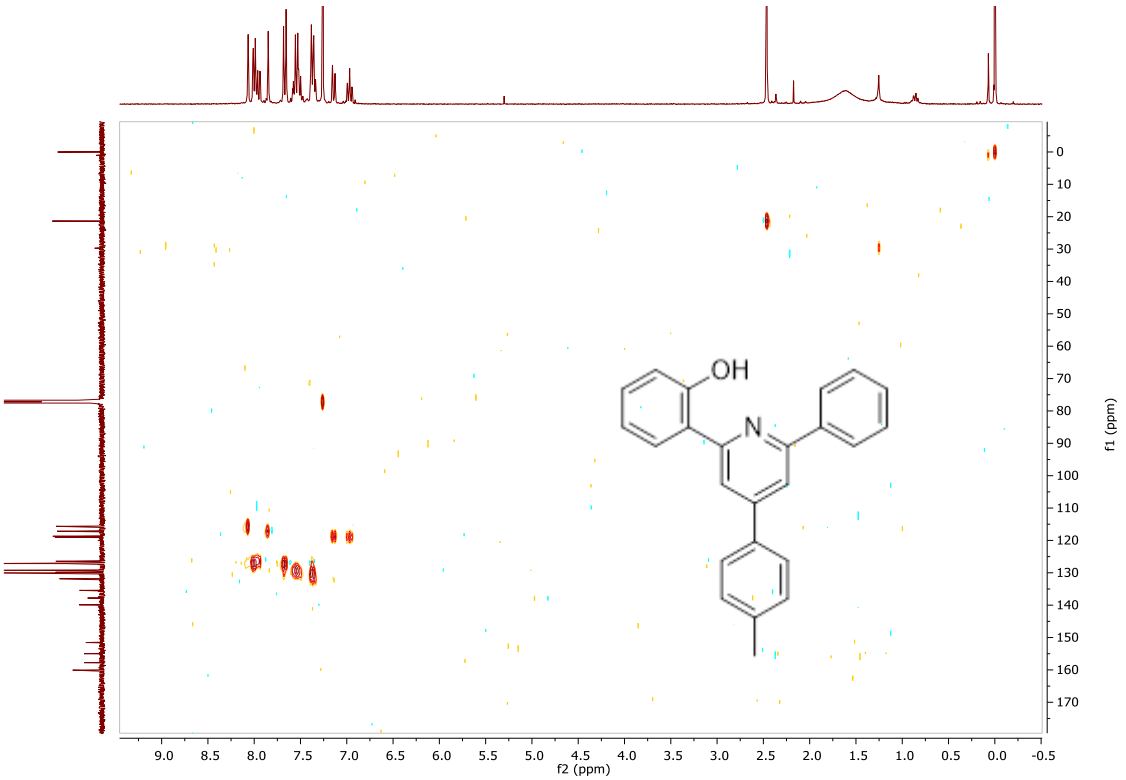

*Figure 63-HSQC spectrum of compound **6b***

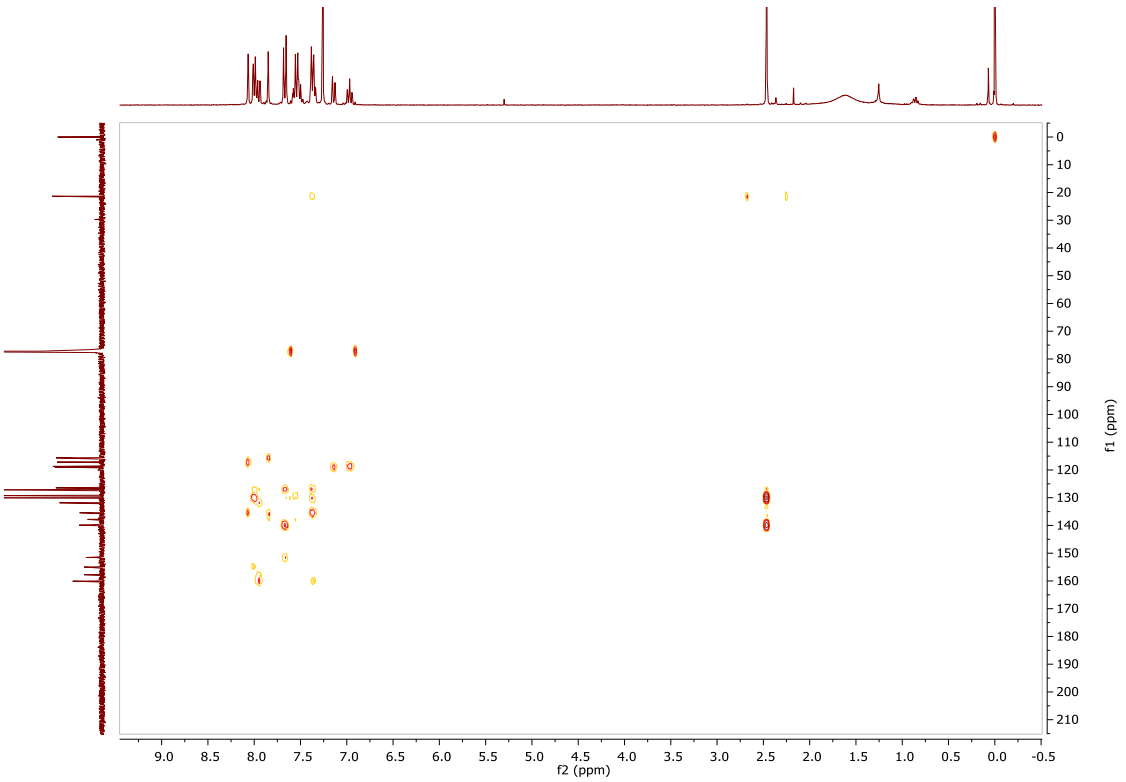

*Figure 64-HMBC spectrum of compound **6b***

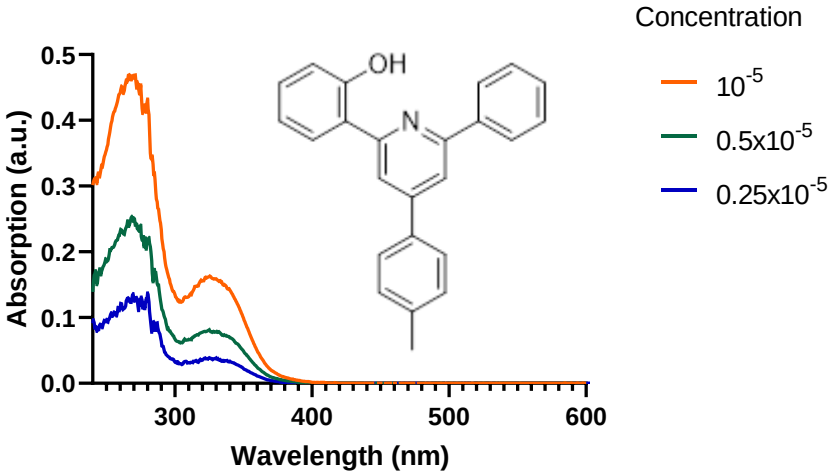

*Figure 65- Absorption spectra of compound **6b***

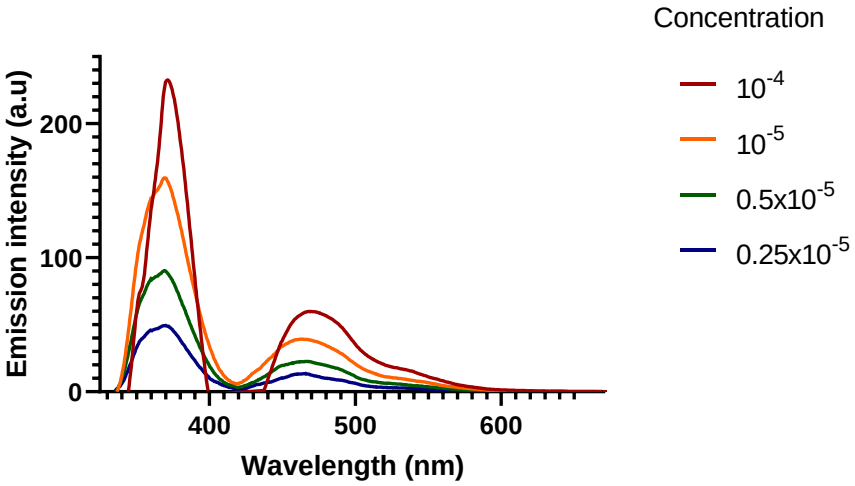

*Figure 66- Emission spectra of compound **6b***

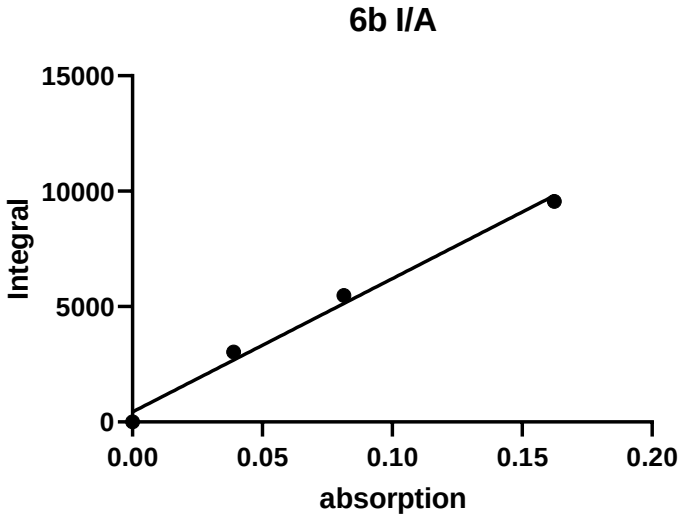

*Figure 67- Ratio of Integrated fluorescence intensity over absorption of compound **6b***

Pyridine 6c

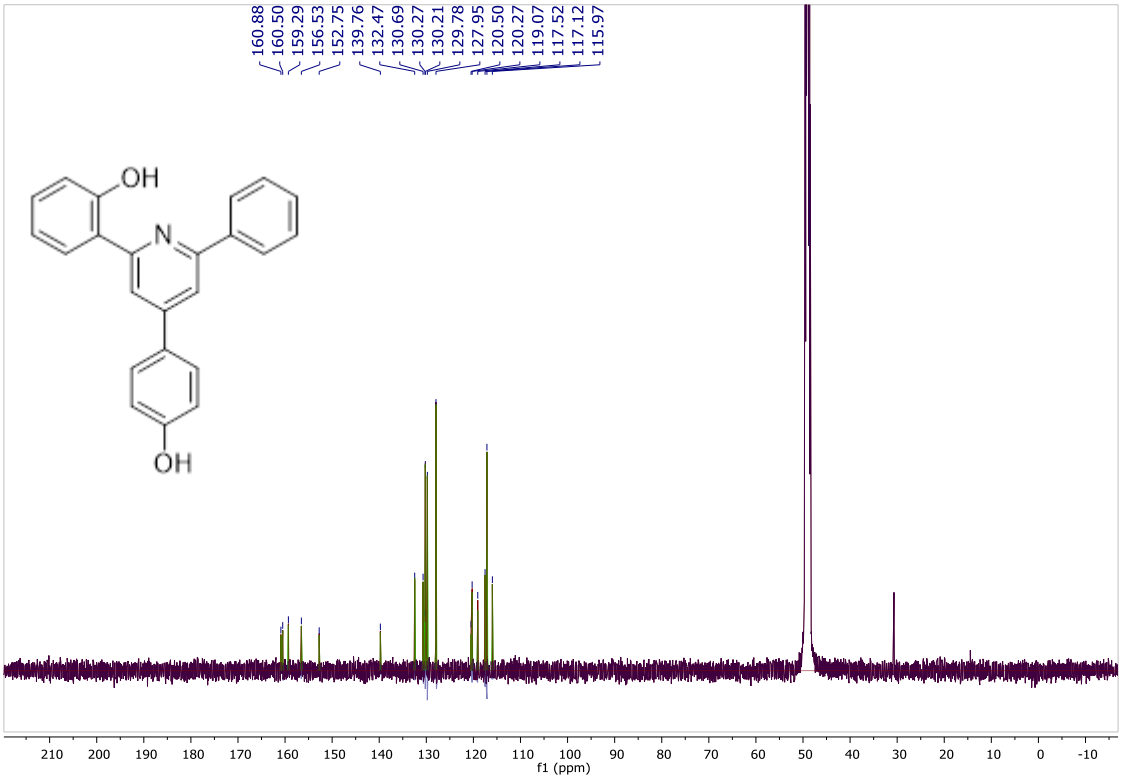

*Figure 68-^{13}C-NMR spectrum of compound **6c***

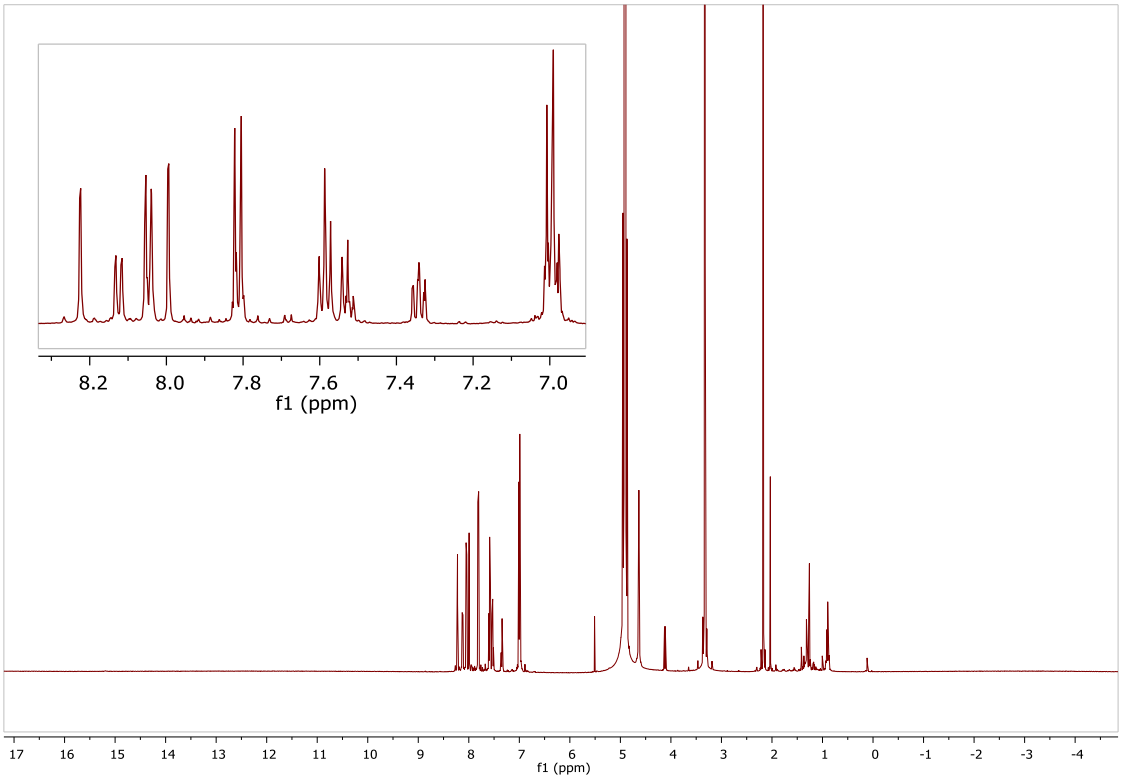

*Figure 69-^{1}H-NMR spectrum of compound **6c***

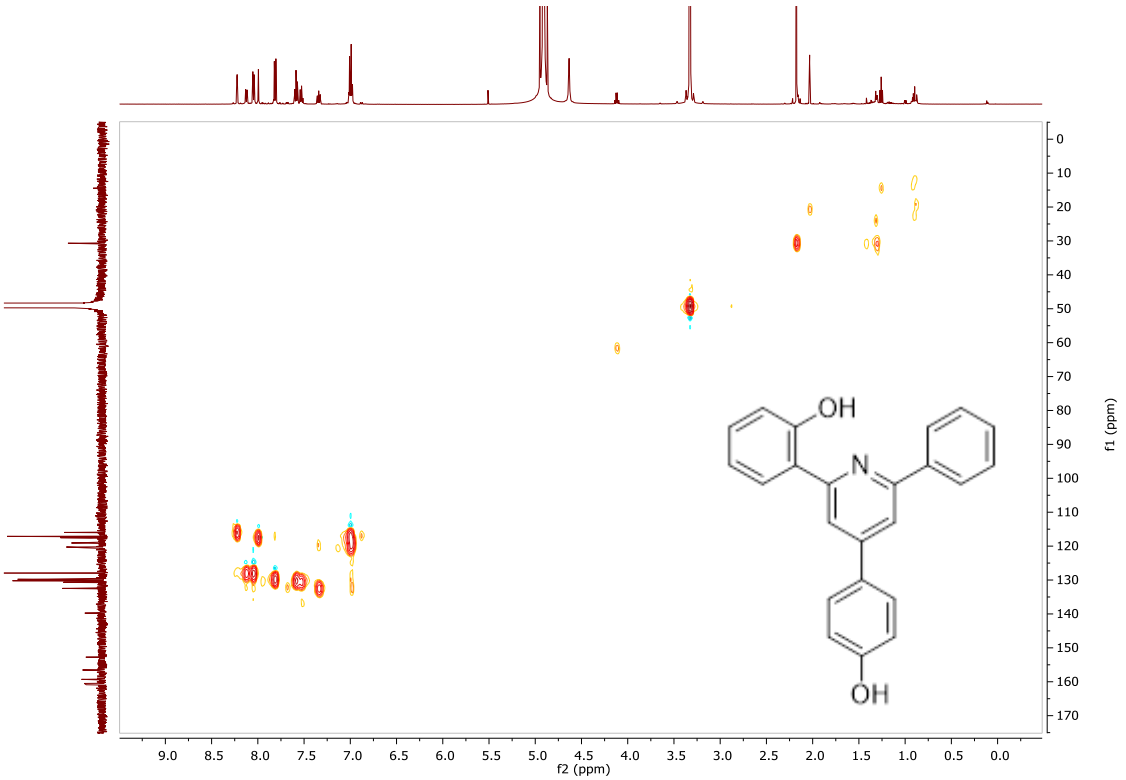

*Figure 70-HSQC spectrum of compound **6c***

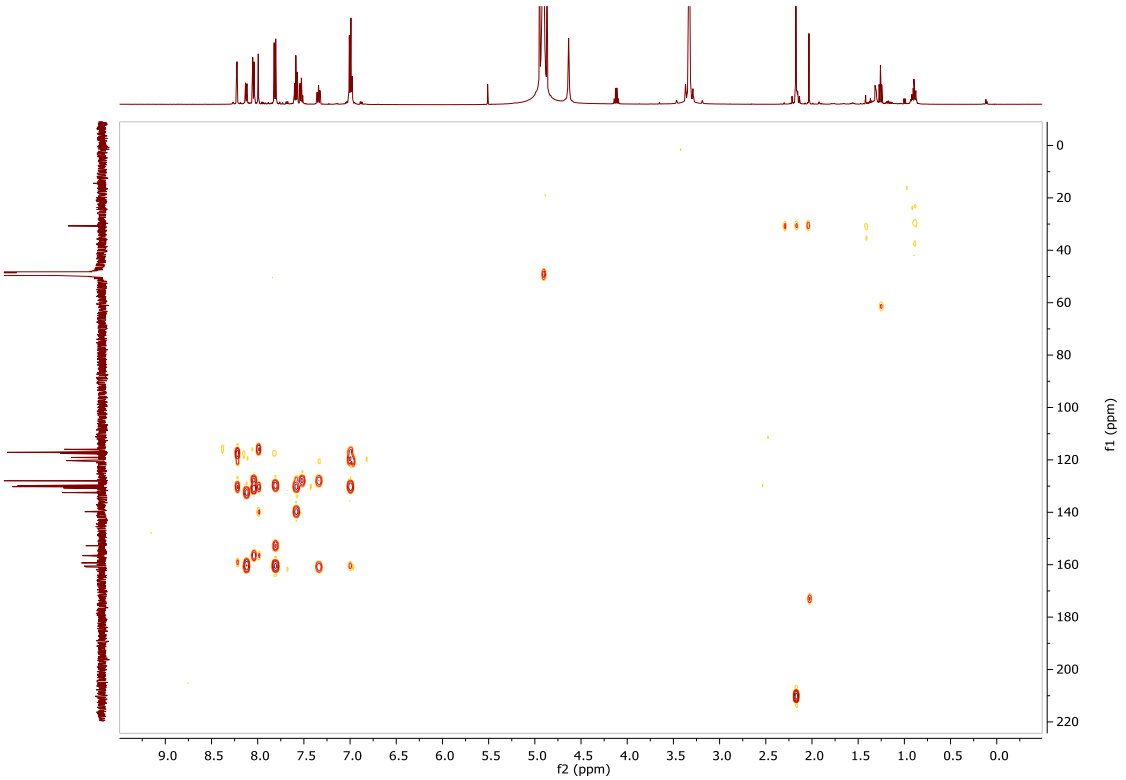

*Figure 71-HMBC spectrum of compound **6c***

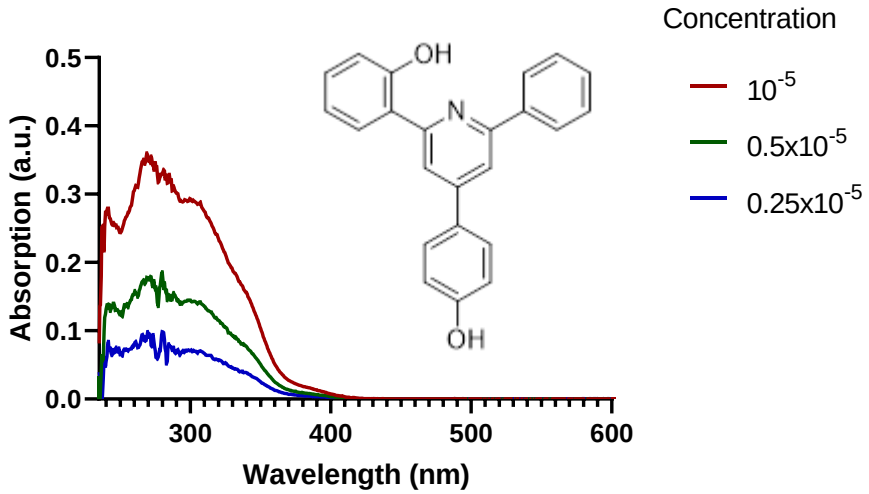

*Figure 72- Absorption spectra of compound **6c***

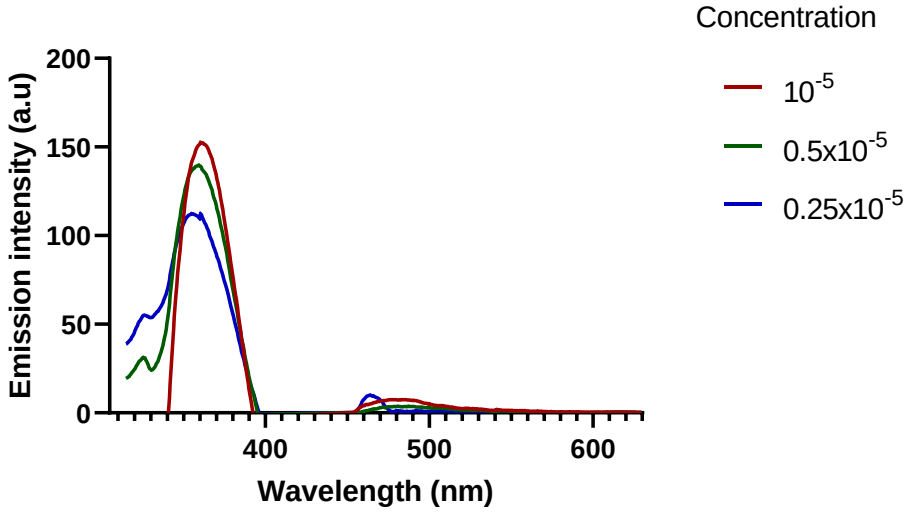

*Figure 73- Emission spectra of compound **6c***

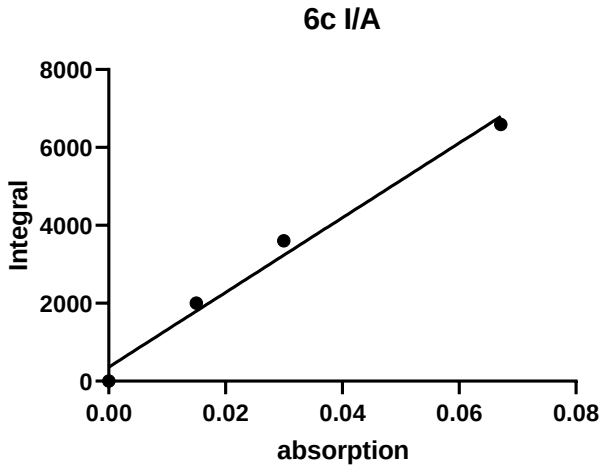

*Figure 74- Ratio of Integrated fluorescence intensity over absorption of compound **6c***

Pyridine 6d

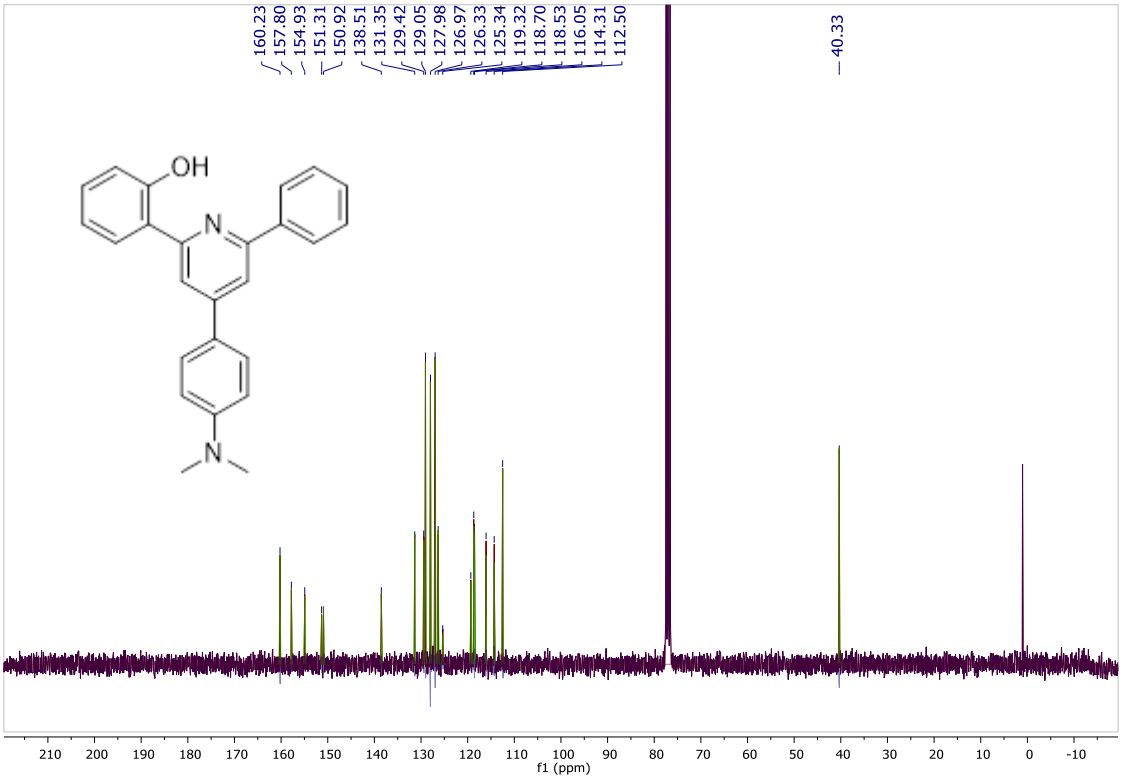

*Figure 75-^{13}C-NMR spectrum of compound **6d***

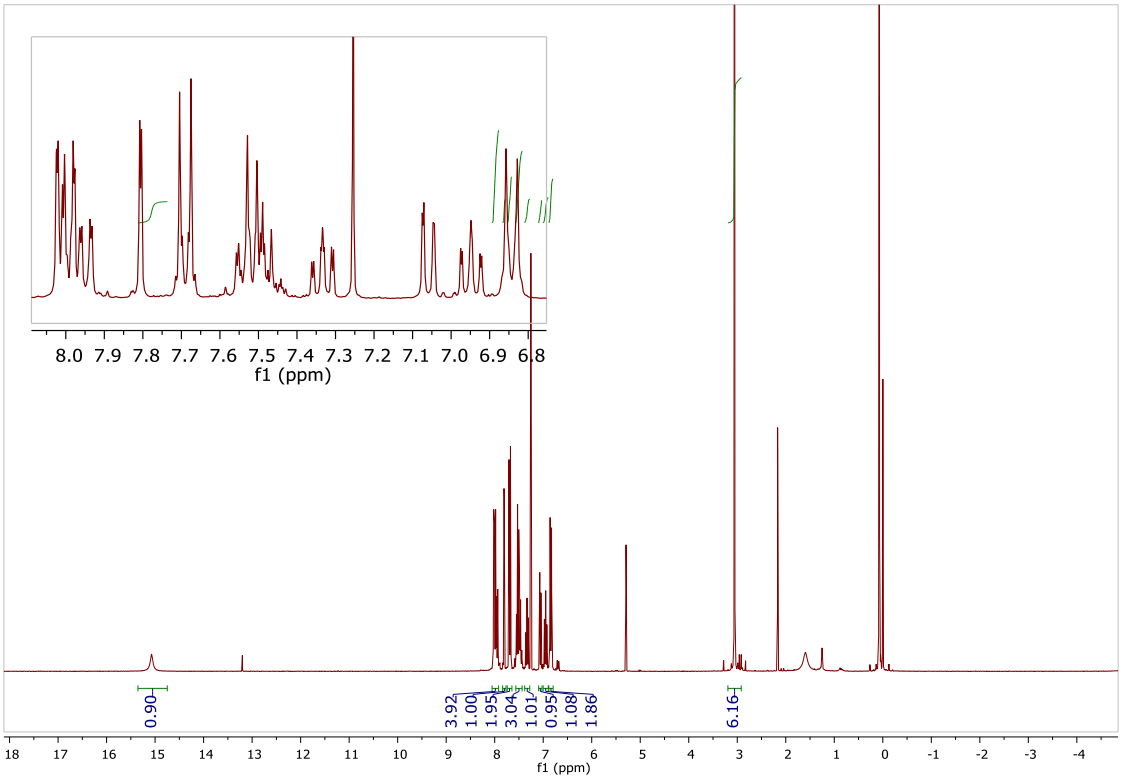

*Figure 76-^{1}H-NMR spectrum of compound **6d***

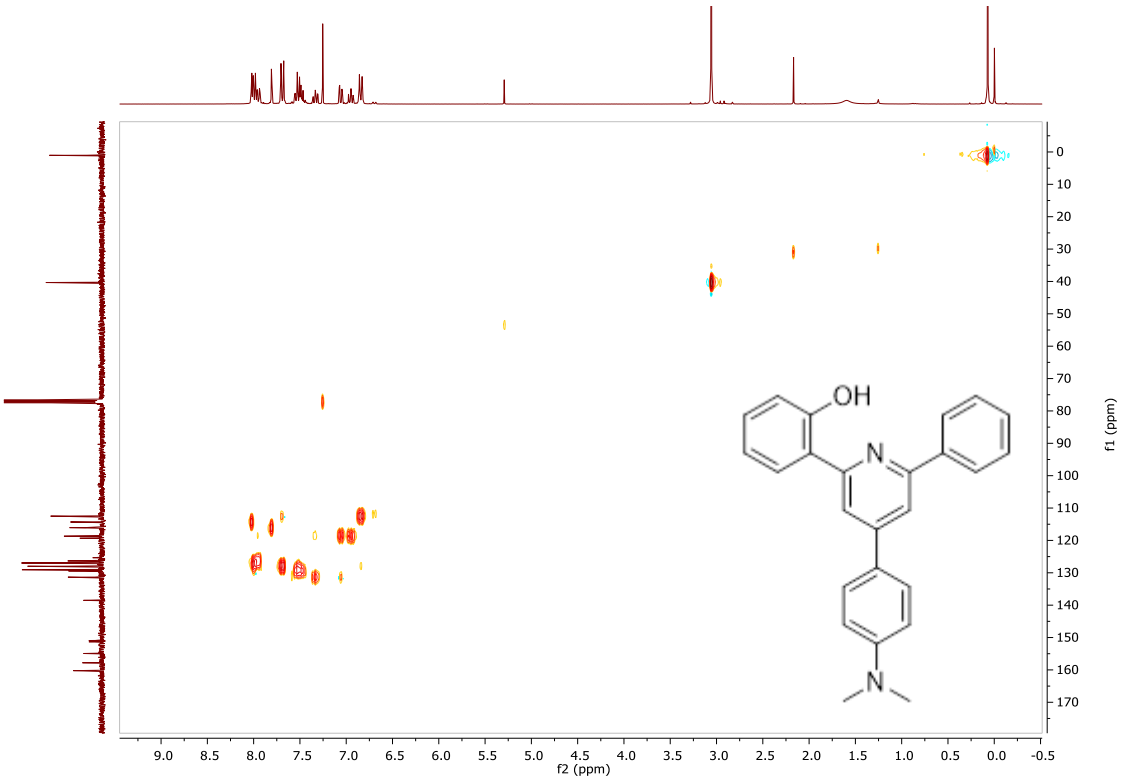

*Figure 77-HSQC spectrum of compound **6d***

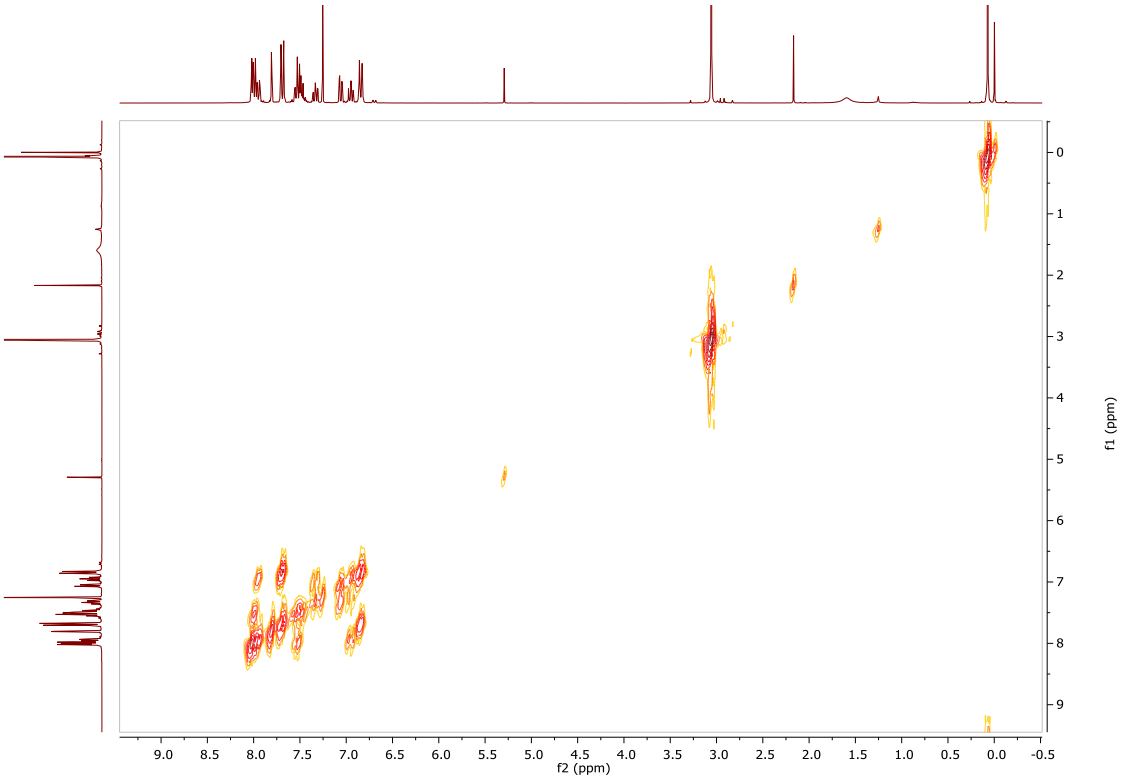

*Figure 78-COSY spectrum of compound **6d***

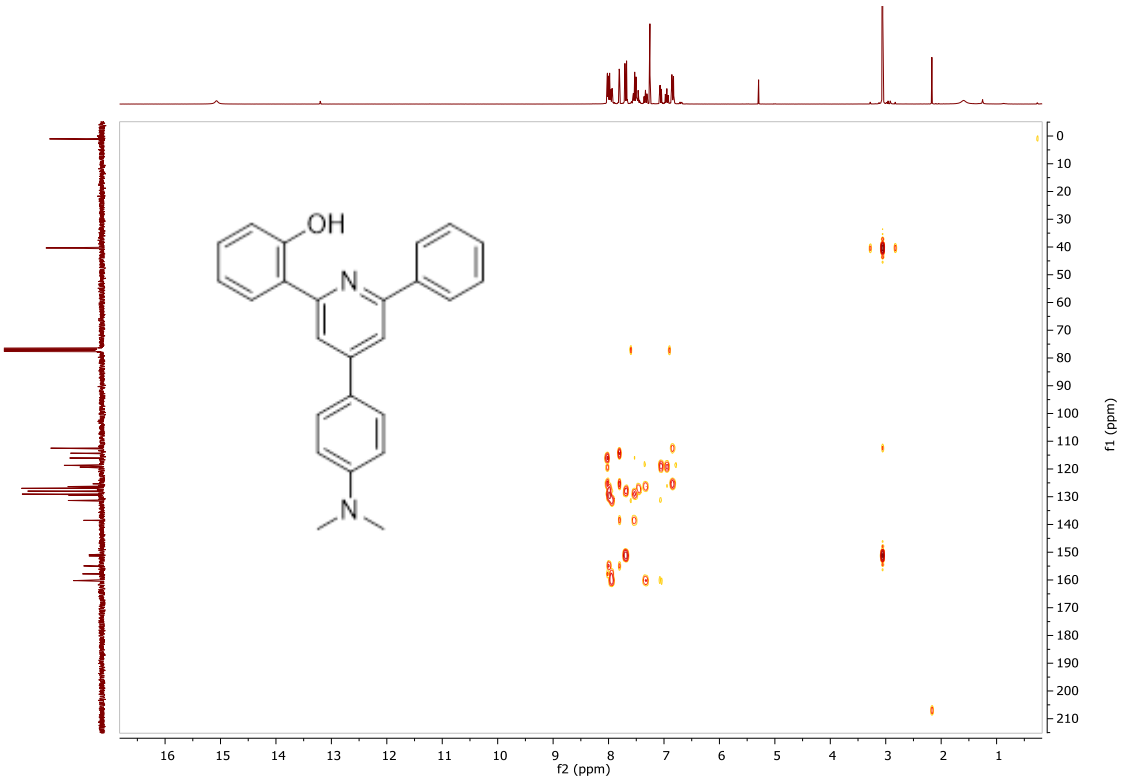

*Figure 79-HMBC spectrum of compound **6d***

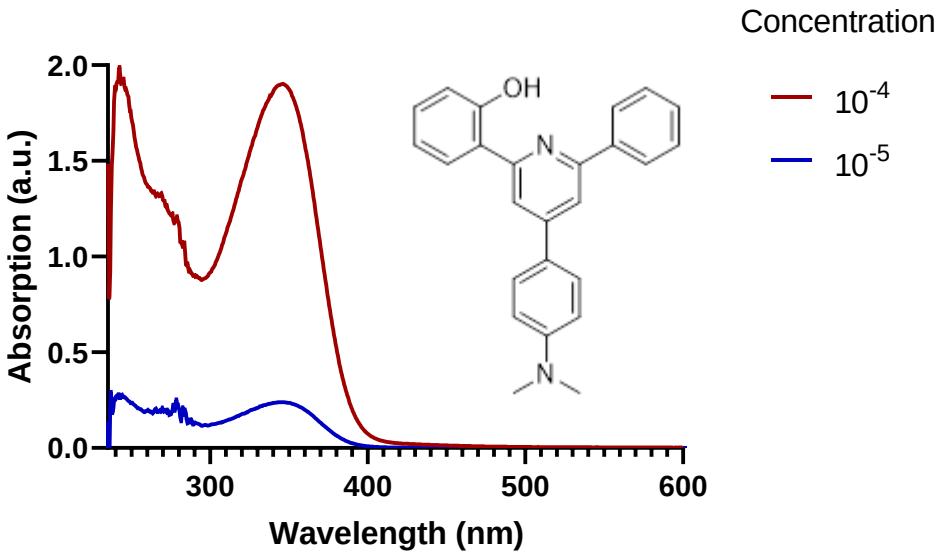

Figure 80- Absorption spectra of compound ***6d***

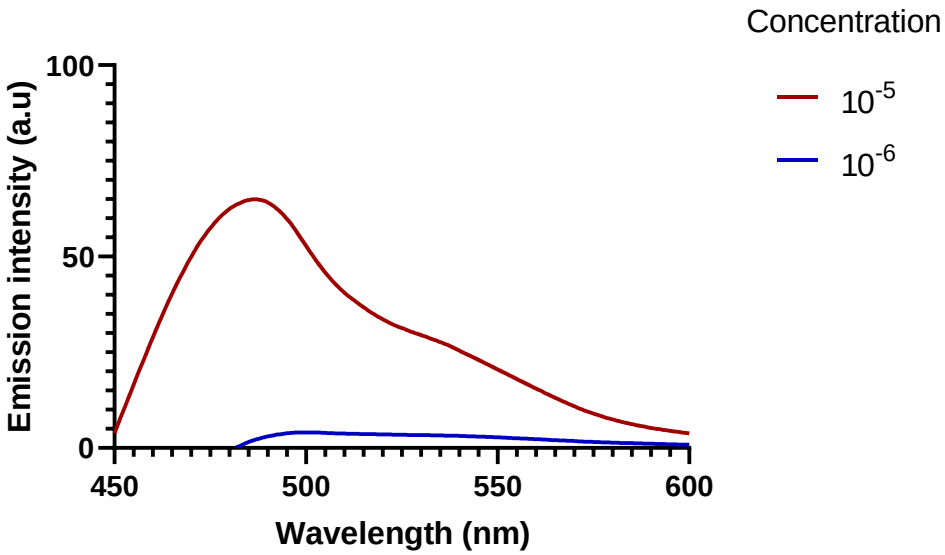

Figure 81- Emission spectra of compound ***6d***

Pyridine 6e

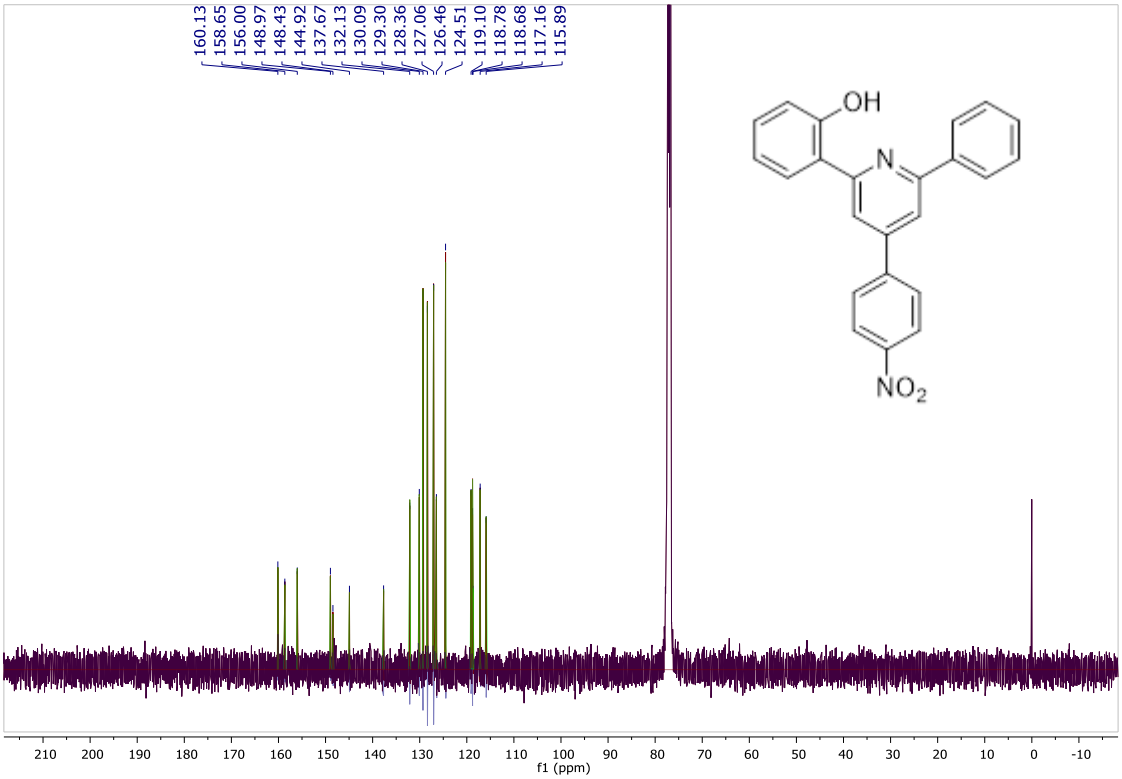

*Figure 82-^{13}C-NMR spectrum of compound **6e***

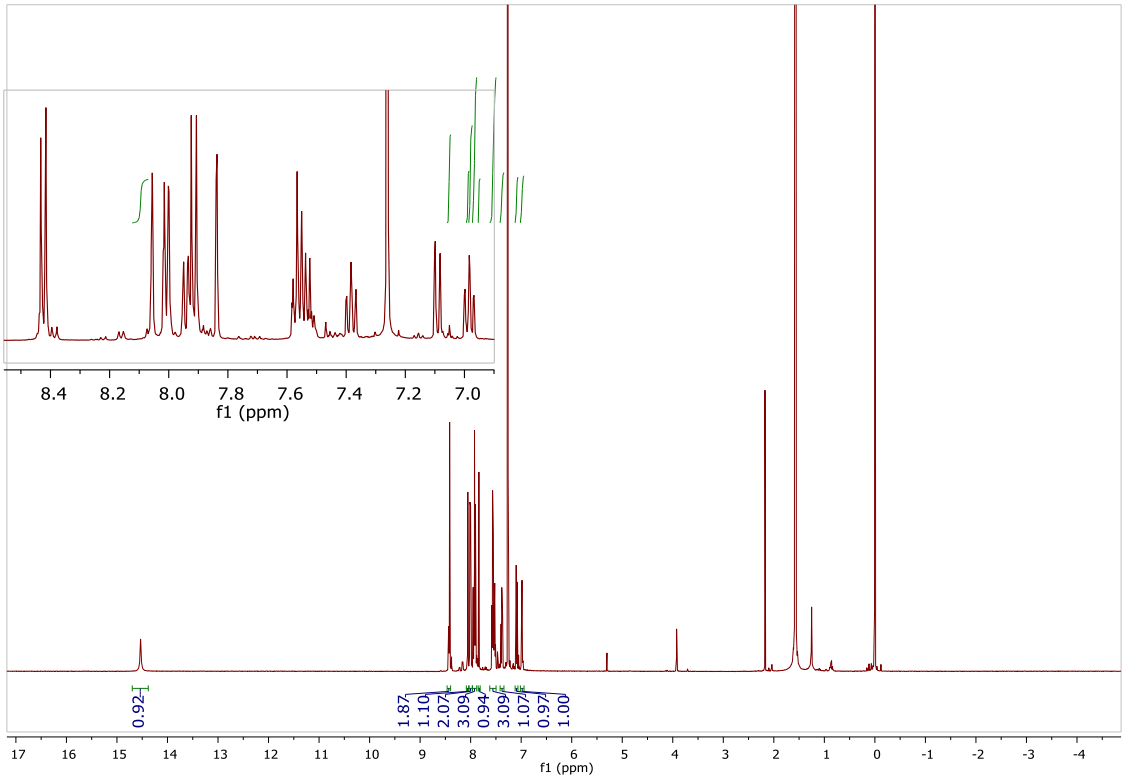

*Figure 83-^{1}H-NMR spectrum of compound **6e***

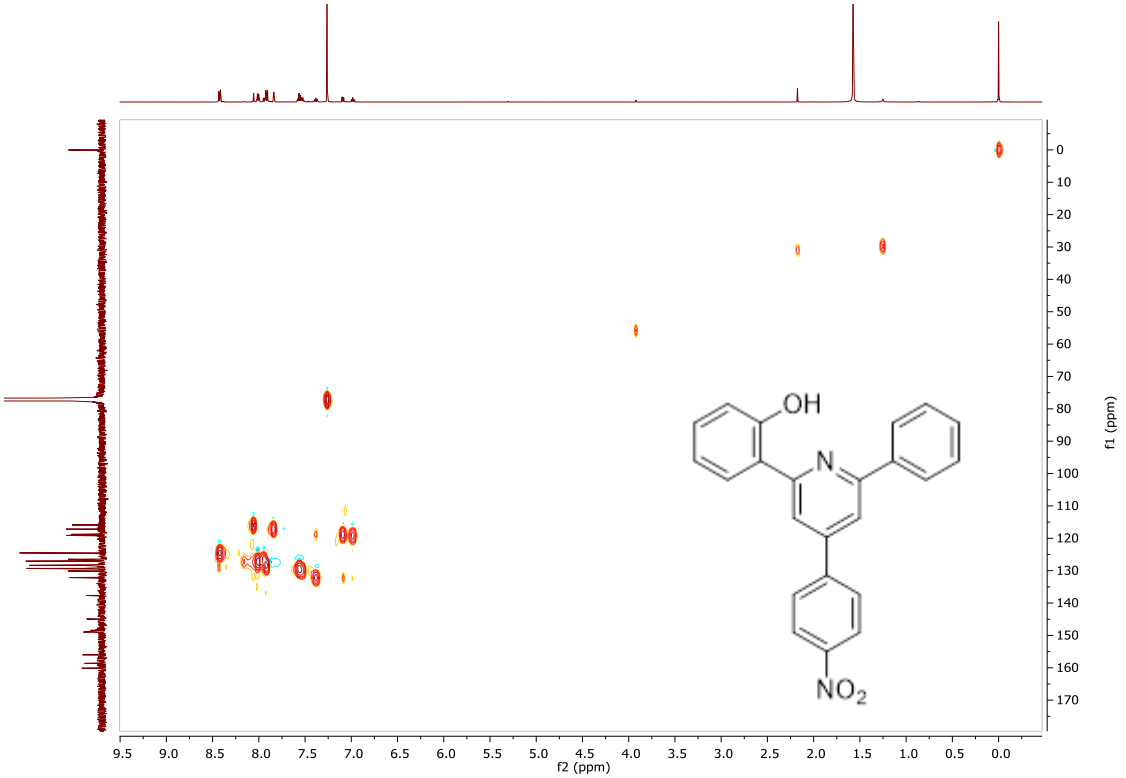

*Figure 84-HSQC spectrum of compound **6e***

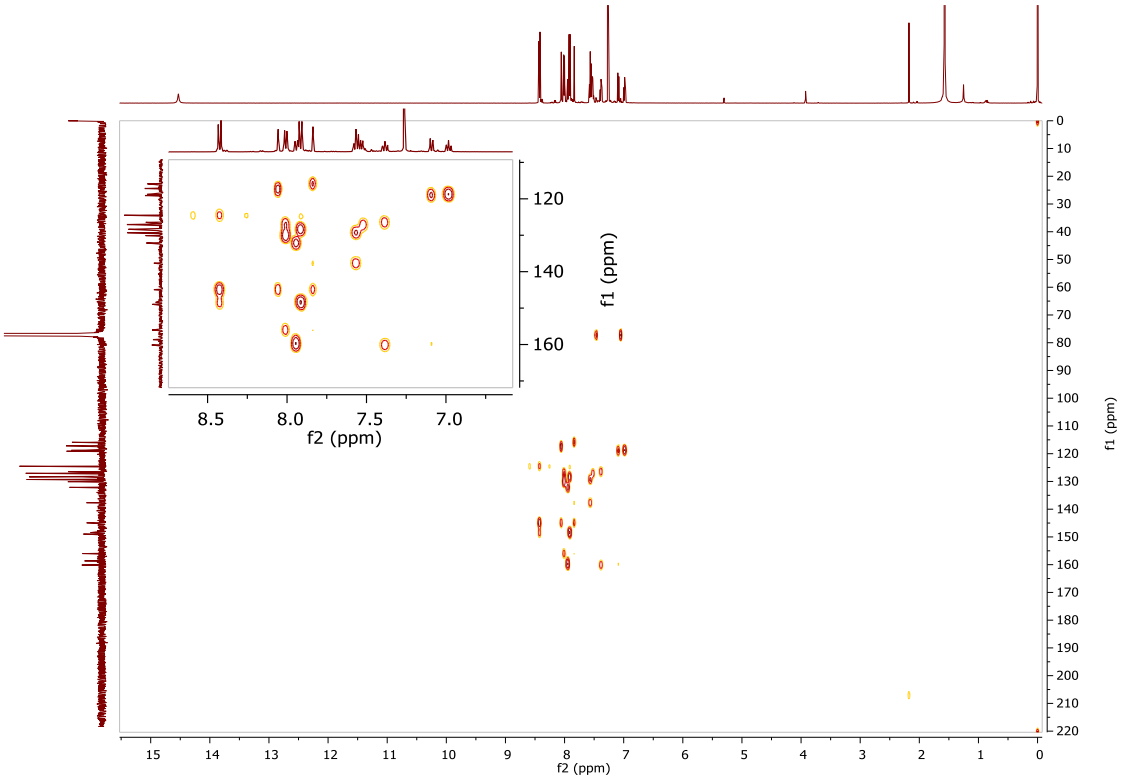

*Figure 85-HMBC spectrum of compound **6e***

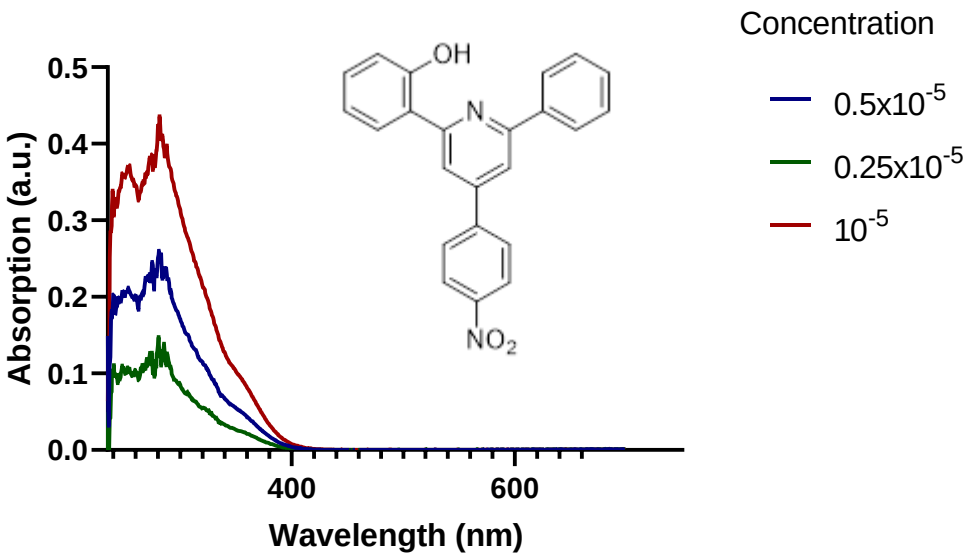

Figure 86- Absorption spectra of compound ***6e***

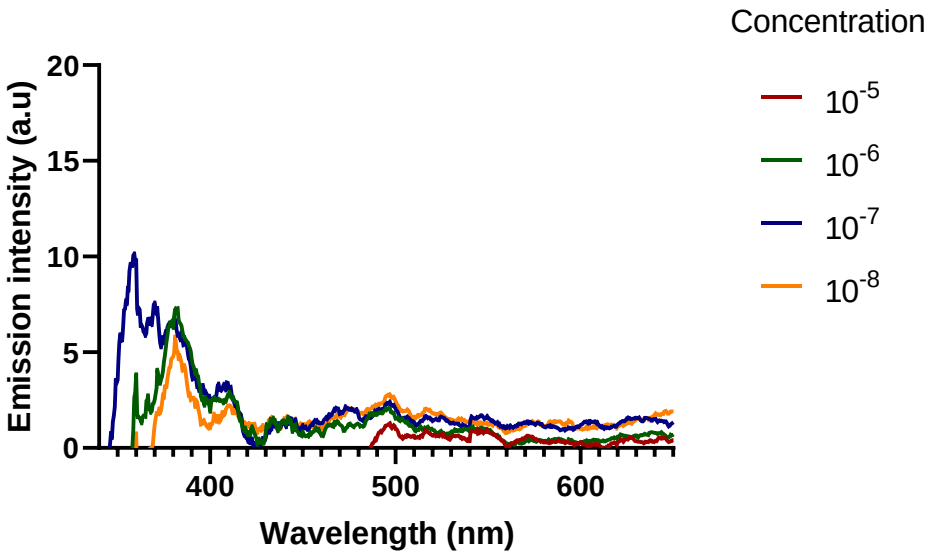

Figure 87- Emission spectra of compound ***6e***

Pyridine 6f

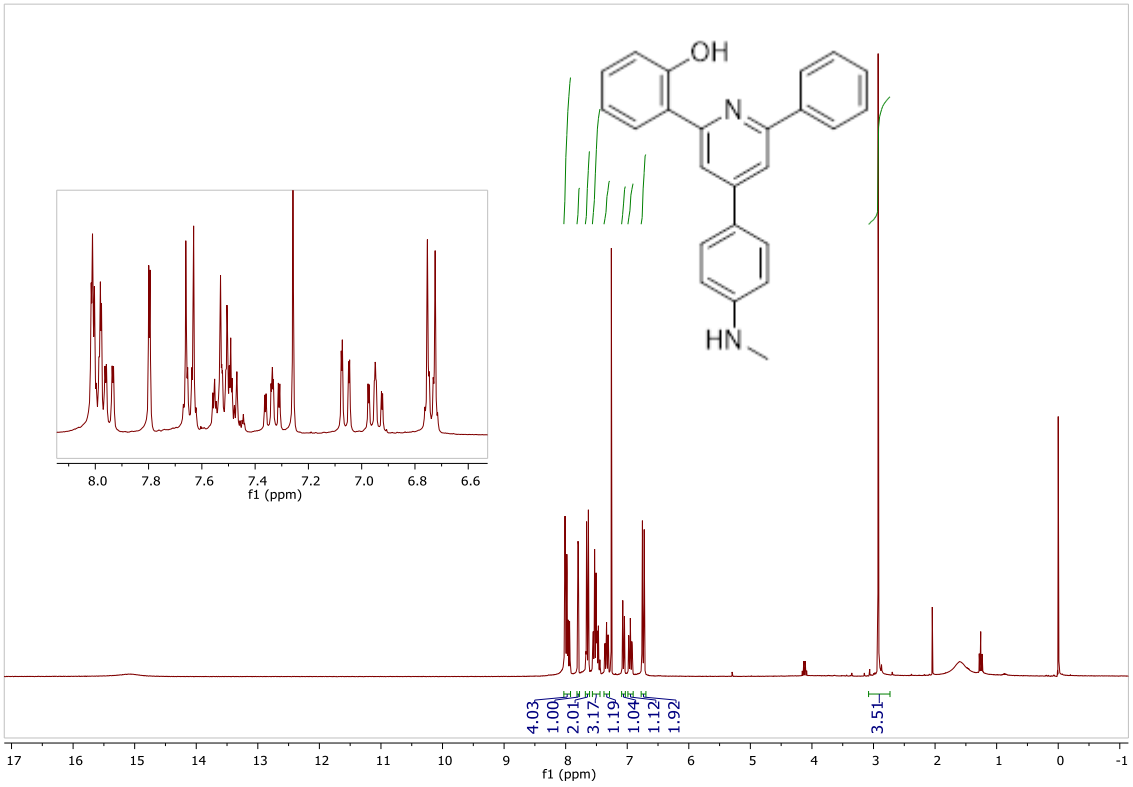

*Figure 88-^{1}H-NMR spectrum of compound **6f***

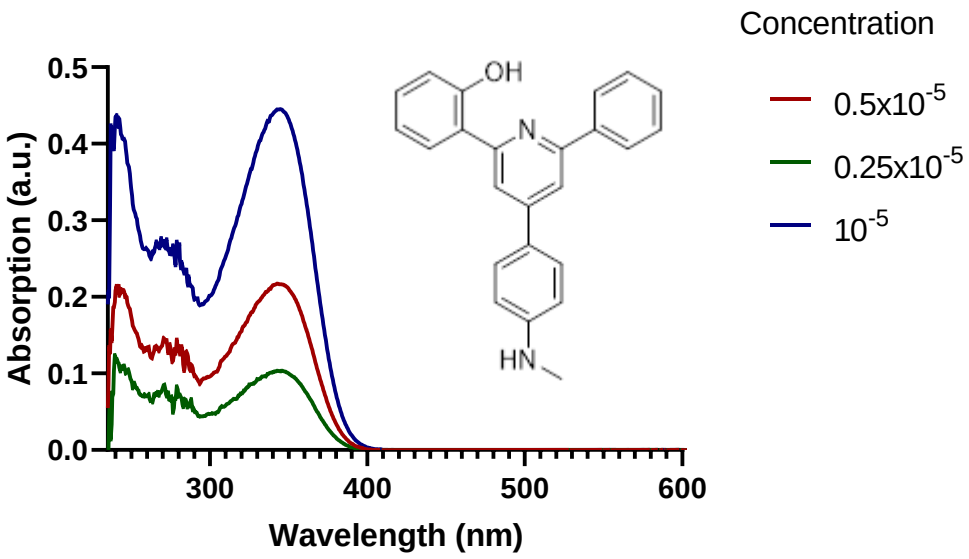

*Figure 89- Absorption spectra of compound **6f***

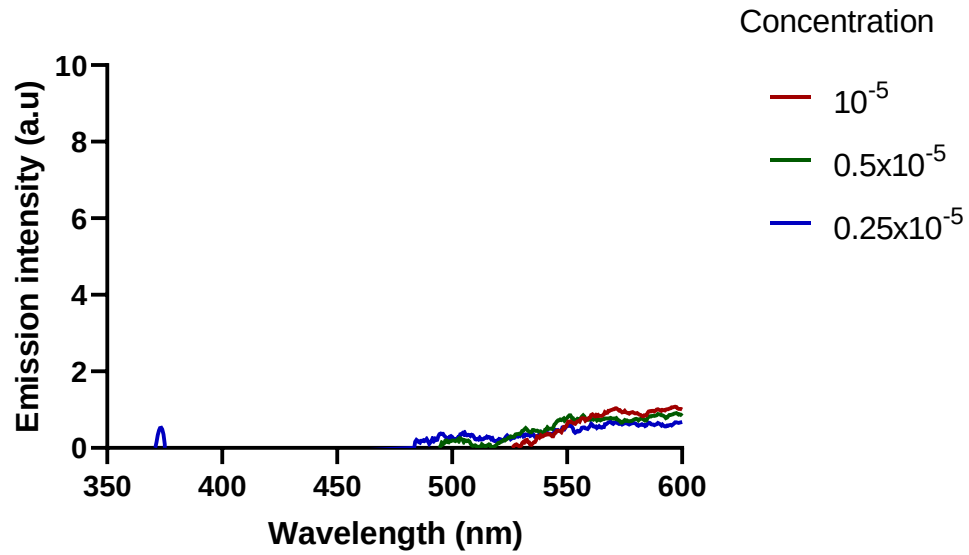

*Figure 90- Emission spectra of compound **6f***

Pyridine 7b

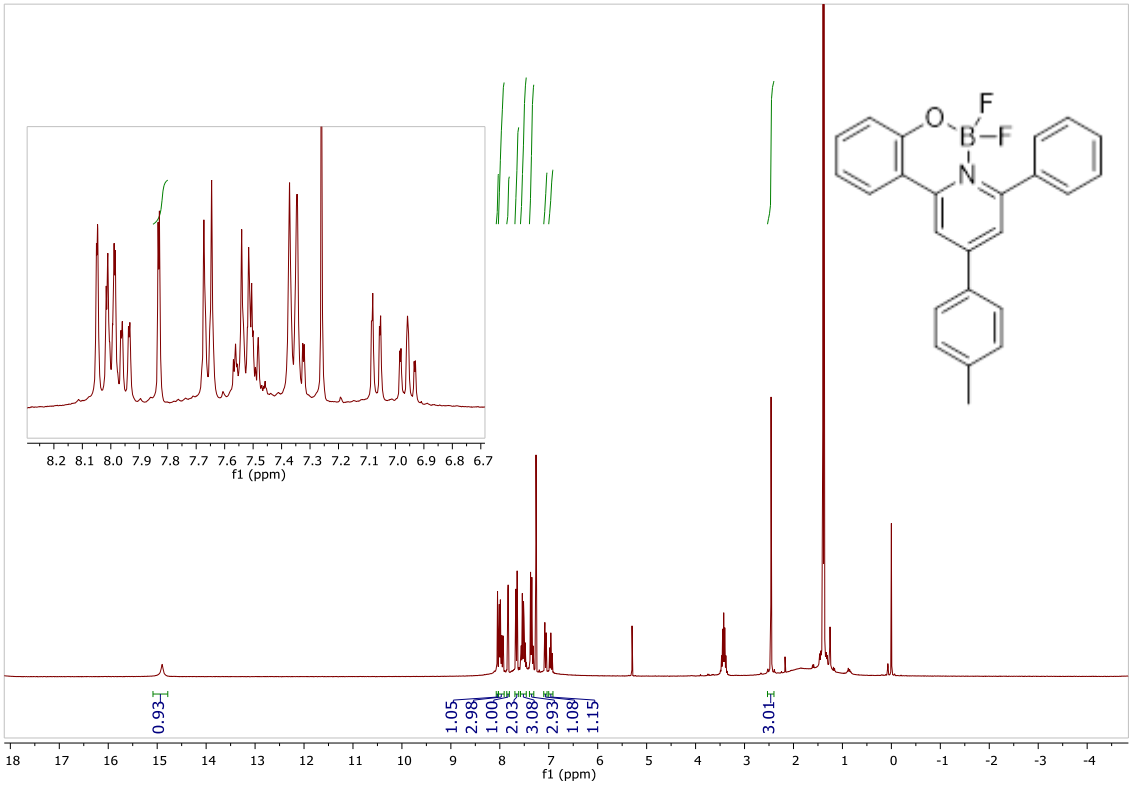

*Figure 91-^{1}H-NMR spectrum of compound **7b***

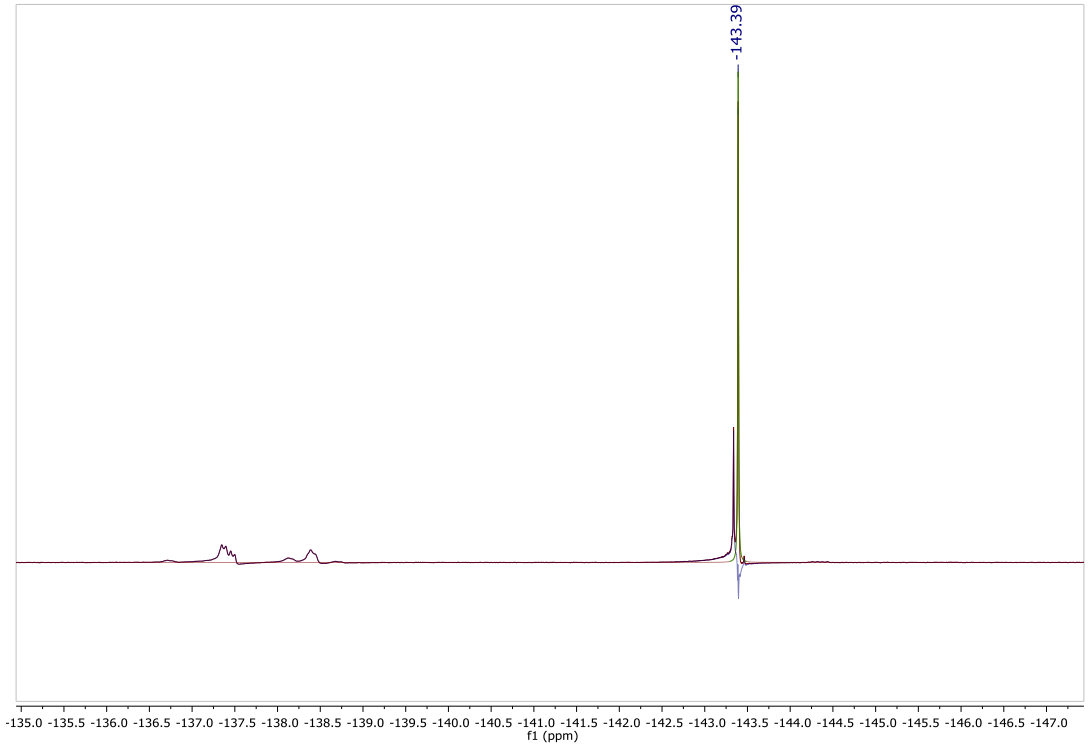

*Figure 92-^{19}F-NMR spectrum of compound **7b***

Pyridine 7d

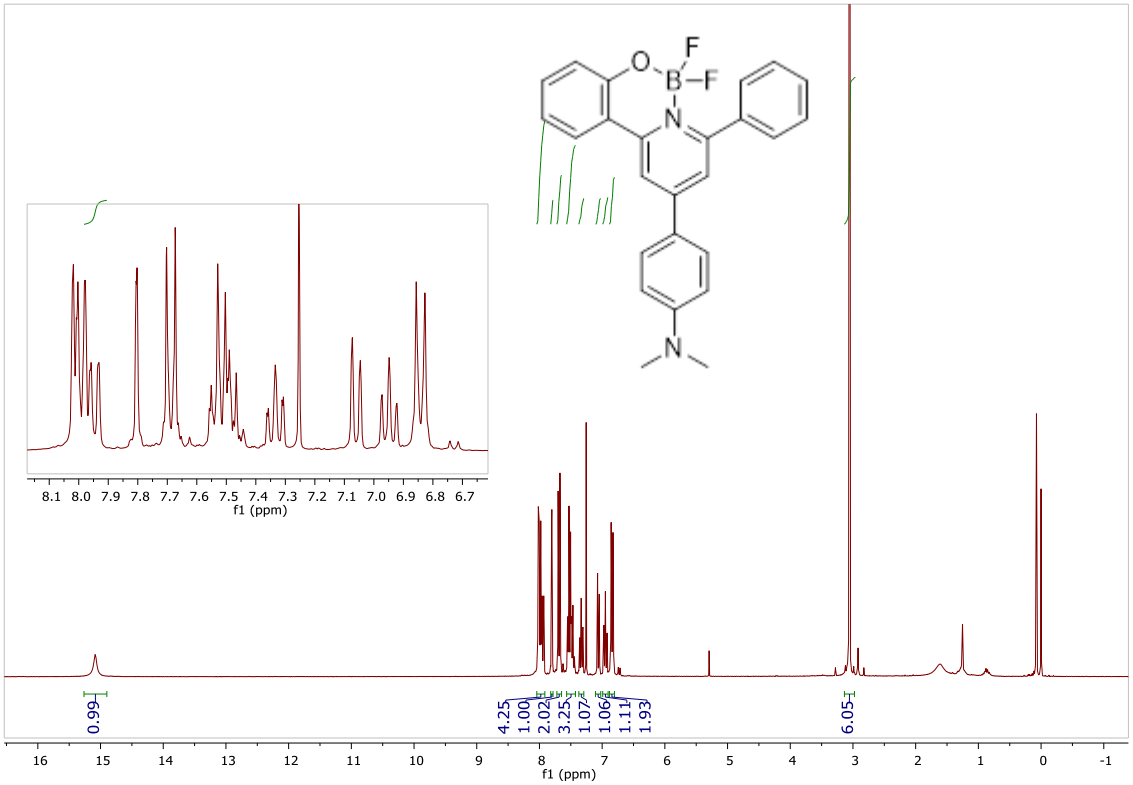

*Figure 93-^{1}H-NMR spectrum of compound **7d***

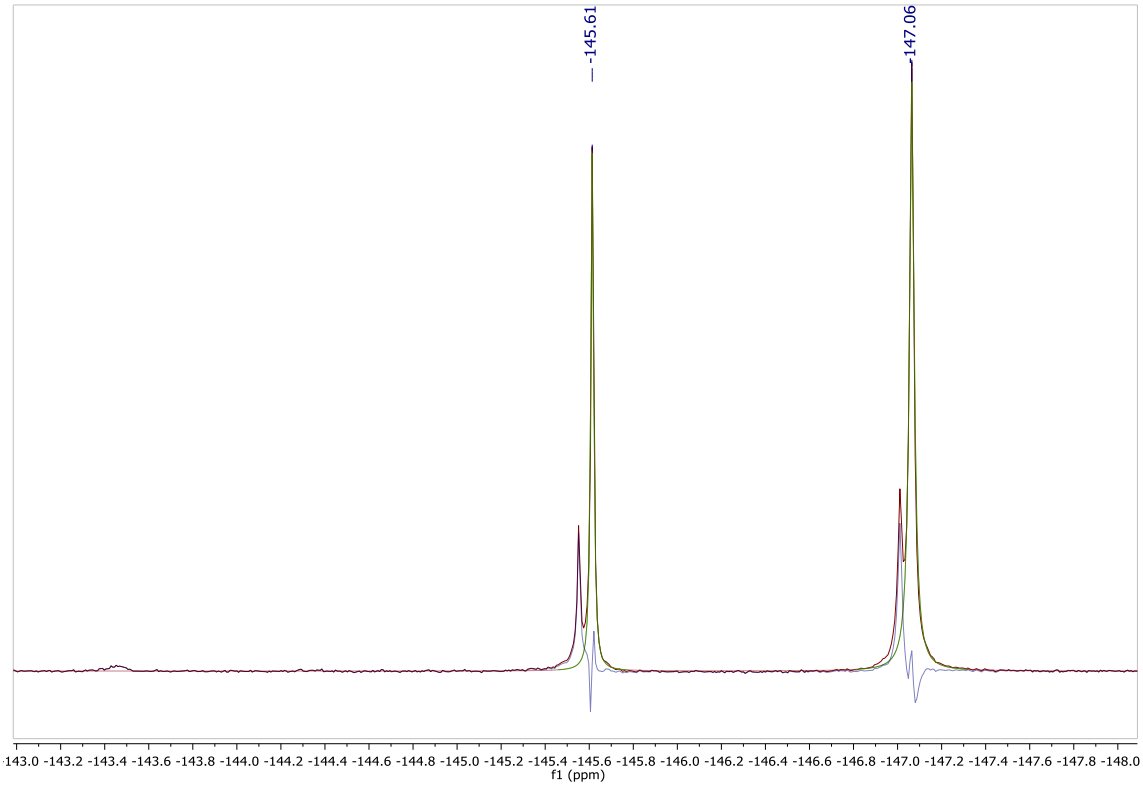

*Figure 94-^{19}F-NMR spectrum of compound **7d***

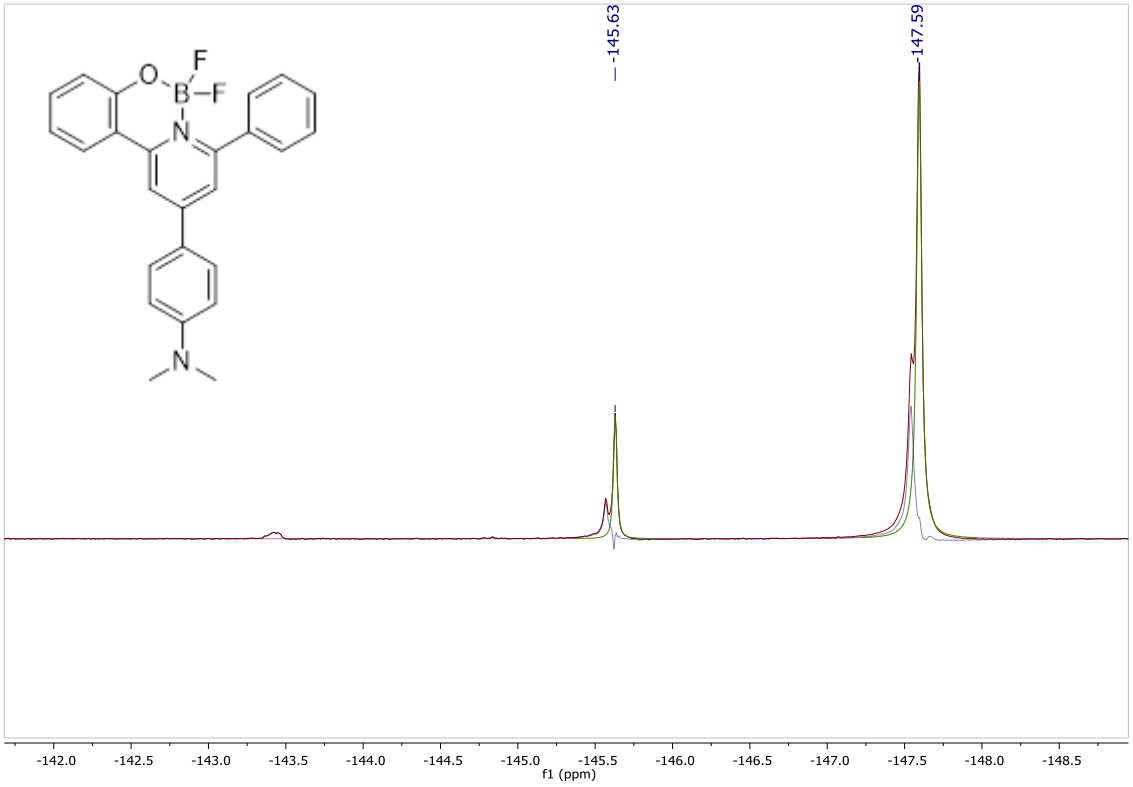

*Figure 95-^{19}F-NMR spectrum of compound **7d** after multiple filtrations.*